Avoiding trade-off when enhancing Fusarium head blight resistance of barley

Rachel Joan Goddard

A thesis submitted to the University of East Anglia

for the degree of Doctor of Philosophy

Department of Crop Genetics

John Innes Centre

September 2015

Abstract

Fusarium head blight (FHB) is an economically important disease of barley caused by mycotoxin-producing *Fusarium* species. Resistance to FHB is associated with several agronomic traits, particularly height. Taller cultivars are generally more resistant; however increased height is less favourable due to the prospect of lodging, creating a trade-off between disease resistance and agronomic qualities.

Disease assays with pathogens of differing trophic lifestyles were conducted using barley *BRI1* mutation lines, which display brassinosteroid (BR) insensitivity and a semi-dwarf phenotype. Interestingly, *bri1* semi-dwarf lines did not display increased susceptibility to FHB. Additionally, *bri1* mutation provided advantageous resistance to necrotrophs but did not increase susceptibility to biotrophs, demonstrating an absence of a resistance trade-off.

The barley cultivars Chevallier and Armelle display significant FHB resistance, yet also possess a tall height phenotype. To determine whether the resistance of these cultivars was associated with height, bi-parental populations were created by crossing to the short, modern variety NFC Tipple. High density genetic maps of the populations were produced using Genotyping-by-Sequencing and 384-SNP BeadXpress assays to enable quantitative trait loci (QTL) mapping of both FHB and agronomic traits. Within the C×T population, a QTL for FHB resistance was identified on chromosome 6H which was not associated with either height or heading date, suggesting that resistance in this region is not due to linkage or pleiotropy with these traits. In contrast, FHB resistance within the A×T population was coincident with both height and heading date QTL on 3H.

QTL analysis of malting traits of Chevallier, an English malting landrace, was also undertaken. Chevallier compared favourably to NFC Tipple, a modern malting cultivar, for several malting characteristics including free amino nitrogen, diastatic power and wort β-glucan content. This demonstrates that Chevallier may be a useful potential source of both FHB disease resistance and quality traits.

Acknowledgements

My funding for this project was provided by BBSRC and Brewlab through a BBSRC-CASE award.

I would firstly like to thank my supervisor Dr. Paul Nicholson for providing me with the opportunity to undertake this PhD. Paul's encouragement, advice and patience throughout my studies has been invaluable and is greatly appreciated. I am especially thankful for his perseverance during those first few months. Additionally, thanks go to Dr. Christopher Ridout and Dr. Keith Thomas who have helped to shape this project with their knowledge and guidance.

I would like to thank both past and present members of the Nicholson group at JIC: Andy Steed, Martha Clarke, Chris Burt, Antoine Peraldi and Marianna Pasquariello for their scientific expertise and for making the group such an enjoyable place to work. Thank you for making me feel welcome and for being so willing to help with various aspects of my project. I would particularly like to thank Andy, Chris, Paul and Martha for all their help with field trial inoculations, scoring and harvesting. Thanks must also go to those at Syngenta Seeds Ltd, KWS UK Ltd. and NIAB who contributed to either the development or phenotyping of the mapping populations used within my study. I am also grateful to the following people who have helped me throughout the past four years: Mark Collins and Joe Nicholson, the JIC Horticultural and Field Services team, Dr. Charles Brearley and colleagues at UEA, Julio Johnson at Brewlab, the Brown group at JIC, Dr. Graham McGrann at SRUC, Dr. Sarah de Vos at New Heritage Barley Ltd. and Dr. Joanne Russell at JHI.

I have been fortunate to get to know some great people at JIC, particularly the students in my year group: Ania Kowalski, Annis Richardson, Artemis Giannakopoulou, Chris Judge, Claire Drurey, Jo Harrison, John Steele, Mike Rugen, Richard Payne and Rowena Fung. I'd especially like to thank Jo and Chris, and also Alex Calderwood, for helping to make this such a great experience both in and out of the lab.

Finally I would like to thank my parents, Raymond and Doreen Goddard, for their continued love and support, for which I will be forever grateful.

Abbreviations

ANOVA	analysis of variance
AUDPC	area under disease progress curve
Bd	*Brachypodium distachyon*
BR	brassinosteroid
BX	BeadXpress
CAP	co-ordinated agricultural project
CER	controlled environment room
CIM	composite interval mapping
cM	centimorgan(s)
cm	centimetre(s)
°C	degrees Celsius
DON	deoxynivalenol
DH	doubled haploid
dpi	day(s) post inoculation
eBL	epibrassinolide
ELISA	enzyme linked immunosorbent assay
ET	ethylene
FCR	Fusarium crown rot
FHB	Fusarium head blight
GA	gibberellic acid
GBS	genotyping-by-sequencing
GLM	general linear model
GS	growth stage
GWAS	genome wide association studies
JA	jasmonic acid
JHI	James Hutton Institute
JIC	John Innes Centre
LOD	logarithm of the odds (to the base 10)
LRR	leucine-rich repeat
ml	millilitre(s)
NIAB	National Institute of Agricultural Botany
NIL	near-isogenic line

NIV	nivalenol
nM	nanomole(s)
OWB	Oregon Wolfe barley
P	probability
PAMP	pathogen associated molecular pattern
PCD	programmed cell death
PCR	polymerase chain reaction
PDA	potato dextrose agar
PLS	physiological leaf spotting
PTI	PAMP-triggered immunity
%	percentage
QTL	quantitative trait loci
RIL	recombinant inbred line
RLS	Ramularia leaf spot
ROS	reactive oxygen species
SA	salicylic acid
SDW	sterile distilled water
SIM	simple interval mapping
SNP	single nucleotide polymorphism
SSD	single seed descent
µg	microgram(s)
µl	microlitre(s)
µM	micromole(s)

List of tables

List of figures

Table of contents

Chapter 1. General introduction

1.1 Head blight and other Fusarium diseases

Fusarium head blight (FHB) is a cereal disease caused by the *Fusarium* species of hemibiotrophic fungal pathogens, causing yield loss and posing a potential health risk to organisms that consume contaminated grain. FHB is primarily a disease of major small grain cereal crops such as barley (*Hordeum vulgare*), bread wheat (*Triticum aestivum*) and durum wheat (*Triticum turgidum*), but it can also affect other cereals such as rice (*Oryza sativa*) and maize (*Zea mays*), causing major economic losses in both agriculture and grain produce industries.

Fusarium species not only cause head blight, but are able to infect the plant host throughout most of its developmental stages and in multiple host tissues. Seedling blight causes poor plant establishment and may be seen after the sowing of *Fusarium* infected seeds or colonisation of clean seeds by *Fusarium* fungi present in the soil (Yang et al. 2011). Root rot, which is indicated by root necrosis, and crown rot, indicated by brown discolouration and weakening of the stem base, are also caused by *Fusarium* species (Beccari et al. 2011). Head blight however is considered to be the most significant of the *Fusarium* diseases, due to the majority of cereal products being generated from grains from the head of the plant and the potential for mycotoxin contamination.

1.2 Symptoms of FHB infection

Following colonisation of plant tissue by *Fusarium* fungi, a number of visible symptoms are presented in the ear and grains of the infected host. The most common symptom of FHB in wheat is the bleaching of infected spikelets prior to senescence (Figure 1.1a). This bleaching can spread from the initial point of infection, producing either partial or complete bleaching of the ear, as the fungus moves into the rachis of the wheat ear and further colonises the host tissue (Guenther and Trail, 2005). The disease may also be manifested as brown or water soaked discolouration on an otherwise green spike, a symptom which is indicative of FHB in barley (Figure 1.1b) (McMullen et al. 2012). Two-row barley cultivars have been demonstrated to be more

resistant to FHB than six-row cultivars Bai and Shaner, 2004). If environmental conditions are favourable for fungal development during anthesis, with prolonged periods of high humidity and warm temperatures, clusters of orange sporodochia may also be present on the glumes, lemma or even entire kernel of infected crops (Scherm et al. 2013). Fusarium infection in floral tissues causes the premature ripening of the grains, resulting in the production of characteristic shrivelled 'tombstone' kernels which are chalky or discoloured in appearance (Maloney et al. 2014). Fusarium damaged kernels (FDK) have a lower grain weight causing them to be more easily dispersed during harvesting, further propagating fungal infection, and are of poor quality resulting in reduced yield. Cereal grains affected by FHB may also contain mycotoxins produced by the fungus, leading to possible health risks depending on the intended use of such products and the toxin(s) present. The economic losses caused by low quality and mycotoxin contaminated wheat and barley grains in the US alone were estimated to total $7.67 billion during 1993 – 2001 (McMullen et al. 2012).

Figure 1.1. The characteristic symptoms of Fusarium head blight infection in barley. a) FHB symptoms in wheat. b). FHB symptoms in two-row (left) and six-row (right) barley. Scale bar = 1cm.

1.3 Causal species

Several *Fusarium* species are known to cause FHB, with environmental conditions, particularly temperature and rainfall, largely determining which particular pathogen species predominates in a specific geographical location. Within a single environment multiple *Fusarium* species may be present, forming a disease complex (Nicholson, 2009). The further pathogens *Microdochium nivale* and *M. majus*, which were formerly recognised as *Fusarium* species before detailed morphological and genetic analysis revealed that they are in a separate genus, are also found within the *Fusarium* disease complex and are known to produce a comparable spectrum of symptoms (Nielsen et al. 2013). Worldwide, *F. graminearum* (teleomorph *Gibberella zeae*) is thought to be the primary causal species of FHB in barley and wheat (McMullen et al. 2012). The warmer climates in Northern America and Asia are more conducive for *F. graminearum* development, as the species displays optimum fungal growth at temperatures between 25 – 30^{o}C (Brennan et al. 2003).

The predominant causal species of FHB in Northern Europe and the UK has historically also been *F. graminearum*, but more recently *F. poae* and *F. avenaceum*, and in particular *F. culmorum* have become increasingly prevalent (Xu and Nicholson, 2009). *F. culmorum*, *F. poae* and *F. avenaceum* exhibit optimal growth at temperatures between approximately 20 – 25^{o}C (Doohan et al. 2003), corresponding with the more moderate climate in Europe. *M. nivale* and *M. majus*, which produce similar symptoms to FHB, are more efficient pathogens in climates of 10 – 15^{o}C (Imathiu et al. 2010) and are therefore isolated from cooler, wetter locations. *F. langsethiae*, which was first identified in 2004 (Torp and Nirenberg, 2004), has also been demonstrated to be an important emerging causal species of FHB in barley and particularly oats (*Avena sativa*). This species is most commonly found in areas such as Northern and Central Europe where temperatures of 20 – 30^{o}C provide an ideal growth environment (Imathiu et al. 2013). The species *F. sporotrichioides* is generally isolated from more moderate regions with temperatures of 20 – 25^{o}C (Doohan et al. 2003), whilst *F. verticillioides*, formerly *F. moniliforme*, and *F. proliferatum* are largely isolated from infected maize stubble and exhibit optimal growth at temperatures of 15 – 30^{o}C.

1.4 Sources of inoculum and mechanisms of infection

Within a field environment, the primary inoculum of FHB is contaminated crop residue from previous harvests (Bai and Shaner, 2004). *F. graminearum* has been demonstrated to survive saprophytically over winter on plant debris from wheat, barley and maize (Goswami and Kistler, 2004). Initiation of the pathogenic phase of the *Fusarium* life cycle and therefore production of inoculum occurs when the environmental conditions become more favourable for fungal development. The conditions during which optimal development occurs are dependent on the species of *Fusarium* that are present within a disease complex and whether they are able to reproduce through sexual or asexual means. For example, *F. poae* and *F. culmorum* are thought to reproduce via asexual means only, whilst *F. graminearum*, *F. avenaceum* and the non-true *Fusarium* species *M. nivale* and *M. majus* are capable of both asexual and sexual reproduction (Doohan et al. 2003). Asexual reproduction results in the production of three main spore types: microconidia, which are one or two celled and produced from the conidiophores, larger multi-septate macroconidia formed in the sporodochia of conidiophores, and round chlamydospores generated from either hyphae or macroconidia (Ma et al. 2013). The production of asexual conidia occurs on the surface of infected crops at the optimal temperature of 28 – 32ºC in *F. graminearum* (Doohan et al. 2003) and studies have determined that they are most often distributed by splash dispersal (Rossi et al. 2002), as demonstrated in Figure 1.2.

Ascospores are produced via sexual means, from sacs called asci within the perithecium, and are discharged during periods of higher humidity due to changes in turgor pressure within the ascus (Trail et al. 2002). The optimal temperature for ascospore generation in *F. graminearum* is 25 – 28ºC and they are considered to be the primary inoculum of FHB due to their airborne dispersal (Trail, 2009). Distribution of the inoculum onto the surface of or inside the spikelets of crops, allows the initiation of infection in the host plant if conditions remain conducive to germination.

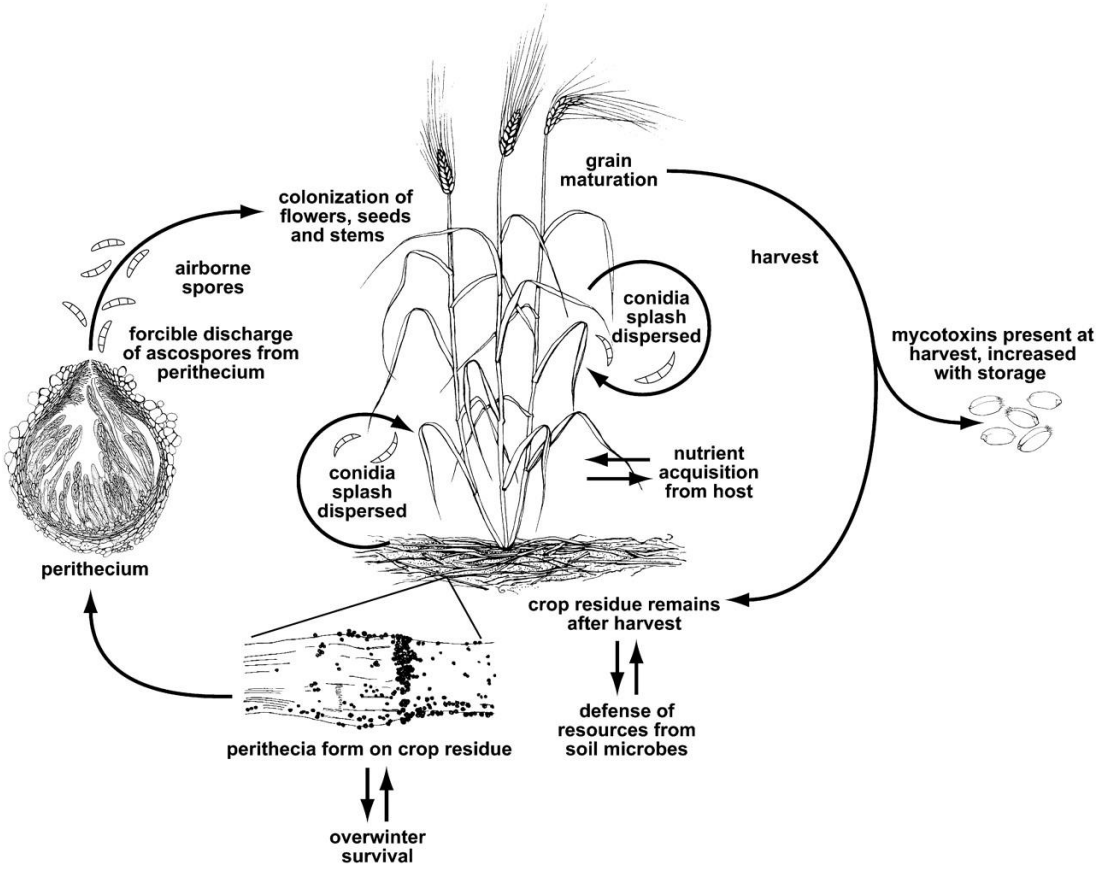

Figure 1.2. The life cycle of *Fusarium graminearum* with wheat as the host cereal. (Taken from Trail, 2009).

1.4.1 Fungal colonisation of the host

Following dispersal of the fungal inoculum, the *Fusarium* fungus is deposited on the external structures of cereal ears, such as the palea, lemma and glumes (Trail, 2009). Anthers are rapidly colonised by *F. graminearum* (Skinnes et al. 2010), therefore cereals are most susceptible to FHB infection during the period of anthesis, but can still be infected during the later stages of kernel development. After germination, *F. graminearum* has been observed to extend its hyphae on the surfaces of these structures without penetrating through the epidermal cells (Boenisch and Schäfer, 2011), before infiltrating the host via the cell wall, epidermis, stomata or cuticle (Wanjiru et al. 2002). *F. graminearum* subsequently undergoes systemic growth, with subcuticular colonisation of wheat glumes being observed as early as 48 hours post

inoculation (hpi) (Pritsch et al. 2000). Two distinct structures, subcuticular hyphae and bulbous infection hyphae, have been observed during this stage of infection (Rittenour and Harris, 2010). Subsequent extension of hyphae in *F. graminearum* is initially confined to the intercellular spaces of the wheat rachis (Brown et al. 2010). This lack of intracellular growth suggests a brief biotrophic stage of asymptomatic host colonisation, leading to *F. graminearum* being considered as a hemibiotroph rather than a truly necrotrophic fungus. Following abundant intercellular growth and hyphal extension, *F. graminearum* begins intracellular establishment, acting in a necrotrophic manner as it causes host cell death. Fungal hyphae are present in the aleurone layer, endosperm and pericarp of infected wheat grain within 72hpi, causing collapse and death of the cells present (Jansen et al. 2005) and ultimately destroying the structure of the caryopses. Colonisation of the rachilla, rachis and the rachis node in wheat occurs through either lateral intercellular or vertically growing intracellular hyphae (Bushnell et al. 2010). Fungal spread within the rachis node is limited in barley, due to the synthesis of cell wall components, such as cellulose, lignin and xylan, preventing the spread of the fungus from the infected spikelet to non-infected grains (Jansen et al. 2005).

1.4.2 Host response to Fusarium colonisation

In response to initial infection by *Fusarium* species the host mounts a number of defence responses. Following infection with *F. graminearum*, the expression of wheat chitinases, β-1,3-glucanases and thaumatin-like proteins were observed (Pritsch et al. 2000). Chitinases and glucanases recognise and target the cell wall components chitin and glucan for degradation (Theis and Stahl, 2004), weakening the *Fusarium* cell wall. Thaumatin-like proteins are also thought to disrupt the integrity of the fungal membrane, as do thionins and lipid transfer proteins which have antifungal activity (van Loon et al. 2006). During this subcuticular and intercellular growth of the fungus within the host, plant cell wall components such as ferulic acid and *p*-coumaric acid are synthesised, which may reinforce the cell wall to prevent additional fungal colonisation (Kang and Buchenauer, 2003). Significant differences in cell wall composition have been determined between FHB resistant and susceptible wheat cultivars, particularly with respect to lignin content, suggesting an important role in

disease resistance (Lionetti et al. 2015). To counteract the strengthening of the host cell wall, *F. graminearum* and *F. culmorum* produce cell wall degrading enzymes including pectinases, xylanases and polygalacturonases (Kikot et al. 2009). Following polygalacturonase secretion by *F. graminearum*, wheat produces polygalacturonase-inhibiting proteins to help inhibit further cell degradation (Walter et al. 2010). Studies have also identified that the production of reactive oxygen species (ROS), peroxidase genes (Desmond et al. 2008), ABC transporters (Xiao et al. 2013) and defensin genes (Gottwald et al. 2012) are activated in response to host invasion by *Fusarium* species. The production of resistance metabolites from a number of biosynthetic pathways has also been observed. For example, higher levels of cinnamic acid, a compound from the phenylpropanoid pathway from which ferulic and *p*-coumaric acid are derived (Ponts et al. 2011), have been observed in resistant wheat cultivars compared to more susceptible cultivars (Paranidharan et al. 2008). Phenylalanine ammonia lyase, an integral component in the phenylpropanoid pathway, is also up-regulated during *F. graminearum* infection (Steiner et al. 2009), again suggesting a role for this pathway in defence. Several phytohormone pathways are also involved in basal immunity and the expression of genes involved in the synthesis of hormones, such as jasmonic acid (JA), have been shown to be upregulated post infection with *F. graminearum* (Li and Yen, 2008). The exact mechanisms of host defence are still being uncovered and further studies should provide more definitive answers to the response of both the host and the *Fusarium* pathogen during the infection process.

1.5 Fusarium mycotoxins

Fusarium fungi have the ability to produce a variety of secondary metabolites known as mycotoxins during host colonisation, which have varying effects on human and animal health should they be ingested. Many *Fusarium* species produce several mycotoxins which are thought to have multiple actions within plant tissue (Table 1.1). Such toxins accumulate in the grains of infected crops and are stable during grain processing methods, meaning they may be detected in food and malt products. Some of the most prevalent mycotoxins include fumonisins, zearalenone, moniliformin, enniatins, beauvericin and the trichothecenes (Desjardins and Proctor, 2007). Fumonisins, such as those produced by *F. verticillioides* and *F. proliferatum*, are

polyketides that disturb sphingolipid metabolism by inhibiting the enzyme ceramide synthase (Lanubile et al. 2013). One of the predominant forms of fumonisin, Fumonisin $B_{1,}$ is most frequently isolated from infected maize and has been demonstrated to induce both intestinal and hepatic toxicity in piglets (Grenier et al. 2012). A further polyketide zearalenone is commonly produced by *F. graminearum* and *F. culmorum*, and a number of studies using several animal models have demonstrated the hyper-estrogenic effects of the toxin (Hueza et al. 2014). Mycotoxins such as moniliformin are also synthesised via polyketide pathways (Jestoi, 2008) and are produced by species such as *F. avenaceum* (Morrison et al. 2002). *F. oxysporum* and *F. langsethiae* have been identified as species that produce enniatins (Thrane et al. 2004), toxins that alter ion homeostasis and disrupt the membrane integrity of mitochondria (Tonshin et al. 2010; Meca et al. 2010). *F. langsethiae* is also known to produce beauvericin (Thrane et al. 2004), a cyclohexadepsipeptide that is able to cause apoptosis of mammalian cells (Logrieco et al. 2002). The class of mycotoxins known as the trichothecenes are currently the most widely understood and investigated form of secondary metabolites produced by the *Fusarium* species, due to the higher prevalence of trichothecene producing strains in Northern Europe and America where cereal crops are commonly grown.

Table 1.1. *Fusarium* species and their known mycotoxins.

Mycotoxin	**Species**	**Reference**
Trichothecenes	*F. graminearum* (DON, NIV), *F. culmorum* (DON, NIV), *F. poae* (NIV), *F. sporotrichioides* (HT-2, T-2), *F. langsethiae* (HT-2, T-2), *F. acuminatum* (T-2)	Bottalico and Perrone, 2002; Desjardins and Proctor, 2007; Imathiu et al. 2013
Fumonisins	*F. verticillioides*, *F. proliferatum*, *F. subglutinans*	Rheeder et al. 2002; Grenier et al. 2012
Enniatins	*F. oxysporum*, *F. langsethiae*, *F. poae*	Thrane et al. 2004
Zearalenone	*F. graminearum, F. culmorum*	Lysoe et al. 2008
Moniliformin	*F. avenaceum, F. tricinctum*,	Morrison et al. 2002
Beauvericin	*F. langsethiae, F. poae*	Thrane et al. 2004; Desjardins and Proctor, 2007

1.5.1 Trichothecene mycotoxins

Several species of true *Fusarium* fungi, therefore excluding *M. nivale* and *M. majus*, produce trichothecene mycotoxins during the colonisation of host plant tissue. Trichothecenes are a large class of structurally similar, water soluble, sesquiterpene secondary metabolites that are produced by some of the most prevalent *Fusarium* species, including *F. graminearum* and *F. culmorum* (McCormick et al. 2011) and are therefore of most interest. Trichothecenes have a fused cyclohexene-tetrahydropyran ring structure around which acetyl and hydroxyl groups are found (Foroud and Eudes, 2009). The different toxins are classified according to their structure at the carbon-8 (C-8) position of the ring. Of the four major types of trichothecene (Type A, B, C, D) Type A and Type B are most common, with Type C and Type D being less associated with FHB (Bennett and Klich, 2003). Type A trichothecenes possess an ester side

chain at the C-8 position, Type B possess a ketone, whilst the less prevalent Type C and Type D possess an epoxide and an additional macrocyclic ring, respectively (McCormick et al. 2011). Type A toxins, such as T-2 and HT-2, are extremely toxic compounds and are approximately ten times more harmful than Type B toxins, such as deoxynivalenol (DON) and nivalenol (NIV) (Desjardins and Proctor, 2007). *F. graminearum* produces DON and its less toxic derivatives 3-acetyl-DON (3-ADON) and 15-acetyl-DON (15-ADON) (Bottalico and Perrone, 2002), whilst *F. sporotrichioides* and *F. langsethiae* produce T-2 and HT-2, although such species are less prevalent.

Trichothecene synthesis occurs via the terpenoid pathway and is initiated by the conversion of the substrate farnesyl pyrophosphate into trichodiene by the enzyme trichodiene synthase. This is encoded for by the gene *Tri5*, which is located at the centre of a 25kb core cluster of 12 co-regulated *Tri* genes (Desjardins and Proctor, 2007). Trichodiene is converted into calonectrin by a series of nine further reactions involving the enzymes *Tri4*, *Tri101*, *Tri11* and *Tri3*, a process which is common in the synthesis of both Type A and Type B trichothecenes (Merhej et al. 2011). A further two common reactions are seen in Type A producing species and *F. graminearum* NIV producers, catalysed by the products of *Tri7* and *Tri13* (Lee et al. 2014). In studies using *F. sporotrichioides*, *Tri7* and *Tri8* are then required for the production of Type A trichothecenes such as T-2 (Foroud and Eudes, 2009). In *F. graminearum*, the Type B trichothecene NIV is then produced by the action of *Tri1* to form 4-ANIV, followed by the conversion into NIV by *Tri8* (McCormick et al. 2011). Isolates of *F. graminearum* and *F. culmorum* that are not capable of producing NIV lack functional *Tri7* and *Tri13* genes, and calonectrin is converted into 3-ADON, 15-ADON or DON by the action of the products of *Tri1* and *Tri8*. The production of the 3- and 15-ADON chemotypes is dependent on the particular mutations present in the coding sequence of the *Tri8* gene. In 3-ADON producers the *Tri8* gene encodes a C-15 esterase which deacetylates 3,15-diacetyldeoxynivalenol at the C-15 position, whilst in 15-ADON producers the *Tri8* gene encodes a C-3 esterase which acts at the C-3 position to produce 15-ADON (Alexander et al. 2011).

The consumption of trichothecene contaminated grain products has been demonstrated to have a negative effect on the health of both humans and animals. Trichothecenes

are classically regarded as inhibitors of eukaryotic protein and mitochondrial synthesis (Pace et al. 1988), by binding to the 60S ribosomal subunit, and have also been demonstrated to inhibit DNA synthesis, cell growth and cause cell cycle arrest (Pestka, 2010). Oxidative stress damage and subsequent cell death caused by the action of DON has been observed in both human and plant cells, as have trichothecene induced chromosomal abnormalities (Arunachalam and Doohan, 2013). Feed refusal in swine and poultry (D'Mello et al. 1999; Borutova et al. 2008) and an inflammatory immune response and irritation of the digestive tract in humans are also associated with trichothecene exposure (Pestka et al. 2004). Due to the health concerns regarding trichothecene contamination strict regulations govern the permitted mycotoxin content of cereal grains and their by-products, such as animal feed and brewed beverages. The US Food and Drug Administration (FDA) recommends a maximum DON level of 1ppm in wheat and barley products for human consumption (US FDA, 2010), whilst within the EU a limit of 1250ppb is acceptable for DON in unprocessed cereals (EC 1881/2006). The increasing prevalence of Type A trichothecene mycotoxins led to new guidance values regarding T-2 and HT-2 being issued in 2013, with advisory limits of 200ppb and 100ppb in unprocessed barley and wheat, respectively, being suggested (EC 2013/165/EU).

1.5.2 The effect of trichothecenes within the host

The actions of trichothecenes such as DON have various effects in cereals. Treatment of wheat leaf segments with up to 90ppm DON causes bleaching, an effect enhanced by the addition of Ca^{2+} (Bushnell et al. 2010). The same study also noted that in response to treatment with non-toxic levels of DON, leaf segments remained green, an observation which was also seen with cycloheximide, another protein synthesis inhibitor. Such results suggest the dual roles of DON in both postponing senescence and causing cell death may be contributed by its effect on protein synthesis. Treatment of wheat leaves with 200ppm DON causes the production of the ROS H_2O_2 and also induces programmed cell death (PCD) within 24 hours (Desmond et al. 2008). However, such levels of toxicity are unlikely to be seen within a natural environment. Contrastingly, treatment of *Arabidopsis thaliana* cells with lower levels of DON (10ppm) inhibits apoptosis-like PCD in response to heat stress treatment (Diamond et

al. 2013). This suggests that trichothecenes may have a role in suppressing cell death, which may be advantageous during the brief biotrophic phase of fungal infection. The results of such studies suggest that trichothecenes produced by *Fusarium* species have a complex role within host tissues.

DON accumulation within the host tissues has been demonstrated to induce the expression of host defence genes. Cytochrome P450s, ABC transporters and glutathione S-transferases are consistently induced by the presence of DON in barley and wheat (Boddu et al. 2007; Gardiner et al. 2010; Walter and Doohan, 2011), suggesting important roles for trichothecene detoxification. Boddu et al. (2007) demonstrated that the barley cultivar Morex shows differential upregulation of defence genes in response to infection with either trichothecene-producing or *tri5* mutant isolates of *F. graminearum* that are incapable of producing trichothecenes. The induction of genes encoding ABC transporters and UDP-glucosyltransferases, which are thought to have a role in DON detoxification, after inoculation with the wild-type fungus but not with the *tri5* isolate suggests that distinct pathways are activated during *Fusarium* infection, with separate roles to both limit mycotoxin accumulation and restrict fungal colonisation (Boddu et al. 2007). In response to point inoculation of DON in wheat ears, the early expression of two ABC transporters are also induced (Walter et al. 2015). ABC transporters are known to play roles in auxin and alkaloid transport, the deposition of cuticular wax and tolerance to heavy metals, though direct transportation of heavy metal ions have not been demonstrated (Rea, 2007). The role of UDP-glucosyltransferases in DON detoxification has been illustrated by the *Arabidopsis* gene *UGT73C5* which is able to convert 15-ADON to the less toxic DON-3-*O*-glucoside, via the transfer of glucose to the 3-OH position (Poppenberger et al. 2003). Barley spike inoculation with DON results in a decrease in DON concentration within the ear over a 72 hour period, but an increase in the content of DON-3-*O*-glucoside, suggesting detoxification of DON (Gardiner et al. 2010). The same study looked at the transcriptional profiles of barley ears treated with DON and again noted the induction of two UDP-glucosyltransferase genes. In a further study four candidate barley UDP-glucosyltransferases were expressed in yeast (Schweiger et al. 2010). *HvUGT13248*, which displayed the lowest sequence identity with the *Arabidopsis* gene *UGT73C5* identified by Poppenberger et al. (2003), was the only gene from the four initial candidates which gave resistance to DON following treatment (Schweiger

et al. 2010). The production of DON-3-*O*-glucoside was found to be greater in both transgenic *Arabidopsis* and wheat lines constitutively expressing *HvUGT13248* than non-transformants (Shin et al. 2012; Li et al. 2015), with the transgenic wheat cultivars also displaying increased Type 2 resistance following infection with *F. graminearum*.

1.5.3 Trichothecene deficient Fusarium strains

The production of mycotoxins by *Fusarium* species has been proposed as a significant factor in the process of infecting host plants. The disruption of key genes in the trichothecene biosynthetic pathway, such as *Tri5* or the closely situated gene *Tri6*, result in a great reduction in mycotoxin biosynthesis, providing targets to enable the investigation into the effects of trichothecenes on fungal virulence and disease incidence (Foroud and Eudes, 2009). In wheat, *Fusarium* isolates which possess disrupted trichothecene biosynthesis pathways show altered infection successes, suggesting a role for these mycotoxins as major factors in disease development. *F. graminearum* isolates which are disrupted in the *Tri5* gene produce reduced FHB symptoms, such as less severe bleaching, when compared to those inoculated with wild-type strains (Desjardins and Hohn, 1997). The trichothecene *tri5* deficient isolates used by Langevin et al. (2004) and the *tri12 F. graminearum* isolates used by Menke et al. (2013) were also determined to be less aggressive than mycotoxin producing isolates during wheat inoculation studies. Further evidence for the role of DON as a virulence factor in wheat can be found in the number of studies which have observed that trichothecene deficient *Fusarium* isolates show a reduced ability to spread from the initial point of inoculation. Bai et al. (2002) demonstrated that whilst DON non-producing strains of *F. graminearum* are still able to infect wheat spikelets, they are restricted in their ability to colonize adjacent spikelets, as did Maier et al. (2006). This inability of the *tri5* knock-out isolate of *F. graminearum* to spread beyond the rachis node during the infection of wheat was demonstrated to be due to the deposition of cell wall components in response to infection, suggesting that the DON mycotoxin has a role in preventing this form of defence response (Jansen et al. 2005). Subsequent studies using green fluorescence protein (GFP) tagged to the *Tri5* gene promoter have further determined that the trichothecene pathway is induced during colonisation of the rachis node (Ilgen et al. 2009). This evidence, combined with the results of the trichothecene mutant studies suggests that the production of DON by

Fusarium species contributes towards not only the aggressiveness of the fungus, but also the ability to colonise plant host tissue in wheat. At present, few studies have investigated the effect of NIV non-producing *Fusarium* strains during host colonisation and NIV has not been demonstrated to be virulence factor in wheat (Ilgen et al. 2008).

Contrastingly, DON does not appear to be a virulence factor in barley. Jansen et al. (2005) observed no differential in the ability of *tri5* disrupted and wild-type *F. graminearum* isolates to spread from infected to non-infected spikelets, with both isolates being inhibited at the rachis nodes. Maier et al. (2006) also identified that there were no significant differences between the visual symptoms caused by *F. graminearum* wild-type isolates or those caused by *tri5* disrupted isolates after spikelet inoculation in both the susceptible Pasadena cultivar and the moderately resistant Chevron. However, whilst Boddu et al. (2007) again observed the inability of both wild-type and *tri5* to spread within infected barley spikes, they determined that trichothecene producing isolates produced more severe FHB symptoms and greater biomass accumulation than the *tri5* mutant strain. The results of such studies suggest that whilst DON may play a role in the aggressiveness of FHB disease, this effect is highly influenced by the host and that the role of DON in the colonisation of barley requires further investigation to be fully understood.

1.6 Molecular methods for identifying the presence of Fusarium species

Whilst visual assessment is useful in detecting the presence of FHB infection, it is important to identify and quantify the exact species causing disease to gain a more complete understanding of the interaction between pathogen and host. Several *Fusarium* species show morphological similarities during growth in axenic culture, so the development of molecular methods has been crucial for more precise identification. Polymerase chain reactions (PCR) have been widely utilised to detect the presence of specific *Fusarium* species and to also quantify the amount of *Fusarium* DNA within a sample. Species specific PCR assays have been designed to ascertain the presence of *F. graminearum* and *F. culmorum* (Nicholson et al. 1998), *F. poae* (Nicholson et al. 1996), *F. subglutinans* and *F. verticillioides* (*F. moniliforme*) (Möller et al. 1999) and *M. nivale* and *M. majus* (Nicholson et al. 1996). Importantly, the

results from competitive PCR employed to quantify *Fusarium* isolates within a sample have been demonstrated to correlate with the results from traditional visual scoring (Nicholson et al. 1998). The presence of *Fusarium* pathogens can also be investigated by the use of PCR primers designed to amplify regions of genes within mycotoxin biosynthetic pathways. Many of these PCR based assays have focused on identifying trichothecene producing *Fusarium* species, particularly those producing Type B trichothecenes, due to the importance of controlling the levels of these mycotoxins in grain products. Characterisation of *Fusarium* species according to their specific chemotypes, such as NIV or DON producing isolates, has been demonstrated in *F. graminearum*, *F. culmorum* and *F. cerealis* (Nicholson et al. 2004). Multiplex quantitative PCR (qPCR) has been developed to successfully identify trichothecene and fumonisin producing *Fusarium* species within maize samples (Preiser et al. 2015). Sarlin et al. (2006) determined a correlation between DON content analysed by gas chromatography-mass spectrometry (GC-MS) and *Fusarium* DNA levels, by using real-time PCR to quantify trichothecene producing species such as *F. graminearum*, *F. culmorum* and *F. sporotrichioides* found in barley grain and malt. Further studies to quantify *F. graminearum* biomass in wheat kernels using real-time PCR, identified that *Fusarium* biomass levels correlate with both *Fusarium* DNA levels and DON quantity, but not disease severity (Horevaj et al. 2011). This again is similar to Hill et al. (2008) who used enzyme linked immunosorbent assays (ELISA) to detect DON levels in barley, and found that whilst the ELISA assay was a quick practical method for indicating the presence of *Fusarium* DON antigens within grain samples, the FHB visual symptoms did not correlate with the DON levels found to be present. Such studies illustrate the importance of quantifying fungal DNA and mycotoxin content within a sample, due to the inconsistencies between the severity of visual symptoms and fungal colonisation and mycotoxin levels.

The identification of *Fusarium* contaminated samples can also be determined by other diagnostic methods. Loop-mediated isothermal amplification (LAMP), a single tube assay which does not require the use of a thermal cycler, has been developed to detect fragments of both the *Tri5* and *Tri6* trichothecene synthesis genes enabling the detection of *F. graminearum* and *F. culmorum* (Denschlag et al. 2014). The detection of *Fusarium* metabolites within grain samples have also been developed using several analytical methods, with high performance liquid chromatography (HPLC) being used

to detect DON, fumonisin and ergosterol content (Plattner et al. 1999; Gang et al. 1998; Bakan et al. 2002) and GC-MS being utilised to detect DON in barley (Olsson et al. 2002; Sarlin et al. 2006) and the presence of several *Fusarium* species in wheat grains (Eifler et al. 2011). The development of biosensor methods such as real-time electrochemical profiling (REP) using electrode arrays have also been demonstrated to be comparable to conventional ELISA assays in detecting the presence of DON in wheat samples (Olcer et al. 2014).

1.7 Resistance derived from cultural practices

A number of cultural practices have been found to affect the incidence of FHB infection in the field. Reduced tillage systems have been found to significantly increase the severity of FHB disease (Dill-Macky and Jones, 2000), with FHB residues being present in up to 60% of the soil in no-till plots compared to only 9% in mouldboard ploughed soil. Wheat residues infected with *F. graminearum* present on the soil surface have been shown to decompose more slowly than those beneath the soil (Pereyra and Dill-Macky, 2004), with tillage systems therefore promoting the burial of these residues and prevention of conidial release. The process of crop rotation also has a significant effect on the incidence of FHB in the field, with crops following maize more prone to FHB infection (Osborne and Stein, 2007). Maize stubble has been identified as a major source of *Fusarium* inoculum, with *F. graminearum* being isolated from maize residues up to three years post-harvest (Pereyra and Dill-Macky, 2008). Marburger et al. (2015) determined that a maize/soybean (*Glycine max*)/wheat rotation system produced higher yields than a maize/wheat/soybean rotation in the presence of FHB, due to the differences in *Fusarium* species which infect soybean compared with major cereals creating a smaller reservoir of inoculum. Alternately, sugar beet (*Beta vulgaris*) has also been suggested as a candidate for crop rotation (Champeil et al. 2004). The developmental stage at which the fungus infects the plant host also contributes to the severity of FHB, with the highest DON content in grain correlating with infection during mid-anthesis (Del Ponte et al. 2007), especially if this coincides with prolonged rainfall (Lacey et al. 1999). Sowing of multiple cultivars on several dates throughout the growing season, therefore producing a variety of flowering stages, or using cultivars with short flowering times could possibly lead to

a reduction in FHB (Champeil et al. 2004) as the most susceptible growing stages are less likely to coincide with inoculum dispersal. However, multiple crop harvesting dates may be less favourable in agriculture. Siou et al. (2014) also determined that infection of wheat spikes up to 28 days post anthesis with *F. graminearum*, *F. culmorum* and *F. poae s*till produced significant levels of FHB and mycotoxin accumulation, suggesting that in the presence of favourable weather conditions this process may be ineffective.

1.7.1 Chemical control measures

The use of fungicides has also been advised as a method for reducing FHB severity. However the outcomes of such treatments are largely dependent on the environmental conditions, the fungicide selected and the *Fusarium* species present. Triazoles, which are sterol demethylation inhibitors (DMIs), inhibit the production of the C-14 sterol which is a known precursor of ergosterol and have been determined to be most effective in the control of FHB incidence (Yin et al. 2009). Combination treatments of metconazole, tebuconazole and prothioconazole have been demonstrated to produce the greatest reduction in FHB severity and DON accumulation in wheat compared to other triazoles such as propiconazole (Paul et al. 2010). However the application of some triazoles, such as epoxiconazole, or combinations of azoles and strobilurin fungicides, such as azoxystrobin, have been reported to result in enhanced DON content of wheat grain when compared to control samples (Mennitti et al. 2003; Blandino et al. 2006), suggesting not all azole fungicides are suitable for use against FHB. Sub-lethal levels of prothioconazole have been shown to increase DON production; however this is thought to be due to such treatments causing oxidative stress responses which in turn stimulate trichothecene production (Audenaert et al. 2010). Tebuconazole treatment, whilst effective against *F. culmorum* and *F. avenaceum* isolates, has little effect on *M. nivale* (Simpson et al. 2001), suggesting one specific fungicide is not appropriate to provide sufficient resistance against the group of *Fusarium* and *Microdochium* pathogens present within the FHB disease complex. Studies with *F. graminearum* and *F. culmorum* have identified azole adapted isolates within a laboratory setting, with some isolates producing larger amounts of the nivalenol mycotoxin than non-adapted strains (Becher et al. 2010; Serfling and

Odon, 2014). The timing of fungicide application is also important when aiming to reduce FHB incidence. Thiophanate-methyl treatment at the optimal growth stage of anthesis reduces both FHB severity and DON accumulation in both wheat and barley, whilst application up to 20 days post anthesis limits the accumulation of mycotoxins but has little effect on the reduction of FHB incidence (Yoshida et al. 2008, 2012). Environmental conditions also affect the action of azole fungicides, as rainfall at the time of fungicide application or during anthesis reduces the efficacy of tebuconazole, prothioconazole and metconazole (Andersen et al. 2014; D'Angelo et al. 2014). Yield improvements gained from fungicide application to control FHB have been proven to be inconsistent. Marburger et al. (2015) saw an average yield increase of 3.9% in tebuconazole and prothioconazole treated wheat in only two out of three trial years, meaning that fungicides alone cannot be reliably used to prevent FHB associated yield loss. The integration of fungicide application with other cultural practices has been proposed as a more reliable method for controlling FHB incidence. For example, the combination of a moderately resistant cultivar and the application of triazole fungicides has been demonstrated to be more effective at reducing FHB incidence and DON accumulation than fungicide application or cultivar genetic resistance alone (Willyerd et al. 2012; Salgado et al. 2014). The inconsistent results produced by fungicides, combined with the high cost of applying such treatments repeatedly with the risk of generating fungicide insensitive *Fusarium* isolates, therefore suggest they are not effective long term solutions to preventing FHB infection and that sources of genetic resistance to FHB must also be identified.

1.8 Host resistance to FHB

As both cultural and chemical control of FHB may be less reliable, the use of genetic mechanisms to minimise the incidence and severity of the disease is favourable. Several types of resistance to FHB in cereal crops have been postulated, although not all described mechanisms have been identified in plant hosts. Resistance to the initial penetration of the host tissue by *Fusarium* fungi is determined to be Type 1 resistance (Schroeder and Christensen, 1963), whilst inhibition of fungal spread from infected to non-infected spikelets comprises Type 2 resistance. Type 2 resistance is primarily important against DON producing isolates of *F. graminearum* and *F. culmorum*, as

other species are not known to spread within the ear (Boenisch and Schäfer, 2011). In barley, *Fusarium* colonisation has been demonstrated to be mostly inhibited from spreading between rachis nodes, restricting the fungus to the original infected spikelet (Jansen et al. 2005). Therefore barley is considered to possess a form of Type 2 resistance. Mesterhazy, (1995) also described three other forms of possible resistance: Type 3, resistance to the infection or damage of kernels, Type 4, resistance to the effect on yield and Type 5, resistance to the accumulation of *Fusarium* mycotoxins such as DON. Whilst resistance to kernel damage and toxin accumulation are advantageous traits for a cereal cultivar to possess, the resistance to initial infection (Type 1) is the primary focus of investigation due to the many practical applications derived from generating resistant cereal crops.

1.9 Resistance to FHB

1.9.1 Germplasm derived resistance

Unlike other crop diseases such as rusts, where durable resistance has been established for wheat leaf rust (*Puccinia triticina)* and stripe rust (*P. striiformis* f. sp. *tritici)* by the introduction of the *Lr34* gene (Risk et al. 2013), identifying genes for stable and reliable resistance to FHB has proven more difficult. The considerable environmental influence on disease incidence makes replication of field studies more complex and numerous studies have identified that resistance to FHB is polygenic with only moderate heritability. In hexaploid wheat germplasm, the Chinese cultivar Sumai 3 is the most widely used source of genetic resistance to FHB (Rudd et al. 2001), due to the consistent and well characterised resistance gained from breeding with this cultivar. A major quantitative trait locus (QTL), titled *Fhb1*, is associated with Type 2 FHB resistance in wheat and has been consistently identified from Sumai 3 mapping populations. *Fhb1* has been fine mapped to the distal segment of 3BS (Cuthbert et al. 2006; Liu et al. 2008) and potential genes within this QTL region are being cloned (Zhuang et al. 2013). Ning 7840, Wangshuibai and Frontana which are derived from the Sumai 3 germplasm, have also been used as additional sources of FHB resistance (Cuthbert et al. 2006).

In barley however, no single cultivar has been identified which produces stable resistance at an appropriate level to effectively combat disease. A number of varieties have been identified which display moderate resistance to FHB such as Chevron a six-row malting variety, the two-row Chinese varieties CIho 4196, Zhedar 1 and Zhedar 2 and the Japanese cultivar Frederickson (Bai and Shaner, 2004), which have all been employed within breeding programs to reduce FHB severity. The recurrent screening of elite germplasm lines, diverse landraces and wild accessions is being undertaken with the aim of identifying potential new sources of resistance for barley breeding (Massman et al. 2011; Linkmeyer et al. 2013; Mamo and Steffenson, 2015), and the advent of new technologies such as genome wide association studies (GWAS) should also enable the increased detection of QTL associated with disease and further exploitation of genetic sources of FHB resistance.

1.9.2 Quantitative trait loci in barley associated with resistance to FHB

QTL associated with FHB and DON accumulation have been identified throughout the barley genome using different bi-parental mapping populations in various environments. Chromosome 2H has been consistently identified as the genomic location of several FHB QTL (Hori et al. 2004; Horsley et al. 2006; Nduulu et al. 2007; Massman et al. 2011). However, such FHB QTL do not always co-locate with QTL associated with reduced DON accumulation (Ma et al. 2001). A number of the FHB or DON QTL previously identified also co-locate with agronomic traits. For example, plant height has been consistently associated with FHB incidence (Zhu et al. 1999; Ma et al. 2001; Choo et al. 2004; Horsley et al. 2006), with taller cultivars appearing to be more resistant. Row type (Mesfin et al. 2003; Sato et al. 2008), flowering time (Mesfin et al. 2003; Horsley et al. 2006; Nduulu et al. 2007) and spike morphology (Hori et al. 2005; Yoshida et al. 2005) are also frequently implicated in FHB resistance. It is therefore important to identify whether the association between QTL for FHB resistance and agronomic traits, such as height, is due to linkage or pleiotropy to avoid the potential trade-off between disease resistance and favourable agronomic traits.

1.9.3 Phytohormone signalling associated resistance

Plant phytohormone pathways regulate numerous aspects of plant development, including growth, organ formation, seed production and senescence. The effects of plant hormones have also been implicated in resistance to *Fusarium* diseases. Exogenous application of JA prior to inoculation with *F. graminearum* in the susceptible wheat landrace Y1193-6 resulted in the upregulation of defence genes and an increase in resistance to a level comparable with that of Sumai 3 (Li and Yen, 2008). Salicylic acid (SA) also appears to decrease susceptibility to FHB, with wheat spikelets which accumulate higher levels of SA following soil drench treatment demonstrating greater resistance to FHB infection and DON accumulation (Makandar et al. 2012). The hormone ethylene (ET) has also been associated with disease resistance. Attenuation of the *Ethylene insensitive 2* (*EIN2*) gene in wheat gives reduced fungal colonisation following *F. graminearum* inoculation, compared with wild-type lines which show more severe bleaching symptoms (Chen et al. 2009). The same study also identified that *Arabidopsis thaliana* ET overproducing lines were also more susceptible to *F. graminearum* infection, suggesting that the ET pathway is also utilised by *Fusarium* fungi during infection of dicotyledonous plant hosts. Evidence from studies such as these provides useful insights into pathways which may be utilised to minimise the incidence of FHB.

1.10 Plant breeding associated trade-offs

The aim of plant breeding is to combine multiple favourable traits, such as disease resistance, reduced height or increased yield, into a single cultivar. However, recent studies have identified that introducing a single desirable trait into breeding programs may result in potential trade-offs which are less favourable. Many European wheat cultivars possess either the *Reduced height* (*Rht*) *Rht-D1b* or *Rht-B1b* alleles which confer reduced sensitivity to the plant growth hormone gibberellic acid (GA) and result in an advantageous semi-dwarf phenotype. However, lines carrying *Rht-D1b* have been demonstrated to show reduced Type 1 resistance to FHB compared to wild-type (*rht-tall*) cultivars (Srinivasachary et al. 2008). Studies with *Rht-B1b* show that the presence of this allele also reduces Type 1 resistance but has a significant positive effect on Type 2 resistance (Srinivasachary et al. 2009). This implicates a trade-off

between reduced plant height, conferred by altered phytohormone signalling, and FHB resistance. Additional studies looking at the effects of the *Rht* alleles on resistance to other fungal diseases determined a more general trade-off between pathogens of differing lifestyles. *Rht* dwarf lines show increased susceptibility to biotrophic fungi, yet display increased resistance to necrotrophs when compared to *rht-tall* lines (Saville et al. 2012), indicating the importance of determining the potential for trade-off when introducing specific alleles into cultivars.

In spring barley broad spectrum disease resistance to powdery mildew, caused by the obligate biotroph *Blumeria graminis* f. sp. *hordei*, has been successfully achieved for over 30 years by the introduction of recessive alleles of the *Mildew resistance locus o* (*Mlo*) gene (Acevedo-Garcia et al. 2014). However, it has been demonstrated that the presence of recessive *mlo* alleles alters resistance to FHB. Jansen et al. (2005) investigated the infection pattern of *F. graminearum* in the caryopses of the mildew resistant cultivars Ingrid-*mlo-5* and Pallas-*mlo-5*, and their respective near-isogenic parental lines (NILs). Colonisation by *F. graminearum* was more rapid in the two *mlo-5* genotypes; with macroconidia being present on the surface of the caryopses at 72hpi compared to 96hpi in the parental NILs (Jansen et al. 2005). The endosperm and aleurone cells within the caryopses of the *mlo-5* cultivars also displayed greater disintegration than in the parental NILs, demonstrating their increased susceptibility to *F. graminearum* infection. The presence of *mlo* alleles has also been observed to affect resistance to other fungal pathogens. Jarosch et al. (1999) demonstrated that the recessive *mlo-1*, *mlo-3* and *mlo-5* alleles confer hypersusceptibility to the hemibiotroph *Magnaporthe grisea*, with a greater degree of sporulation and enlarged lesion development observed in cultivars possessing these alleles. Investigation into the recent emergence of the hemibiotrophic barley pathogen *Ramularia collo-cygni*, which causes Ramularia leaf spot (RLS), also identified that cultivars possessing the *mlo-11* allele show an increased susceptibility to *R. collo-cygni* (McGrann et al. 2014). Further analysis of this association using doubled-haploid mapping populations determined that a QTL for RLS susceptibility and the *mlo-11* resistance allele co-localise on 4H.

Trade-offs may also be associated with quality traits. The translocation between the 1BL chromosome segment in bread wheat (*T. aestivum*) and 1RS in rye (*Secale cereale*) was originally created to introduce the rye resistance genes to leaf rust, stem

rust and powdery mildew (*Lr26,Yr9, Lr26, Pm8*) into commercial wheat (Dhaliwal et al. 1987). This translocation has also been observed to be associated with increased resistance to FHB. A study by Ittu et al. (2000) identified that increased resistance to FHB is associated with the presence of the *GliR1* allele, which resides within the 1BL/1RS translocation region. QTL mapping of the Romanian wheat variety Fundulea 201R, which also carries the 1RS segment, resulted in the detection of a major QTL associated with Type 2 resistance on chromosome 1B within the 1BL/1RS region (Shen et al. 2003). Whilst this may appear to be a potentially useful source of Type 2 resistance, quality studies have identified that the presence of the 1BL/1RS translocation results in poor performance during the commercial bread making process. Lines possessing the translocation show a reduction in glutenin content, causing a decline in gluten strength (Lee et al. 1995) and also have lower kernel hardness, affecting the milling quality of such lines (Zhao et al. 2012). Dough 'stickiness' and reduced tolerance to mixing processes are also associated with the 1BL/1RS translocation (Martín et al. 2001), which is thought to be due to the presence of genes encoding secalins, which are gluten associated storage proteins, in the 1RS segment (Jiang et al. 2010). This suggests that selecting for FHB resistance within the 1BL/1RS region may give the potential for trade-off.

Results from the above studies suggest that it is vital to investigate the potential for trade-off between disease resistance and agronomically and economically important quality traits. Determining whether genes for resistance affect other traits by either pleiotropy or linkage will determine whether such resistance is useful for breeding purposes. Whilst specific traits may still be bred for due to their agronomic importance regardless of associated undesirable effects, such as the *Rht* semi-dwarfing alleles, the prior knowledge of potential trade-off will allow more informed breeding decisions to be made.

1.11 Overall objectives

There is little genetic resistance to FHB in barley which performs consistently across environments and does not cause a potential trade-off with other traits. Therefore, identifying sources of resistance which do not have pleiotropic effects would be

advantageous when aiming to breed for FHB resistance and lower mycotoxin content whilst retaining agronomically significant quality traits.

The specific objectives for this research are:

i) To investigate the effect of altered phytohormone signalling through the brassinosteroid pathway on resistance to FHB and a range of other economically important cereal diseases. Barley *bri1* cultivars have a mutation in the brassinosteroid receptor (*BRI1*) gene and possess a semi-dwarf phenotype, therefore the prospect of trade-off between growth and disease resistance within these lines will be determined.

ii) To identify whether the barley cultivars Chevallier or Armelle may be used as a possible source of resistance to FHB. Chevallier is a tall English landrace and Armelle is a tall French cultivar, yet both have been demonstrated to show significant FHB resistance. The potential for pleiotropy between FHB resistance, agronomic traits such as height and flowering time, and quality traits within these two cultivars will be investigated.

Chapter 2. Evaluation of the role of BRI1 in disease resistance and potential trade-offs

Many of the results in this chapter have been previously published in:

Goddard R, Peraldi A, Ridout C, Nicholson P. 2014. Enhanced disease resistance caused by *BRI1* mutation is conserved between *Brachypodium distachyon* and barley (*Hordeum vulgare*). *Molecular Plant-Microbe Interactions* **27**, 1095–1106.

2.1 Introduction

Plant hormones play a critical role in regulating development including growth, senescence and response to both abiotic and biotic stresses. Salicylic acid (SA), jasmonic acid (JA) and ethylene (ET) are three hormones considered to be at the core of plant regulatory mechanisms involved in response to pathogen infection and they are known to act in a largely antagonistic manner. Resistance to biotrophs is predominantly dependent on signalling through the SA pathway. Defence responses activated by SA signalling include the hypersensitive response (HR), which acts to deprive biotrophic pathogens of living tissue by causing the death of infected host cells. In contrast, JA and ET signalling often work in concert and are considered to be more important in resistance towards necrotrophic pathogens that feed off dead plant tissue and insects which cause host cell death (Glazebrook, 2005; Kliebenstein and Rowe, 2008). However, recent evidence suggests a more complex picture where several growth-promoting phytohormones can greatly modulate the outcome of pathogen infection (Robert-Seilaniantz et al. 2011). Further hormones such as cytokinins (CKs), auxin and abscisic acid (ABA) are also known to regulate both physiological and stress-related responses and it has become increasingly clear that the integration of phytohormone signals is much more complex than previously thought, particularly with respect to regulating the trade-off between growth and immunity.

Gibberellic acid (GA) is a hormone which has been shown to play a role in both development, such as growth and seed germination, and also immunity. GA-responsive growth is modulated by DELLA proteins which act as growth repressors (Peng at al. 1999). In the presence of GA, DELLAs are ubiquitinated by the SCF

complex (Alvey and Harberd, 2005), promoting recognition of DELLA proteins by the 26S proteasome protein complex and targeting them for degradation and so relieving growth inhibition (Hussain and Peng, 2003). The *Reduced height* (*Rht*) gene was a major dwarfing gene used during the Green Revolution, and the semi-dominant gain-of-function alleles *Rht-B1b* and *Rht-D1b* encode truncated growth repressor DELLA proteins which are hyposensitive to GA (Hedden, 2003). In the presence of GA these mutant forms of DELLA are constitutively active, causing inhibition of stem elongation and resulting in a semi-dwarf phenotype. Under higher nitrogen inputs, semi-dwarf *Rht* lines show an increased yield due to a greater biomass accumulation in the grain, and are also more resistant to lodging as the shorter stem is more able to support this increased biomass.

Whilst the presence of the *Rht* alleles produces a favourable semi-dwarf phenotype, it has been demonstrated that these alleles also confer a trade-off between height and altered disease resistance. *Arabidopsis thaliana* DELLA proteins have been implicated in plant immunity, with mutations in GAI (one of the five *At*DELLA proteins) giving an increased resistance to *Alternaria brassicicola*, a necrotrophic fungus which causes cell apoptosis in plants, but also an increased susceptibility to hemibiotrophic fungi (Navarro et al. 2008). The presence of the *Rht-B1b* allele in wheat has also been significantly associated with susceptibility to Fusarium head blight (FHB), with semi-dwarf varieties showing compromised initial resistance (Type 1) to FHB compared to tall varieties with the wild-type allele (Srinivasachary et al. 2009). Investigation into the effects of *Rht* and *Slender 1* (*Sln1*), the barley (*Hordeum vulgare*) *Rht* orthologue, to a range of fungal pathogens has also determined that dwarf (gain-of-function) DELLA mutants have greater resistance to necrotrophic pathogens but an increased susceptibility to biotrophic pathogens. *Rht* and *Sln1* alleles have been demonstrated to confer an increased susceptibility to the brief initial biotrophic stage of infection displayed by hemibiotrophic fungi such as *F. graminearum*, but an increased resistance to the necrotrophic colonisation phase that follows (Saville et al. 2012). A higher susceptibility to biotrophs, for example *Blumeria graminis*, was also observed in semi-dwarf lines suggesting that GA signalling has a pleiotropic effect on plant growth and disease resistance (Saville et al. 2012). Recent studies have implicated DELLA proteins as having a function for pathway control and signal integration, particularly with respect to JA signalling which mediates resistance to necrotrophic

pathogens. JA ZIM-domain (JAZ) proteins act as repressors of JA signalling (Song et al. 2014) and bind to MYC2, the activator of JA transcription, inhibiting its activity (Kazan and Manners, 2013). In the presence of GA, DELLA proteins are targeted for degradation and growth repression is released (Alvey and Harberd, 2005). Under less favourable conditions, in the absence of GA, DELLA proteins are not degraded and have been demonstrated to compete with MYC2 to bind to JAZ proteins (Wild et al. 2012). The transcription factor MYC2 is then free to activate JA responsive genes, releasing JA repression and therefore providing enhanced resistance to necrotrophic pathogens (De Bruyne et al. 2014). As the JA and SA pathways are generally thought to act in an antagonistic manner, increased JA signalling is assumed to cause the suppression of SA-mediated defence responses, resulting in greater susceptibility to biotrophs. This hypothesis, based on cross-talk between several phytohormone pathways, provides a molecular basis for resistance trade-offs between pathogens of differing lifestyles. The implications of these studies suggest that alternative semi-dwarfing alleles, which act through alteration of signalling in phytohormone pathways other than GA, could be investigated to determine whether a similar trade-off between growth and immunity is evident.

Brassinosteroids (BRs) are one such class of plant growth hormones. BRs regulate a wide range of developmental processes, such as cell elongation, root growth, and senescence, yet have also been implicated as having an important role in regulating plant defence (Bari and Jones, 2009). BR is perceived by the extracellular domain of the receptor Brassinosteroid-insensitive 1 (BRI1), an LRR (leucine-rich repeat) receptor-like kinase (Nam and Li, 2002). Once BR is bound, BRI1 then heterodimerizes with BRI1-associated receptor kinase 1 (BAK1), the co-receptor of BRI1, removing the inhibitory protein BRI1-kinase inhibitor 1 (BKI1) from the plasma membrane (Wang and Chory, 2006). BRI1 and BAK1 undergo transphosphorylation and phosphorylated BKI1 is able to promote BR signalling (Zhu et al. 2013). In *Arabidopsis*, BR signalling is known to act antagonistically with pathogen-associated molecular pattern (PAMP)-triggered immunity (PTI), (Albrecht et al. 2012; Belkhadir et al. 2012). Lozano-Durán et al. (2013) showed that BR-mediated suppression of immune signalling requires expression of Brassinazole-resistant 1 (BZR1), one of two major BR-activated transcription factors in *Arabidopsis*, which induces expression of several WRKY transcription factors that

negatively control early immune response. An antagonistic relationship between BR and PTI signalling has also been demonstrated in rice where *Pythium graminicola*, a pathogenic oomycete of roots, exploits endogenous BRs as virulence factors for host colonization (De Vleesschauwer et al. 2012). The authors showed that the immunosuppressive effect of BRs is, at least partially, due to negative cross-talk with both the SA and GA pathways. In addition, Nahar et al. (2013) showed that BRs can suppress rice defence mechanisms against the root-knot nematode *Meloidogyne graminicola*, at least partially through negative cross-talk with the JA signalling pathway. The results of such studies demonstrate a function for BR in plant immunity and signal integration, though further work is needed to determine the extent of the role of BR signalling in both pathogen defence and crosstalk between phytohormone pathways.

Mutation of *BRI1* also results in dwarfism in both dicot and monocot species (Clouse et al. 1996; Yamamuro et al. 2000; Chono et al. 2003; Thole et al. 2012). Japanese semi-dwarf '*uzu'* barley (*bri1*) varieties possess a spontaneous single nucleotide substitution (A > G at position 2612) in a conserved region of the kinase domain of the BRI1 gene, as seen in Figure 2.1, which is thought to alter kinase activity and therefore signal transduction, ultimately rendering the plant insensitive to exogenously applied BR (Chono et al. 2003). The effect of *BRI1* mutation on disease resistance in barley is unknown, but the semi-dwarf *uzu* lines provide an ideal background in which to investigate whether altered signalling through the BR pathway has a similar pleiotropic effect on growth and disease resistance as demonstrated by GA.

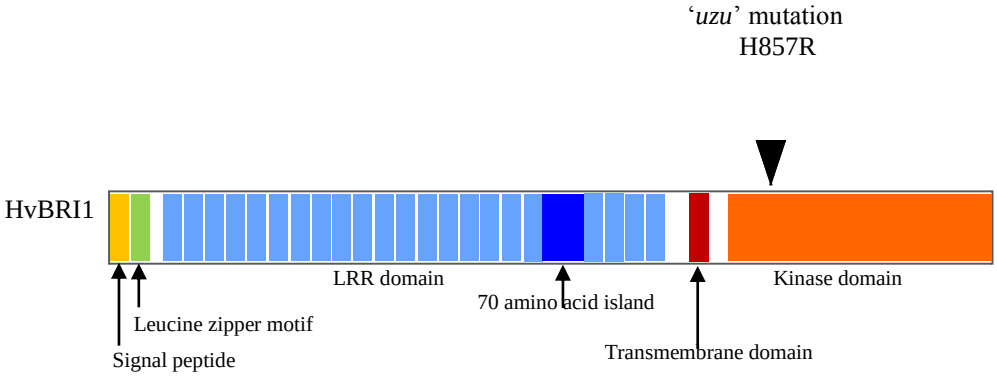

Figure 2.1. Schematic representation of the missense mutation of the *HvBRI1* protein in '*uzu*' barley. (Taken from Goddard et al. 2014).

The availability of the semi-dwarf *bri1* lines permit the investigation of the effect of BR mutation to a range of economically important pathogens exhibiting different infection strategies, trophic lifestyles and tissue compatibility (Table 2.1). *Magnaporthe oryzae*, which causes rice blast, is a hemibiotrophic pathogen that exhibits a brief biotrophic phase characterised by the development of haustoria within host cells (Parker et al. 2008), which can also infect other cereals including wheat and barley (Jarosch et al. 2003; Urashima et al. 2004). Ramularia leaf spot (RLS), a newly important disease of barley, is caused by *Ramularia collo-cygni*, a hemibiotrophic fungus with a very prolonged endophytic phase of asymptomatic, intercellular colonisation (Stabentheiner et al. 2009). *Oculimacula* species *O. yallundae* and *O. acuformis* are the causal pathogens of eyespot of wheat, barley and rye. While *O. acuformis* is considered to be entirely necrotrophic, *O. yallundae* exhibits a brief initial asymptomatic phase of infection before colonising in a necrotrophic manner (Blein et al. 2009). Several *Fusarium* species, including *F. culmorum*, can infect the roots, stem bases and heads of cereals, with the mode of infection dependent on tissue. FHB is an economically devastating disease due to the production of mycotoxins, such as deoxynivalenol (DON), by the fungus that contaminate the grain (Bottalico and Perrone, 2002). *F. culmorum* can also infect vegetative tissues i.e. roots and stem bases causing root rot (FRR) and crown rot (FCR) respectively (Miedaner, 1997). Take-all is a serious disease of wheat, barley and triticale, caused by the necrotrophic pathogen

Gaeumannomyces graminis var. *tritici* (*G. graminis*). In contrast, *Blumeria graminis* is an obligate biotrophic pathogen that causes powdery mildew (Both et al. 2005).

Table 2.1. Tissue compatibility and trophic lifestyle of the major cereal pathogen species used. (Taken from Goddard et al. 2014).

Pathogen	**Tissue**	**Trophic lifestyle**	**Reference**
Blumeria graminis f.sp. *hordei*	Foliar	Biotroph	Both et al. (2005)
Fusarium culmorum	Floral	Hemibiotroph (short biotrophic stage)	Brown et al. (2010)
	Root	Necrotroph	Beccari et al. (2011)
	Stem base	Necrotroph	Beccari et al. (2011); Chen et al. (2013)
Gaeumannomyces graminis var. *tritici*	Root	Necrotroph	Freeman and Ward. (2004)
Magnaporthe oryzae	Foliar	Hemibiotroph (short biotrophic stage)	Parker et al. (2008)
Ramularia collo-cygni	Foliar	Hemibiotroph (long asymptomatic stage)	Stabentheiner et al. (2009)
Oculimacula acuformis	Stem base	Necrotroph	Blein et al. (2009)
Oculimacula yallundae	Stem base	Hemibiotroph (short biotrophic stage)	Blein et al. (2009)

Whilst the role of BR in plant disease response has become increasingly apparent, little is known about the effect of disruption of BR perception mutation in barley. The following research investigated the effect of the semi-dwarfing *BRI1* mutation on disease resistance to a range of cereal fungal pathogens, exhibiting a range of trophic lifestyles, with the aim of determining whether there was a trade-off between BR-mediated growth and disease resistance.

2.2 Materials and methods

2.2.1 Plant material and growth conditions

Near-isogenic line pairs (NILs) of barley two-row cultivar Bowman (*BRI1*) and Bowman-Uzu (*bri1*) (as characterised by Druka et al. 2011), and six-row Akashinriki (*BRI1*) and Akashinriki-Uzu (*bri1*) were obtained from the Barley and Wild Plant Resource Center, Okayama University, Japan. In all experiments except for take-all, seeds were pre-germinated in Petri dishes on damp filter paper for 48 h in the dark at 4^{o}C and then incubated at 24^{o}C for 24 h, before being transferred to F2 soil (Levington, Scotts Professional, UK).

2.2.2 Fungal inoculum

Magnaporthe oryzae (*M. oryzae*) wheat-adapted isolate BR32 (kindly provided by Dr G.R.D. McGrann, John Innes Centre (JIC), UK) was maintained at 24^{o}C as detailed by Tufan et al. (2009). Wheat-adapted T5 isolate of *Gaeumannomyces graminis* var. *tritici* (*G. graminis*) (kindly provided by Prof A. Osbourn, JIC) was cultured on potato dextrose agar (PDA) under 16 h/8 h light-dark cycle at 24 °C. *Ramularia collo-cygni* (*R. collo-cygni*) isolate Rcc09B4 was maintained and inoculum prepared as detailed by Peraldi et al. (2014). A mixture of *Oculimacula acuformis* and *O. yallundae* isolates (as described by Chapman et al. 2008) were maintained on V8 agar plates (9g bactoagar, 50 ml V8 vegetable juice in 450 ml deionized water) at 16^{o}C for 21 days prior to use as inoculum. DON-producing *Fusarium culmorum* (*F. culmorum*) isolate Fu42 from the culture collections at JIC was maintained and conidial inoculum prepared as detailed by Peraldi et al. (2011). For stem base infection tests, *F. culmorum*

Fu42 colonies were grown on V8 agar for 14 days at 20ºC. *Blumeria graminis* f.sp. *hordei* (*B. graminis*) isolates CC148 and DH14 from the culture collections at JIC were maintained on the barley line Golden Promise as described by Brown and Wolfe (1990).

2.2.3 Leaf unfurling standard assay

To confirm the altered BR responsiveness of the *uzu* lines and to determine the sensitivity of the lines to brassinosteroid the leaf unrolling protocol of Chono et al. (2003) was followed. Seeds of each line were grown in the dark for 7 days (17ºC/15ºC 16/8 h temperature regime) to cause leaf etiolation before two segments (top and bottom) of 1.5cm were cut from each leaf. Sections were floated in 2ml of appropriate concentrations (80nm, 800nm) of epibrassinolide (eBL) and incubated for 4 days in the dark. Photographs of each plate were taken on the final day of incubation and Image J was used to measure leaf unrolling. Experiments were repeated twice.

2.2.4 Seedling spray inoculations

Seeds were sown 10 per 5 x 5 cm pot and grown at 18/15ºC under a 16 h/8 h light-dark photoperiod. Seedlings were inoculated with *M. oryzae* isolate BR32 as described by Tufan et al. (2009), and incubated under a 16/8 h light-dark photoperiod at 24ºC/16ºC to induce fungal development. At 6dpi, disease symptoms were scored as the number of lesions on the first leaf (Jarosch et al. 2003). *M. oryzae* inoculations were repeated twice. *R. collo-cygni* inoculations with Rcc09B4 were performed as three independent experiments, as described by Makepeace et al. (2008). Symptoms were scored from 10 – 28dpi as a percentage of the first leaf showing Ramularia leaf spot (RLS) lesions. Scores were then calculated as a percentage of the maximum possible area under disease progress curve (% max AUDPC), assuming a value of 100% for every score date, to standardise scores across experiments.

2.2.5 Root and leaf inoculations

Inoculum was prepared by homogenising 14 day old *G. graminis* T5 culture plates with H_2O (2:1) and thoroughly mixing with autoclaved H_2O-saturated medium

vermiculite (William Sinclair Horticulture Ltd). Inoculum was added to 50ml Falcon tubes, with 5 seeds placed on top of the inoculum and 5 replicates per genotype. Seedlings were incubated at 18/15^{o}C under a 16 h/8 h light-dark photoperiod for 3 weeks and scored using a numerical system (0 – 10 scale incorporating symptoms in both roots and leaves, with 0 = no infection, 10 = whole seedling diseased). Three seedling inoculations with *G. graminis* were conducted. Detached leaf assays with *B. graminis* f. sp. *hordei* isolates (DH14 and CC148) were performed using the protocol of Boyd et al. (1994). Agar boxes were incubated at 18/12^{o}C under a 16 h/8 h light-dark photoperiod and symptoms were scored at 7 and 10dpi, using the 0 – 4 scale devised by Moseman et al. (1965), in three independent experiments.

2.2.6 Stem base inoculations

All plants for *F. culmorum* stem base infections were grown at 18/15^{o}C under a 16 h/8 h light-dark photoperiod. Seedlings for *F. culmorum* non-wound stem base infection were grown 5 seeds per 5 x 5cm pot, with 5 replicates per line. Seedlings were inoculated using the method of Simpson et al. (2000), using the following modifications. Inoculum was prepared by homogenising Fu42 culture plates with H_2O (2:1) and seedlings were inoculated with 2ml of homogenate. Seedlings were kept in the dark for 24 h after inoculation to induce fungal growth and symptoms were scored at 21dpi. *F. culmorum* wounded stem base assays followed the protocol of Knight and Sutherland (2013). Wounds were inoculated with 10µl of conidia ($1x10^7$ ml^{-1}) and incubated in the dark at 25^{o}C for 24 h. Seedlings were returned to normal growth conditions and scored at 21dpi. Non-wounded stem base assays were repeated three times and wounded assays were repeated twice.

For *Oculimacula* stem base infection, plants were grown and inoculated with either *O. acuformis* or *O. yallundae* using the method of Burt et al. (2010). Plants were incubated at 10^{o}C under a 16/8 h light-dark photoperiod and harvested 8 weeks post inoculation. Assays were repeated twice with *O. yallundae* isolates and once with *O. acuformis*. Disease symptoms for all stem base assays were assessed as the penetration of leaf sheaths by the pathogen, using the 0 – 10 scoring system devised by Scott (1971).

2.2.7 Field experiment inoculation

Seeds were sown in $1m^2$ plots in a randomised complete block design experiment, in the spring of 2012 and 2013 at JIC. Eight and five replicates per genotype were used in the 2012 and 2013 trials, respectively. Plants were spray inoculated from anthesis with an *F. culmorum* Fu42 conidial suspension of $1x10^5$ ml^{-1} spores ($0.5x10^5 ml^{-1}$ spores in 2013) and 0.05% Tween 20, with repeated spraying to ensure even inoculation. Disease was assessed visually as the percentage of disease per plot at 4 separate time points, beginning 2 weeks after the first inoculation. Data from both experimental years were combined for analysis.

2.2.8 Statistical analysis

All experiments were performed at least twice. All disease data scores were analysed using a generalized linear model (GLM) in the software package GenStat v16.0 (Lawes Agricultural Trust, Rothamsted Experimental Station, UK). ANOVA tables are displayed within the Appendix. Within the GLMs paired t-tests were used to assess differences in disease symptom severity for each of the *BRI1/bri1* pairs.

2.3 BRI1 results

2.3.1 BR Insensitivity of semi-dwarf bri1 uzu lines

In response to the control treatment (H_2O) neither NIL pair showed any significant difference in leaf unfurling between the *BRI1* tall and *bri1* semi-dwarf line with the leaf segments remaining tightly furled ($P = 0.097$ and $P = 0.122$ in Akashinriki and Bowman backgrounds, respectively). When treated with 80nm of eBL, both *BRI1* lines showed a significant increase in leaf unrolling ($P < 0.001$ in both backgrounds), whilst both the semi-dwarf *bri1* lines were insensitive to the treatment ($P = 0.181$ and $P = 0.154$ in Akashinriki and Bowman backgrounds, respectively). The wild-type *BRI1* lines again showed a further increase in leaf unrolling after 800nm eBL treatment ($P < 0.001$ in both backgrounds). After treatment with 800nm eBL, the semi-dwarf *bri1*

lines displayed a significant increase in unrolling compared to the control treatments ($P < 0.001$ in both backgrounds), indicating that the *bri1* lines are attenuated in their sensitivity to BR but that they remain responsive to high concentrations of exogenously applied BR.

2.3.2 Influence of BRI1 mutation on resistance to M. oryzae

The wheat-adapted isolate of *M. oryzae* BR32, which also infects barley, was used to investigate the impact of *BRI1* mutation on disease resistance to this hemibiotrophic pathogen. Following spray inoculation with BR32 conidia, large lesions developed rapidly on both Bowman and Akashinriki *BRI1* lines, with disease symptoms being more severe on the former. By 6dpi, large areas of chlorosis had also begun to develop around the *M. oryzae* infection lesions on both *BRI1* lines (Figure 2.2a). Both *bri1* semi-dwarf lines were more resistant to blast infection than their respective *BRI1* lines, with leaves of the *bri1* genotypes having significantly fewer and smaller necrosis-ringed lesions than those of *BRI1* ($P < 0.001$ and $P = 0.015$ in the Bowman and Akashinriki pairs, respectively, Appendix Table A.1) (Figure 2.2b).

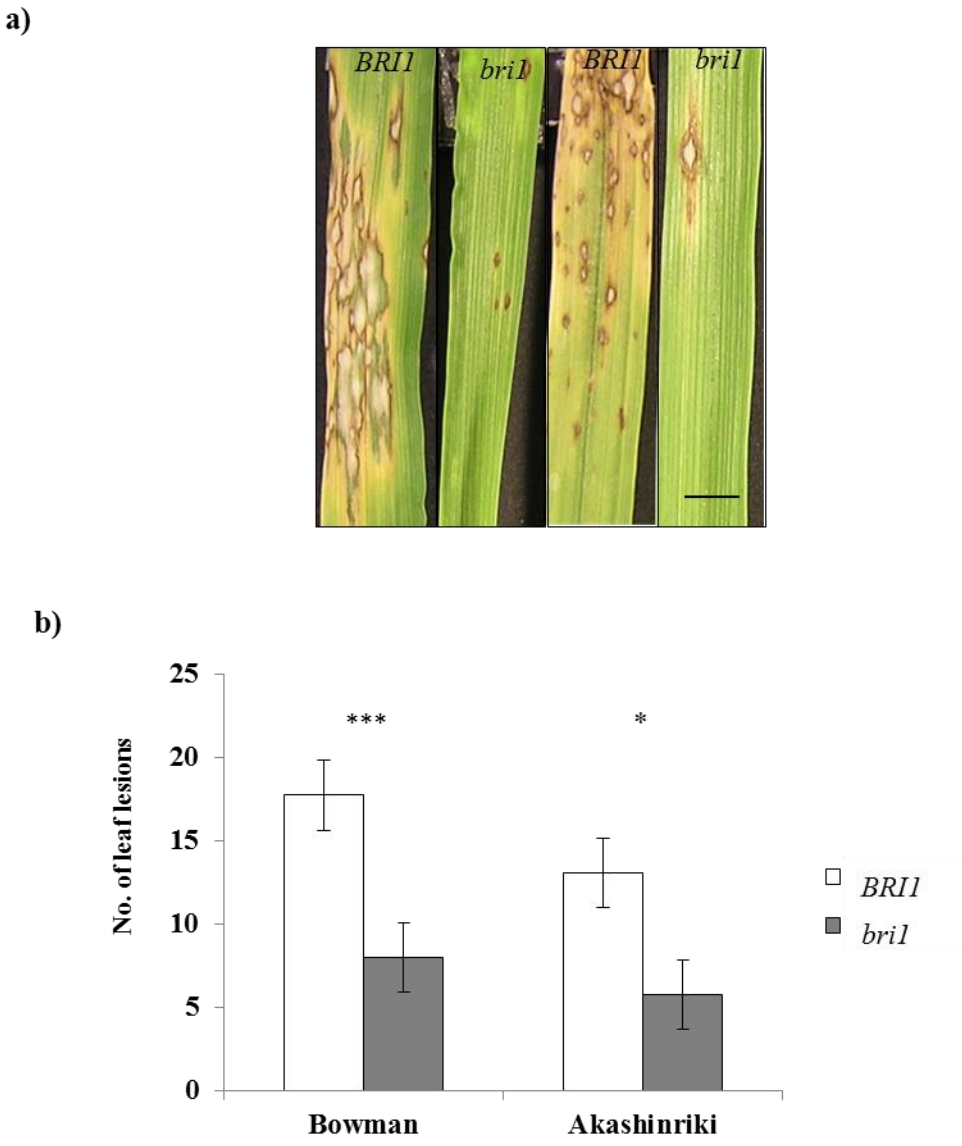

Figure 2.2. The effect of the *bri1* mutation on *Magnaporthe* infection. a) Leaf blast symptoms in Bowman (left pair) and Akashinriki backgrounds (right pair) at 6dpi. Scale bar = 1cm. b) The number of blast leaf lesions on seedlings inoculated with *M. oryzae* BR32 isolate (6dpi). Means ± s.e. were calculated from 2 independent experiments. *, *** Significant differences ($P < 0.05$ and $P < 0.001$ respectively) from the wild-type NILs.

2.3.3 Influence of BRI1 mutation on resistance to G. graminis var. tritici

In response to inoculation with *G. graminis*, the necrotrophic causal agent of take-all disease, Bowman and Akashinriki *BRI1* wild-type seedlings were more susceptible than *bri1* seedlings and displayed blackened roots and stems (Figure 2.3a). In the *BRI1* lines, a greater proportion of the roots per seedling were continuously infected (no patches of uninfected tissue), with characteristic black discolouration progressing up the stems and causing curling and yellowing of the leaves. In *bri1* lines the extent of root infection by the fungus was much less severe, with roots only showing patches of light brown discolouration and with fewer seedlings displaying foliar disease symptoms. The *bri1* NILs displayed a significantly lower disease score ($P < 0.001$, Appendix Table A.2) than the *BRI1* NILs (Figure 2.3b).

2.3.4 Influence of BRI1 mutation on resistance to Oculimacula spp.

The disease symptoms of *Oculimacula* infection were more apparent in the *BRI1* tall NILs, with the semi-dwarf *bri1* NILs displaying less severe browning of the stem base (Figure 2.4a). In response to stem base infection with the hemibiotrophic fungus *O. yallundae*, the semi-dwarf *bri1* lines were significantly more resistant to infection than *BRI1* lines ($P < 0.001$), with the fungus penetrating through fewer successive leaf sheaths (Figure 2.4b). To determine the effect of *BRI1* mutation to a truly necrotrophic species of *Oculimacula*, lines were inoculated with *O. acuformis* isolates in a single experiment. Similar results were obtained to those for *O. yallundae* infection as the *bri1* lines were more resistant than the Bowman and Akashinriki *BRI1* lines but the differential was less pronounced ($P = 0.004$ and 0.002 in Bowman and Akashinriki pairs, respectively, Appendix Table A.3).

a)

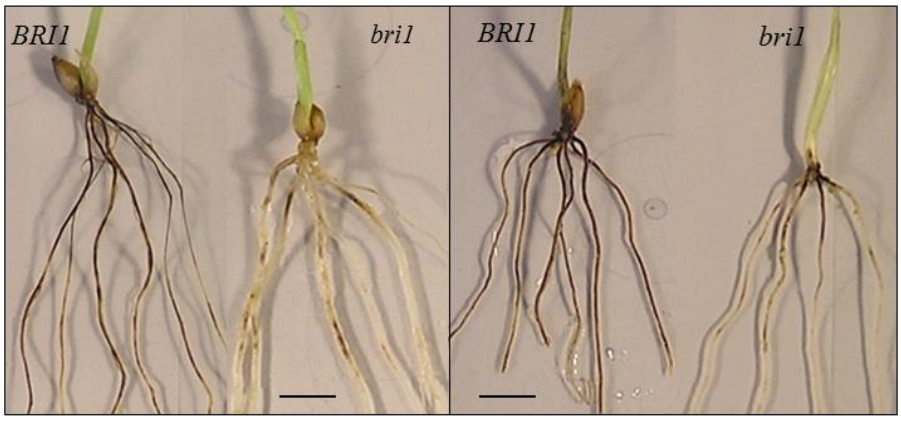

b)

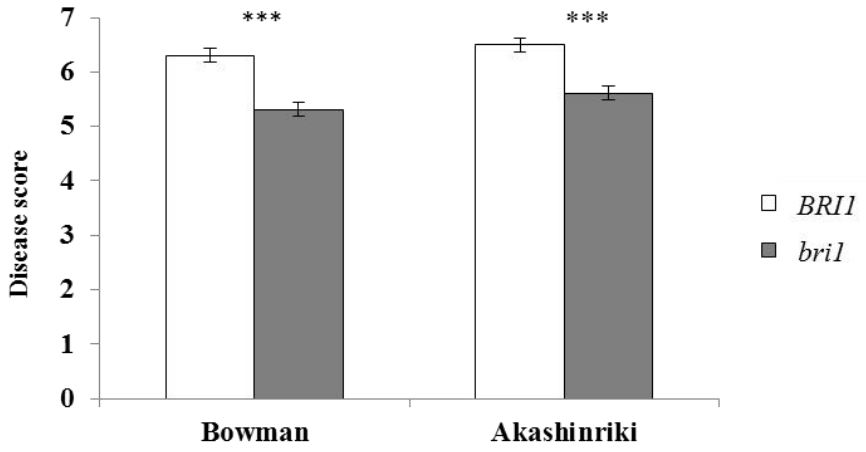

Figure 2.3.The effect of the *bri1* mutation on *Gaeumannomyces* infection. a) Take- all disease symptoms in both Bowman (left pair) and Akashinriki backgrounds (right pair) at 21dpi. Scale bars = 1 cm. b) Disease scores (0 – 10 severity scale) of NIL pairs inoculated with *G. graminis* (21dpi). Means ± s.e. were calculated from 3 independent experiments. *** Significant difference ($P < 0.001$) from the respective wild-type NILs.

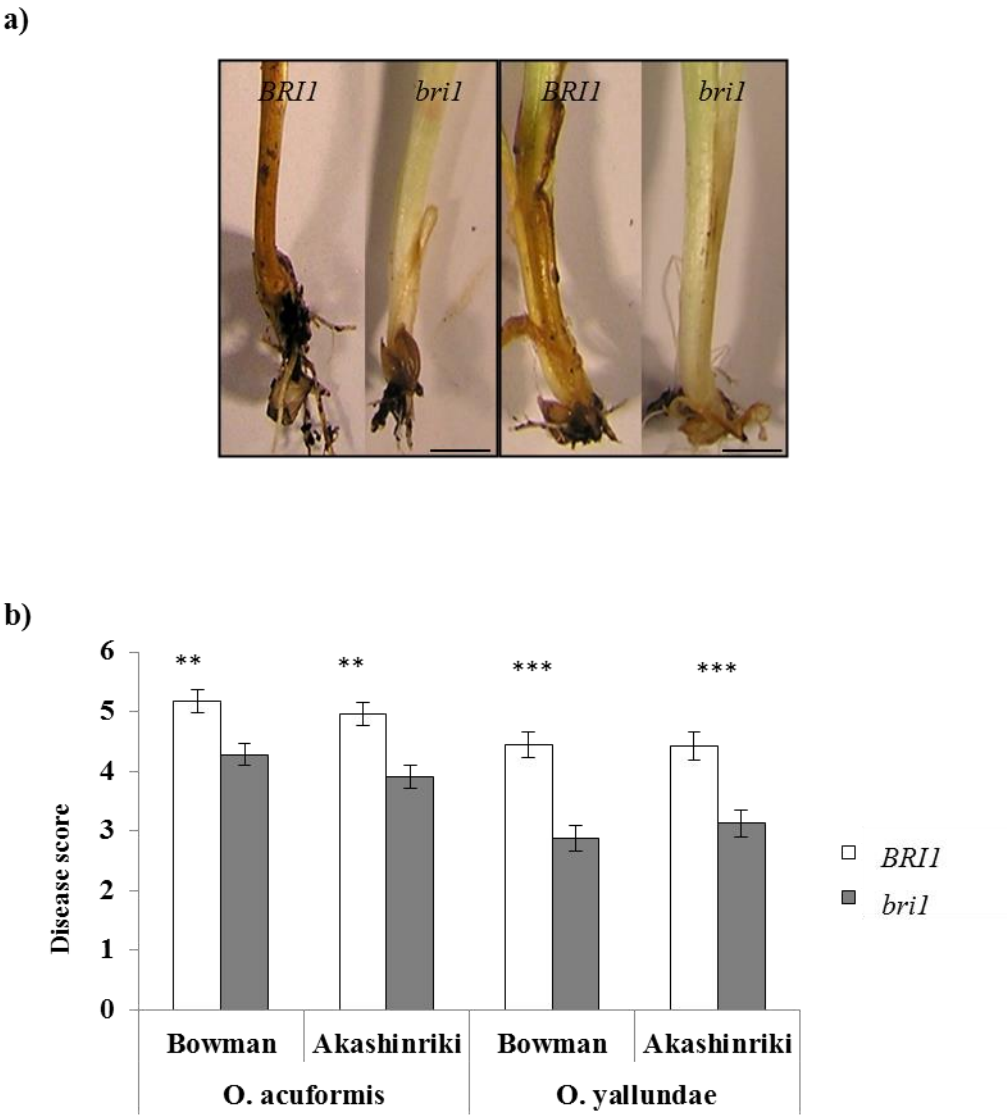

Figure 2.4. The effect of the *bri1* mutation on *Oculimacula* infection. a) *O. yallundae* symptoms in both Bowman (left pair) and Akashinriki background (right pair) at 56dpi. Scale bars = 1 cm. b) Stem base disease scores of *O. yallundae/acuformis* inoculated NIL pairs at 56dpi. Means ± s.e. were calculated from 2 independent experiments (*O. yallundae*). The experiment was repeated once with *O. acuformis* to confirm findings. **, *** Significant differences ($P < 0.01$ and $P < 0.001$) from the respective wild-type NILs.

2.3.5 Influence of BRI1 mutation on resistance to F. culmorum

Barley *bri1* and *BRI1* lines were assessed for their response to both FHB and FCR. Susceptibility to FHB was assessed through spray inoculation of field plots in two successive years (2012 and 2013) followed by visual disease scoring. Interestingly, in the 2012 field trial, plants were subjected to a short period of drought stress before normal watering was resumed. The heads of semi-dwarf *bri1* lines which had emerged during the period of stress were much smaller, more compact and had fewer grains than those in the *BRI1* lines (Figure 2.5a). Heads of the *bri1* lines that emerged subsequently during the more favourable conditions were less compact than those produced during the drought stress but they were still more compact than those of the *BRI1* lines. However, no significant difference in the combined FHB disease scores between semi-dwarf *bri1* and *BRI1* lines (P = 0.457 and 0.197 in Bowman and Akashinriki pairs, respectively, Appendix Table A.4) was visible (Figure 2.5b).

Susceptibility to FCR was determined by the ability of the pathogen to penetrate through successive leaf sheaths at the stem base following stem base infection. The *BRI1* lines of both Bowman and Akashinriki displayed more severe visual disease symptoms than the *bri1* lines, with a greater number of leaf sheaths exhibiting the brown discolouration characteristic of the disease (Figure 2.6a). The differences in FCR scores between tall and semi-dwarf NILs were found to be significant in both the Bowman and Akashinriki pairs ($P < 0.001$, Appendix Table A.5) (Figure 2.6b). In an additional set of experiments, seedlings were wounded at the stem base prior to inoculation to encourage infection by the fungus (Knight and Sutherland, 2013). With this procedure, the differential susceptibility observed in the non-wounded assays was lost (Figure 2.7a) and no significant difference in FCR symptoms were seen between *BRI1* and *bri1* lines (P = 0.103 and 0.064 in Bowman and Akashinriki pairs, respectively, Appendix Table A.6) (Figure 2.7b).

a)

b)

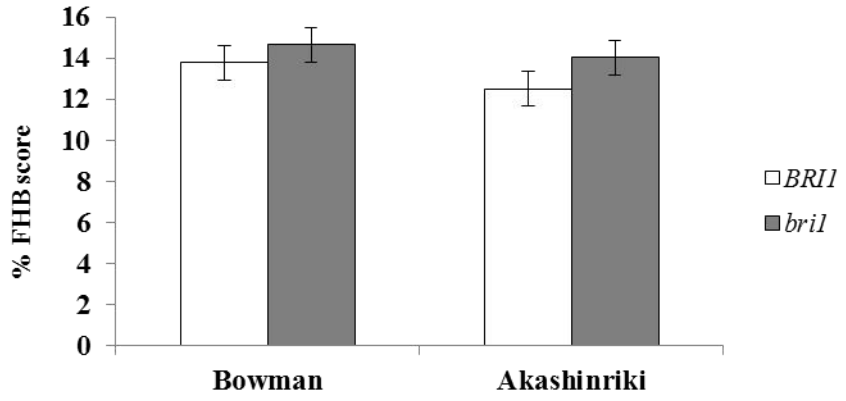

Figure 2.5. The effect of the *bri1* mutation on *Fusarium* infection. a) FHB symptoms on barley heads spray inoculated with *F. culmorum* conidia from the 2012 field trial; Bowman (left pairs) Akashinriki backgrounds (right pairs) at 21dpi. Heads on the left of each pair represent heads subjected to drought stress, whilst those on the right represent non stressed heads. Scale bars = 1cm. b) Visual FHB disease assessment scores for 2012 and 2013 field plots spray inoculated with *F. culmorum* Fu42 conidia (21dpi). Bars indicate means ± s.e. from 2 years of trial data.

a)

b)

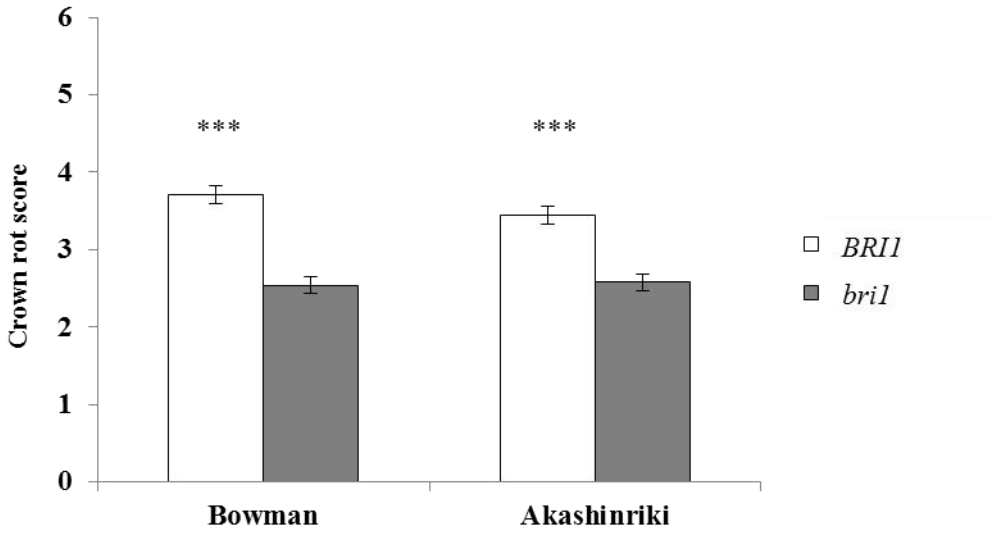

Figure 2.6. The effect of the *bri1* mutation on *Fusarium* infection. a) Images of FCR in non-wounded stem bases in both Bowman (left pair) and Akashinriki background (right pair) at 21dpi. Scale bars = 1cm. b) Crown rot scores of non-wounded *F. culmorum* Fu42 inoculated NIL pairs at 21dpi. Means ± s.e. were calculated from 3 independent experiments. *** Significant difference ($P < 0.001$) from the respective wild-type NILs.

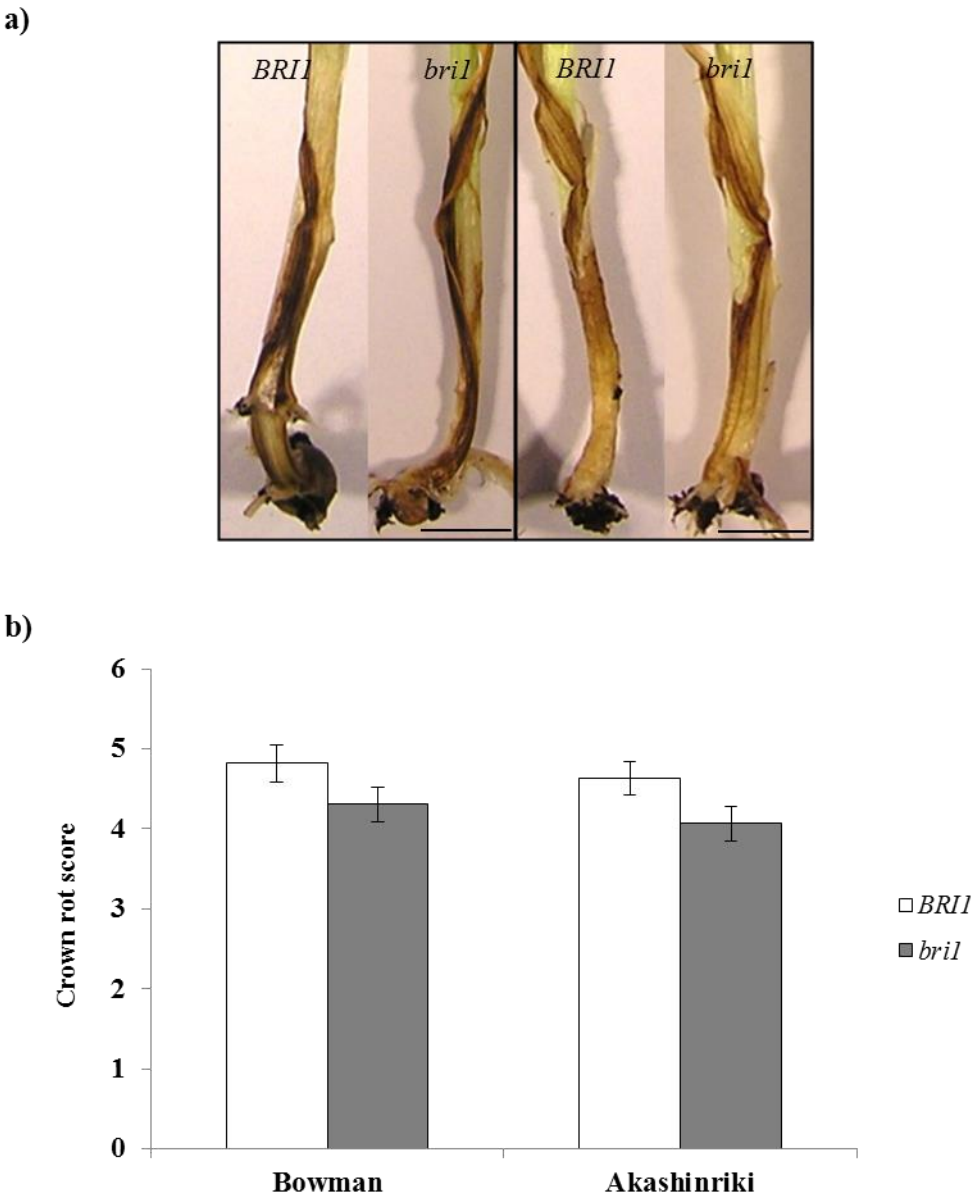

Figure 2.7. The effect of the *bri1* mutation on *Fusarium* infection. a) Images of FCR on wounded stem bases in both Bowman (left pair) and Akashinriki backgrounds (right pair) at 21dpi. Scale bars = 1cm. b) Crown rot scores of wounded *F. culmorum* Fu42 inoculated NIL pairs at 21dpi. Means ± s.e. were calculated from 2 independent experiments.

2.3.6 Influence of BRI1 mutation on resistance to R. collo-cygni

R. collo-cygni is a hemibiotrophic fungal pathogen which displays a long endophytic colonisation phase, before switching to a necrotrophic lifestyle. Foliar spray inoculation with *R. collo-cygni* produced characteristic RLS brown lesions visible on both the abaxial and adaxial leaf surface from 10dpi in the Bowman background and 12dpi in the Akashinriki background. Disease symptoms were consistently more severe in the Bowman background across all experiments, with both *BRI1* and *bri1* lines displaying a greater percentage of RLS lesions per leaf than both of the Akashinriki lines (Figure 2.8a). However, no significant difference in percentage maximum area under disease progress curve (%AUDPC) score was observed between lines possessing the *bri1* mutation ($P = 0.175$ and 0.278 in Bowman and Akashinriki pairs, respectively, Appendix Table A.7) and those possessing the *BRI1* gene in any of 3 independent inoculation experiments (Figure 2.8b).

2.3.7 Influence of BRI1 mutation on resistance to B. graminis f.sp. hordei

The role of *BRI1* in resistance to *B. graminis* f.sp. *hordei* was investigated as an example of an interaction with an obligate biotrophic pathogen. Disease susceptibility was scored taking into account the amount of mycelial growth, necrosis and chlorosis visible on the leaf surface. The two-row variety Bowman was more susceptible to the *B. graminis* f.sp. *hordei* isolates used than the six-row variety Akashinriki, with both *BRI1* and *bri1* lines in the Bowman background displaying a greater number of mycelial colonies (Figure 2.9a). However, no significant difference in susceptibility to *B. graminis* f.sp. *hordei* was observed in detached leaf assays between the *BRI1* tall and *bri1* semi-dwarf lines for either of the NIL pairs ($P = 0.374$ and 0.183 in Bowman and Akashinriki pairs, respectively, Appendix Table A.8) at either of the time points scored (7, 10dpi) (Figure 2.9b).

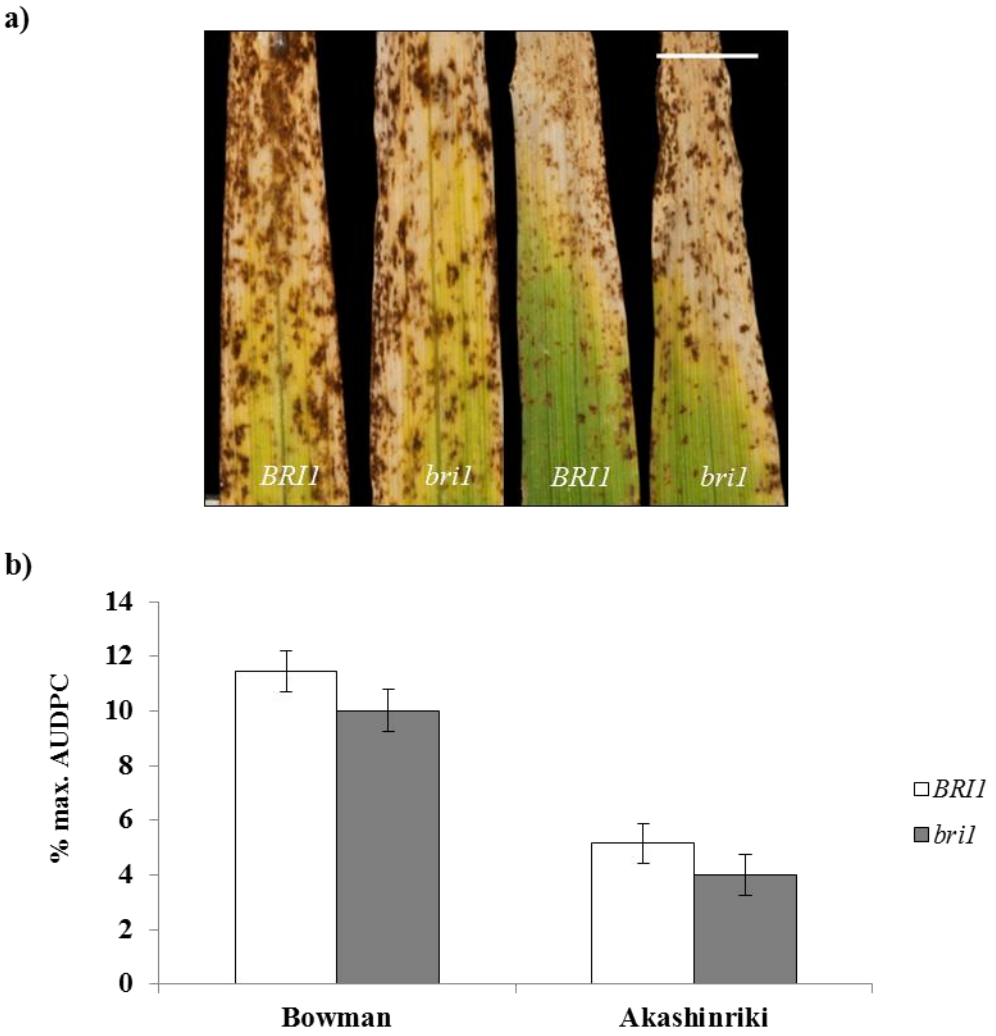

Figure 2.8. The effect of the *bri1* mutation on *Ramularia* infection. a) Ramularia leaf spot symptoms on barley seedlings in both Bowman (left pair) and Akashinriki backgrounds (right pair) at 28dpi. Scale bar = 1cm. b) The % of the maximum area under disease progress curve (% max AUDPC, 28dpi) for leaves inoculated with *R. collo-cygni*. Means ± s.e. were calculated from 3 independent experiments.

a)

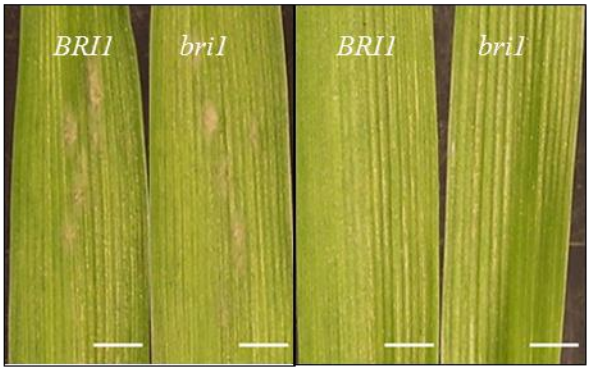

b)

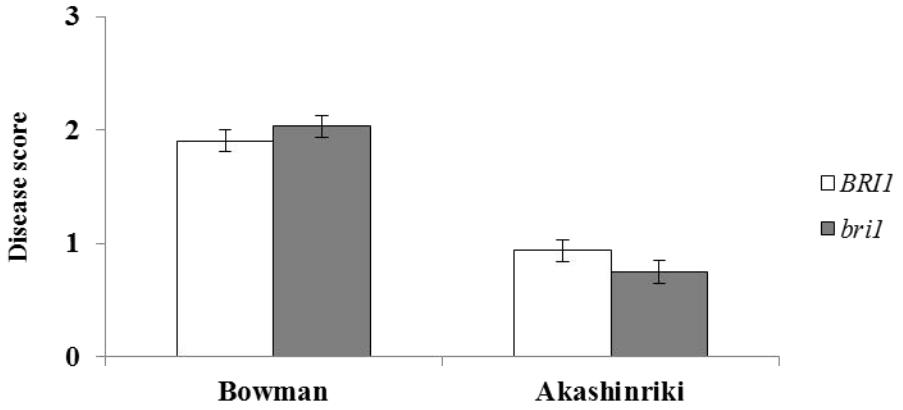

Figure 2.9. The effect of the *bri1* mutation on *Blumeria* infection. a) Powdery mildew disease symptoms following spray inoculation in both Bowman (left pair) and Akashinriki backgrounds (right pair) at 10dpi. Scale bars = 1 cm. b) Disease scores for detached first leaves inoculated with *B. graminis* spores (10dpi). Means ± s.e. were calculated from 3 independent experiments.

2.4 Discussion

Brassinosteroids along with a second phytohormone, GA, have been demonstrated to have increasingly important roles in the interplay between plant growth and immunity (De Bruyne et al. 2014). Attenuating GA signalling through mutation of DELLA proteins was very important in agriculture, with the wheat *Rht* semi-dwarfing alleles being central to advances in crop yield that occurred during the so-called 'Green Revolution' (Peng et al. 1999; Achard et al. 2006; Navarro et al. 2008). However, *Rht* and *Sln1* (the *Rht* DELLA equivalent in barley) alleles have pleiotropic effects on immunity. In response to biotrophic fungi the dwarf gain-of-function barley *Sln1d* line is more susceptible than the wild-type tall line, yet *Sln1d* is more resistant to disease caused by necrotrophic fungi (Saville et al. 2012).

BRI1 mutation in barley confers a semi-dwarf phenotype, much less extreme than the reduction in height seen in barley lines possessing the *Sln1d* GA-insensitive allele. Disruption of *BRI1* led to an increase in disease resistance to necrotrophic pathogens (*G. graminis* var. *tritici*, *O. acuformis*) and hemibiotrophs with a short biotrophic phase (*M. oryzae*, *O. yallundae*) in leaf and root tissues. In contrast, disruption of *BRI1* had no discernible effect on resistance towards *B. graminis* var. *hordei* and *R. collo-cygni*. *B. graminis* is an obligate biotroph (Both et al. 2005), whilst *R. collo-cygni* is a hemibiotroph with a prolonged asymptomatic endophytic phase (Stabentheiner et al. 2009).

Interestingly the effect of *BRI1* mutation on infection by the hemibiotroph *F. culmorum* appeared to differ with tissue. Semi-dwarf *bri1* lines were more resistant than tall *BRI1* lines to stem base infection, yet no difference in susceptibility was seen after floral inoculation. This probably reflects differences in the mode of infection in the two tissues. During infection of floral tissues of wheat, *F. culmorum* initially grows intercellularly with little or no disruption of the host tissues before adopting a necrotrophic growth style (Brown et al. 2010). In contrast, no such stage has been observed during the infection and colonisation of stem base or root tissues where the fungus appears to grow in an entirely necrotrophic manner (Beccari et al. 2011; Chen et al. 2013). It has been previously shown that in response to FHB infection, the model species *Brachypodium distachyon* (Bd) mirrors more closely the situation in wheat, as the fungus is able to move through head tissues to infect adjacent spikelets (Peraldi et

al. 2011). Parallel to the investigation of disease response assays in barley *uzu bri1* lines, similar studies were conducted by A. Peraldi using a Bd T-DNA insertional *BRI1* homozygous mutant (*Bdbri1*) line and a null segregant control line (*BdBRI1*) (Goddard et al. 2014). Following spray-inoculation of heads of *Bdbri1* and *BdBRI1* with *F. culmorum*, there was no difference in the rate and magnitude of FHB symptom appearance up to 5dpi (Goddard et al. 2014). Disease then developed more rapidly on *BdBRI1* than on the *Bdbri1* line as the fungus spread through rachis tissues to infect additional spikelets. The movement of *Fusarium* through infected floral tissues of Bd contrasts with the lack of movement in barley. This conforms to the different types of FHB resistance described by Schroeder and Christensen (1963). Type 1 defines the resistance of the spike to initial fungal penetration and Type 2 is interpreted as resistance to spread through the rachis from infected to non-infected spikelets. Most wheat varieties have little or no Type 2 resistance, whilst barley varieties have inherently high levels of Type 2 resistance and differences in FHB susceptibility are due to different degrees of Type 1 resistance (Bai and Shaner, 2004). The data from Bd floral infection indicate that disruption of *BRI1* had no effect on resistance to initial infection (Type 1 resistance) but did lead to an increase in Type 2 resistance. Data from the two replicated field experiments involving the barley *BRI1* NILs provided no evidence for a role of *BRI1* in FHB resistance of barley. As FHB symptoms do not spread in barley (Type 2 resistance) it is concluded that this also reflects a lack of effect of *BRI1* mutation on Type 1 resistance (resistance to initial infection). Therefore, this concurs with the situation in Bd where disruption of *BRI1* had no effect on Type 1 resistance. The results from the FHB inoculation experiments, in both *B. distachyon* and barley, together support the view that *BRI1* mutation impacts on mechanisms associated with Type 2 resistance to FHB, the phase where the fungus adopts a necrotrophic mode of colonisation.

The effect of *BRI1* mutation on stem base infection by *F. culmorum* was also dependent upon inoculation method. When unwounded, the *bri1* lines were significantly more resistant to *F. culmorum* than their wild-type NILs. However, this difference was lost when the stems were wounded immediately prior to inoculation. Physical trauma of plant tissues through wounding or herbivory activates a signalling cascade that leads to the production of different mobile signals, the predominant of which are ET and JA (Savatin et al. 2014). In *Arabidopsis*, Makandar et al. (2010)

reported that mutation of some of the core signalling components of the JA pathway (*opr3, coi1* and *jar1*) induces hyper-resistance in *Arabidopsis* plants challenged with *F. graminearum*, a very close relative of *F. culmorum*. The observation of increased induction of Pathogenesis-related protein 1 (PR1) transcripts and SA accumulation in *opr3* and *jar1* mutants compared to the wild-type plants, led the authors to conclude that the JA-induced susceptibility may function via attenuation of SA-induced defence mechanisms (Makandar et al. 2010). Antagonism between the JA/ET and SA signalling pathways is well documented (Robert-Seilaniantz et al. 2011) and in *Arabidopsis* both SA and JA signalling have been demonstrated to be required for resistance against *F. graminearum* (Makandar et al. 2012). Similarly ET signalling was shown to be a factor of susceptibility to infection by *Fusarium* species in *Arabidopsis*, wheat and barley (Chen et al. 2009). Therefore, it is reasonable to assume that wounding of barley stem bases may activate JA and ET signalling pathways, both of which have been shown to increase susceptibility to *Fusarium* species. It is possible that signalling resulting from the wounding pre-treatment may antagonise the effect of the *BRI1*-related differential response observed between the *BRI1* and *bri1* lines in the absence of wounding.

Whilst my results demonstrate that BR signalling has pleiotropic effects on growth and disease resistance, it is of interest to note that unlike the GA-insensitive *Sln1d* mutation, *BRI1* mutation does not incur a disease resistance trade-off between pathogens of differing trophic lifestyles. Semi-dwarf *bri1* lines were more resistant to infection by pathogens exhibiting a necrotrophic lifestyle but such lines did not exhibit the increased susceptibility to biotrophic pathogens associated with attenuation of GA signalling (Saville et al. 2012). The absence of the biotroph-necrotroph disease trade-off following impairment of BR signalling suggests that manipulation of this pathway or downstream BR-regulated genes may have potential agricultural use in breeding varieties with reduced height, enhanced resistance to necrotrophic pathogens but without compromising resistance to biotrophic pathogens.

An emerging body of evidence suggests that BR signalling is involved in the regulation of plant defence responses. Belkhadir et al. (2012) reported that BRs function in an antagonistic manner to PTI that is triggered by PAMPs such as chitin and flagellin. BAK1, the BRI1 co-receptor, has been demonstrated to also act as a co-receptor with Flagellin-sensing 2 (FLS2), an LRR receptor-like kinase that recognises

the flagellin PAMP flg22-peptide (Chinchilla et al. 2007). Overexpression of BRI1 in *Arabidopsis* compromised PTI activity in response to flg22 treatment, possibly due to competition between BRI1 and FLS2 for BAK1 (Belkhadir et al. 2012), which may be responsible for the observed antagonism. Further studies conducted in *Arabidopsis* showed that activation of the BRI1 pathway inhibits the PTI signalling mediated by several pattern-recognition receptors (PRRs). Co-treatment of wild-type plants with exogenous eBL and flg22 caused a significant decrease in flg22-induced immune responses (Albrecht et al. 2012). However, the same study showed that exogenous BR treatment also reduced chitin induced PTI activity, which is detected independently of BAK1, suggesting that BR-mediated inhibition occurs downstream of BAK1. The cause of the antagonism may actually lay with BZR1, the key transcription factor regulating BR-responsive genes. BZR1 promotes the expression of a number of WRKY transcription factors that act as negative regulators of the reactive oxygen species (ROS) production associated with the onset of PTI, which is thought to suppress defence gene expression (Lozano-Durán and Zipfel, 2015). Mutation of *BRI1* might be anticipated to alleviate this antagonism and perhaps lead to enhanced efficiency of PTI. My data would support the view that BR signalling functions antagonistically with basal defence mechanisms as *BRI1* mutation enhanced resistance against a broad range of pathogenic micro-organisms despite differences in their infection and virulence strategies. Currently, little is known about the molecular components controlling the antagonistic relationship between growth and immunity in monocotyledons. However, recent work in *Arabidopsis* from two independent groups demonstrated that the basic helix-loop-helix transcription factor Homolog of brassinosteroid enhanced expression2 interacting with IBH1 (HBI1), negatively regulates genes involved in the onset of PTI while positively regulating BR-triggered responses (Fan et al. 2014; Malinovsky et al. 2014). The above studies suggest that HBI1 and BZR1 both negatively mediate immunity, although the mechanisms through which these transcription factors act is still unclear (Belkhadir and Jallais, 2015).

In contrast to the effects of BRs on PTI, other studies have proposed that BRs have a positive role in resistance. For example, exogenous application of BRs was shown to increase resistance to *M. grisea* and *Xanthomonas oryzae* pv. *oryzae* in rice and resistance to tobacco mosaic virus, *Pseudomonas syringae* pv. *tabaci* and *Oidium* sp. in tobacco (Nakashita et al. 2003). This report appears difficult to reconcile with the

findings here that *BRI1* mutation reduced disease caused by *M. oryzae*. Similarly, Ali et al. (2013) reported the first study implicating BRs in resistance to *Fusarium* in barley. The authors observed that exogenous application of eBL, whether applied to floral tissue or added in the soil, enhanced the resistance of barley to FHB and FCR, respectively, caused by *F. culmorum*. This appears contradictory to the present findings that mutation of *BRI1* enhances resistance. Recent reports taking a genetic rather than chemical approach, however, support the findings from the present work that disruption of *BRI1* in barley leads to enhanced resistance to necrotrophic pathogens. Barley semi-dwarf *uzu* (*bri1*) lines not only showed less severe symptoms to FCR than their tall equivalents (Chen et al. 2014), but also displayed slower development of *Fusarium* throughout the leaf sheaths and reduced fungal biomass within infected tissues (Bai and Liu, 2015). The results of these genetic studies indicate that reduced BR signalling enhances resistance to *Fusarium*. A further study by Ali et al. (2014), using the Bowman and Akashinriki *uzu bri1* lines used within this research, also demonstrated that altered *BRI1* signalling gives increased resistance to the necrotrophic net blotch fungus *Pyrenophora teres* and also to barley stripe mosaic virus (BSMV). Interestingly, both the studies of Ali et al. (2013) and Nakashita et al. (2003) employed a chemical approach to investigate the effect of BRs on disease resistance. Their findings therefore reflect the effect of exogenous application of phytohormone to plants whose cellular signalling machinery is intact and therefore fully responsive to the hormone. Recent studies (Ali et al. 2014; Chen et al. 2014; Bai and Liu, 2015) employing a genetic approach to investigate the impact of BR signalling on disease resistance have utilised *bri1* lines which are hyposensitive to the BR signal. Plants carrying genetic mutations that impair or prevent activation of a particular phytohormone pathway may compensate for such a defect via differential regulation of other hormonal signalling pathways to re-equilibrate overall hormone ratios and outputs. Hence, it is not surprising that the findings from genetic studies may not correspond directly to those from studies using chemical approaches, as the former examines the effect of constitutive disruption of a pathway while the latter generally examines the effect of supplementing or overloading a pathway. In addition, responses to phytohormone application are frequently dependent upon concentration. For example, Clouse et al. (1996) reported that root growth of *Arabidopsis* seedlings was reduced when exposed to high concentrations of eBL but stimulated at low concentrations. Similarly, Zhao et al. (2004) reported that production of the

phytoalexin β-thujaplicin was stimulated by moderate ET concentrations, whereas excessive concentrations of ET reduced β-thujaplicin levels to below those in untreated plants.

In conclusion, my data demonstrates that BR signalling plays a complex role in the trade-off between growth and immunity. Mutation of *BRI1*, the gene encoding the main barley BR receptor, not only resulted in a reduction in plant height when compared to wild-type plants, it also provided increased disease resistance in response to infection with pathogens of specific trophic lifestyles. Unlike GA-insensitive alleles which confer a resistance trade-off between biotrophic and necrotrophic fungal pathogens, I was able to demonstrate that the *BRI1 uzu* mutation provides advantageous resistance to necrotrophs without increasing susceptibility to biotrophs. The knowledge that *BRI1* mutation results in both a favourable shorter stem phenotype and increased necrotroph resistance demonstrates the potential for the BR pathway to be manipulated when aiming to reduce plant height and increase resistance to a range of economically important diseases.

Chapter 3. Production of high density barley genetic maps for quantitative trait loci analysis

3.1 Introduction

Quantitative trait loci (QTL) identify regions of the genome that are associated with a particular agronomic trait, such as height or disease resistance. The detection of QTL for specific traits is reliant on the production of a segregating population, such as a recombinant inbred (RIL) or doubled haploid (DH) population, with known polymorphisms between the parental lines (Collard et al. 2005). Genetic linkage maps are then created based on the recombination frequency of these polymorphisms throughout the entire population, allowing QTL to be identified by determining the statistical association between the genetic markers within the map and the phenotype observed (Würschum, 2012). The detection of QTL therefore depends on the identification of a sufficient number of reliable polymorphisms to produce an adequately marker dense genetic linkage map.

Restriction fragment length polymorphisms (RFLPs) were widely utilised as some of the first DNA markers to generate genetic maps (Yang et al. 2015), including the maps used to identify QTL for FHB and other associated agronomic traits. For example, Zhu et al. (1999) located eight QTL associated with FHB, within a population of 144 DH barley lines, from a linkage map of only 97 RFLPs. Ma et al. (2001) also located eight FHB QTL using a map derived from 211 RFLPs genotyped across a 147 line DH barley population. The total map distance covered 1,026cM, with a mean distance of 13.5cM between markers (Ma et al. 2001). As marker technology has developed towards more PCR-based methods, such as amplified fragment length polymorphisms (AFLPs) and simple sequence repeats (SSRs), the inclusion of multiple forms of genetic markers within a map has been used to give an increased marker density and to aid QTL identification. Hori et al. (2005) used a combination of AFLPs, SSRs, expressed sequence tags (ESTs) and resistance gene analog (RGA) markers from 95 barley RILs to produce a high density map of 1,172 markers. Dahleen et al. (2003) produced a linkage map of 1,330.8cM containing 7 RGA, 29 SSR, 53 RFLP and 123 AFLP markers using 75 DH barley lines, which enabled the detection of nine FHB QTL. The same authors subsequently produced a higher density map of the same population by genotyping an additional 85 DH lines and including a further 369

markers, increasing the map distance to 1,385.5cM (Dahleen et al. 2012). Although the aforementioned genetic markers have been demonstrated to produce sufficient linkage maps for QTL identification, their higher cost and lower efficiency mean they have been increasingly replaced by higher throughput technologies.

Genotyping methods have rapidly developed within the last decade, providing new tools for identification of genetic polymorphisms. A number of arrays designed to identify single nucleotide polymorphisms (SNPs) have been developed using Illumina BeadChip® genotyping technology (Illumina Inc, San Diego, CA) allowing a large number of samples to be queried for a greater number of SNPs within a single run. The Illumina BeadChip system is based on the hybridisation of three oligonucleotides (two SNP specific probes and one locus specific probe) to a DNA sample, PCR amplification and the addition of cyanine fluorescent probes, followed by hybridisation to a BeadChip and analysis of the fluorescent signal to identify the SNP (Shen et al. 2005). The barley SNPs used within these arrays have been primarily derived from expressed sequence tags (ESTs) from a relatively small, yet well characterised, set of parental lines. The 1,536 SNP Barley Oligonucleotide Pool Assay (BOPA1) devised by Rostoks et al. (2005, 2006) used the parents of the Oregon Wolfe Barley (OWB) population, in addition to Morex, Steptoe and Optic amongst the cultivars from which to identify polymorphisms. From this assay, Moragues et al. (2010) developed two separate 384-SNP subsets, specifically optimised for genotyping either barley landraces or cultivars, with a view to reducing the ascertainment bias seen by using a single SNP set. Three pilot OPAs were also generated by Close et al. (2009), before the creation of two final production OPAs (BOPA1 and BOPA2) each testing 1,536 SNPs which were selected from the pilot OPAs based on their genomic location and biological relevance. These again use the parents and progeny from four common barley mapping populations, Steptoe × Morex, Haruna Nijo × OHU602, Morex × Barke and the OWB population, for SNP identification (Close et al. 2009). A selection of 2,832 SNPs from the BOPA1 and BOPA2 assays developed by Close et al. (2009) have also been combined with 5,010 SNPs identified from RNA sequencing (RNA-seq) reads of 10 barley cultivars (including Barke, Betzes, Morex and Optic), to form the iSelect SNP chip capable querying 7,842 markers (Comadran et al. 2012).

Next-generation sequencing (NGS) technologies have also been widely posited as one approach for the identification of large numbers of genetic markers within a species. Such genotyping methods include restriction-site-associated DNA sequencing (RAD-seq), Genotyping-by-Sequencing (GBS), reduced representation libraries (RRL) and complexity reduction of polymorphic sequences (CRoPS). Most NGS technologies are based on the digestion of DNA with specific restriction enzymes (RE), followed by the ligation of either common and barcode adapters to allow multiplexing of samples and then subsequent pooling and sequencing of these samples (Davey et al. 2011). NGS methods have been demonstrated to be suitable for numerous different downstream applications, such as phylogeography (Emerson et al. 2010) and genome wide association studies (Parchman et al. 2012), with both RAD-seq and GBS being particularly utilised for QTL mapping studies in numerous species. RAD-seq uses size selection to identify DNA fragments of 300-700bp for sequencing which have been digested and randomly sheared (Cronn et al. 2012). A smaller region of the genome is sequenced at a higher coverage level with RAD-seq, proving a useful method for studying species without a reference genome as each marker is genotyped with an increased level of precision (Davey et al. 2011). Using the RAD-seq method, 445 RAD markers were mapped within the OWB population to identify QTL for agronomic traits such as height and row type (Chutimanitsakun et al. 2011).

GBS differs from RAD-seq in that digested fragments (170-350bp) are not sheared or size selected, simplifying the workflow process (Elshire et al. 2011). In barley, the GBS protocol was initially optimised using a single methylation-sensitive RE ApeKI, as the cut sites for this enzyme were demonstrated to be distributed throughout the barley genome (Elshire et al. 2011). The ApeKI enzyme subsequently generates three types of DNA fragments containing either a barcode and a common reverse adapter, or either both common or both barcoded adapters (Elshire et al. 2011). This method was validated by the mapping of 24,186 sequence tags from the OWB population to the OWB framework map, with both the reference and the GBS markers being demonstrated to be in agreement (Elshire et al. 2011). A two-enzyme approach has also been developed by Poland et al. (2012), where all digested DNA fragments possess both a common adapter and a barcoded forward adapter, which was again validated in the OWB population by the mapping of 9,545 SNPs. GBS technology further differs from RAD-seq in that a larger proportion of the genome is sequenced

but at low coverage. This has proven to be highly useful for species with a reference genome, particularly with respect to QTL mapping and MAS studies (Davey et al. 2011), as it easier to impute missing data from the low coverage sequencing reads with increased accuracy. The use of GBS for generating genetic maps with the aim of QTL identification has been demonstrated by Liu et al. (2014).The authors used a map with 1,391 SNPs derived from a Golden Promise × Morex population to locate a QTL associated with the height gene *Breviaristatum-e* (*ari-e*) on 5H, which was previously mapped to the same genomic region by QTL analysis.

With the aim of generating high quality genetic maps suitable for identifying QTL associated with FHB, three barley populations were produced in this study. Chevallier is an English landrace from 1820 (Beaven, 1936) which has been demonstrated to show significant resistance to FHB (Muhammed, 2012). Chevallier was crossed with NFC Tipple, a short modern malting variety (Syngenta Seeds, Ltd), which is susceptible to FHB and has been demonstrated to be genetically distant to Chevallier by phylogenetic analysis (J. Russell, personal communication). Two separate Chevallier × NFC Tipple populations were produced by single seed descent (SSD) and one was advanced to the F_5 generation, while the second was advanced to the F_7 generation. A further bi-parental cross between NFC Tipple and the French cultivar Armelle was created. Armelle was released in 1974 and has also been shown to have FHB resistance (Muhammed, 2012). A single Armelle × NFC Tipple population was produced by SSD and advanced to the F_6 generation. All three populations were genotyped using the 384-SNP cultivar optimised array (Moragues et al. 2010) and the two Chevallier × NFC Tipple populations were additionally genotyped using the GBS method described by Elshire et al. (2011).

3.2 Materials and methods

3.2.1 Generation of mapping populations

Two separate bi-parental crosses were developed to provide two mapping populations with the common parents Chevallier (JIC accession number 4851 or 4817), and NFC Tipple (hereafter referred to as Tipple) (Syngenta Seeds, Ltd). An F_5 population of 188 RILs (C×T F_5) was produced by KWS UK Ltd., Cambridge, UK. I produced a separate

population resulting in 188 F_7 RILs (C×T F_7) at JIC. Both populations were developed by single seed descent (SSD). A bi-parental cross between Armelle and Tipple (A×T) was also developed by Syngenta Seeds Ltd, creating a population of 250 F_6 RILs developed by SSD.

3.2.2 384-SNP BeadXpress genotyping

For both the C×T F_5 and A×T F_6 populations leaf material was sampled from 3-week-old seedlings, with a pool of five seedlings per genotype. For the C×T F_7 population, leaf material was sampled from a single seedling per genotype. Genomic DNA for each population was extracted using the DNeasy 96 Plant Kit and the protocol for frozen plant tissue (Qiagen) by R. Goram (JIC), and diluted to 50ng/µl. The 384-plex cultivar optimised genotyping panel (as described in Moragues et al. (2010) was used to genotype the C×T F_5, C×T F_7 and A×T F_6 populations using the Illumina BeadXpress (BX) platform at the James Hutton Institute (JHI). SNP calls were analysed using Illumina BeadStudio software.

Marker data for 384 SNPs was produced by the BX genotyping platform. From the returned SNP calls, RILs which displayed an apparent high level of heterozygosity (over 20% of total SNP calls returned as heterozygous) were removed from the dataset. In the C×T F_5 population, 23 RILs were removed leaving 165 RILs for subsequent analysis. (It was later determined that the high level of heterozygosity in the C×T F_5 population was an artefact of incorrect calling by the software, perhaps due to issues with SNP genotyping). In the C×T F_7 (188 RILs) and A×T F_6 populations (250 RILs) all of the genotyped lines were retained in the dataset as they displayed sufficiently low heterozygosity. Monomorphic markers were then removed from each dataset, providing an initial set of markers for the genetic mapping of each population.

3.2.3 Genotyping-by-Sequencing

Leaf material from a single 3-week-old seedling per genotype was sampled for both the C×T F_5 and F_7 populations. Genomic DNA for each population was extracted using the DNeasy 96 Plant Kit and the protocol for frozen plant tissue (Qiagen) by R. Goram

(JIC). DNA was then quantified using the Quant-iT™ PicoGreen® dsDNA assay and diluted to 50ng/µl. GBS libraries for the C×T F_5 and C×T F_7 populations were produced at the Biotechnology Resource Centre (BRC) Genomic Diversity Facility at Cornell University (US), using the 96-plex ApeKI restriction enzyme approach (Elshire et al. 2011). Libraries were sequenced using the Illumina HiSeq 2000/2500 generating 100bp single end reads. On average, 2,066,581 reads were produced for the C×T F_5 population and 2,230,103 were produced for the F_7 population per DNA sample. Raw sequence reads were trimmed and the barcodes removed and the 64bp tags were mapped to the Morex reference genome (IBSC, 2012) to call the SNPs. Failed sequences were determined as those displaying less than 10% of the total mean reads per population and were removed from analysis. Raw and filtered (those with a minor allele frequency of above 1% and merged duplicate SNPs) SNP calls aligned to the Morex reference sequence were provided for both populations.

Sequencing of a single C×T F_5 line (line 5) and a single C×T F_7 line (line 568) failed providing genotype data for 187 lines for both populations. Within Excel, further data filtering was performed on the 8,754 filtered SNP calls provided for each population. SNPs which were monomorphic or displayed missing calls for either of the parental genotypes were removed from the analyses as were SNPs with over 20% missing values for the C×T progeny, providing an initial set of markers for the genetic mapping of each population.

3.2.4 Combined BeadXpress and Genotyping-by-Sequencing data

To provide the most complete linkage group for each chromosome, the GBS and BX SNP initial data sets (containing all the filtered polymorphic SNPs) were combined for both the C×T F_5 and F_7 populations.

3.2.5 Genetic mapping

All maps were created using JoinMap® 3.0 software (van Ooijen and Voorrips, 2001). Within JoinMap, individual marker chi-squared values were calculated and markers which deviated significantly from the expected 1:1 ratio were either re-coded or removed from the marker set. The Kosambi mapping function was used to generate

genetic distances between markers and a LOD score of 7.0 was used to create the linkage groups for both the BX and GBS datasets. For the BeadXpress datasets the marker order of each linkage group was referenced against the marker order in the barley consensus map (Close et al. 2009), whilst for the GBS datasets the marker order was referenced against the Morex reference genome (IBSC, 2012). Genetically redundant markers were removed from the initial maps. Markers which appeared to have been ordered incorrectly, for example mapping to either the wrong chromosome or the wrong chromosome arm to the reference map, were also removed to ensure that the most accurate map was generated for subsequent QTL analysis. The final map for each population was then generated by re-running the mapping software. Linkage maps for each population were drawn using MapChart (Voorips, 2002).

3.3 Results

3.3.1 384-SNP BeadXpress genotyping

Genotyping of both of the C×T populations with the 384-SNP assay identified 212 SNPs (55.2% of total SNPs) within the cultivar optimised 384-SNP set which were monomorphic between the Chevallier and Tipple parental lines. A total of 172 markers were determined to be polymorphic in both the C×T F_5 and F_7 populations, with these polymorphic markers displaying uneven distribution across the seven chromosomes during the linkage mapping process (Table 3.1). Chromosomes 1H and 7H were particularly sparsely populated in both populations using this genotyping platform.

Within the C×T F_5 population 164 progeny lines were used to create the genetic map. In the initial mapping process nine linkage groups (with 1H and 5H each represented across two groups) containing 158 markers were identified, although some of the markers appeared to be incorrectly ordered and were removed. In the final map nine linkage groups were again present, with the marker number per linkage group ranging from five on 7H to 32 on 6H. Of the initial 172 markers, 14 could not be linked. Only 14 polymorphic markers were identified that mapped to chromosome 1H and only nine of these could be identified at a LOD score of 7.0. Therefore, chromosome 1H was mapped as two linkage groups containing four and five markers. Even fewer markers correctly mapped to chromosome 7H (2.9% of the total markers), with only

11 markers being polymorphic on this chromosome and only five markers being present in the 7H linkage group at a LOD of 7.0 (Table 3.1). Chromosomes 3H and 6H displayed the greatest marker coverage, with 16% (28) of the markers mapping to 3H and 19% (32) of the markers available mapping to 6H. The final C×T F_5 map covered a genetic distance of 684.8cM with a total of 133 markers (Table 3.4). This represented a marker density of one marker every 5.1cM, with the largest distance between markers being 17.1cM.

Within the C×T F_7 population none of the progeny lines displayed more than 20% heterozygosity, so all 188 lines were included within the genetic mapping process. In the initial genetic map 10 linkage groups were identified (with 1H, 2H and 5H each represented across two groups) containing a total of 168 markers, some of which were incorrectly ordered and therefore removed. Of the initial 172 markers, four could not be linked. The final F_7 map covered a distance of 820.6cM with a total of 154 markers, representing one marker every 5.3cM (Table 3.4). The genetic marker number per linkage group in the final map ranged from five on 7H to 34 on 3H. Of the 14 polymorphic markers identified to chromosome 1H, 12 of these markers (7.8% of the total polymorphic markers) were mapped to two linkage groups of five and seven markers at a LOD score of 7.0. As with the C×T F_5 population, only 2.9% of markers mapped to the 7H chromosome within the F_7 genetic map. The largest distance between markers was observed to be 20.1cM on chromosome 7H.

Of the SNP set assayed, 221 (57.6%) of the markers were monomorphic between the Armelle and Tipple parents, leaving 163 polymorphic markers. This is comparable with the C×T populations, where 55.2% of the markers were also determined to be monomorphic. In the initial mapping process 145 markers were clustered into eight linkage groups, with 18 markers which could not be linked to any group. After removal of the incorrectly ordered markers, a final A×T genetic map consisted of 129 markers covering 717.9cM was created, giving a marker density of one marker every 5.6cM (Table 3.4). The largest distance between markers was observed to be 23.7cM on chromosome 1H. The 129 markers formed eight linkage groups, with chromosome 2H represented as two separate groups of 11 and 13 markers. As with both of the C×T populations, chromosome 1H in the A×T map contained the fewest markers, with only 14 SNPs for 1H being polymorphic in the parental lines, resulting in only 5.4% of the total markers mapping to this linkage group. Only 5.4% of the markers were located

to 6H, despite this chromosome being more marker dense (containing over 16% of SNPs) in both the C×T populations. The linkage groups representing chromosomes 5H and 3H contained the highest number of markers, with 27.9% (36 markers) and 21.7% (28 markers) mapping to each of these chromosomes, respectively.

3.3.2 Genotyping-by-Sequencing

The GBS platform provided a much greater number of SNPs with which to create a genetic map than the BX genotyping method. Large attrition rates were observed in the number of SNPs initially produced by the GBS method compared to those suitable for inclusion in the genetic mapping process (with 82% of SNPs removed from the initial dataset in both of the C×T populations). From the linkage mapping analysis, a single linkage group per chromosome was identified for both populations (Table 3.2), compared to the multiple linkage groups identified in the BX data set. An increase in both marker number and genetic distance was also seen in both populations.

None of the lines assayed with the GBS genotyping method displayed over 20% heterozygous SNP calls in the GBS data produced for the C×T F_5 population. All lines were therefore retained in the analysis, providing 187 out of 188 C×T progeny lines for linkage analysis. A total of 1,565 SNPs were included in the initial linkage analysis, which formed seven linkage groups containing a total of 892 markers. Of the initial 1,565 markers, 673 markers could not be correctly linked to a group. As with the BX data, some of these markers were incorrectly ordered or genetically redundant and were therefore removed. The final GBS C×T F_5 linkage map covered a genetic distance of 1,188.2cM, representing an increase of 42.4% compared to the BX map (684.8cM). The number of genetic markers ranged from 59 on 4H, to 158 on 7H. Chromosome 1H, which was previously poorly represented by markers in the BX dataset, was extended from 29.1cM to 209.3cM with a total of 84 GBS markers. An additional 153 markers were mapped to chromosome 7H in the GBS map, expanding the genetic distance covered from 36.4cM to 170.9cM. The total number of markers included in the map increased from 133 to 817 using the GBS SNPs, with an average of 116 markers per chromosome (Table 3.2). The marker density was improved from one genetic marker every 5.1cM in the BX map to one marker every 1.5cM. The greatest distance between markers was also reduced to 15.0cM.

A total of 1,577 SNPs were included in the initial linkage analysis of the C×T F_7 GBS data, forming seven linkage groups containing a total of 897 markers. Of the initial markers, 680 markers could not be correctly linked. After the removal of incorrectly ordered markers, a final C×T F_7 linkage map covering 968.1cM with a total of 733 markers across seven linkage groups was created. The final map displayed a 15% increase in map distance compared to the BX map, (from 820.6cM to 968.1cM) and an increase in marker number from 154 to 733 markers (Table 3.2). The number of genetic markers ranged from 59 on 4H, to 162 on 2H, with an average of 104 SNPs per chromosome. As with the C×T F_5 population the marker coverage of chromosomes 1H and 7H, which previously displayed the lowest marker density, was greatly improved. Chromosome 1H included 80 more markers than in the original BX map, giving a total of 93 markers and an increase of 107.4cM in linkage group distance. A total of 72 further markers were included in the chromosome 7H linkage group using the GBS dataset, however this only represented an expansion in map distance of 14.3cM (from 69.9cM in the BX map to 84.2cM in the GBS). The total marker density was increased in the F_7 population; with one marker every 1.3cM in the GBS map compared to one marker every 5.3cM in the BX map. The largest distance between two genetic markers was 16.6cM on chromosome 5H.

3.3.3 Combined 384-SNP array BeadXpress and Genotyping-by-Sequencing

The SNPs from both the BX and GBS methods for each population were combined into a single data set with the aim of to creating the most complete linkage group for each chromosome. The inclusion of the BX SNP markers allowed a greater number of markers to be anchored into the genetic maps for each population (Table 3.3).

The C×T F_5 combined map contained 936 markers (95 BX and 841 GBS markers) covering 1,224.4cM, an increase of 36.2cM and an addition of 119 markers (Table 3.3). Of the 1,737 markers used in the initial combined map, 711 markers could not be correctly linked to any group. The number of genetic markers per linkage group in the final combined map ranged from 77 on 4H, to 179 on 2H. Chromosome 2H, the longest linkage group in the GBS map, was expanded by 22.8cM through the addition of 27 markers by combining the two datasets (Table 3.3). However, the addition of 18 extra markers to the linkage group representing 4H reduced the map distance from

132.9cM in the GBS map to 121.9cM in the combined map. An additional 14 markers were introduced to chromosome 5H in the combined map, again contracting the genetic distance from 128.0cM to 119.9cM. The marker density of the combined map was also improved on that of the map containing solely GBS markers, with one marker every 1.3cM compared to one marker every 1.5cM. The largest distance between two adjacent genetic markers was similar to the GBS map (15.0cM), with a distance of 15.1cM on 1H.

The C×T F_7 combined final map contained 962 markers (135 BX and 827 GBS markers), covering 1,078.4cM (Table 3.3). This gave an increase of 229 markers and an extension of 110.3cM compared to the GBS map. Of the 1,749 markers used in the initial combined map, 726 markers could not be correctly linked to any group. The number of genetic markers per linkage group in the final combined map ranged from 76 on 4H, to 176 on 2H. Linkage groups which displayed a higher number of markers in the GBS map were also extended by combining the datasets. For example, 55 extra markers were identified on chromosome 3H giving a marker total of 172 and extending the linkage group by 43.6cM to a distance of 198.4cM (Figure 3.1). The GBS linkage group for 7H contained 77 markers covering 84.2cM, making it the shortest linkage group in the GBS map. The addition of the BX markers to the GBS dataset allowed the inclusion of 60 extra GBS markers on chromosome 7H, increasing the total from 77 markers to 139 in the final combined map (Table 3.3). The final map distance of 7H was also extended by 63.2cM to 147.4cM. As with the C×T F_5 map, some chromosomes appeared shorter in the combined GBS/BX map than the GBS map. The linkage group for 2H was contracted from 191.6cM to 174.2cM by the addition of 14 markers, whilst 17 further markers were added to 4H reducing the map length by 4.4cM. Combining both the GBS and BX markers also improved the marker density of the map, with one marker placed every 1.1cM compared with one every 1.3cM in the GBS map. However, the largest distance between two markers was not greatly reduced by combining the two datasets, with a gap of 16.5cM being observed on 1H.

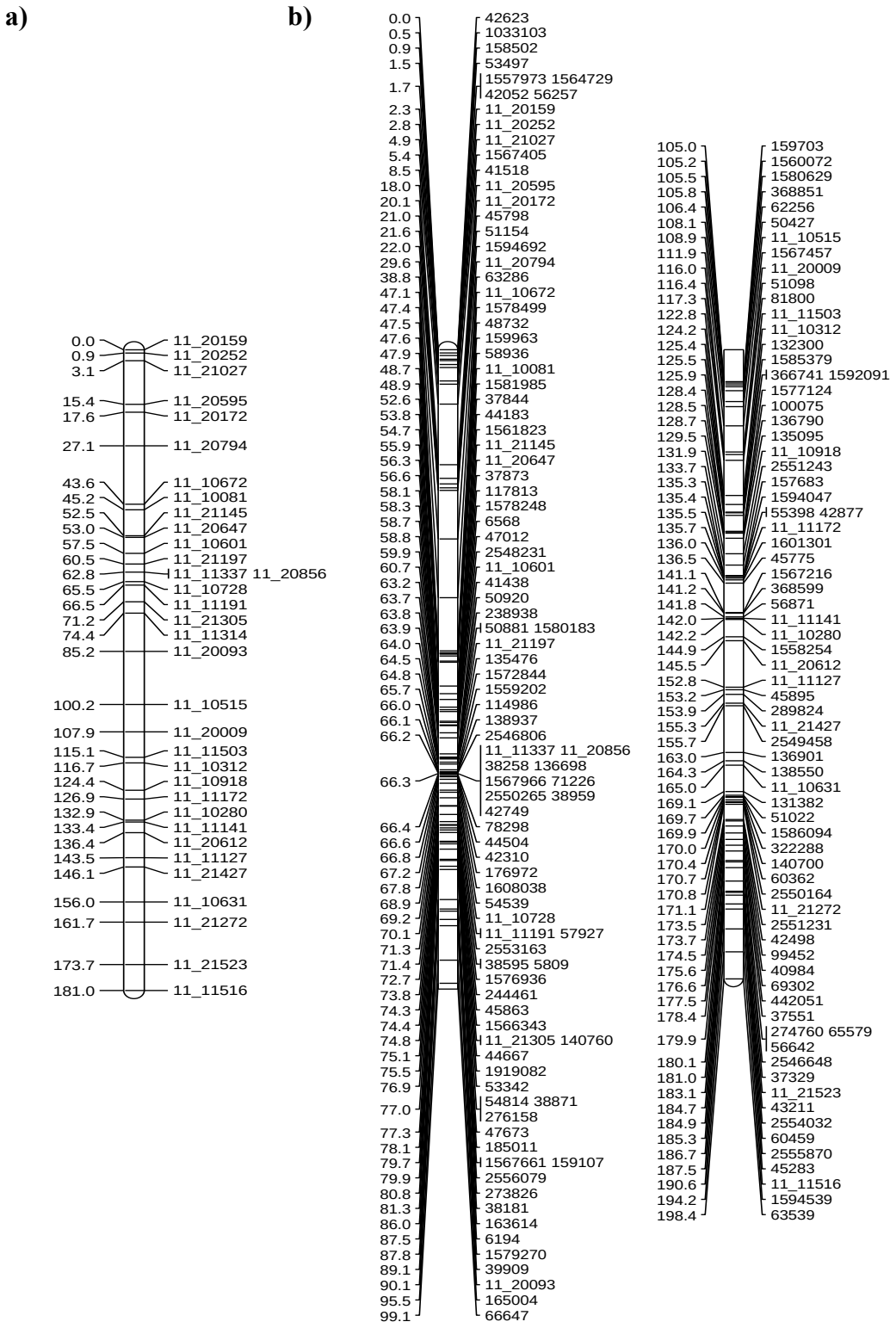

Figure 3.1. Genetic maps of C×T F_7 chromosome 3H. a) Linkage group for 3H with 34 BeadXpress markers. b) Linkage group for 3H with 172 combined 384-SNP array BeadXpress and Genotyping-by-Sequencing markers.

Table 3.1. Genetic maps produced by 384-SNP BeadXpress genotyping.

Population	1H		2H		3H		4H		5H		6H		7H		Total	
	Markers	(cM)	Markers	(cM)	Markers	(cM)	Markers	(cM)	Markers	(cM)	Markers	(cM)	Markers	(cM)	Markers	(cM)
C×T F_5	9	29.1	27	154.2	28	151.8	15	81.2	20	110.5	32	131.5	5	36.4	133	684.8
C×T F_7	12	72.7	27	147.1	34	181.0	20	120.9	25	137.7	31	118.5	5	42.6	154	820.6
A×T F_6	7	55.2	24	159.2	28	159.2	18	97.8	36	126.0	7	50.6	9	69.9	129	717.9

Table 3.2. Genetic maps produced by Genotyping-by-Sequencing.

Population	1H		2H		3H		4H		5H		6H		7H		Total	
	Markers	(cM)	Markers	(cM)	Markers	(cM)	Markers	(cM)	Markers	(cM)	Markers	(cM)	Markers	(cM)	Markers	(cM)
C×T F_5	93	209.3	152	207.2	115	190.4	59	132.9	113	128.0	127	149.5	158	170.9	817	1188.2
C×T F_7	92	180.1	162	191.6	117	154.8	59	128.1	112	121.4	114	108.0	77	84.2	733	968.1

Table 3.3. Genetic maps produced by combined 384-SNP BeadXpress genotyping and Genotyping-by-Sequencing.

Population	1H		2H		3H		4H		5H		6H		7H		Total	
	Markers	(cM)	Markers	(cM)	Markers	(cM)	Markers	(cM)	Markers	(cM)	Markers	(cM)	Markers	(cM)	Markers	(cM)
C×T F_5	104	200.8	179	230.0	143	201.7	77	121.9	127	119.9	143	173.8	163	176.7	936	1224.4
C×T F_7	106	180.5	176	174.2	172	198.4	76	123.7	126	121.7	167	132.5	139	147.4	962	1078.4

3.4 Discussion

The production of genetic maps for the same mapping populations with both the 384-SNP BX Illumina array and the GBS protocol provided an opportunity to compare the two methods. SNP chip arrays have been widely utilised and the production of the BOPA assays (Close et al. 2009) and the iSelect chip (Comadran et al. 2012) have allowed ease of genotyping for a large number of SNPs of interest. GBS technology has only more recently been developed and the pipelines with which to analyse data produced by this method are still being improved upon (Davey et al. 2011).

The three populations used within this study display a wide range of genetic diversity. The common parent within both populations is Tipple, a modern malting variety, which was crossed with both the English landrace Chevallier, and the French cultivar Armelle. The aim of using two populations with the same parental genotypes but of different generations (C×T F_5 and F_7) and separate initial crosses was to allow the validation of any subsequent QTL associated with FHB or agronomic traits. This also provided the opportunity to evaluate how the different genotyping platforms performed with regard to the different levels of possible heterozygosity within the two populations. The A×T population was genotyped using the BX technology only, but gave the opportunity to compare the ability of the 384-SNP set to identify polymorphisms in two diverse populations.

The cultivar optimised 384-SNP array devised by Moragues et al. (2010) was used alongside the Illumina BeadXpress technology to genotype both the A×T and two C×T populations. Using this method a large number of SNPs were identified (55.2% in both the C×T F_5 and F_7 populations and 57.7% in the A×T population,) which were monomorphic between the parental genotypes and were therefore uninformative in the genetic mapping process. Chevallier and Tipple are thought to be genetically diverse (J. Russell, personal communication), so it was surprising that so few polymorphic markers were identified from the 384-SNP assay. A number of lines within C×T F_5 population also appeared to display particularly high levels of heterozygosity (over 20% heterozygous SNP calls per line), leading to the removal of 23 F_5 lines and reducing the population available for mapping to 165 progeny lines. The percentage heterozygosity in the F_5 population was calculated to be 12.6%, which is indicative of an $F_{4:5}$ RIL population. A similar level of heterozygosity was not displayed in either

the C×T F_7 population or the A×T F_6 population, which was thought to be due to the additional cycles of inbreeding that these populations were subjected to. It is possible that the protocols used for each genotyping method may also contribute to the higher levels of heterozygosity seen within the C×T F_5 population. Genomic DNA from pools of five seedlings per line were used to genotype the C×T F_5 and A×T F_6 populations using the BX system, with the aim of accounting for a higher percentage of heterozygosity within the less advanced mapping populations, whilst the C×T F_5 and F_7 populations were genotyped from a single seed per line using the GBS method. It is possible that the process of pooling DNA from multiple seedlings may contribute to the increased heterozygosity displayed within the C×T F_5 BX dataset, however such heterozygosity was not seen in the A×T F_6 population genotyped using the same technique. I subsequently designed KASP markers to validate the genotypic status of the heterozygous C×T F_5 lines as determined by the BX method. Such lines were confirmed to be homozygous, suggesting that several markers had been miscalled by the automated software when analysing the BeadChip data. This illustrates that QTL analysis using the C×T F_5 genetic map can be considered to be as informative as the F_7 map if using the data derived from the GBS genotyping method.

The genetic maps produced using the 384-SNP assay dataset contained a similar number of markers, with 133 and 154 markers in the C×T F_5 and F_7 populations, respectively, and 129 markers in the A×T population. In two spring barley populations (Power × Braemar and Decanter × Cocktail) which were also genotyped using the cultivar optimised 384-SNP subset, 125 and 127 polymorphic SNPs respectively, were identified between the parental lines, of which 122 and 120 SNPs could be mapped (McGrann et al. 2014). Bertholdsson et al. (2015) also used the 384-SNP assay to generate a 196 SNP genetic map for a Psaknon × SLUdt1398//Mona population. However, as the populations presented within this study were generated using more diverse parental lines it might be expected that a greater number of SNPs would have been identified. This suggests that genotyping using the 384-SNP assay is useful for adapted germplasm but is not able to provide additional SNP information when used to genotype diverse parental lines. The map distances generated from the BX SNPs ranged from 684.8cM in the C×T F_5 population, to 820.6cM in the C×T F_7 population, with the marker distribution in both the C×T and A×T populations being uneven. In both populations chromosomes 1H and 7H contained the fewest markers. In contrast,

chromosomes 2H and 3H generally displayed the greatest number of SNPs. This is reflected in the design of the 384-SNP set. SNPs were selected for inclusion in the assay if they were evenly distributed across the genome, with a 10cM maximum interval distance between markers. The frequency of SNPs located on each chromosome was also calculated, with approximately 40 SNPs being attributed to 1H and 7H, and over 70 markers being positioned to 2H and 5H (Moragues et al. 2010). Of the SNPs assayed for 7H, only 11 were identified as being polymorphic in the C×T parental lines and only five of these could be linked at a LOD of 7.0. This resulted in linkage groups which had distances of up to 20cM between markers in both of the C×T populations. This is again comparable to the maps produced using the same genotyping method by McGrann et al. (2014), where chromosome 7H in the Decanter × Cocktail map was represented as three linkage groups, with distances of up to 38cM between SNP markers. Similarly, only 14 SNPs were polymorphic for 7H in the A×T dataset, with nine markers forming a linkage group. Contrastingly, certain chromosomes for which SNPs were represented at a higher frequency in the 384-SNP subset were represented by linkage groups displaying relatively low marker numbers. For example, approximately 50 markers in the subset were assigned to chromosome 6H, of which 31 and 32 were mapped in the C×T F_5 and F_7 populations respectively. However, the A×T 6H linkage map only contained 15 polymorphic 6H markers, of which only 7 were genetically linked using mapping software. Moragues et al. (2010) determined that using an optimised 384-SNP set is generally a more cost effective genotyping method than using a larger 1,536 SNP BOPA1 assay. However, the lack of polymorphic SNPs within the parental genotypes of both populations using the cultivar optimised 384-SNP set resulted in sparsely populated linkage groups, particularly for 1H and 7H. This lack of markers may be due to ascertainment bias. This arises when markers are identified from a relatively small panel of cultivars used to create the SNP assay, which are then not represented at the same frequency in the population which is genotyped (Heslot et al. 2013). Therefore less common polymorphisms are less likely to be detected than frequently occurring polymorphisms. Using a cultivar optimised 384-SNP assay to genotype the landrace Chevallier and the older Armelle variety may have resulted in rarer SNPs being undiscovered. This lack of markers on particular chromosomes may be expected to have an effect when using these linkage maps for QTL analysis. The effect of a QTL is known to be minimised when DNA markers are more than 15cM apart, especially

using single marker analysis methods, resulting in a QTL being less likely to be identified (Collard et al. 2005). This therefore means that FHB or agronomic trait QTL present on some of the chromosomes produced from the 384-SNP genotyping method may be less precisely located or possibly even undetected due to the sparse distribution of markers.

NGS methods should reduce the effects of ascertainment bias as they identify polymorphisms based on the population being genotyped (Rife et al. 2015). The GBS linkage maps generated for the C×T F_5 and F_7 populations contained up to six times more markers than the BX maps, and markers were more evenly distributed throughout the genome. Chromosome 7H which was previously the least represented linkage group in the BX map, was increased from five to 158 markers, suggesting that the lack of markers in the BX map was not due to a lack of polymorphisms between the Chevallier and Tipple lines on this chromosome but due to the SNPs selected in the 384-SNP assay.

Whilst the GBS genotyping method provided a much larger initial number of SNPs than the BX data (8,754 SNPs compared to 384 SNPs in the BX dataset), 82% of these were removed from the mapping dataset through a series of quality control steps to give two robust final sets of 1565 (F_5) and 1577 (F_7) SNP markers . A total of 817 and 733 markers, in the C×T F_5 and F_7 populations respectively, were included in the final genetic maps produced using solely the GBS markers. This attrition rate is similar to that seen in the study by Honsdorf et al. (2014) who identified approximately 41,000 SNPs from initial GBS sequencing of a set of barley introgression lines, a total which was reduced to 3,744 SNPs after data filtering. Mascher et al. (2013) also identified an initial 33,000 SNPs using a two enzyme GBS method, but numbers were reduced to approximately 8,000 SNPs by filtering for minor allele frequency (MAF) and missing data values, and only 1,584 SNPs were successfully incorporated into the final genetic map. Further work by Liu et al. (2014) identified 1,949 reliable SNPs from a total of 461,000,000 sequencing reads within their 138 RIL Golden Promise × Morex GBS dataset, of which only 1,332 SNPs were genetically informative. This evidence suggests that whilst the low coverage GBS method produces genetic information for a large number of SNPs throughout the genome, a high proportion of these will be less reliably genotyped and that using a stringent set of criteria is important for identifying robust SNPs which can used in further applications.

Using the GBS dataset the marker density of the genetic maps increased from approximately one marker every 5cM in the BX map to one marker every 1cM using the GBS data, producing a genetic map of high density. However despite there being an average of 116 and 104 markers per chromosome in the C×T F_5 and F_7 populations respectively, some linkage groups still displayed marker intervals of over 15cM. This observation is not limited to the populations genotyped here, as despite the high density of GBS-derived linkage maps a number of studies have also reported larger than expected distances between markers. For example, the markers surrounding the *ari-e* height QTL identified by Liu et al. (2014) were separated by a distance of 7cM. Similarly, within the 3,000 SNP map created by Igartua et al. (2015) marker intervals of up to 10.5cM were observed, whilst Poland et al. (2012) noted distances of up to 18cM between markers despite the genetic map containing over 9,000 SNPs. This issue is not only confined to barley GBS derived maps, as the bread wheat map produced by Li et al. (2015) contained 3,757 unique SNPs yet had marker intervals of up to 28cM and the durum wheat map created by van Poecke et al. (2013) using a bin-mapping approach noted 38 bins devoid of markers. Even within the relatively small genome of rice, a total of 86 out of 1,550 marker bins were empty in the map produced by Spindel et al. (2013). This lack of even marker distribution in certain genomic regions may correlate with known areas of reduced recombination (Poland et al. 2012), a lack of polymorphism between the parental genotypes (Liu et al. 2014; Igartua et al. 2015) or possibly low read coverage due to less even distribution of restriction enzyme sites (Spindel et al. 2013). The results from the present study combined with the current literature suggest that whilst the GBS method can be used to produce high density linkage maps, a number of factors may still result in regions of low marker coverage during map production.

The advantages of combining different early generation DNA markers into a single map to improve genetic density has been widely demonstrated (Yang et al. 2015). The BX and GBS SNP datasets for the two C×T populations were also combined in an effort to populate the larger intervals between markers with SNPs and to produce the most accurately ordered maps. Merging the datasets allowed the addition of 119 and 229 markers in the C×T F_5 and F_7 maps, respectively, and extended the genetic distance by 110cM in the F_7 population. This represented an increase of up to 10% in map distance and an addition of up to 23% more markers. This inclusion of further

markers not only increased the length of the shortest linkage groups, but also extended some of the most densely populated chromosomes such as 2H and 3H. The marker density was increased from one marker every 1.3cM in the C×T F_7 map to one every 1.1cM, demonstrating that it was possible to improve map resolution even in a well populated GBS map by the addition of the BX SNPs. The total length of the linkage maps produced by combining the BX and GBS SNPs were 1,224.4cM (936 markers) in the F_5 map and 1,078.4cM (962 markers) in the F_7 map. The map lengths produced are comparable to those obtained in other barley GBS studies, for example an introgression map of 55 wild barleys spanning 989.2cM (Honsdorf et al. 2014), the 1,200cM map produced by Liu et al. (2014) from a Golden Promise × Morex population of 138 RILs and also SNP array studies such as the original BOPA1 and BOPA2 map covering 1,099cM (Close et al. 2009). The map produced by Honsdorf et al. (2014) contained a combination of 457 BOPA1 SNPs and 3,744 GBS derived SNPs, the addition of which gave a tenfold increase in resolution compared to the original map created with solely BOPA1 markers. Within the C×T maps, the incorporation of GBS and BX SNPs into a single dataset allowed a larger number of GBS SNPs to be incorporated within linkage groups than in the initial GBS map. For example, a total of 827 GBS SNPs were included in the final C×T F_7 combined map, whilst only 733 were included in the original GBS map, representing an increase of 23.8%. A similar effect was seen by Chutimanitsakun et al. (2011), where 445 RAD markers were initially mapped covering 1,260cM, yet inclusion of 2,383 RFLPs, SSR and SNPs allowed the integration of 463 RAD markers to give a map of 2,846 markers over a total distance of 1,286cM.

Whilst the overall C×T map distances were extended by the integration of markers some of the linkage groups were actually contracted in length by inclusion of the BX SNPs, such as chromosome 2H in the C×T F_7 map which was shortened by 17.4cM through the addition of 14 markers. The expansion of genetic maps are predominantly due to errors in genotyping, which falsely represent double recombination events and cause the distance of a linkage group to be inflated (Cartwright et al. 2007). Error checking in large datasets can be time consuming as it generally involves removing single markers and testing for map distortion, and if a large proportion of markers all possess a low error rate it may not be possible to remove them all from subsequent analysis. In an effort to identify errors during the mapping processes described here,

the markers (BX and GBS data) for both the A×T and C×T populations were analysed using the JoinMap chi-squared analysis function and those which were significantly different from the expected 1:1 ratio and could not be re-coded or were thought to be indicative of double recombination were removed from the analysis. It is possible that the markers which appeared to be under segregation distortion and were removed from the datasets may actually be informative during the QTL mapping process (Xu, 2008) and could be included in subsequent genetic maps to provide more marker loci. The marker orders of subsequent maps were also referenced against the BOPA1 and BOPA2 SNP positions determined by Close et al. (2009) and the Morex reference sequence (IBSC, 2012). However, it appears that there may still have been instances where errors occurred in the ordering of the SNP markers, such as in the F_7 2H linkage group. By incorporating both sets of genotype data into the mapping process it appears that some of these errors have been corrected for, suggesting that the combined BX and GBS maps not only contain a higher density of markers, but are also more accurate and reliable in the order of these markers.

This study allowed the comparison between two genotyping methods, with the aim of producing the most accurate linkage maps for subsequent QTL identification. By utilising both the 384-SNP array and GBS genotyping methods and amalgamating the subsequent SNP data it has been possible to produce high density genetic maps which correlate with the marker order of the barley reference maps. This should enable the more precise identification and positioning of QTL associated with FHB and agronomic traits.

Chapter 4. FHB resistance and the potential for trade-off with agronomic traits in heritage barley

4.1 Introduction

Determination of the genetic resistance of barley and wheat to FHB has primarily been investigated through quantitative trait loci (QTL) mapping approaches. Reported FHB QTL in barley all relate to Type 1 resistance (disease incidence), whilst QTL in wheat have been reported for Type 1 and Type 2 resistance (disease spread within the infected ear). Several methods of inoculation are used within mapping studies, with differing methods being favoured to investigate the separate forms of resistance. In barley the grain-spawn method is the most widely used inoculation technique for QTL studies and involves the distribution of *Fusarium* infected cereal grains on the soil surface (Zhu et al. 1999; Ma et al. 2001; Dahleen et al. 2003; Mesfin et. al 2003; Choo et al. 2004; Horsley et al. 2006; Lamb et al. 2009; Yu et al. 2010; Dahleen et al. 2012). This method mimics the natural infection process observed due to the accumulation of *Fusarium* infected crop debris in the soil from prior harvests, with inoculum being present throughout the growing season. The spray inoculation method (Canci et al. 2004; Nduulu et al. 2007) and the cut-spike test (Hori et al. 2005; Sato et al. 2008) are more labour intensive techniques and involve the spraying of *Fusarium* conidia directly onto the ears during anthesis. These two methods most represent either splash or windborne spore dispersal and can be used to ensure equivalent inoculum application across varieties differing in flowering time (Hori et al. 2005). All three of these methods have been used to identify Type 1 resistance QTL in barley.

Similarly in wheat both the grain-spawn and spray inoculation methods are used to identify QTL for Type 1 resistance (Draeger et al. 2007; Haberle et al. 2007; Schmolke et al. 2008; Srinivasachary et al. 2008; Srinivasachary et al. 2009; Szabó-Hevér et al. 2014). Assessing this form of resistance is inherently more difficult than in barley however, due to the propensity of the fungus to spread through the rachis within the wheat ear to infect adjacent spikelets (Buerstmayr et al. 2009). Type 2 resistance in wheat may be specifically investigated using the single spikelet inoculation method where *Fusarium* conidia are directly injected into a defined area of the wheat ear, with

resistance determined as the rate or extent of fungal spread from the point of inoculation (Buerstmayr et al. 2002; Srinivasachary et al. 2009; Ruan et al. 2012). QTL associated with mycotoxin accumulation, usually identified by quantification of DON within harvested grains, may be detected using the grain spawn, spray inoculation and spikelet inoculation techniques but not by the cut-spike method as the ear is removed from the plant prior to maturity preventing mycotoxin accumulation within the grain (as grain do not develop in the cut spike).

QTL associated with FHB resistance have been located on every chromosome in barley, as demonstrated in Figure 4.1, and also in wheat (Massman et al. 2011; Buerstmayr et al. 2011). The detection of multiple QTL each contributing a low phenotypic effect on FHB resistance within a single mapping population is a common occurrence in both of these cereal species (Buerstmayr et al. 2009). In barley, Ma et al. (2001) detected eight QTL (2HS, 2HL, 3HS, 3HL, 5HS, 5HL, 6HL, 7HS) associated with Type 1 resistance which each accounted for between 7 – 20% of the variance in a Chevron × Stander cross. Similarly, Yang et al. (2005) identified eight QTL (1DL, 2DS, 3BC, 3BS, 4DL, 5AS, 6BS, 7BL) associated with both Type 1 and 2 resistance from a population derived from the wheat cultivars DH181 × AC Foremost, which each accounted for between 6 – 24% of the population variance. QTL detection is often extremely variable and can be highly dependent on the environment and year in which the phenotyping took place. Mesfin et al. (2003) identified 13 barley QTL associated with FHB across six trials within a single year in a Fredrickson × Stander cross, however only three of these QTL were significant across multiple environments.

QTL associated with lower DON concentration have also been identified on every barley chromosome (Massman et al. 2011). In wheat, fewer studies have assessed the potential relationship between FHB and DON, with QTL for DON accumulation being identified on 1AL, 2A, 2DS, 3BS, 4B, 5AS, 5DL (Buerstmayr et al. 2009). QTL associated with FHB resistance and a reduction in DON accumulation in both barley and wheat are often non-coincident. Only five of the eight barley FHB QTL detected by Ma et al. (2001), co-located with the genomic region of QTL for reduced DON accumulation within the grain. Dahleen et al. (2003) located nine FHB QTL in a Zhedar 2 × ND9712//Foster barley population, yet were only able to detect three QTL associated with lower DON concentration which co-located with FHB QTL. In

wheat, Somers et al. (2003) used a Wuhan × Nyu Bai DH population to identify four QTL associated with both Type 1 and 2 FHB resistance and also identified three genomic regions associated with reduced toxin concentration, only one of which was coincident with an FHB QTL.

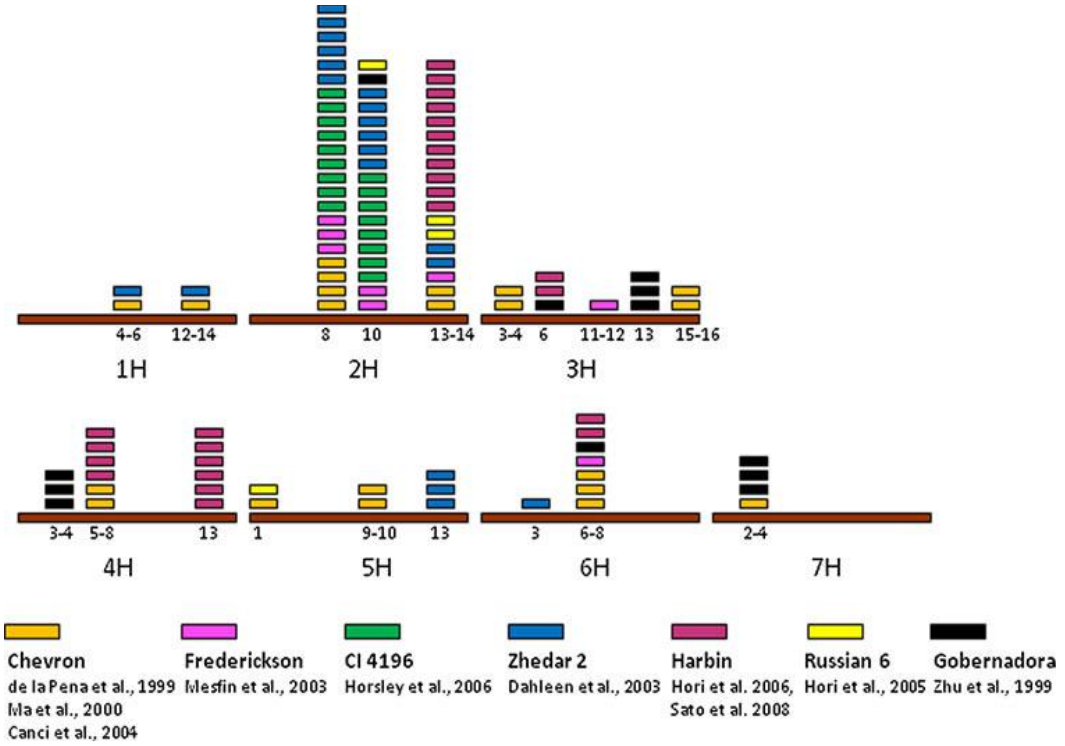

Figure 4.1. Quantitative trait loci identified in various barley cultivars and the bin positions on the specific chromosomes. Each square represents a different environment within a study where a QTL was detected and each colour represents the cultivar from which resistance was contributed. (Taken from Massman et al. 2011).

FHB resistance and DON accumulation QTL are also frequently coincident with QTL for agronomic traits. Plant height and heading date (HD) have been particularly implicated as having a role in FHB resistance in barley and wheat, whilst QTL for ear morphology traits are also frequently associated with FHB (Bai and Shaner, 2004). In barley, both row type and flowering type are also thought to be highly influential on disease susceptibility (Hori et al. 2005). The co-location of QTL for FHB and

agronomic traits is often transient across environments and trial years in both wheat and barley, suggesting that much of the resistance associated with agronomic characteristics is due to disease escape (Buerstmayr et al. 2009). However, determining the potential for either linkage or pleiotropy between genes for agronomic traits and disease resistance is important for informed cereal breeding.

In both barley and wheat, taller cultivars are thought to be more resistant than those which have shorter stature (Srinivasachary et al. 2009), which has been suggested to be due to the microclimate of the shorter lines being more conducive to *Fusarium* infection as shorter cultivars may be subject to increased humidity favouring disease development. The reduced distance between leaf layers observed in shorter plants may also aid the dispersal of splash borne conidia, further reducing Type 1 resistance (Buerstmayr and Buerstmayr, 2015). This poses a trade-off between the short height phenotype which is favoured in agriculture and the potential for breeding for FHB resistance. Numerous studies in barley have identified major FHB QTL which are coincident with those for plant height. A study using two sets of DH lines, derived from a three-way Zhedar 2 × ND9712//Foster cross, identified two QTL with resistance derived from Zhedar 2, at 62 – 70cM and 106 – 122cM on 2H which co-located with plant height (Dahleen et al. 2012). Zhu et al. (1999) identified several potent FHB resistance QTL on 1H, 3H and 4H in a Gobernadora × CMB643 population, which again were all coincident with height QTL. Of the eight FHB QTL identified by Ma et al. (2001), four were co-incident with plant height (2H, 3H, 5H and 7H) QTL and the other five co-located with other morphological traits. Yu et al. (2010) detected a potent FHB QTL accounting for 14% of the phenotypic variance within a Zhenongda 7 × PI 643302 cross on 2H, however the QTL interval also overlapped partially with a minor QTL for height. A single QTL for FHB resistance was detected at the centromeric region of 5HS in a Russia 6 × H.E.S 4 population (Hori et al. 2005), with resistance derived from Russia 6, which co-located with a QTL for height. GWAS studies of two-row and six-row barley CAP (Co-ordinated Agricultural Project) lines by Massman et al. (2011) also identified an association between plant height and FHB resistance, with QTL on 4H at 24 – 36cM and 6H at 42 – 67cM co-locating with QTL for height. An association between FHB and plant height has also been demonstrated in wheat, with QTL for both Type 1 and Type 2 resistance on 1A, 2BS, 2DS, 3A, 4DS, 5BL coinciding with height QTL (Schmolke et

al. 2008; Gervais et al. 2003; Ban and Handa, 2008; Mao et al. 2010; Draeger et al. 2007; Srinivasachary et al. 2008; Paillard et al. 2004). A major QTL associated with Type 1 resistance to FHB was detected in a Soissons × Orvantis DH population, which co-located with a major QTL associated with height at the *Rht-D1* locus on 4DS (Srinivasachary et al. 2008). The Soissons allele was associated with both increased Type 1 resistance and increased plant height at this locus. Interestingly, the *Fhb1* QTL on 3BS which is associated with potent Type 2 resistance and is derived from the Chinese cultivar Sumai 3 does not appear to have any major associations with plant height (Xie et al. 2007; McCartney et al. 2007; Pumphrey et al. 2007; Buerstmayr et al. 2009). The identification of QTL in both barley and wheat which do not always coincide with those for plant height suggests that resistance seen in tall varieties is not solely due to disease escape.

The role of HD has also been implicated in FHB resistance with a number of QTL being identified on wheat chromosomes, such as 2AL, 6DL, 7AL and 7BS, which co-locate with QTL for FHB severity in Arina × Forno, Dream × Lynx and Cansas × Ritmo populations (Liu et al. 2013; Paillard et al. 2004; Klahr et al. 2007; Haberle et al. 2007). Studies in barley have identified chromosome 2H as being a particular genomic region associated with both FHB and HD QTL. A study by de la Pena et al. (1999) identified a potent QTL for FHB between markers *MWG887 – ABC306* on 2H which accounted for up to 14% of the phenotypic variation. This FHB QTL coincided with a QTL for HD also detected in the same marker interval. Mesfin et al. (2003) detected three further QTL associated with FHB on 2H, between the markers *Ebmac0521a – Bmag0140*, *Vrs1 – Bmag0125* and *ABC252 – ABC153*. One of the major QTL in this region, located between *Ebmac0521a – Bmag0140* markers, was also associated with later heading. QTL analysis of two mapping populations by Canci et al. (2004), using two partially susceptible lines from the Chevron × M69 population crossed to the elite cultivars Stander and M81, detected QTL on 2H for both resistance to FHB incidence and DON accumulation within a 6.7cM region. The Chevron allele at this locus reduced FHB susceptibility by approximately 42%, but increased the heading date by 3.8 days. An FHB QTL in the same region of 2H (Qrgz-2H-8) was also identified by Lamb et al. (2009) from a C93-3230-24 × Foster cross, which again co-located with both a HD QTL and also a QTL for plant height in the *hvm23 – abc162* marker region. A further HD QTL flanked by the markers

ABG46c-MWG865 at the Qrgz-2H-8 region on 2H, where HD correlated negatively with FHB severity, was mapped to the same region as the *Early maturing 6* (*Eam6*) gene (Horsley et al. 2006), suggesting that the QTL detected may actually be *Eam6*. Previously HD was thought to have a pleiotropic effect on disease resistance, with later heading cultivars being exposed to the *Fusarium* inoculum present in the environment for a shorter period of time and therefore displaying less severe FHB symptoms (Dahleen et al. 2003). Nduulu et al. (2007) developed a NIL population derived from a CM62 × M69 cross to fine map the relationship between FHB and HD at the Qrgz-2H-8 region to determine whether disease resistance was due to pleiotropy or linkage with HD associated genes. The authors determined that the QTL for FHB resistance displayed a close association with the *GMS03* marker, whilst the HD QTL was more closely associated with the *GBM1023 – Bmac0132* marker interval which was 1.0cM away from the *GMS03* marker. The same study also identified a resistant yet early-heading recombinant, suggesting that the relationship between FHB resistance and HD is actually due to very close linkage at the Qrgz-2H-8 region of 2H and not due to the pleiotropic effect of a HD gene.

Other important agronomic traits, such as row type in barley, have been associated with FHB severity demonstrating that there are multiple trade-offs to be considered when breeding for resistance. The *Six-rowed spike 1* (*Vrs1*) gene, which acts with the *Intermedium-C* (*Int-C*) gene to determine row type, is located on 2H (Ramsay et al. 2011). The *Vrs1.b* wild-type allele confers a two-row phenotype and is associated with FHB resistance, whilst six-row cultivars (*vrs1.a*) are thought to be more susceptible (Bai and Shaner, 2004). A study by Mesfin et al. (2003), using a mapping population derived from a two-row Fredrickson and six-row Stander cross, identified two FHB QTL on 2H. One of these was associated with HD, whilst the other was coincident with *Vrs1* at the *Vrs1 – Bmag0125* interval. An FHB QTL which was coincident with *Vrs1* and a major QTL for HD was also identified using the 125 RIL population derived from a Russia 6 (two-row) and H.E.S 4 (six-row) cross developed by Hori et al. (2005). It is possible that the ear morphology of six-rowed cultivars is more conducive to *Fusarium* infection than that of two-row varieties, either by providing a larger surface area for the deposition of inoculum or for the collection of water following rainfall, which would provide a more humid microclimate for pathogen growth (Yoshida et al. 2005). However, as the *Vrs1* locus appears to be very close to

a major HD QTL, as demonstrated in multiple mapping populations (Dahleen et al. 2003; Mesfin et al. 2003; Hori et al. 2005), it has not yet been possible to fully determine whether the effect of row type on FHB resistance is due to pleiotropy or linkage with *Vrs1*. Interestingly, Massman et al. (2011) also detected two co-locating QTL for DON accumulation and HD which were close to *Vrs1* in the six-row CAP population, suggesting that within six-row populations there may be a closely linked HD effect within the region of *Vrs1*. The development of a NIL population to precisely map both FHB and row type QTL within the *Vrs1* region may be necessary to determine the relationship between FHB and *Vrs1* on 2H.

The long arm of 2H is also the location of the *cly1*/*Cly2* locus which confers cleistogamy, or closed flowering, in barley (Wang et al. 2013). An FHB QTL was identified within 1.7cM of the *cly1*/*Cly2* locus in a study by Hori et al. (2005), whilst QTL for FHB resistance were coincident with the cleistogamy locus in all five of the RIL populations investigated by Sato et al. (2008). Anther extrusion is associated with increased Type 1 resistance in wheat, as retained or partially extruded anthers are thought to provide a favourable substrate within the floret for *Fusarium* colonisation (Lu et al. 2013). Closed flowering may also provide another means to reduce FHB susceptibility. However, Dahleen et al. (2012) also studied the effect of the flowering type on resistance yet were unable to identify any QTL co-locating with the *cly1*/*Cly2* locus, with the authors noting that disease severity in closed or open flowering lines appeared to differ between environments. Yoshida et al. (2007) demonstrated that cleistogamous cultivars display increased resistance to infection compared to chasmogamous (open flowering) varieties when inoculation occurs at anthesis, however this resistance was lost by 10 days post-anthesis, when both cleistogamous and chasmogamous cultivars display similar levels of susceptibility.

FHB resistance has also been demonstrated to be correlated with other characteristics such as glume length, spike density, floret size and spike angle in barley (Zhu et al. 1999; Ma et al. 2001; Choo et al. 2004; Hori et al. 2005; Horsley et al. 2006). The major QTL associated with FHB on 2H was coincident with those for inflorescence density and lateral floret size in a study by Zhu et al. (1999), as was a QTL for lateral floret size on 4H which also co-located with a QTL for DON. Ma et al. (2001) identified a spike angle QTL on 2H at *Xcdo373 – Xcdo684b*, which overlapped QTL for lower FHB incidence and DON concentration, and also two QTL associated with

the number of nodes on the rachis on 1H and 2H which co-located with QTL for DON. Increased spikelet density within the ear may provide a more favourable microclimate for fungal proliferation, whilst a more upright spike angle may promote water accumulation in the ear following rainfall (Yoshida et al. 2005). Increased floret size may simply provide a larger surface area for inoculum to collect. In wheat, narrow flower opening and compactness of the ear have also been associated with FHB (Gilsinger et al. 2005; Schmolke et al. 2005). A potent FHB QTL on 2B explaining 29% of the phenotypic variation which was associated with narrow flower opening in a Patterson × Goldfield cross (Gilsinger et al. 2005). Such studies in both barley and wheat illustrate the importance of ear morphology as a potential means of disease escape.

The results of QTL and association studies illustrate the complexity of breeding for genetic resistance to FHB, as a trade-off between resistance and a number of favourable traits is often evident. In the current study, two separate mapping populations were developed from a cross between the significantly FHB resistant, yet tall, heritage Chevallier parent and the short susceptible parent Tipple. The aim of this study was to phenotype both of these populations for FHB susceptibility, plant height, HD and other characteristics to determine whether the resistance of Chevallier conferred a potential trade-off with agronomic traits, therefore affecting the potential of such resistance to be introgressed into elite barley cultivars. An additional mapping population, derived from an Armelle × Tipple cross, was also phenotyped to evaluate the possibility of a trade-off in another FHB resistant cultivar.

4.2 Methods and materials

4.2.1 Production of Fusarium inoculum

DON producing *F. culmorum* Fu42 was grown on V8 agar (9 g bactoagar, 50 mL V8 vegetable juice in 450 mL deionized water) for 14 days at 20^{o}C. Small squares of agar (1cm) were added to flasks of sterilized oat grains and kept at room temperature for 3 – 4 weeks. The conidia were harvested by adding SDW to each flask and filtering the solution through muslin, before centrifuging for 5 min at 3000g. The remaining pellet

was washed and re-suspended with SDW at a concentration of 1×10^6 conidia ml^{-1} and stored at -20°C until use.

4.2.2 Chevallier × Tipple F_5 phenotyping

The 188 line F_5 Chevallier × Tipple population was sown in a whole plot, single replicate design containing 18 randomized controls, including the parental lines, at the JIC field trial site in 2013. The population was scored for multiple agronomic traits. Height (distance from the soil to the tip of the barley spike, excluding awns at Zadoks growth stage (GS) 83 (Zadoks et al. 1974)) and heading date (number of days from initial sowing to Zadok's GS 55) were scored. Growth habit (GH) was recorded on a 1 – 6 scale at Zadok's GS 20, (1 = very prostrate, 6 = very erect) and tillering was scored on a 1 – 9 scale (1 = very poor, 9 = very good). Mildew was scored on a 1 – 9 scale (1 = no mildew, 9 = all upper leaves more than 50% infected) on five score dates from Zadok's GS 14 – 39, and a mean value for each RIL was calculated. Spike angle was recorded using the UPOV (1994) 1 – 9 scale (1 = erect, 9 = recurved). Physiological leaf spotting (PLS) was observed as dark brown spots on both sides of the leaf, and scored on a 1 – 10 scale (1 = no spotting, 10 = more than 50% of leaves covered). To investigate FHB susceptibility plots were sprayed 7 – 8 times from mid-anthesis with *F. culmorum* Fu42 conidial suspension ($0.5x10^5$ conidia per ml^{-1} and 0.05% Tween 20) using a knapsack sprayer and were mist irrigated to increase humidity and promote fungal infection. Spraying was continued throughout anthesis to ensure that all emerging spikes were inoculated, as *Fusarium* species are not known to spread within the ear in barley. FHB severity (percentage of disease per plot) was scored at four separate time points, beginning 2 weeks after the first inoculation. Grain was hand-harvested from each plot for subsequent DON analysis.

A further FHB trial containing the 188 C×T F_5 lines in a three row split plot design, with two replicates per line, was sown in spring 2013 at KWS, Thriplow, UK. Height and HD was recorded at this site. FHB scores were taken on a single date with each replicate being scored by a different individual. The phenotype data for each replicate was therefore analysed separately as two trials (designated KWS1 and KWS2) to account for any differences in scoring.

4.2.3 Chevallier × Tipple F_5 mildew seedling inoculation

The C×T F_5 population, Chevallier, Tipple and the susceptible control line Manchuria were sown three seeds per 5 x 5 cm pot and grown at 18^{o}C in a CER. Lines were randomised within each tray, with 30 pots per tray including pots of Chevallier, Tipple and Manchuria. The *B. graminis* isolate CC148 was maintained on separate pots of Manchuria seedlings at 18^{o}C. After 9 days, seedlings were inoculated with *B. graminis* by distributing spores from the inoculation pots onto the seedlings, which were then kept at 18^{o}C with high humidity for 24 h. After 7 days the 1st leaf of each seedling was scored separately for mildew and necrosis symptoms, using a 0 – 4 scale (0 = no mildew/necrosis, 4 = 100% of leaf covered). The experiment was repeated twice.

4.2.4 Chevallier × Tipple gibberellic acid (GA) response assay.

The protocol of Gale and Gregory (1977) was followed. Chevallier and Tipple seeds were sown randomly in two P40 Pak trays (20 seeds per line, per treatment) and grown in a CER (18/15^{o}C under a 16 h/8 h light-dark photoperiod). Seedlings were watered as necessary with either 10ppm gibberellic acid (GA_3) solution (Sigma Aldrich, product G7645) or control treatment of H_2O. Measurements (total plant height, length from first to second leaf node, length from second to third leaf node) were recorded at 31dpi and the percentage difference in height between the GA_3 and control treatment for each line was calculated. The experiment was conducted once.

4.2.5 Chevallier × Tipple F_5 phytase analysis

A sub-set of 105 lines from the C×T F_5 population were selected on the basis of seed availability and were milled for subsequent analysis of the phytate content of the flour. Inositol phosphate levels of these samples were analysed by HPLC. The peak areas associated with the presence of inositol 1,3,4,5-tetrakisphosphate (IP_4), two isomers of inositol pentakisphosphate (IP_{5a} and IP_{5b}) and phytate (*myo*-inositol-(1,2,3,4,5,6)-hexakisphosphate or IP_6) were measured. Five replicates of the parental lines were

included, with a single replicate for the RILs. This work was conducted by the group of Dr. Charles Brearley at the University of East Anglia, UK.

4.2.6 Chevallier × Tipple F_7 phenotyping

The 188 line C×T F_7 population developed at JIC was sown in a whole plot single replicate design containing 12 randomized controls, including the parental lines, at JIC in 2014. The population was inoculated and scored as in the C×T F_5 trial in 2013. Phenotype data for height and HD and mildew severity (two score dates) was also recorded.

A further trial with the same population was sown at JIC in 2015, using a split plot two replicate design also containing 12 randomized controls. The population was inoculated as described in 2013. Height, HD, tillering, GH, PLS and mildew severity were scored as in the C×T F_5 2013 trial. The population was scored for FHB as in 2013 and grain was hand harvested for DON toxin analysis.

4.2.7 Armelle × Tipple F_6 phenotyping

From the Armelle × Tipple F_6 population developed by Syngenta, 198 lines from the total 250 RIL population were selected on the basis of seed availability. These lines were sown in a randomised whole plot single replicate design, containing the parental controls in 2013 at NIAB, Cambridge, UK. The population was inoculated from mid-anthesis with an *F. culmorum* Fu42 conidial suspension at $0.5x10^5$ conidia per ml^{-1} and was scored for FHB at two separate time points, beginning 2 weeks after the first inoculation. FHB measurements were recorded as the percentage of ears infected per plot. Height was also recorded.

The same population was sown in a randomised whole plot single replicate design also containing the parental controls at the JIC field trial site in 2014. The population was inoculated as in the C×T F_5 trial in 2013. The population was scored for FHB severity at two separate time points, beginning 2 weeks after the first inoculation. Height and HD were also recorded.

4.2.8 DON analysis

The same subset of 105 lines used in the C×T F_5 phytase assays were selected from the FHB trial at JIC in 2013 for DON analysis. The DON concentration of four replicates of each of the parental lines from the C×T F_7 FHB trial in 2014 was also analysed, however the levels were so low that the RIL population was not tested. The entire 188 C×T F_7 RIL population from the 2015 JIC FHB trial was also analysed for DON accumulation. From the C×T F_5 2013 trial five replicates of each parent were analysed, whilst for the C×T F_7 2015 trial four replicates were analysed. A single replicate per RIL, per population, was analysed. A sample of grain (~40g) from each line was milled to gain a representative sample for each plot. The DON ELISA assay was carried out using a Ridascreen Fast DON ELISA kit (R-Biopharm) and the initial DON extraction was conducted as per the manufacturer's instructions. Mycotoxin analysis of the C×T F_7 population was conducted by M. Collins and J. Nicholson (JIC).

4.2.9 Statistical analysis

The analyses of variance (ANOVA) for phenotypic traits recorded during the field trials were conducted separately for each environment by means of a general linear model (GLM) within Genstat 16th edition (Lawes Agricultural Trust, Rothamsted Experimental Station, UK), to account for the effect of line, row (within the field) and replicate. The analyses of variance for FHB susceptibility were also analysed separately for each environment using a GLM to account for the effect of score date, line, row and replicate. Disease severity was found to differ across environments therefore combined analyses of variance were not conducted. Spatial analysis was not performed on the experimental data due to the single replicate nature of the trials. The mildew CER experiments were analysed using a GLM to account for experimental, tray and line variation, whilst a two-sample t-test was used to compare the parental lines for both the DON accumulation values and the inositol phosphate measurements. A simple linear regression was fitted for FHB and DON values for both the 2013 and 2015 trial data.

4.2.10 QTL analysis

Genstat 16th edition (Lawes Agricultural Trust, Rothamsted Experimental Station, UK) was used for QTL analysis. The combined 384-SNP BeadXpress and Genotyping-by-Sequencing genetic maps were used for the C×T F_5 and F_7 populations, whilst the 384-SNP BeadXpress genetic map was used for the A×T F_6 population. Predicted mean values calculated within a GLM in Genstat were used for the phenotype data for each trait, except for the C×T F_5 and F_7 DON accumulation data and the C×T F_5 phytase (inositol) data where the raw data values were used. Traits were analysed as a single trait linkage analysis using the Kosambi mapping function and LOD threshold of 3.0 was used to detect significant QTL. QTL analysis of the Chevallier × Tipple F_5 and F_7 populations and the Armelle × Tipple F_6 population was initially performed using a maximum step size of 10cM along the genome for QTL detection. The analysis was subsequently repeated using a maximum step size of 2cM to determine if QTL could be more precisely located. However, reducing the step size affected only the size of the QTL interval, both increasing and decreasing it, but did not affect the location of the peak QTL marker. Therefore, all further reported QTL for all three populations were generated as in the original analysis. Simple interval mapping (SIM) was used for the initial QTL search, followed by composite interval mapping (CIM) to finalise the QTL location using the detected candidate QTL as co-factors. A final QTL model was then fitted to produce the estimated QTL effects. QTL images were produced using MapChart.

4.3 Results

4.3.1 Chevallier × Tipple F_5 phenotyping

In all three *Fusarium* inoculation experiments (JIC, KWS1, KWS2) the parental line Tipple consistently displayed the characteristic symptoms of FHB, with multiple *Fusarium* infected kernels per spike (Figure 4.2), whilst disease was mainly absent in Chevallier. FHB disease severity at the KWS1 and KWS2 trials was much lower than that observed at the JIC site. Within the GLM, score date, line and row were all deemed to have significant effects on FHB at the JIC trial ($P < 0.001$) (Appendix, Table A.9). Neither line nor row were significant at KWS1 ($P = 0.255$ and 0.628, respectively,

Appendix, Table A.10). The positional effect of row was significant at KWS2 (P = 0.023) but again line did not affect FHB severity (P = 0.124) (Appendix, Table A.11). The predicted mean FHB score for Chevallier ranged from 0.25% in at KWS1, to 0.87% in the JIC trial (Table 4.1), whilst for Tipple ranged from 12.3% at KWS2 to 17.6% at JIC. The difference in predicted mean FHB scores between the parental lines was significant in all three datasets at the P <0.01 level or higher (Table 4.1). The mean FHB scores for the RILs were 7.2, 3.4 and 4.7% in the JIC, KWS1 and KWS2 trials respectively, illustrating the lower disease incidence in both of the KWS trials. (Table 4.1).

Figure 4.2. *Fusarium culmorum* Fu42 isolate inoculated Chevallier (left) and Tipple (right) heads from the 2013 John Innes Centre field trial. Scale bar = 1cm.

Line had a significant effect on plant height in all three trials (P < 0.001 at KWS1 and KWS2, P = 0.017 at JIC, Appendix Tables A.12 – A.14). The row effect was not significant at JIC (P = 0.793), but was at both KWS1 and KWS2 (P = 0.034 and 0.020, respectively). Tipple consistently displayed a short height phenotype throughout all three trials (Table 4.1). The difference in height values between the two parental lines

was significant in all three datasets at the $P = 0.01$ level (Table 4.1). The mean heights for the RILs were 112.5, 110.1 and 111.2cm in the JIC, KWS1 and KWS2 trials respectively (Table 4.1).

Within the GLM, the effect of line on HD score was significant in all three trials ($P < 0.001$ at KWS1 and KWS2, $P = 0.010$ at JIC, Appendix Tables A.15 – A.17). The row effect was deemed significant at JIC ($P = 0.011$), but not at either KWS trial ($P = 0.144$ and 0.286 at KWS1 and KWS2 respectively). Tipple took significantly fewer days than Chevallier to reach head emergence in all three trials (Table 4.1). The RIL plots emerged earlier at the JIC trial site in 2013. The mean HD scores for the RILs were 106.0, 110.0 and 110.0 days at JIC, KWS1 and KWS2 respectively, (Table 4.1). As the range in HD scores in the RILs exceed the range of the parents, it is probable that both of the parental lines contribute towards HD.

At the JIC trial site phenotype data for GH, tillering, PLS and spike angle was collected. The presence of *B. graminis* within the field resulted in natural powdery mildew infection, allowing disease severity to also be recorded. Significant differences in predicted mean score values for the parental lines were observed for GH, PLS and mildew (Table 4.1).

Table 4.1. Predicted mean values from general linear modelling of phenotypic traits at each trial site for Chevallier and Tipple, and the range of predicted means for the 188 C×T F_5 recombinant inbred lines.

			Parents		RILs		
Trait	**Environment**	**Year**	**Chevallier**	**Tipple**	**Mean**	**Range**	**t- probability***
Height	JIC	2013	144.5	79.1	112.5	71.0 – 152.0	0.002
Height	KWS 1	2013	138.5	85.0	110.1	80.0 – 160.0	0.010
Height	KWS 2	2013	129.0	84.0	111.2	80.0 – 155.0	0.010
Heading date	JIC	2013	109.0	105.0	106.0	100.0 – 116.0	0.002
Heading date	KWS 1	2013	113.0	111.0	110.0	103.0 – 120.0	0.046
Heading date	KWS 2	2013	114.0	110.0	110.0	102.0 – 121.0	0.030
FHB	JIC	2013	0.9	17.6	7.2	1.5 – 23.0	<0.001
FHB	KWS 1	2013	0.3	15.8	3.4	0.5 – 10.0	<0.001
FHB	KWS 2	2013	0.5	12.3	4.7	0.0 – 15.0	0.002
Growth habit	JIC	2013	4.0	3.0	3.0	1.0 – 6.0	0.042
Tillering	JIC	2013	6.0	7.0	6.0	2.0 – 9.0	0.053
Mildew	JIC	2013	6.0	4.0	5.0	2.0 – 9.0	0.048
Physiological leaf spotting	JIC	2013	7.0	6.0	6.0	1.0 – 10.0	0.045
Spike angle	JIC	2013	3.0	2.0	3.0	1.0 – 5.0	0.050

* The statistical significance of the difference between predicted mean scores for Chevallier and Tipple were calculated by t-probabilities within the GLM.

The level of DON accumulation in 105 of the C×T F_5 RILs at the JIC trial was investigated with the aim of identifying whether reduced FHB symptoms also correlated with a reduction in DON concentration. The mean DON content of the milled grain for Chevallier was 0.4ppm, whilst for Tipple it was 14.9ppm. The mean values for the parental lines were significantly different at the $P = 0.025$ level. The mean DON accumulation values in the RILs calculated from one replicate was 3.7ppm, with a range between 0.1 – 15.8ppm. An R^2 value of 0.206 was determined for the relationship between the FHB score from the JIC trial and the DON values calculated from the ELISA. This indicates a weak positive correlation between the visual symptoms of FHB recorded and the subsequent levels of DON accumulation within the grain.

Inositol phosphate analysis was undertaken on the same sub-set of the C×T F_5 RILs as used for the DON accumulation analysis. The mean peak areas for IP_{5a} and IP_{5b} were determined to be significantly different between Chevallier and Tipple (Table 4.2). The peak area values for the RILs were lower than the mean peak areas for the parental lines, but were only calculated from a single replicate which may account for this discrepancy.

Table 4.2. The mean peak areas associated with inositol phosphates for Chevallier and Tipple, and the range of peak areas for 105 C×T F_5 recombinant inbred lines.

	Means		**Range**	
Trait	**Chevallier**	**Tipple**	**RILs**	**t- probability***
IP_4	347148	318882	65022 – 193860	0.357
IP_{5a}	462524	127849	1090 – 20318	0.002
IP_{5b}	653283	767112	8369 - 22719	0.020
IP_6	2899245	2344212	824870 – 1504600	0.094

* The statistical significance of the difference between peak area values for Chevallier and Tipple was calculated from a t-test.

To investigate the resistance of the C×T F_5 RILs and the parental lines to powdery mildew infection in a controlled environment, two seedling inoculation experiments

within a CER were conducted. Symptoms of mildew and necrosis appeared to be segregating within the population so were scored separately. There was no significant effect of experiment ($P = 0.174$) on mildew severity, whilst the experiment – tray interaction and the effect of line were determined significant at the $P < 0.001$ level (Table 4.3). As with the field environment, Chevallier displayed more severe mildew symptoms than Tipple, with pustules covering a larger proportion of the Chevallier leaf surface. Very few mildew pustules were observed on Tipple leaves. Predicted mean scores of 2.0 and 0.0 for Chevallier and Tipple, respectively, were obtained from the GLM, with a score of 2.5 for the susceptible control line Manchuria. T-probabilities were calculated and the mean scores for Chevallier and Tipple were found to be significantly different ($P < 0.001$), whilst the scores for Chevallier and Manchuria were not ($P = 0.164$). The predicted mean scores for the RILs ranged between 0.0 – 3.0.

Table 4.3. Analysis of variance for mildew scores from two *B. graminis* seedling inoculation experiments, calculated within a general linear model.

Term	**d.f**	**m.s**	**v.r**	**F.pr**
Experiment	1	0.48	1.86	0.174
Experiment.Tray	12	1.27	4.93	<0.001
Line	148	1.60	6.23	<0.001
Residual	172	0.26		
Total	333	0.89		

Necrotic symptoms were also scored in the two experiments. The effect of experiment and the experiment – tray interaction were not significant ($P = 0.052$ and 0.583 respectively), whilst line had a significant effect at the $P < 0.001$ level (Table 4.4). Only mild necrotic symptoms were observed in the control lines, with a predicted mean score of 0.30 in Tipple, 0.04 in Chevallier and 0.01 in Manchuria, corresponding to less than 25.0% of the leaf surface displaying necrosis. None of these values were significantly different. The predicted means for the RILs ranged from 0.0 – 2.0.

Table 4.4. Analysis of variance for necrosis scores from two *B. graminis* seedling inoculation experiments, calculated within a general linear model.

Term	d.f	m.s	v.r	F.pr
Experiment	1	1.09	3.82	0.052
Experiment.Tray	12	0.25	0.87	0.583
Line	148	0.55	1.94	<0.001
Residual	172	0.28		
Total	333	0.40		

4.3.2 QTL analysis of Chevallier × Tipple F_5 traits

Two QTL associated with plant height were identified at the JIC site (Table 4.5). The major height QTL was identified on the long arm of 3H at position 139.8cM (Figure 4.5) with a LOD score of 35.5 and accounted for 68.0% of the variance. A minor QTL was located at 32.6cM on 3H. For both of these QTL the contributing parental allele came from Chevallier, which was expected due to its tall height. Two height QTL were also detected at KWS1 and KWS2 which mapped to exactly the same locations as the JIC height QTL, giving confidence in the accuracy of the phenotype data collected at both trials.

QTL for HD were mapped to chromosomes 3H and 7H in the JIC dataset. A major QTL was identified at 139.8cM on 3H, corresponding to marker 11_11172 (Table 4.5), with a LOD score of 15.7 and explaining 34.5% of the variance. This QTL therefore co-localises with the major 3H height QTL identified in both the JIC and KWS datasets. A further HD QTL was located on 7H at position 28.7cM (Figure 4.7). The late HD phenotype was contributed to by both parents, with Tipple providing the high value (later) allele at the 3H QTL and Chevallier contributing the later allele at the minor 7H QTL (Table 4.5). This possible additive effect may explain why several of the RIL lines showed significantly later (higher) predicted mean HD scores than either of the parental lines (Table 4.1). The HD QTL detected at KWS1 and KWS2 were located at the same map positions as in the JIC data (Table 4.5), along with an additional minor QTL on 2H with the later allele contributed by Chevallier.

A single major QTL associated with FHB was identified using the JIC dataset with a LOD score of 5.6. This was located on 6H at position 114.5cM corresponding to

marker 11_11246 (Figure 4.6). Up to 15.3% of the phenotypic variance within the dataset was accounted for by this QTL and higher levels of disease were associated with the Tipple allele (Table 4.5), illustrating that resistance was being provided by Chevallier. No QTL associated with FHB could be identified from either of the KWS datasets. This may be due to the low disease pressure observed within both of the replicates at the KWS1 and KWS2.

Phenotype data from ELISA assays were used to identify any QTL associated with DON accumulation. A single QTL was detected on 6H at position 119.5cM, accounting for 10.5% of the variance within the RIL population. Susceptibility to DON accumulation was associated with the allele contributed by Tipple. The QTL associated with DON accumulation co-located with the 6H FHB QTL (Figure 4.6).

QTL for GH, tillering and spike angle all co-located at position 139.3cM (marker 11_11172) on 3H corresponding to the location of the major height and HD QTL (Figure 4.5). A QTL for PLS was also detected on 3H at position 144.5cM. QTL associated with powdery mildew were identified on 1H, with a major QTL at 11_10332 at position 43.9cM (Figure 4.3). A single QTL for IP_{5a} and two QTL for IP_{5b} were identified. The IP_{5a} QTL was located on 3H at position 23.2cM and the IP_{5b} QTL were located on 1H at 29.1cM and 6H at 104.1cM (Table 4.5). It was not possible to identify any QTL associated with IP_4 or IP_6.

Table 4.5. Quantitative trait loci identified from the 188 C×T F_5 recombinant inbred lines phenotyped at JIC, KWS1 and KWS2 in 2013.

Trait	Environment	Marker	Chr*	Position*	LB*	UB*	-LOG(P) *	% Var*	Add. *	Allele*	s.e. *
Height	JIC	11_21197	3	32.63	22.13	43.13	11.59	14.66	7.65	Chevallier	1.02
Height	JIC	11_11172	3	139.83	137.91	141.75	35.54	68.00	16.48	Chevallier	1.04
Height	KWS	11_21197	3	32.63	22.13	43.13	4.60	4.53	3.33	Chevallier	0.77
Height	KWS	11_11172	3	139.83	138.15	141.51	42.16	77.29	13.75	Chevallier	0.76
Heading date	JIC	11_11172	3	139.83	135.89	143.77	15.69	34.47	2.23	Tipple	0.25
Heading date	JIC	11_21326	7	28.74	19.80	37.68	8.67	16.72	1.55	Chevallier	0.25
Heading date	KWS	11_21459	2	202.94	164.84	230.00	6.38	6.43	1.24	Chevallier	0.24
Heading date	KWS	11_11172	3	139.83	137.67	141.99	34.59	60.66	3.81	Tipple	0.25
Heading date	KWS	309695	7	31.05	10.99	51.11	9.62	9.11	1.48	Chevallier	0.22
FHB	JIC	11_11246	6	114.50	104.56	124.44	5.59	15.32	1.44	Tipple	0.30
DON	JIC	50359	6	119.51	103.15	135.87	3.20	10.47	1.39	Tipple	0.42
Growth habit	JIC	11_11172	3	139.83	135.34	144.32	11.65	30.60	0.44	Chevallier	0.06
Tillering	JIC	11_11172	3	139.83	135.52	144.15	12.10	31.70	0.90	Tipple	0.12
Mildew field score	JIC	11_10332	1	43.92	25.31	62.53	3.87	9.58	0.41	Chevallier	0.10
Mildew CER score	JIC	11_10332	1	43.92	40.31	47.53	9.79	37.42	0.46	Chevallier	0.07
Physiological leaf spotting	JIC	11_10312	3	144.47	131.60	152.51	5.235	15.567	0.795	Chevallier	0.17
Spike angle	JIC	11_11172	3	139.83	136.15	143.51	14.22	36.73	0.62	Chevallier	0.07
IP5a	JIC	11_21145	3	23.28	18.28	28.28	5.25	27.72	2088.42	Tipple	434.61
IP5b	JIC	59596	1	29.11	14.30	43.92	3.24	11.24	1110.79	Chevallier	311.76
IP5b	JIC	100039	6	104.11	93.08	115.14	3.92	14.09	1243.59	Chevallier	310.19

* Chr : chromosome, Position: peak marker position in cM, LB: QTL lower bound in cM, UB: QTL upper bound in cM, -LOG(P): significance value, % Var: % of phenotypic variance, Add.: additive effect, Allele: high value allele, s.e.: standard error.

Figure 4.3. Quantitative trait loci identified on chromosome 1H of the Chevallier × Tipple F_5 mapping population by trait phenotyping.

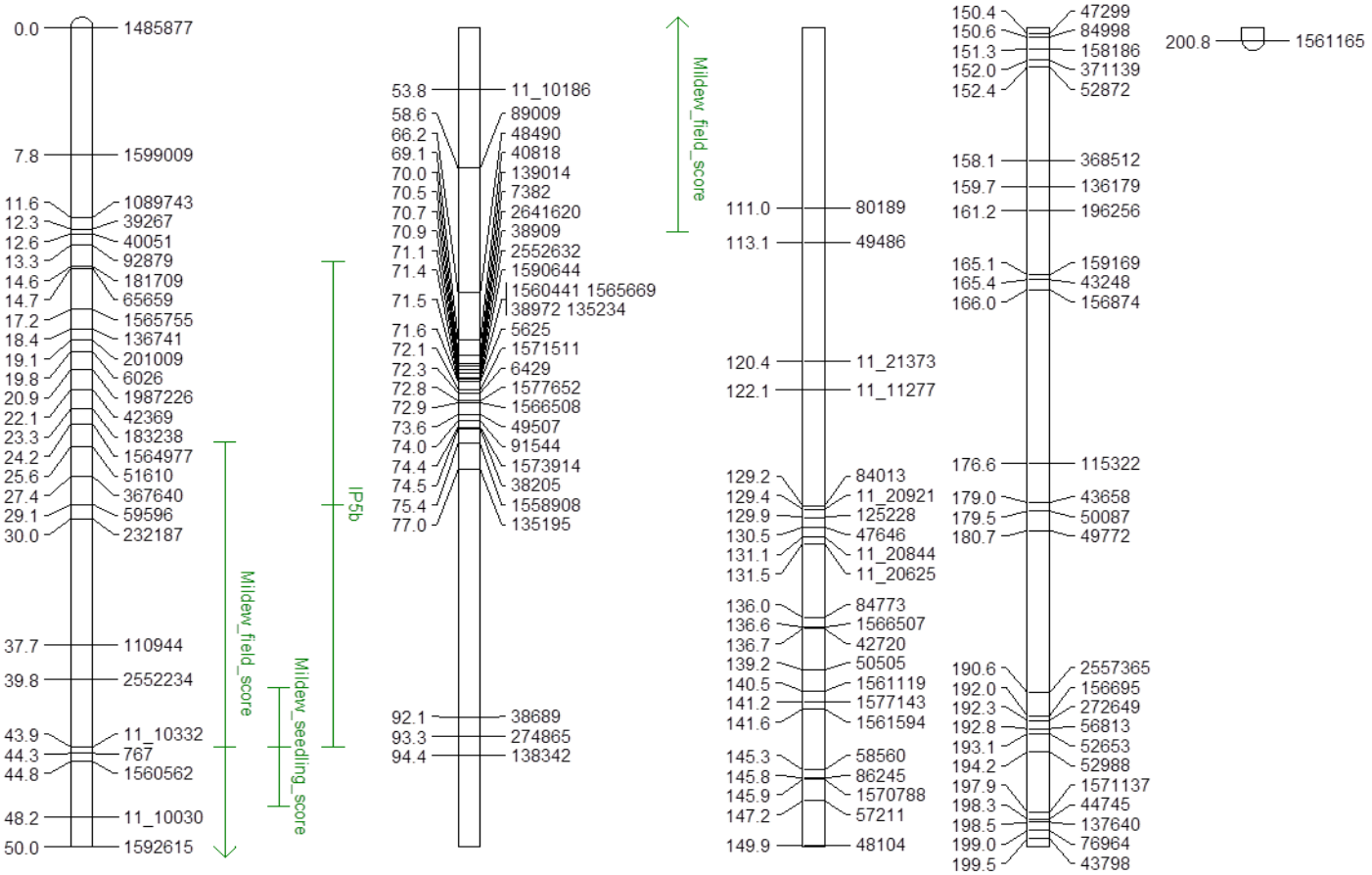

Figure 4.4. Quantitative trait loci identified on chromosome 2H of the Chevallier × Tipple F_5 mapping population by trait phenotyping.

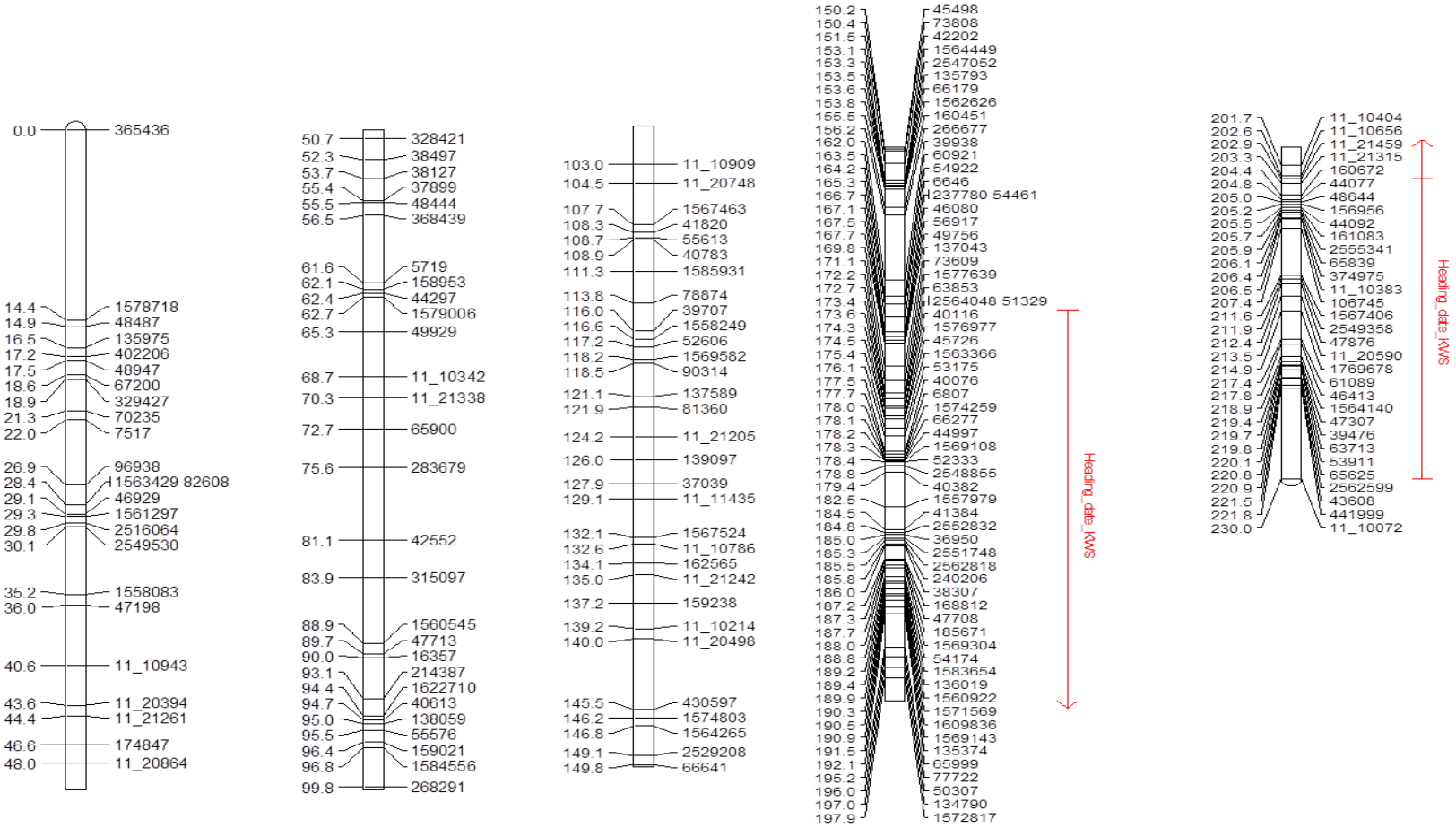

Figure 4.5. Quantitative trait loci identified on chromosome 3H of the Chevallier × Tipple F_5 mapping population by trait phenotyping.

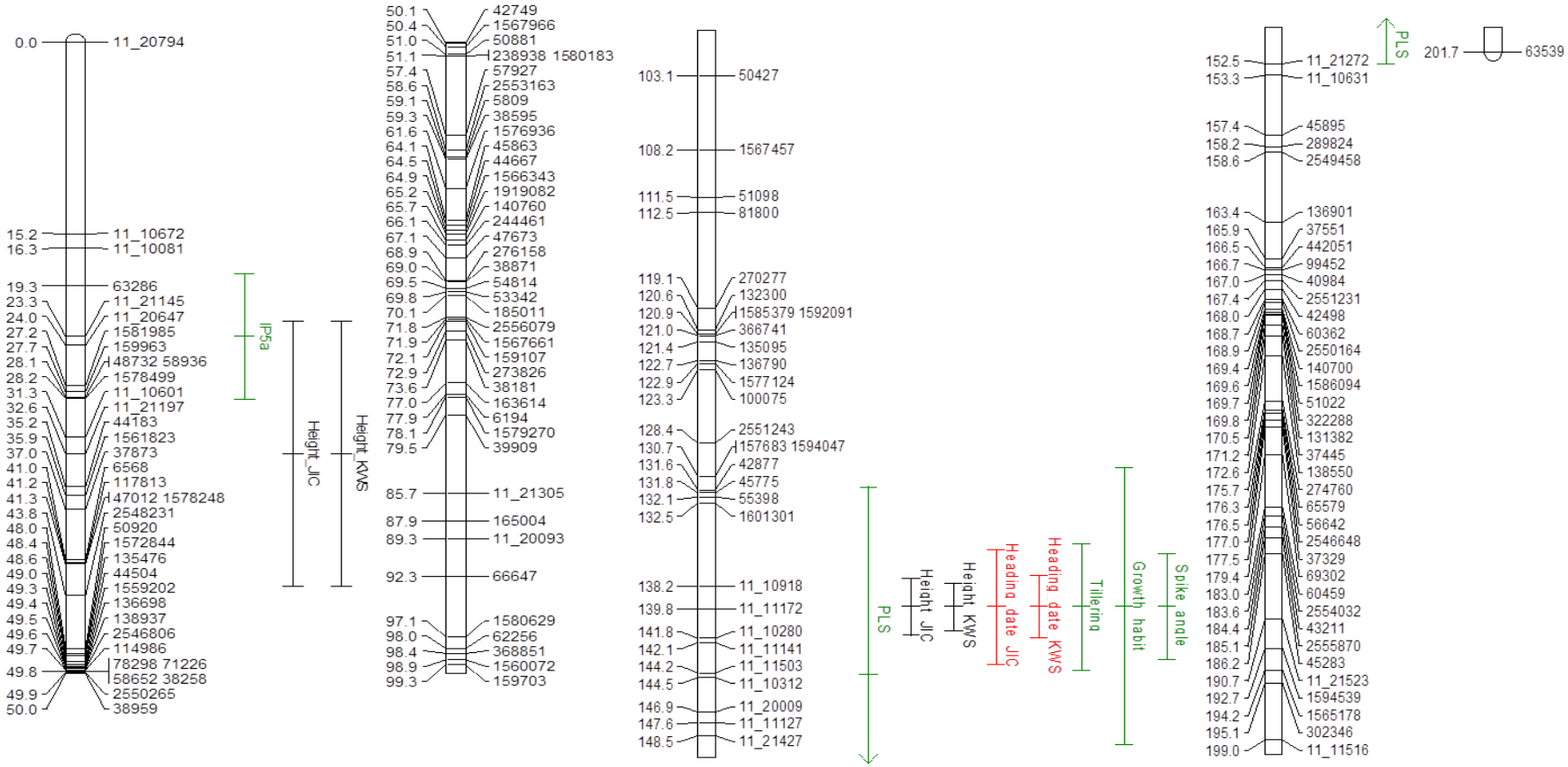

Figure 4.6. Quantitative trait loci identified on chromosome 6H of the Chevallier × Tipple F_5 mapping population by trait phenotyping.

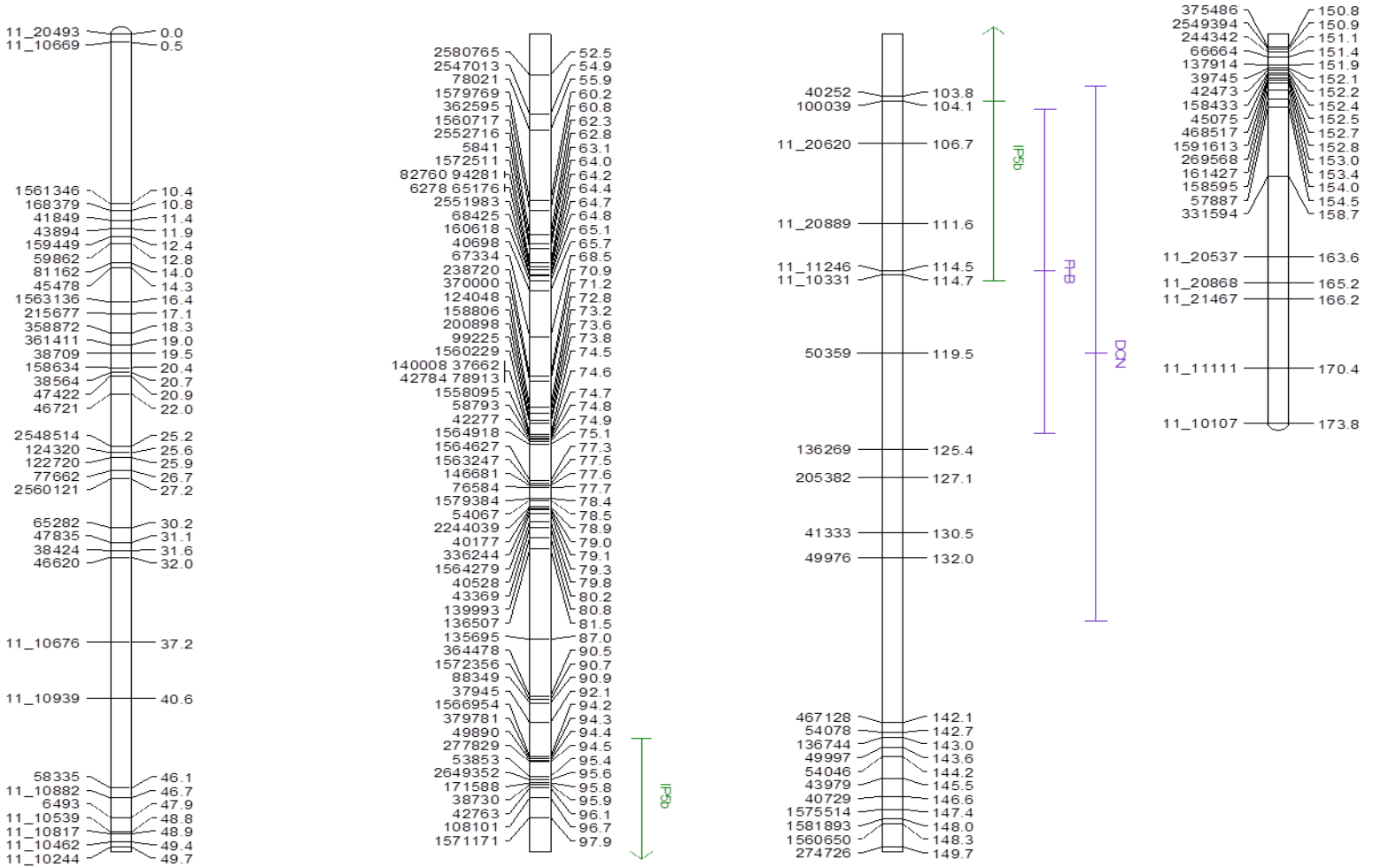

Figure 4.7. Quantitative trait loci identified on chromosome 7H of the Chevallier × Tipple F_5 mapping population by trait phenotyping.

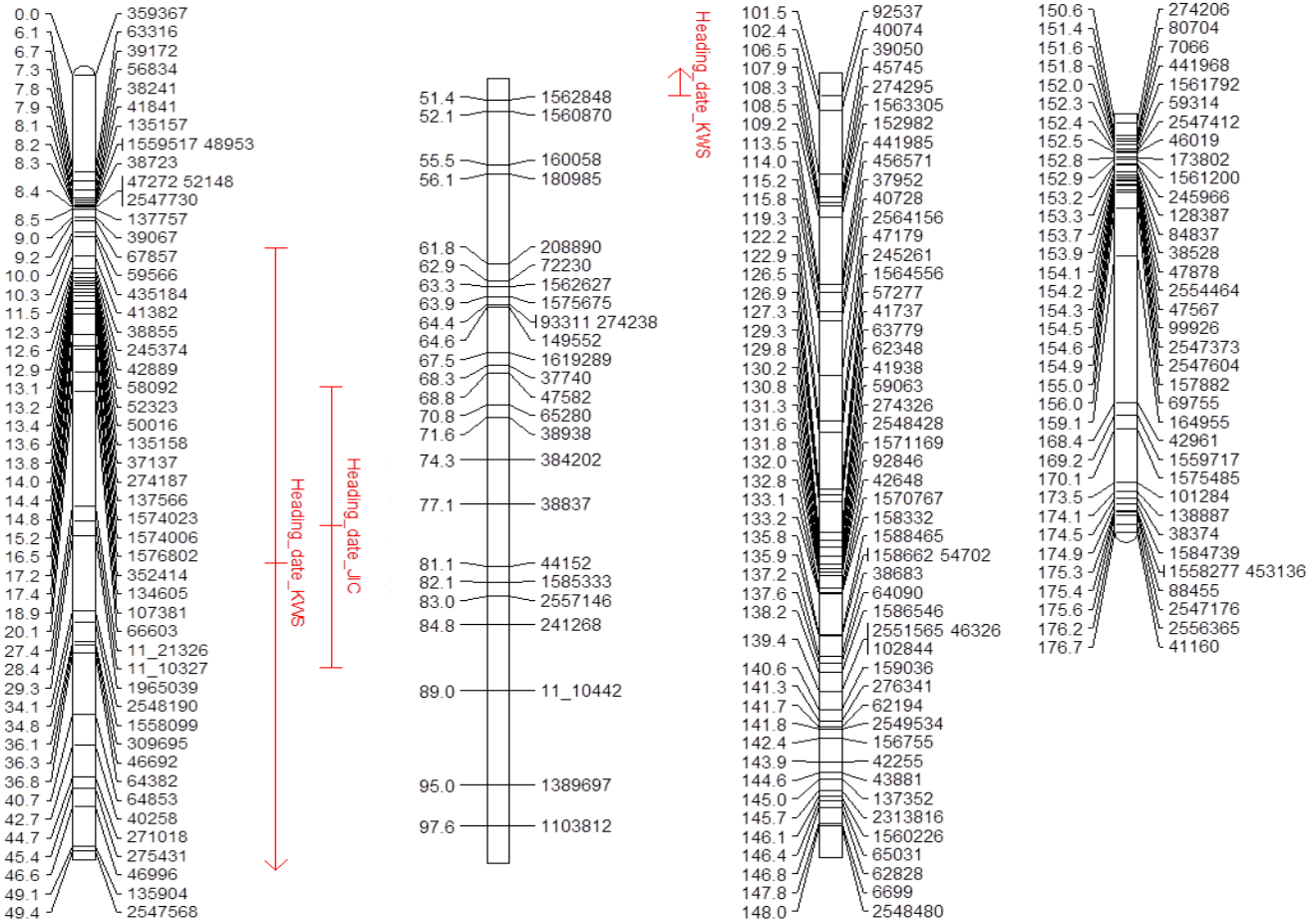

4.3.3 Chevallier and Tipple GA assay

The *sdw1* gene on 3H confers a semi-dwarf phenotype and the candidate gene has been proposed as a gibberellin 20-oxidase or *Hv20ox* (Jia et al. 2011). The response of the parental lines to GA was investigated with the aim of identifying whether a GA response might be contributing towards the major 3H height QTL. Treatment with 10ppm GA_3 had a significant positive effect on all three measurements of plant height (total height, first to second and second to third leaf node) compared with the control in both Chevallier and Tipple (P <0.001). The height measurements of Chevallier and Tipple under the control treatment were also deemed to be significantly different (P = 0.026), therefore the percentage difference in height values between the control and 10ppm GA_3 treatment for each measurement were calculated to account for this. Treatment of 10ppm GA_3 resulted in a 67.7% and 68.7% increase in distance between the second and third leaf nodes in Chevallier and Tipple, respectively (Figure 4.8). A similar increase of 67.0% and 68.0% in length was also observed in the total height measurement of Chevallier and Tipple respectively, when comparing the 10ppm GA_3 treatment to the control. A less pronounced effect in seedling growth in response to 10ppm GA_3 was displayed in the distance between the first to second leaf node, as the percentage difference in length between the control and GA treatment was 47.1% in Chevallier and 48.0% in Tipple (Figure 4.8). Whilst the application of 10ppm GA_3 had a significant effect on increasing plant height, no significant variation (P = 0.646) in the percentage differences between 10ppm GA_3 and control treatments for any of the three height measurements were observed between Chevallier and Tipple.

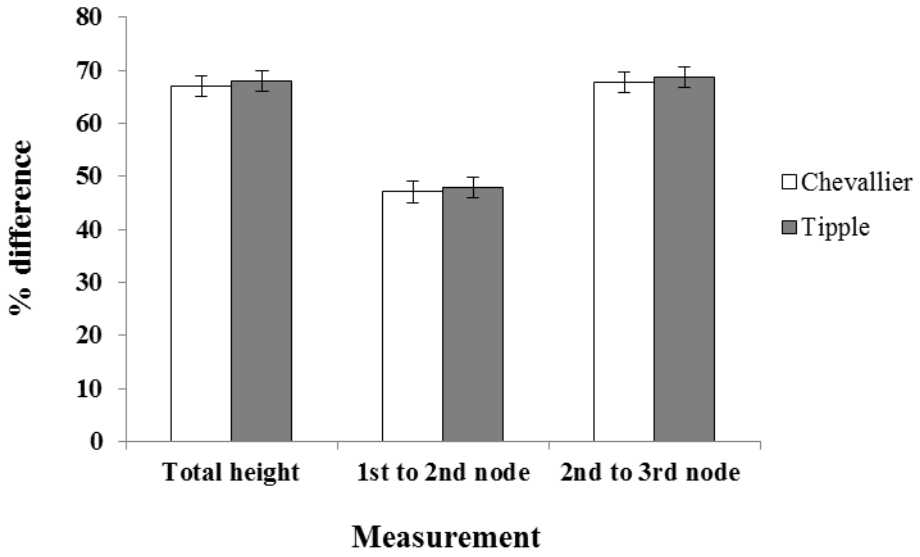

Figure 4.8. The percentage difference in total height, first to second and second to third leaf node distance, between Chevallier and Tipple seedlings treated with either 10ppm GA_3 or H_2O.

4.3.4 Chevallier × Tipple F_7 phenotyping

There were a number of phenotyping issues with the C×T F_7 trial at the JIC site in 2014. The herbicides applied to the trial failed to control weed growth, resulting in barley plants displaying stunted growth due to competition with naturally occurring plants within the environment. This stress led to shorter plants in which the peduncle failed to extend, resulting in the ears being trapped within the boot during anthesis, hindering the inoculation process. Within the GLM, score date, line and row were deemed to have a significant effect on FHB severity ($P < 0.001$), (Appendix Table A.18). The predicted mean FHB scores for Chevallier and Tipple were 2.3 and 14.0% respectively (Table 4.6), with Tipple displaying a lower disease score than expected from previous JIC trials. The difference in predicted means between the two parental lines was still significant at the $P < 0.001$ level however. The range of scores for the RILs was 2.1 – 20.3%, with a total of 15 RILs displaying a higher predicted FHB score than the susceptible Tipple parent. The mean FHB score for the RILs was 8.3% (Table 4.6). Growth conditions in the 2015 trial were favourable and plants were not subject to the weed competition seen in 2014. Within the GLM, score date, line and row were deemed to have a significant effect on FHB severity ($P < 0.001$), whilst replicate was

not significant ($P = 0.187$), (Appendix Table A.19). Tipple had a predicted mean FHB score of 19.2%, whilst Chevallier scored 1.5% (Table 4.6). Predicted scores for the RILs ranged from 1.1 – 12.9%, with a mean score of 7.2%.

DON analysis of the 2015 F_7 trial was undertaken. The mean DON content of the milled grain for Chevallier was 0.5ppm, whilst for Tipple it was 3.6ppm. The mean values for the parental lines were significantly different at the $P = 0.014$ level. The mean DON accumulation values in the RILs calculated from one replicate was 1.8ppm, with a range of 0.1 – 5.6ppm. This range of values for DON concentration in the 2015 trial of F_7 RILs is much lower than in the 2013 trial of the C×T F_5 population where the range was 0.1 – 15.8ppm. An R^2 value of 0.177 was determined for the relationship between FHB score in 2015 and the DON values calculated from the ELISA. This indicates a very weak positive correlation between visual symptoms of FHB severity and the concentration of DON within the grain.

In the 2014 trial, line had a significant effect on plant height ($P < 0.001$) whilst the positional effect of row did not ($P = 0.343$), (Appendix Table A.20). The predicted height values for the parental lines were 119.5 and 70.0cm in Chevallier and Tipple, respectively (Table 4.6). The mean height of the RILs was 94.8cm. From the 2015 trial line was again significant in the GLM ($P < 0.001$), whilst both row and replicate were not significant ($P = 0.079$ and 0.501, respectively), (Appendix Table A.21). Under the more favourable growth conditions of the 2015 trial the predicted height values for Chevallier and Tipple were 140.8 and 90.7cm, an increase in height of approximately 20cm compared to that of the 2014 trial. The predicted height values for the parental lines were significantly different at the $P < 0.001$ level (Table 4.6). The predicted mean height score of the RILs was 109.8cm, an increase of 15cm compared to the mean height in 2014.

HD was significantly affected by line ($P < 0.001$) in the 2014 trial, but not by row ($P = 0.409$), (Appendix Table A.22). There was a difference of five days between the HD scores of Chevallier and Tipple, with predicted scores of 77.0 and 82.0 days respectively (Table 4.6). The predicted scores suggest that the Chevallier line had an earlier HD than Tipple, which is in contrast to all three previous trials (JIC, KWS1 and KWS2 in 2013) where the Chevallier parent consistently emerged from the boot at a later date than Tipple (Table 4.6). This change in HD pattern may be due to the

stressful growth conditions experienced in 2014. Within the GLM for the 2015 trial, line was also deemed significant ($P < 0.001$), but row and replicate were not ($P = 0.930$ and 0.710, respectively), (Appendix Table A.23). The predicted HD scores for the parental lines were 94.0 and 90.0 days in Chevallier and Tipple respectively, illustrating that under more favourable growth conditions the Tipple parent displayed the expected earlier HD phenotype (Table 4.6). The HD scores observed in the RILs ranged from 74.0 – 92.0 days in the 2014 trial and from 87.0 – 99.0 days in the 2015 trial (Table 4.6). The mean score for the RILs was 81.0 days in 2014 and 92.0 days in 2015.

Phenotype data for GH, tillering and PLS was only collected during the 2015 trial, with the parental lines being significantly different for all traits except tillering (Table 4.6).

Table 4.6. Predicted mean values from general linear modelling of phenotypic traits at the JIC trial site in 2014 and 2015 for Chevallier and Tipple, and the range of predicted means for the 188 C×T F_7 recombinant inbred lines.

		Parents		RILs		
Trait	**Year**	**Chevallier**	**Tipple**	**Mean**	**Range**	**t- probability***
FHB	2014	2.3	14.0	8.3	2.1 – 20.3	<0.001
FHB	2015	1.5	19.2	7.2	1.1 – 12.9	<0.001
Height	2014	119.5	70.0	94.8	61.0 – 124.0	<0.001
Height	2015	140.8	90.7	109.8	79.9 – 140.0	<0.001
Heading date	2014	77.0	82.0	81.0	74.0 – 92.0	<0.001
Heading date	2015	94.0	90.0	92.0	87.0 – 99.0	<0.001
Growth habit	2015	4.0	2.0	3.0	2.0 – 5.0	<0.001
Tillering	2015	6.0	7.0	6.0	3.0 – 8.0	0.061
Mildew	2014	6.0	3.0	4.0	2.0 – 7.0	<0.001
Mildew	2015	5.0	3.0	5.0	2.0 – 9.0	0.010
Physiological leaf spotting	2015	4.0	5.0	4.0	2.0 – 9.0	0.042

* The statistical significance of the difference between predicted mean scores for Chevallier and Tipple were calculated by t-probabilities within the GLM.

4.3.5 QTL analysis of Chevallier × Tipple F_7 traits

As with the C×T F_5 population, two QTL were associated with height in the F_7 RILs, both of which were identified in the same locations on 3H in both 2014 and 2015. The major height QTL on 3H was identified at positions 136.5 and 135.5cM from the 2014 and 2015 trials respectively, which accounted for 67.9 and 61.6% of the phenotypic variance within the RILs. A minor height QTL was also located on 3H in both years (Table 4.7).

Three QTL associated with HD were identified in each trial year, with a major QTL at position 136.5cM on 3H. The two QTL on 3H co-located with the minor and major height QTL also present on this chromosome (Figure 4.11) and a further minor HD QTL was detected at the telomeric region of 7H in both years. The Chevallier parental allele was associated with a later HD score for the 3H and 7H QTL, whilst the Tipple allele was associated with a later score at the major 3H QTL (Table 4.7). This contribution from both parental genotypes may explain the transgressive segregation seen in the range of HD scores in the F_7 RIL population in both trial years.

It was not possible to identify any QTL associated with FHB from the C×T F_7 2014 trial using the predicted mean values calculated across the four score dates, which was thought to be due to the issues with accurately phenotyping the FHB trait. The predicted mean values for each score date were then analysed separately with the aim of identifying potential QTL. Analysis of the first score date identified two QTL associated with FHB. The 6H QTL was detected at position 122.14cM and accounted for 6.7 % of the variation within the population. A further QTL on 7H was detected accounting for 7.5% of the variance (Table 4.7). Higher FHB values were associated with the presence of the Tipple allele. No QTL could be identified during the analysis of the second and third score datasets individually. Analysis of the fourth and final score dataset resulted in the detection of a single QTL associated with FHB on 3H at position 135.41cM. This QTL co-located with the major 3H height and HD QTL (Figure 4.11) with the Tipple allele contributing to the higher FHB score, shorter plant height and later flowering. Analysis of the 2015 predicted mean FHB scores calculated across the four score dates resulted in the detection of four QTL. The 6H QTL was again identified at position 114.6cM accounting for 8.6% of the phenotypic variance in the RILs. A single QTL was identified on 2H at position 130.5cM. Two QTL were

identified on 7H, at positions 7.4 and 103.5cM (Table 4.7), accounting for 7.8 and 10.8% of the variance, respectively. The major 7H FHB QTL co-located with the FHB QTL identified during the initial score for the 2014 trial, whilst the QTL interval for the minor 7H QTL interval partially overlapped the location of two HD QTL identified in both 2014 and 2015 (Figure 4.13). For all four QTL identified in the 2015 trial the Chevallier parent was associated with increased resistance to FHB.

Four QTL associated with DON accumulation were identified from the 2015 trial (Table 4.7). A single QTL was detected on 1H at position 101.8cM, with the Chevallier allele contributing to higher DON concentration. Two QTL were identified on 3H at 76.9 and 126.4cM, with the Tipple allele being associated with higher DON accumulation. A final QTL was identified on 6H at 89.7cM, with the Chevallier allele contributing to higher DON. The combined phenotypic variance accounted for by the two QTL where Tipple contributes the high value allele (both on 3H) was 14.2%, whilst for the two QTL where Chevallier contributes the high value allele (1H, 6H) the combined variance was 15.6%.

From the 2015 trial data, the major QTL for GH and tillering and co-located on 3H, in a similar location as the major height and HD QTL (Table 4.7). Two minor GH QTL were identified on 1H and 2H, whilst a further tillering QTL was identified on 2H (Table 4.7). A major QTL associated with powdery mildew was again detected on 1H from the 2015 data, with two additional minor QTL on 1H and 2H. A single QTL on 2H for powdery mildew was identified from the 2014 trial. Finally, three QTL associated with PLS were also identified, with two QTL on 7H and a single QTL on 3H (Table 4.7). Tipple contributed the higher scoring allele for the major 7H QTL and Chevallier contributed the higher scoring allele for the other two QTL.

Table 4.7. Quantitative trait loci identified from the 188 C×T F_7 recombinant inbred lines phenotyped at JIC in 2014 and 2015.

Trait	Year	Marker	Chr*	Position*	LB*	UB*	-LOG(P) *	% Var. *	Add. *	Allele*	s.e. *
Height	2014	44504	3	66.59	32.13	73.13	9.28	4.33	3.70	Chevallier	0.56
Height	2014	45775	3	136.46	134.80	138.12	67.93	79.38	15.85	Chevallier	0.56
Height	2015	135476	3	64.55	45.67	83.43	16.51	9.64	5.06	Chevallier	0.54
Height	2015	42877	3	135.51	133.66	137.36	61.62	71.62	13.78	Chevallier	0.54
HD	2014	176972	3	67.16	36.46	97.07	9.54	7.32	1.20	Chevallier	0.18
HD	2014	45775	3	136.46	133.69	139.66	36.12	42.51	2.90	Tipple	0.18
HD	2014	309695	7	0.00	0.00	8.42	18.69	17.85	1.88	Chevallier	0.19
Heading date	2015	2553163	3	71.27	42.46	97.07	7.06	4.00	0.62	Chevallier	0.11
Heading date	2015	45775	3	136.46	131.89	141.03	34.45	32.50	1.71	Tipple	0.11
Heading date	2015	46692	7	1.15	0.00	5.42	34.07	30.58	1.76	Chevallier	0.11
FHB score 1	2014	66664	6	122.14	85.77	132.53	3.57	6.66	0.35	Tipple	0.10
FHB score 1	2014	1570767	7	97.88	69.59	126.17	4.02	7.54	0.38	Tipple	0.09
FHB score 4	2014	1594047	3	135.41	110.39	160.43	3.99	8.07	1.52	Tipple	0.38
FHB	2015	11_21315	2	130.51	124.14	154.22	4.11	8.41	0.35	Tipple	0.09
FHB	2015	1562670	6	114.56	95.74	132.53	4.23	8.64	0.31	Tipple	0.09
FHB	2015	64853	7	7.43	0.00	34.11	3.89	7.61	0.37	Tipple	0.09
FHB	2015	64090	7	103.48	69.85	137.11	4.49	10.78	0.45	Tipple	0.09
DON	2015	49486	1	101.871	80.215	134.248	3.264	4.803	0.251	Chevallier	0.06
DON	2015	54814	3	76.956	59.541	106.757	4.325	8.891	0.311	Tipple	0.06
DON	2015	51098	3	126.362	106.797	169.698	3.362	5.314	0.24	Tipple	0.06
DON	2015	11_10331	6	89.77	73.215	105.292	4.496	10.808	0.343	Chevallier	0.07
Growth habit	2015	1561594	1	128.46	112.54	144.38	8.18	10.39	0.22	Chevallier	0.04
Growth habit	2015	1564449	2	109.10	80.73	137.47	6.09	7.53	0.19	Tipple	0.04
Growth habit	2015	42877	3	135.51	131.28	139.74	18.95	32.82	0.39	Chevallier	0.04
Tillering	2015	137043	2	123.41	89.24	157.59	4.40	6.85	0.21	Chevallier	0.05
Tillering	2015	1594047	3	135.41	129.44	141.39	12.63	24.02	0.38	Tipple	0.05
Mildew	2014	66277	2	129.55	106.13	152.97	4.07	8.40	0.34	Chevallier	0.09
Mildew	2015	42369	1	18.30	10.53	26.07	10.32	19.12	0.50	Chevallier	0.07
Mildew	2015	139014	1	62.97	36.73	89.22	4.80	7.86	0.32	Chevallier	0.07
Physiological leaf spotting	2015	1919082	3	75.51	55.05	95.97	5.56	9.14	0.43	Chevallier	0.09
Physiological leaf spotting	2015	435184	7	54.98	46.12	63.84	9.27	17.12	0.58	Tipple	0.09
Physiological leaf spotting	2015	41160	7	146.65	107.67	157.35	4.00	6.47	0.36	Chevallier	0.09

* Chr : chromosome, Position: peak marker position in cM, LB: QTL lower bound in cM, UB: QTL upper bound in cM, -LOG(P): significance value, % Var: % of phenotypic variance, Add.: additive effect, Allele: high value allele, s.e.: standard error.

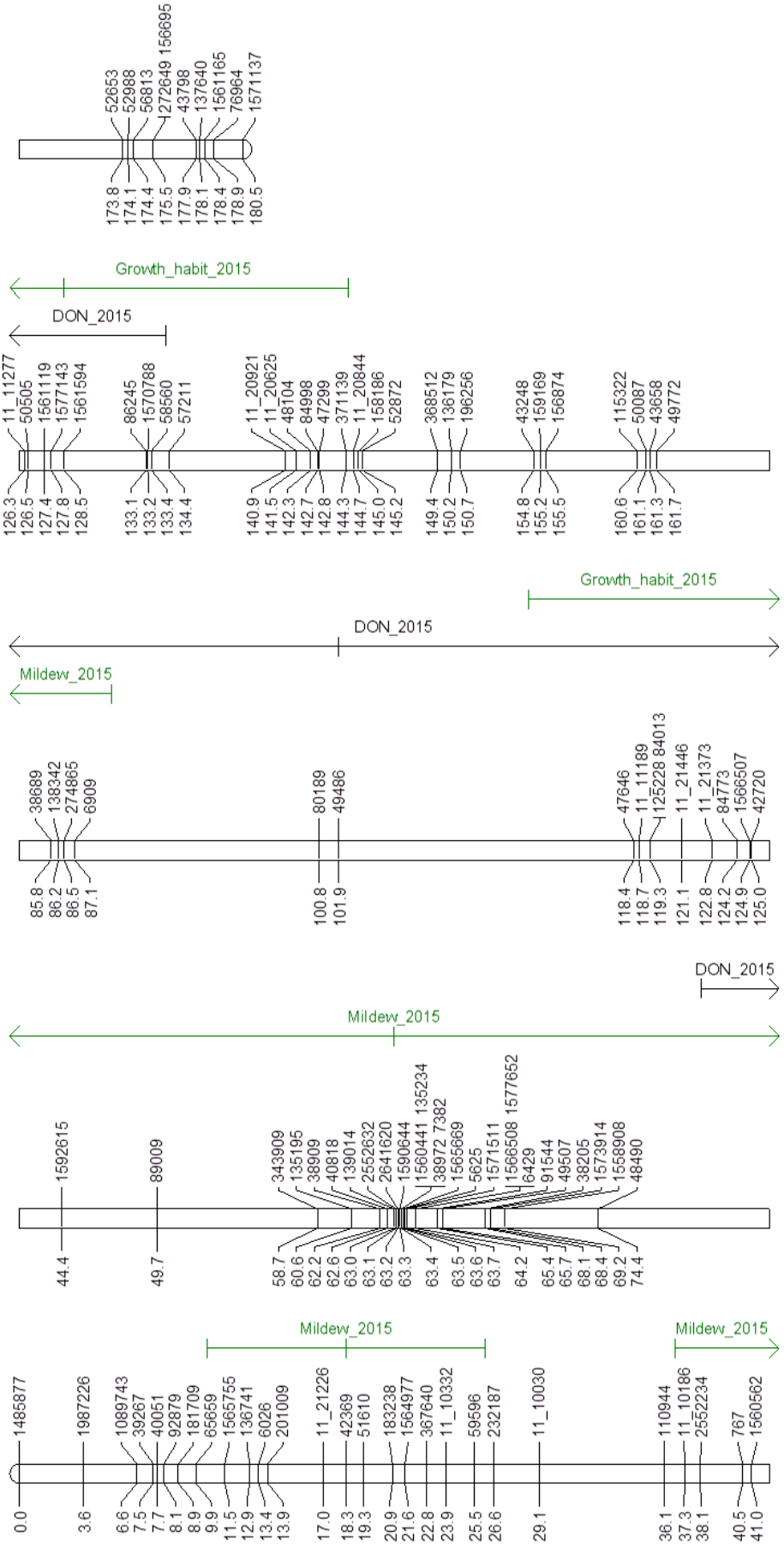

Figure 4.9. Quantitative trait loci identified on chromosome 1H of the Chevallier × Tipple F_7 mapping population by trait phenotyping.

Figure 4.10. Quantitative trait loci identified on chromosome 2H of the Chevallier × Tipple F_7 mapping population by trait phenotyping.

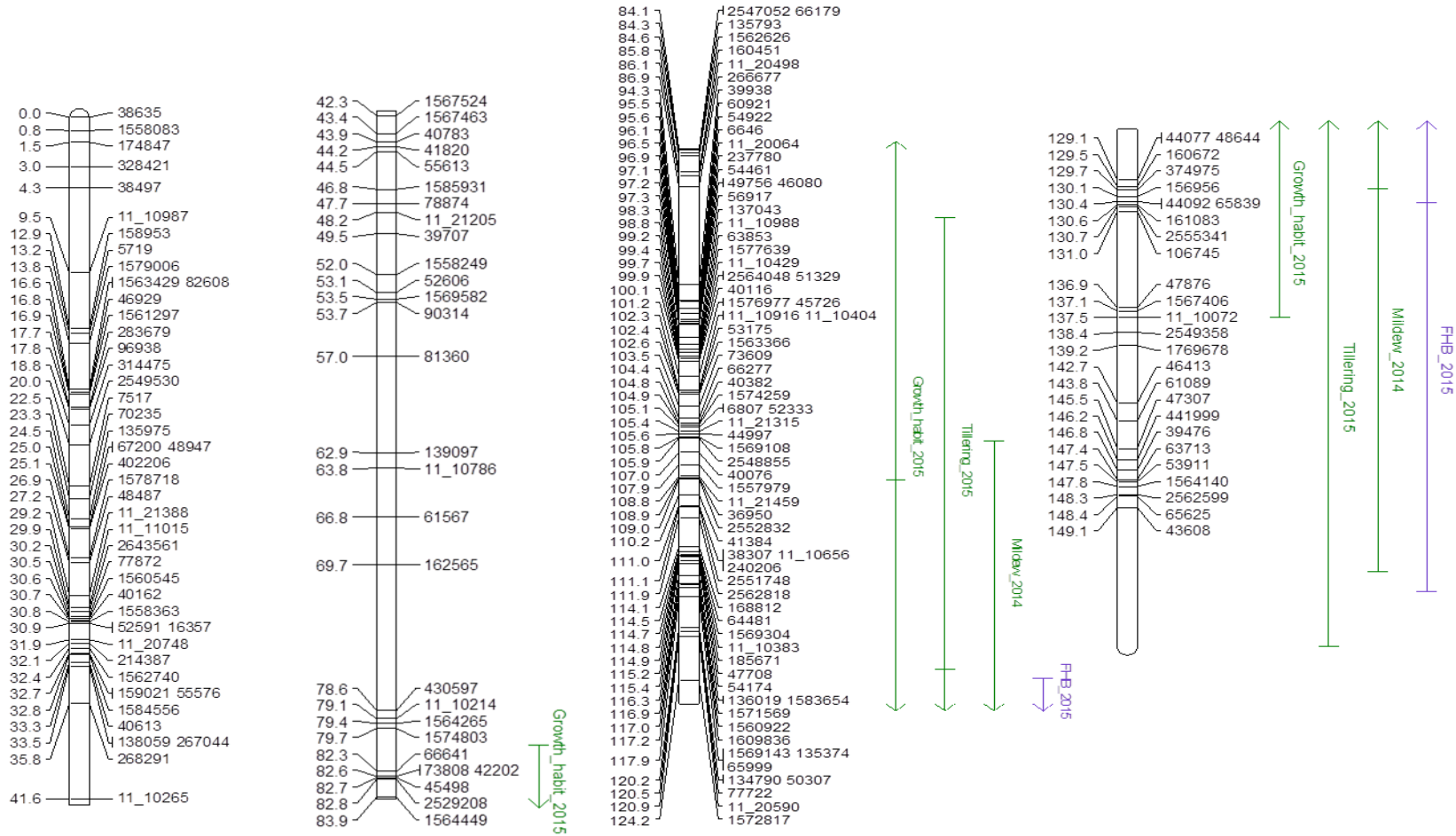

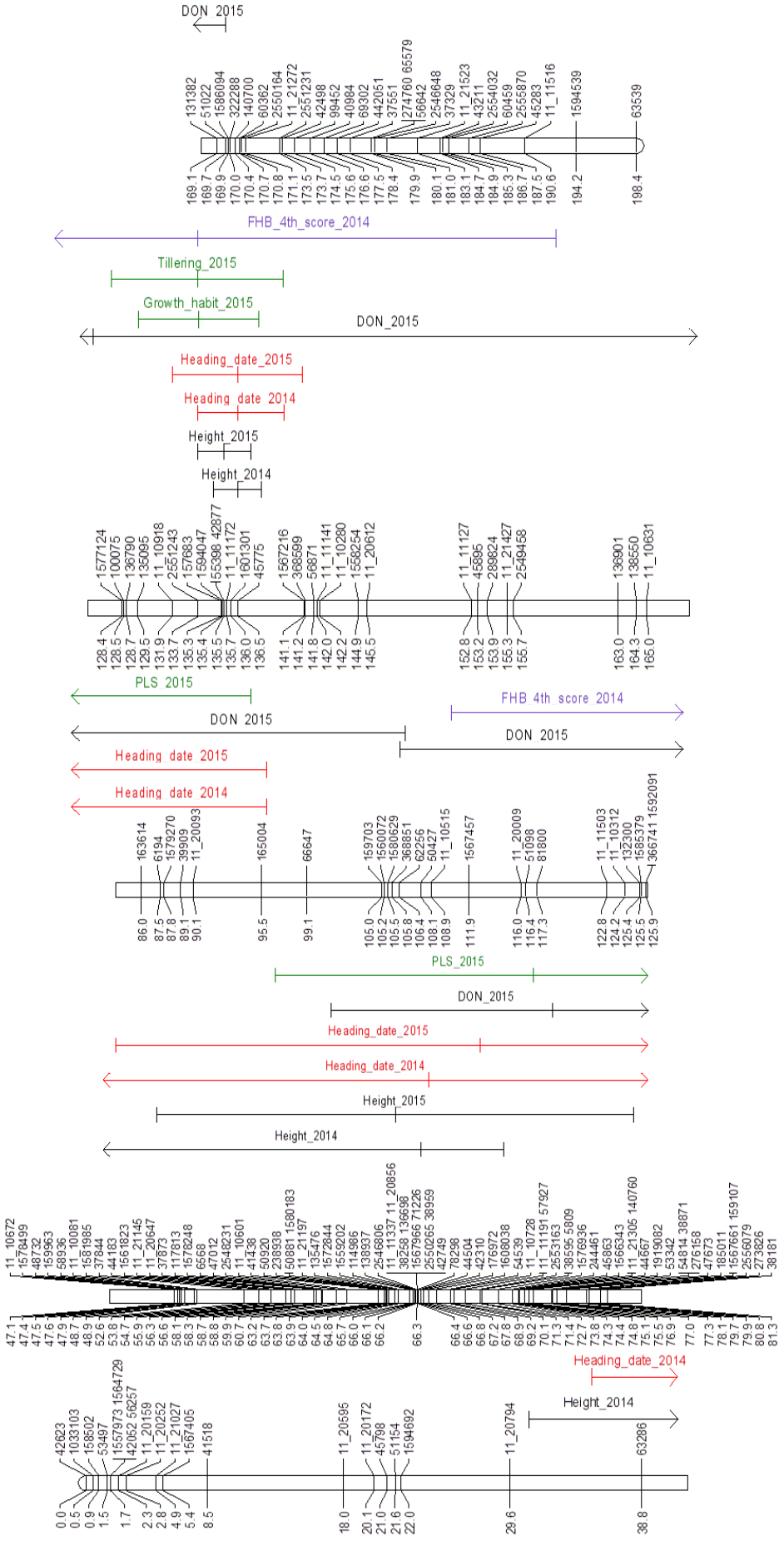

Figure 4.11. Quantitative trait loci identified on chromosome 3H of the Chevallier × Tipple F_7 mapping population by trait phenotyping.

Figure 4.12. Quantitative trait loci identified on chromosome 6H of the Chevallier × Tipple F_7 mapping population by trait phenotyping.

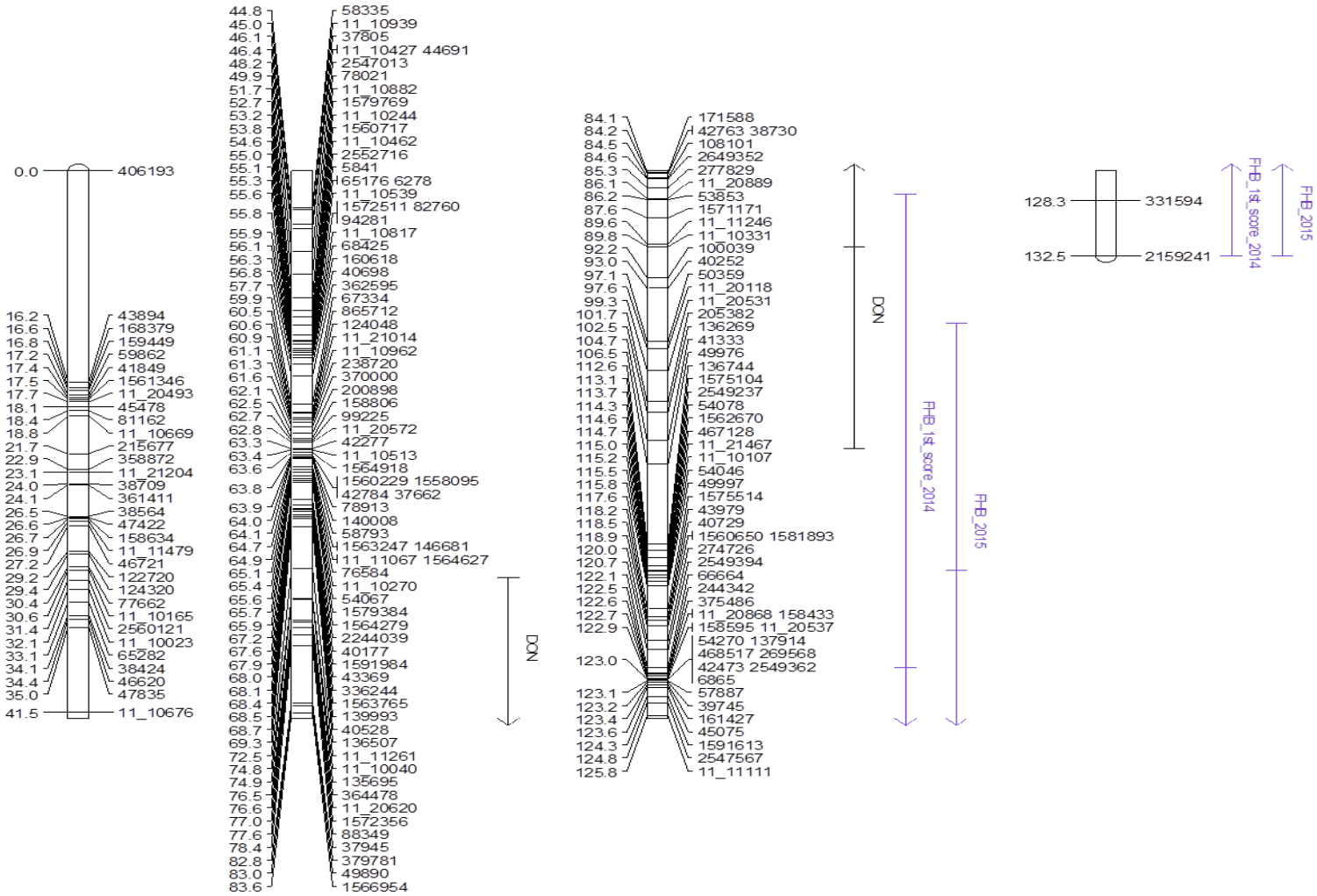

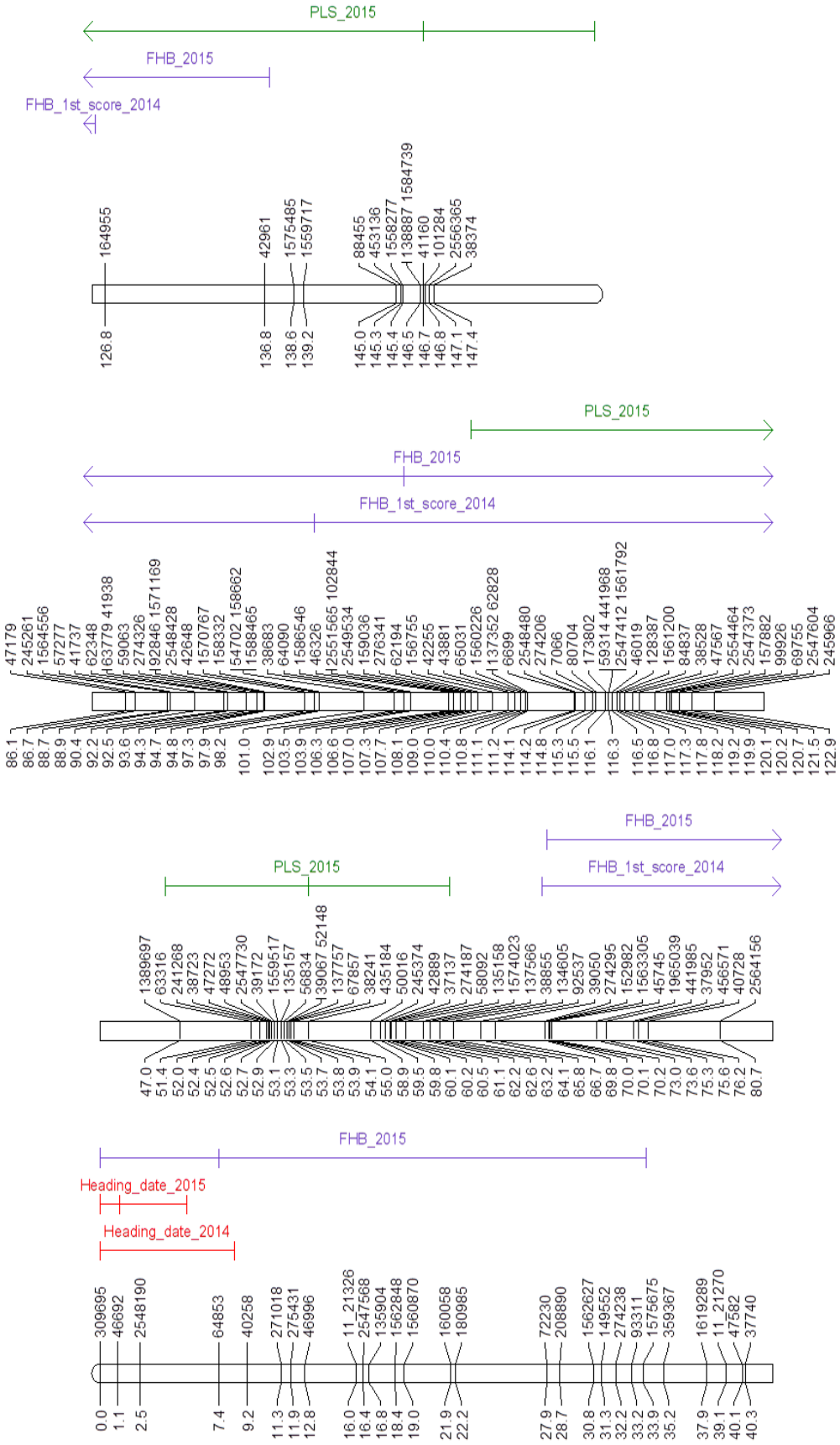

Figure 4.13. Quantitative trait loci identified on chromosome 7H of the Chevallier × Tipple F_7 mapping population by trait phenotyping.

4.3.6 Chevallier × Tipple F_7 DON QTL

From the QTL analysis of the DON accumulation data recorded in the C×T F_7 population in 2015 four QTL were identified (1H, 3HS, 3HL and 6H). The Chevallier parent (allele A) contributed high value alleles at the 1H and 6H QTL, whilst the Tipple parent (allele B) contributed high value alleles at both 3H QTL. Lines which possessed either the high value allele at all four of the DON QTL loci (ABBA), the low value allele at each loci (BAAB) or those possessing all the parental alleles (AAAA or BBBB) were selected and the mean DON values (ppm) for each of these classes was calculated. The mean DON value for the ABBA class (all high value alleles) was 2.5ppm whilst the value for the BAAB class (all low value alleles) was 0.9ppm. The mean values for classes AAAA and BBBB were 1.3 and 2.3ppm respectively, with these combinations of alleles displaying intermediate DON accumulation compared to the ABBA or BAAB classes (Figure 4.14).

Figure 4.14. Box plots of each of the four DON genotype classes identified from quantitative trait loci analysis of the C×T F_7 population in 2015.

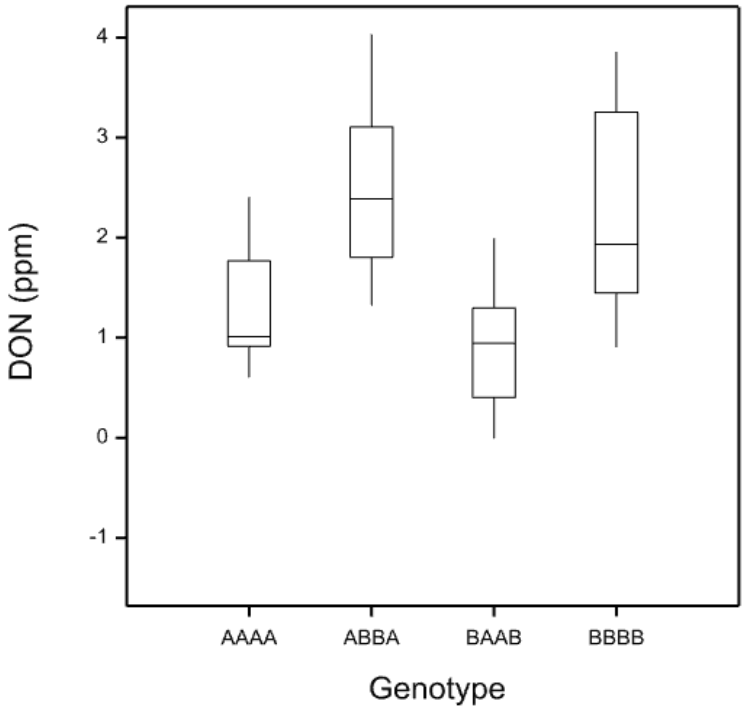

4.3.7 Armelle × Tipple F_6 phenotyping

At the 2013 NIAB trial (NIAB13) score date was observed to have a significant effect on FHB severity ($P < 0.001$), (Appendix Table A.24). The effect of line and row were also significant ($P = 0.008$ and 0.037, respectively). Disease pressure at this trial was not high. Tipple displayed significantly more severe FHB symptoms than the Armelle parent ($P = 0.043$), with a score of 9.7% compared to 3.0% in Armelle (Table 4.8). The mean score for the RILs was 8.2%. The 2014 trial (JIC14) was subject to the same weed-choked and stressful conditions as the C×T F_7 trial at the same site, therefore accurate phenotyping of FHB was compromised. Within the GLM, score date had a significant effect ($P = 0.020$), but line and row did not ($P = 0.252$ and 0.156, respectively, Appendix Table A.25). Tipple displayed more severe FHB symptoms, with a score of 17.0%, whilst Armelle scored 3.0%. The predicted mean scores of the parental lines were found to be significantly different at the $P = 0.01$ level. The range of predicted scores within the RILs varied from 0.5 – 22.0% (Table 4.8), and the mean score for the RILs was 10.4%.

Within the NIAB13 trial, the predicted height values for the parental lines were 81.4 and 108.0cm in Tipple and Armelle, respectively (Table 4.8). The predicted height values for the RIL lines varied from 73.0 – 135.0cm, with a mean score of 97.7cm (Table 4.8). Within the GLM, the effect of line on plant height was insignificant ($P = 0.055$), as was the positional effect of row ($P = 0.155$), (Appendix Table A.26). The heights of the parental lines at JIC14 were shorter than at NIAB13 most probably due to the less favourable growth conditions. Within the GLM, neither line nor row were deemed to have a significant effect on plant height ($P = 0.249$ and 0.319, respectively), (Appendix Table A.27). The predicted height values for Armelle and Tipple were 97.0 and 59.0cm, respectively (Table 4.8). The scores for the RILs ranged from 58.0 – 122.0cm, with a mean score of 92.9cm.

HD scores were only recorded at JIC14. Line was determined to significantly affect heading ($P < 0.001$) but row did not ($P = 0.056$), (Appendix Table A.28). Predicted HD scores for the parental lines were 83.0 and 77.0 in Armelle and Tipple, respectively, which were found to be significantly different at the $P < 0.001$ level (Table 4.8). The HD values for the RILs ranged between 74.0 – 95.0 days, with a mean score of 84.0 days.

Table 4.8. Predicted mean values from general linear modelling of phenotypic traits at the NIAB and JIC trial site in 2013 and 2014 for Armelle and Tipple, and the range of predicted means for the 198 A×T F_6 recombinant inbred lines.

			Parents		RILs		
Trait	**Environment**	**Year**	**Armelle**	**Tipple**	**Mean**	**Range**	**t- probability***
FHB	NIAB	2013	3.0	9.7	8.2	0.0 – 27.0	0.043
FHB	JIC	2014	3.0	17.0	10.4	0.5 – 22.0	0.010
Height	NIAB	2013	108.0	81.4	97.7	73.0 – 135.0	0.027
Height	JIC	2014	97.0	59.0	92.9	58.0 – 122.0	<0.010
Heading date	JIC	2014	83.0	77.0	84.0	74.0 – 95.0	<0.001

* The statistical significance of the difference between predicted mean scores for Armelle and Tipple were calculated by t-probabilities within the GLM.

Table 4.9. Quantitative trait loci identified from the 198 A×T F_6 recombinant inbred lines phenotyped at NIAB and JIC in 2013 and 2014.

Trait	**Environment**	**Year**	**Marker**	**Chr***	**Position***	**LB***	**UB***	**-LOG(P) ***	**% Var. ***	**Add. ***	**Allele***	**s.e. ***
Height	NIAB	2013	11_10918	3	147.62	136.13	159.11	4.25	10.42	4.53	Armelle	1.10
Height	JIC	2014	11_10918	3	147.62	138.25	154.68	4.06	8.21	4.30	Armelle	1.10
Heading date	JIC	2014	11_10280	3	154.39	137.43	159.23	3.44	7.80	1.20	Tipple	0.34
FHB	NIAB	2013	11_11172	3	149.22	130.92	159.23	3.46	7.40	1.94	Tipple	0.53

* Chr : chromosome, Position: peak marker position in cM, LB: QTL lower bound in cM, UB: QTL upper bound in cM, -LOG(P): significance value, % Var: % of phenotypic variance, Add.: additive effect, Allele: high value allele, s.e.: standard error.

4.3.8 QTL analysis of Armelle × Tipple F_6 traits

A single QTL associated with height was identified from the NIAB13 data. This QTL was located on 3H at position 147.6cM, corresponding to marker 11_10918, and represented 10.4% of the phenotypic variance within the population (Table 4.9). A height QTL locating to the same marker position was also identified from the JIC14 data, representing 8.2% of the phenotypic variance within the population. The high value allele was contributed by the tall Armelle parent for both of the QTL. HD was only recorded at JIC14 and a QTL associated with this trait was also detected on 3H at 154.4cM (marker 11_10280), explaining 7.8% of the population variance (Table 4.9). This HD QTL overlapped with the height QTL, with a later HD score being associated with the presence of the Tipple allele. QTL associated with FHB could only be detected using NIAB13 data, with no QTL being identified using a LOD threshold of 3.0 using the JIC14 dataset. The NIAB13 FHB QTL mapped to marker 11_11172 at position 149.2cM on chromosome 3H, therefore co-locating with the previously identified QTL for both height and HD (Figure 4.15). The FHB QTL explained 7.4% of the population variance and higher FHB susceptibility was associated with the Tipple parental genotype.

Figure 4.15. Quantitative trait loci identified on chromosome 3H of the Armelle × Tipple F_6 mapping population by trait phenotyping.

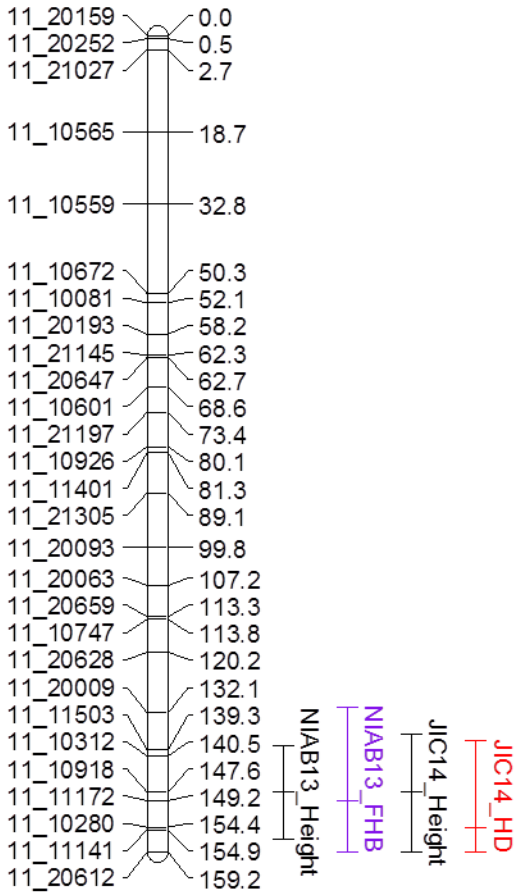

4.4 Discussion

Phenotyping of both the Chevallier × Tipple F_5 and F_7 populations enabled QTL for several agronomic traits to be identified, with many of these QTL being detected in the same location across both populations and in different trial environments. A major QTL associated with plant height, accounting for up to 77% of the phenotypic variance, was identified on chromosome 3H in both the C×T populations. There are various groups of barley semi-dwarfing genes such as *breviaristatum* (*ari*), *erectoides* (*ert*), *brachytic* (*brh*), *semi-brachytic* (*uzu*) and *short culm* (*hcm*), with several of these genes located on chromosome 3H (Wang et al. 2014; Dockter et al. 2014). The *uzu* or *Hvbri1* semi-dwarfing gene, associated with reduced sensitivity to brassinosteroid, is present at the centromeric region of 3HL (Chono et al. 2003). However the major height QTL in the C×T population is located at the distal end of 3HL, suggesting the *uzu* gene is unlikely to be associated with the shorter height phenotype seen in the present study. The *erectoides-c* semi-dwarfing gene has also been mapped close to the centromere on 3HL (Lundqvist et al. 1997); however the spikes of cultivars possessing the *erectoides-c* allele display a compact appearance due to a shorter internode distance within the ear. The semi-dwarfing *sdw1* gene is also located on 3HL and is associated with late heading, a decrease in 1000-grain weight, prostrate growth habit and an increase in tiller number (Thomas et al. 1991; Bezant et al. 1996; Malosetti et al. 2011; Jia et al. 2011). The major QTL for height on 3HL at 136.0 – 139.8cM in both the C×T F_5 and F_7 populations also co-locates with the major QTL for HD, GH, tillering and spike angle. It seems apparent that the *sdw1* gene is the likely candidate underlying the major height QTL on 3HL, as the Tipple allele is associated with reduced height, increased heading, a prostrate GH and increased tiller number at this region. A recent study suggests that the effect of *sdw1* on height and HD may be due to pleiotropy as these traits are consistently associated with this locus (Kuczyńska et al. 2014). *Sdw1* and *denso*, which were originally identified from the cultivars Jotun and Diamant, have been proven to be allelic (Kuczyńska et al. 2013), with the *denso* allele being favoured for use in malting cultivars and *sdw1* being utilised for feed barley (Jia et al. 2009). Jia et al. (2011) proposed the *sdw1* locus to be a gibberellin 20-oxidase or *Hv20ox* due to its location in the syntenic region of rice containing the semi-dwarf *sd1*gene which also encodes a GA 20-oxidase. GA treatment assays have been utilised to confirm the presence of the *denso* semi-dwarfing allele in the Baudin

cultivar, which displays increased growth following GA_3 application compared to the control cultivar AC Metcalfe (Jia et al. 2011), however following the exogenous application of GA_3 to Chevallier and Tipple seedlings both parental lines were equally responsive. It may therefore be possible that at least within the C×T population, the height QTL on 3H may not be associated with a GA response. The relative expression levels of *Hv20ox* have been proposed as a method of determining the presence of either the *sdw1* or *denso* allele (Jia et al. 2011), suggesting that this may be a necessary method to confirm the allelic status of Chevallier and Tipple at the *sdw1* locus.

Chromosome 4H is the site of the major *B. graminis* resistance gene known as *Mlo*, which provides broad spectrum resistance to powdery mildew, yet it was not possible to detect a QTL associated with mildew resistance on 4H in either C×T population. It is very unlikely that the heritage cultivar Chevallier possesses any form of *Mlo* associated resistance, as illustrated by its high level of susceptibility. While Tipple is highly resistant to mildew, the *Mlo* status of Tipple remains unclear. Tipple displayed significant resistance to powdery mildew in both natural and controlled inoculation experiments, yet does not appear to possess either the *mlo-9* or *mlo-11* alleles, which are most commonly used in spring barley, or the *mlo-5* allele (G. McGrann, personal communication).

The major QTL associated with susceptibility to mildew in both the F_5 and F_7 C×T populations were located on chromosome 1H. The short arm of chromosome 1H is the site of the major *Mla* locus for race specific resistance to powdery mildew. Alleles at this locus encode multiple NB-LRR proteins and promote specific host – pathogen interactions resulting in various mildew resistance phenotypes (Xu et al. 2014). There are 30 recognised *Mla* alleles and due to the complexity at the *Mla* locus designing molecular markers for easy characterisation of these alleles has proven difficult (Moscou et al. 2011). Several mapping studies have also identified resistance QTL on 1H associated with the *Mla* locus. Hickey et al. (2012) identified a major QTL on 1H bin 2 at position 29.2cM, whilst Schmalenbach et al. (2008) identified two QTL associated with powdery mildew resistance between 0 – 85.0cM which accounted for a 50.0% reduction in mildew susceptibility. The *Mlra* minor resistance gene is also present on 1H and is located distally to the *Mla* locus (Aghnoum et al. 2010), however it is unlikely the resistance conferred by alleles at this locus could explain the apparent high levels of resistance demonstrated by Tipple. The further mildew resistance gene

Ror1 is also present on 1H and has been fine mapped to the pericentric region of the long arm of 1H (Acevedo-Garcia et al. 2013), however the positioning of the QTL identified within the present research suggests that this gene is unlikely to be associated with mildew susceptibility in the C×T population. The mildew resistance gene *Mlp* has also been posited to be located on 1H (Jørgensen, 1994). It appears probable that the resistance to powdery mildew in the Tipple parent is associated with the *Mla* locus although the results of the present study are unable to confirm the specific allelic status of Tipple, and further experiments using *Mla*-, *Mlra*- and *Mlp*-virulent *B. graminis* isolates should be undertaken to characterise the resistance seen in Tipple. In the F_7 2015 trial, a single minor QTL associated with mildew was identified on 2H at position 129.6cM, which was not identified in any other trial year or population. Shtaya et al. (2006) identified a QTL on 2H in two successive years using a L94 × Vada population, at positions 100.5 and 86.0cM, whilst Silvar et al. (2011) also detected two minor QTL on 2H accounting for a combined phenotypic variance of 7.3%. The *MlLa* resistance gene, which causes an intermediate response to avirulent *B. graminis* isolates, is also located on 2H (Giese et al. 1993), suggesting this may have a role in resistance in the C×T population.

Physiological leaf spots (PLS), also known as abiotic or non-parasitic leaf spots (NPLS), are distinct from fungal spotting diseases such as net blotch caused by *Pyrenophora teres* f. *teres* and Ramularia leaf spot, and are thought to be caused by oxidative stress (Wu and von Tiedemann, 2004). The presence of PLS is associated with yield loss in highly susceptible cultivars. A single QTL on the long arm of 3H for PLS was detected in the F_5 RILs, whilst a major 7HS QTL and two minor QTL were identified on 3HS and 7HL in the F_7 RILs. The recessive *mlo* alleles which confer powdery mildew resistance are associated with increased susceptibility to abiotic spotting, such as target spot, in a field environment (Makepeace et al. 2007). However, an absence of QTL for both mildew severity and PLS on 4H, the location of the *Mlo* gene, suggests that *mlo* is not associated with the PLS symptoms seen within the C×T population. Behn et al. (2004) identified several QTL for NPLS on 1H, 4H and 7H from a PZ24727 × Barke DH population, with the 7HS being mapped to 25cM. A further study by the same authors again detected a QTL on 7HL at 90cM which co-located with QTL for height and 1000-grain weight; however this had a lesser effect on the phenotypic variance than the 4H *mlo* associated QTL (Behn et al. 2005). The

presence of PLS QTL on both the short and long arm of 7H within these studies and at similar genomic regions in the F_7 RILs suggests that 7H may be an important genomic region associated with PLS. The 3H PLS QTL identified in the F_5 RILs partially overlapped with the minor 3H QTL for height and HD. It has been noted that in some environments, the appearance of PLS coincides with generative growth (Behn et al. 2004), which may offer an explanation for the partial co-location of the PLS and HD QTL. A number of lesion mimic mutants, known as *nec* mutants, which display necrotic lesions in the absence of pathogenic organisms (Rostoks et al. 2003) have been identified on 3H in barley. The *nec8* mutant (also known as *necS1-1*) was induced through fast-neutron (FN) treatment of the cultivar Steptoe and has been mapped to 3H bin 6, with a possible candidate gene being a cation or proton exchanging protein (Zhang et al. 2009). A further mutant designated *nec9.3091*, which also displayed dark brown leaf spots, was mapped to the AFLP marker *E37M33-6* at 128.1cM on 3H in a Proctor × Nudinka map (Wright et al. 2013). Further investigation into the underlying mechanisms which result in leaf spotting in barley may allow clarification of the 3H QTL which are associated with similar symptoms in the C×T populations.

The availability of phosphate is an important target for plant breeding. Up to 70% of the phosphate in seeds is stored as phytic acid (*myo*-inositol-(1,2,3,4,5,6)-hexakisphosphate or IP_6) in the aleurone layer, where it is thought to act a store of cations, phosphoryl groups and act as a chelating agent (Brinch-Pedersen et al. 2002). Phytases (*myo*-inositol hexakisphosphate phosphohydrolases) hydrolyse phytic acid into *myo*-inositol and inorganic phosphate, providing bioavailable phosphate which was previously inaccessible in the seed (Lott et al. 2011). Monogastric livestock display low phytase activity, meaning much of the phosphate in their feed is unavailable, and the seeds of many crops also display low phytase activity meaning that increasing phytase levels is a favourable breeding target in cereals (Brinch-Pedersen et al. 2014). Three QTL for different isomers of inositol pentakisphosphate (IP_5) were identified on 1H, 3H and 6H in the C×T F_5 population. A single major QTL on 3H was detected for IP_{5a} and two minor QTL were identified for IP_{5b} on 1H and 6H, with the 6H QTL partially overlapping the FHB QTL. Further definition of the intervals for the 6H IP_{5b} and FHB QTL should determine the extent of any association between these traits. IP_5 is a lower inositol phosphate which is associated with IP_6 hydrolysis (Rapp et al. 2001) and it is possible that the different isomers of IP_5, such

as IP_{5a} and IP_{5b}, may also be phytase enzymes (C. Brearley, personal communication). In plants two forms of phytases have been identified; histidine acid phosphatase phytases (HAP), a family of enzymes which include multiple inositol polyphosphate phosphatase (MINPPs), and purple acid phosphatase phytases (PAP) (Brinch-Pedersen et al. 2014). A major QTL associated with a PAP was identified on 5H at 58.9cM, with the *HvPAPa* gene mapping to the same location, whilst a minor QTL on 3H at 54.1cM corresponded to the location of the *HvPAPb* gene in a Yerong × Franklin DH population (Dai et al. 2011). A QTL on 1H was also detected from the same study at 44 – 76cM, although this could not be linked to any gene. The positioning of common markers within the map produced by Dai et al. (2011) and the C×T map determines that the location of the *HvPAPb* gene does not correspond with the position of the 3H IP_{5a} QTL interval. This suggests that *HvPAPb* is not likely to be responsible for the IP5a effect observed in the C×T population. At present, only nine PAP cDNAs have been cloned from cereals (Brinch-Pedersen et al. 2014) and there do not appear to be any known PAPs or MINPPs on 1H or 6H in the literature. The identification of three QTL which may potentially have an effect on mature grain phytase activity therefore requires further investigation.

The primary objective of the present study was to determine the possibility of a trade-off between FHB resistance and agronomic traits in the tall, heritage cultivar Chevallier. A QTL associated with reduced FHB incidence was consistently identified on the long arm of chromosome 6H in the two separate C×T populations across multiple trial years, giving confidence in the potency of this QTL. This QTL was not coincident with any other agronomic QTL conventionally associated with FHB resistance such as height or HD, as the major QTL for these traits were identified on chromosome 3H within the region of the *sdw1* gene. This suggests that the resistance of the 6H QTL is not a consequence of pleiotropy or linkage with genes for these traits.

The phenotyping of disease traits is difficult due to the complex interaction between genotype and environment, therefore FHB QTL are less easy to define than those for highly heritable traits such as height. The interval distance for the 6H FHB QTL was defined as 19.9cM in the C×T F_5 RILs which was expanded to 36.8cM in the C×T F_7 RILs. The QTL interval for the F_7 population is likely to be more accurately defined than in the F_5 population, even though the interval appears larger, due to the increased genetic map resolution in this population. It is therefore favourable to further define

the QTL interval within the F_7 population by back-crossing RILs which possess the resistance haplotype at the 6H QTL interval to the Tipple parent and conducting additional phenotyping of these lines.

Chromosome 6H is not generally associated with FHB resistance, with 2H being most frequently identified as the location of most major QTL detected for FHB (Zhu et al. 1999; Hori et al. 2005; Horsley et al. 2006; Lamb et al. 2009; Yu et al. 2010; Massman et al. 2011). In studies where QTL for FHB have been identified on this chromosome, many of these have been associated with agronomic traits and are therefore difficult to further characterise without attempting to determine the potential of pleiotropy or linkage within these regions (Ma et al. 2001; Dahleen et al. 2003; Canci et al. 2004). FHB QTL which do not appear to co-locate with other traits have however been identified on the short arm of 6H. Mesfin et al. (2003) identified two minor effect QTL on 6HS at 46 and 58cM within a Frederickson × Stander cross, however these were determined to have an opposite allelic effect on resistance. Dahleen et al. (2012) identified an FHB QTL located on 6HS between 0 – 6cM from a Zhedar 2 × ND9712//Foster population, with resistance provided by the Zhedar 2 allele. The peak marker underlying this QTL locates to chromosome 6H bin 2 in the integrated SNP based consensus map produced by Muñoz-Amatriaín et al. (2011). Massman et al. (2011) also identified two FHB QTL on 6H from the US CAP populations. One of these QTL co-located with a DON QTL on 6HS at 42 – 61cM and the other was positioned on 6HL at 124 – 126cM. However, only the 6HS QTL was present in both the two-row and the six-row CAP populations while the 6HL QTL was only detected in the six-row population (Massman et al. 2011). The 6H FHB QTL in the Chevallier × Tipple population is located on 6HL at position 114.5cM in both the F_5 and F_7 populations and does not appear to correlate with any of the previous approximate QTL locations on 6H identified within two-row barley. The QTL detailed in the literature at present were identified from mapping populations using the cultivars Zhedar 2 or Frederickson, or the advanced breeding CAP populations which are predominantly American, Japanese and Chinese elite modern germplasm lines. The 6H resistance QTL identified within this research is provided from the English landrace Chevallier, which may account for the identification of what appears to be a previously unidentified QTL in a two-row cultivar. That this QTL has not been previously described in the literature and also does not appear to provide a trade-off

with other agronomic traits suggests this resistance may be unique to Chevallier. The extent to which the SNPs underlying the 6H QTL associated with Chevallier are present in both modern and heritage barley varieties can be determined by designing KASP markers within the QTL region. Several other Chevallier accessions from various geographic locations, (obtained from the JIC Germplasm Resources Unit), have also been genotyped using the Genotyping-by-Sequencing method, yet not all possess the same SNP at the 6H peak marker.

Chromosome 6H is also known to be the location of several QTL associated with resistance to other barley diseases. Niks et al. (2004) identified a major novel gene designated *Ryd3,* for resistance to barley yellow dwarf virus (BYDV) at 58cM on 6H in a L94 × Vada RIL population. *P. teres* is the causal organism of the net form of net blotch, (NFNB), a foliar disease of barley. Resistance to NFNB is associated with the centromeric region of 6H, with Abu Qamar et al. (2008) identifying two resistance genes, approximately 1.8cM apart, at this position and a study by Gupta et al. (2011) detecting a single major gene for resistance at this location. Resistance to a small secreted proteinaceous necrotrophic effector known as PttNE1, associated with *P. teres* infection, was also detected on 6H at 46cM in a Hector × NDB 112 population (Liu et al. 2015). The centromeric region of 6H has also been proposed as the location of a number of genes which affect resistance to *Rhynchosporium secali*s, the causal species of leaf scald. Wagner et al. (2008) identified a minor QTL associated with *R. secalis* resistance near the centromere of 6H, whilst Zhan et al. (2008) also determined there was a cluster of resistance genes at this region, in addition to a major resistance gene named *Rrs13* on the short arm of 6H. Low levels of leaf scald symptoms, caused by natural *Rhynchosporium* infection, were present in the JIC C×T F_7 trial in 2014; however the distribution of disease was sporadic and disease levels were not adequate enough to accurately phenotype the whole population. It is unlikely that the 6H FHB QTL identified from the C×T populations will have an effect on resistance to either *R. secalis* or *P. teres,* as resistance to both leaf scald and NFNB is consistently associated with either the centromeric region or the short arm of 6H, whilst the FHB QTL is located on the long arm of 6H. However, it may be pertinent to conduct inoculation experiments with both of these fungal pathogens to determine whether any QTL for resistance can be identified from the population and if these QTL co-locate with the FHB resistance QTL.

Barley mapping studies frequently result in the detection of multiple QTL associated with a reduction in FHB incidence (Ma et al. 2001; Dahleen et al. 2003; Hori et al. 2005; Dahleen et al. 2012). In addition to the 6H QTL, three further QTL associated with FHB were identified on 2H and 7H in the C×T F_7 population during the 2015 trial, none of which were detected in the C×T F_5 population. The increase in the number of detected QTL may be due to the more fixed genetic nature of the F_7 population compared to the C×T F_5 RILs. Chromosome 2H is the genomic region which is most associated with the presence of major FHB QTL, however these frequently co-locate with HD QTL (Zhu et al. 1999; Canci et al. 2004; Hori et al. 2005; Horsley et al. 2006; Sato et al. 2008; Lamb et al. 2009). In the current study, only a single minor FHB QTL was detected at this location and no association with HD was identified. The 2H QTL does however partially overlap minor QTL identified for GH and tillering which were also identified in the same year and a QTL associated with powdery mildew detected in 2014. The peak markers for each of these traits do not co-locate with that of the FHB QTL but it is not possible at present to conclude that these traits are not associated. QTL for FHB resistance have also been identified on 7H in previous studies (Ma et al. 2001; Dahleen et al. 2012). In this study, QTL on 7HS and 7HL partially overlapped QTL for HD and PLS, respectively. The peak markers for the FHB and PLS QTL on 7HL are separated by 42.2cM meaning it is unlikely that there is an association between the two traits, although this cannot be fully disregarded. The 7HS QTL peak marker is 7.4cM from the peak marker of the minor HD QTL, with the Chevallier allele providing increased resistance to FHB but also an increase in the number of days to head emergence at the HD QTL. This suggests there may be the possibility of trade-off between FHB and HD at this QTL position.

The strong interaction between genotype and environment can greatly affect the ability to detect FHB QTL (Canci et al. 2004). During the 2014 trial of the F_7 population when plant growth conditions were not optimal, it was not possible to detect any QTL using the mean FHB score but it was possible to identify QTL using the individual scores from each of the four score dates. Interestingly, the 6H QTL was identified from the first score date, as was a 7H QTL, however these were absent in the final score when a single 3H QTL was present. This suggests that the 6H QTL may represent a form of host resistance during the early stages of infection, which in the

2014 trial was then masked by the effect of the 3H QTL during the later infection stages. The 3H FHB QTL was coincident with the major QTL for plant height and other agronomic traits. Competition with weeds resulted in very short plants and spikes remained partially surrounded by the flag leaf sheath. It was noted that such spikes in the shorter, later heading RILs frequently exhibited severe FHB symptoms at the base of the spike, most probably as a result of the retention of inoculum and associated high humidity aiding infection.

In barley, QTL associated with reduced DON concentration do not always coincide with those for FHB. An association mapping study by Massman et al. (2011), using American two-row and six-row CAP lines, identified eight commonly detected QTL for reduced DON concentration on 1H, 2H, 3H, 4H, 5H and 6H with only two of these QTL (4H at 24 – 36cM and 6H at 42 – 67cM) being associated with Type 1 FHB resistance. Studies by both Yu et al. (2010) and Dahleen et al. (2012), detected multiple QTL for FHB on 2H, 5H and 7H, however QTL associated with a reduction in DON concentration were only identified on chromosomes 3H and 2H in each study, respectively. Several other mapping studies within barley have identified either QTL for DON or FHB resistance which also do not co-locate (Ma et al. 2001; Dahleen et al. 2003; Lamb et al. 2009). Such studies suggest that breeding for both decreased FHB incidence and DON accumulation in barley is a complex process as it appears that these traits are often under separate genetic control.

In the C×T F_5 population a single QTL associated with reduced DON accumulation was identified that co-located with the 6H FHB QTL, with resistance to DON and reduced FHB incidence being conferred by the Chevallier allele. However, from the 2015 trial of the C×T F_7 RILs four QTL were identified on 1H, 3HS, 3HL and 6H with only one of these partially overlapping with an FHB QTL. The detected DON QTL were located within large marker intervals, with the 3HL interval spanning up to 43.3cM. The reduced precision of DON QTL location observed from the 2015 phenotype data may be due to the limited range of DON values of the F_7 RILs. The weather following inoculation was very cool and this may have adversely influenced DON production by the fungus. For example, the FHB scores and DON concentration in Tipple at the JIC 2013 trial were 17.6% and 14.9ppm respectively, whilst in 2015 the disease score for Tipple was 19.2% yet DON levels were much lower than in 2013, at only 3.6ppm. It may even be possible that the Chevallier allele confers reduced

DON accumulation during years of high DON production, yet has a lesser effect when DON levels are relatively low.

Of the four DON QTL identified in 2015, Chevallier and Tipple each contributed two alleles for reduced DON accumulation. The contribution of alleles from both the resistant and susceptible parental lines which are associated with lower DON has been observed in other mapping studies. For example, Dahleen et al. (2003) detected three DON QTL on chromosome 6H in a Zhedar 2 × ND9712//Foster population, with only one of these QTL being associated with the allele from the FHB resistant parent Zhedar 2. Similarly, lower DON was associated with the resistant Chevron parental allele for five QTL identified by Ma et al. (2001), whilst the susceptible Stander parent contributed to lower DON levels for two detected QTL. The F_7 RILs possessing the low value alleles at each of the four DON QTL (1H, 3HS, 3HL, 6H) identified in the 2015 trial exhibited a lower mean DON concentration in the grain than those possessing all of the alleles associated with the Chevallier parent. This suggests that by selecting specific alleles at each of these four loci it may be possible to produce lines which show increased resistance to DON accumulation compared to the Chevallier parent.

Most interestingly, within the C×T F_7 population a single DON QTL on 6H was identified from the 2015 trial. Unexpectedly, however, it was the Chevallier allele at this QTL that was associated with an increase in DON accumulation within the grain. The peak markers of the 6H FHB and DON QTL are 24.8cM apart, although it is not possible from the present QTL resolution to fully determine whether these are indeed different QTL. It is likely that the effect of the 6H DON QTL is dependent on the environment, which may explain why the Chevallier allele was associated with lower DON levels in 2013 but was associated with higher DON in 2015. A significant environmental effect on the detection of resistance QTL has been observed in several other studies. Horsley et al. (2006) identified four QTL associated with reduced DON accumulation on 2H (bins 5 – 10) in a Foster × CIho 4196 RIL population. At three of the four trial environments, the CIho 4196 allele contributed to lower DON concentration within the grain, yet in a single environment the Foster allele was associated with lower DON. This considerable genotype × environment interaction provides further difficulty in the identification of QTL associated with DON accumulation.

Three additional QTL associated with DON were identified on 1H, 3HS and 3HL and QTL for reduced DON accumulation have been identified on these chromosomes in previous mapping studies (Ma et al. 2001; Canci et al. 2004). The 1H DON QTL located at 101.8cM explained the lowest phenotypic variance within the F_7 population and partially overlapped the QTL for mildew and GH also detected on this chromosome. Ma et al. (2001) also identified a minor QTL associated with lower DON on 1HL, between markers *Xcdo431 – Xcmwg706*, which did not co-locate with other traits. The intervals of the two 3H QTL partially overlapped the minor and major QTL associated with agronomic traits such as height and HD, with the allele for lower DON being contributed by Chevallier. Interestingly, the 3H DON QTL which accounts for the largest phenotypic variance overlaps the minor QTL for height and HD, whilst the minor DON QTL overlaps the major 3HL agronomic trait cluster found in the region of the *sdw1* gene. The minor DON QTL overlapping with the *sdw1* locus on 3HL may reflect a pleiotropic effect associated with this major height and HD QTL. In contrast the reduction in DON contributed by the Chevallier allele at the 3HS QTL is less likely to be associated with the effects of the environment or as a consequence of disease escape resulting from a greater plant height, but may be due to an as-yet-unknown developmental process.

Reduced DON accumulation in barley grain has been associated with the expression of UDP-glucosyltransferases which convert the mycotoxin 15-ADON to DON-3-*O*-glucoside, a compound which exhibits reduced toxicity (Gardiner et al. 2010). Schweiger et al. (2010) identified four candidate barley UDP-glucosyltransferases which were observed to be greatly induced by DON. After expression in yeast only a single gene from the four candidates, *HvUGT13248*, conferred resistance to DON and was associated with the production of DON-3-*O*-glucoside (Schweiger at al. 2010). *Arabidopsis thaliana* lines displaying constitutive expression of *HvUGT13248* exhibited less growth inhibition following culture on DON containing media than non-transformed lines, which displayed restricted germination and reduced root and cotyledon growth (Shin et al. 2012). Transgenic *HvUGT13248* lines also produced increased concentrations of DON-3-*O*-glucoside than non-transformants following DON treatment (Shin et al. 2012). The wheat cultivars Bobwhite and CBO37 have since been transformed to express *HvUGT13248*, and display both increased Type 2 FHB resistance (spread within the ear) and greater production of DON-3-*O*-glucoside

than non-transgenic lines, suggesting this may be a useful source of resistance to DON accumulation (Li et al. 2015). Homology searches of the *HvUGT13248* genomic sequence using the Ensembl Plant genome browser position this gene on chromosome 5H in barley, which does not correspond with the locations of any of the four DON QTL identified within the C×T study indicating the QTL identified are not associated with this gene.

The Armelle × Tipple population was included within the present study to determine whether the resistance of Armelle, another tall cultivar, was also due to a trade-off between height or other agronomic traits. A single QTL for both height and HD co-located on the long arm of chromosome 3H, suggesting that the *sdw1* locus is also associated with these traits in this population. The single FHB QTL detected, with resistance derived from Armelle, directly coincided with the height QTL on 3HL. This suggests that the FHB resistance seen in Armelle may be due to an association with a gene controlling plant height and HD on 3H. It is not possible to determine whether this is due to pleiotropy or linkage from the present study, however. That the resistance of the taller variety Armelle appears to be associated with both height and HD, suggests that the resistance on 6H in Chevallier, which is not associated with either trait, is unique.

The phenotyping of two separate Chevallier × Tipple populations for FHB susceptibility has validated the identification of a potent QTL associated with reduced FHB incidence on chromosome 6H of Chevallier. In contrast to many mapping studies, the FHB QTL is not associated with agronomic traits such as height or HD. This indicates that the resistance of Chevallier is unlikely to be due to either pleiotropy or linkage with agronomic traits and may be a form of physiological resistance rather than a consequence of disease escape.

Chapter 5. Quantitative trait loci analysis of malting quality traits within a Chevallier × Tipple barley population

5.1 Introduction

The quality of barley malt is influenced by a number of specific components, all of which have an effect on the colour, flavour, reproducibility and stability of the finished beer. The optimal proportions of such components, including β-glucan, α-amylase and free amino nitrogen (FAN), have been determined to facilitate the production of beer with a consistent quality. During malting and mashing there are three main recognised biochemical processes; amylolysis (breakdown of starches); cytolysis (breakdown of structural components such as cell walls) and proteolysis (modification of proteins) (Hu et al. 2014). There are several methods for the analysis of the extent to which these processes have occurred, including those approved by the Institute of Brewing (IoB), the European Brewing Convention (EBC) and the American Society of Brewing Chemists (ASBC). Malt specifications may be expressed as either 'as is' values, which are representative of normal moisture conditions, or 'dry basis' values which are derived from dry extract (O'Rourke, 2002).

β-glucan or (1-3)(1-4)-β-d-glucan (BG) content is one quality parameter which is assessed during malting analysis. β-glucan is a cell wall non-starch polysaccharide which is a major component of the barley endosperm and is degraded by the cytolytic enzyme (1-3)(1-4)-β-d-glucan-4-glucanohydrolase or β-glucanase (Wang et al. 2004). The breakdown of β-glucan is an important step in the malting process as it allows the movement of enzymes, such as α-amylases, into the starchy endosperm which was previously inaccessible to these enzymes (Matthies et al. 2009). Raw barley grains contain very little β-glucanase activity and production of this enzyme is induced during the germination stage of the malting process (de Sa and Palmer, 2004). The β-glucan content of malt provides an indication of modification (the extent of endosperm breakdown), therefore high wort β-glucan content is a sign of poor modification of the grain (Gianinetti, 2009). Higher β-glucan levels are associated with increased wort viscosity, which can affect filtration processes and result in a haze in the finished product (Speers et al. 2003). Low β-glucan malts are therefore favoured within the brewing industry.

The enzyme α-amylase is one of the principle amylolytic enzymes involved in the malting process. α-amylase causes the random hydrolysis of α-1-4-D-glycosidic bonds within amylose and amylopectin, generating oligosaccharides and dextrins which are converted by β-amylase into fermentable sugars, such as glucose and maltose, for yeast metabolism (Adefila et al. 2012). Higher α-amylase levels are therefore desirable yet have been linked to pre-harvest sprouting (PHS) under humid conditions, with QTL for both traits co-locating in some mapping studies (Yang and Ham, 2012). PHS has a negative effect on grain quality and results in uncontrolled germination, demonstrating the potential for trade-off when breeding for desired malting quality traits. Diastatic power is a measure of the combined enzyme activity of α-amylase and the further diastatic enzymes β-amylase and limit dextrinase, and acts as an indicator of the amount of starch degradation possible during malting and mashing (Gibson et al. 1995). Higher values of diastatic power in malt have become more desirable due to the increased use of adjuncts, such as rice or corn, in brewing because these grains possess limited endogenous diastatic power (Wang et al. 2015). However, in 100% malt beers high diastatic power values are less favoured.

The moisture level of malt is important, as higher moisture levels are associated with lower extract values and the increased potential for growth of microorganisms. Malts with higher moisture values may have been subject to poor kilning processes, which may also have an adverse effect on malt colour and flavour (Hamalainen and Reinikainen, 2007). The IoB extract measurement is produced on coarsely ground material (0.7mm as opposed to 0.2mm). It provides an estimate of the amount of extract, or sugars, within the malt providing an indication of the level of starch modification (O'Rourke, 2002).

Parameters associated with the nitrogen content of the malt are also important in the brewing process. The total nitrogen (TN) provides a representation of all the nitrogenous compounds within the malt, whilst the total soluble nitrogen (TSN) signifies only the soluble forms (Abernathy et al. 2009). The soluble nitrogen ratio (SNR) represents the ratio between TSN and TN. The SNR and the Kolbach Index denote the same measurement, but refer to the methods approved by the IoB and the EBC, respectively. The TN value gives an indication of the protein content within the grain (Angelino et al. 1997), whilst TSN and SNR provide a representation of the extent of the modification of proteins into different molecular weight forms and amino

acids during malting. Protein levels need to be moderately high during the brewing process due to their enzymatic role in starch degradation and contribution to body and flavour (Steiner et al. 2010). However, excessive protein levels are thought to contribute towards haziness in the finished beer and also reduce the available starch resulting in a lower extract yield.

FAN refers to the complex mix of free amino acids and peptides present within the wort, which provide an essential source of yeast nutrition (Mugode et al. 2011). The measurement of FAN serves as an indicator for potential yeast fermentation, but does not take into the account the preferential uptake of specific amino acids by yeast (Stewart et al. 2013). Adequate FAN levels are required to provide the necessary source of nitrogen for sufficient yeast fermentation; however excessive FAN in the wort, which yeast is unable to metabolise, is associated with flavour instability due to the promotion of ester flavours and also poor mouthfeel (Steiner et al. 2012). Contrastingly, low FAN levels within the wort reduce the availability of amino acids, such as valine, which in turn can affect the formation of diacetyl compounds that contribute towards specific flavour tones within beer (Krogerus and Gibson, 2013). FAN levels of 140 – 180mg/l are considered to be optimal for both yeast metabolism and flavour development (Fox et al. 2003).

The contamination of barley grain by *Fusarium* species, and the subsequent accumulation of mycotoxins, is known to affect several malt quality parameters. *Fusarium* infected grains show severe structural damage, with the degradation of cell walls and starch granules observed prior to the malting process (Oliveira et al. 2012b). Nielsen et al. (2014) found that in the UK malting cultivars Tipple, Quench and Optic an increase in *F. poae* biomass was associated with a decrease in both malt extract and germinative energy. *F. culmorum* infection alters the protein content of grain, with an increase proteolytic activity and protein extractability observed compared to control grains (Oliveira et al. 2013). Wort produced from *Fusarium* infected malt is observed to have higher FAN and β-glucan levels than non-infected malt and is also associated with premature yeast flocculation (Oliveira et al. 2012a). Furthermore, the presence of DON within the malt correlates with a darker wort colour, which is thought to be due to the production of proteolytic enzymes during *Fusarium* infection (Schwarz et al. 2006). Hydrophobins are low molecular weight hydrophobic proteins produced by filamentous fungi, which are involved in a range of biological functions during the

fungal life cycle such as sporulation and surface interactions (Bayry et al. 2012). Hydrophobin production by *F. graminearum*, *F. culmorum* and *F. poae* has been observed not only during the development of barley grain but also throughout the steeping and germination steps of malting, before the subsequent release of hydrophobins into the wort during mashing (Sarlin et al. 2007). The presence of *Fusarium* associated hydrophobins in the finished brewed product causes gushing (uncontrolled foaming) of bottled beer upon opening (Sarlin et al. 2012). Gushing is therefore considered to be a serious quality defect, as such products cannot be sold to consumers. The results of these studies demonstrate the negative effects of FHB on the quality of brewed products and illustrate the need for advances in breeding for resistance to reduce FHB associated losses.

Chevallier barley was cultivated throughout England during the 1800s and early 1900s and was considered one of the best malting barleys at this time (Beaven, 1936). However, the desired characteristics and performance of malting cultivars have evolved throughout the last century and it is unknown how the malting quality of Chevallier compares to modern varieties. The creation of a recombinant in-bred line (RIL) population between Chevallier and the contemporary malting barley Tipple provides a unique opportunity to identify any favourable malting traits within the Chevallier germplasm. Malt quality is known to be affected by *Fusarium* infection; therefore the significant FHB resistance of Chevallier provides an additional aspect for identifying the potential for trade-off between disease resistance and quality traits. With this aim, Chevallier, Tipple and 105 RILs were micromalted to identify potential QTL associated with either malt quality or yeast fermentation activity.

5.2 Materials and methods

5.2.1 Chevallier × Tipple F_5 field trial

A trial containing a subset of 105 lines of the 188 Chevallier × Tipple F_5 population was sown at Morley Farm, Norfolk, UK in 2013. A single replicate of each RIL was sown in a 2 x 6m plot and nitrogen was applied at 65kg/ha. The 105 RILs were identical to those used in the DON accumulation/inositol phytase assays in Chapter 4.

5.2.2 Micromalting analysis

Micromalting analysis using 500g of seed per genotype was undertaken by Crisp Malting Ltd. using their standard methods of analysis. A single replicate of each RIL and two replicates for each parental line were micromalted. The malt quality traits α-amylase (as is and dry basis, dextrin units/du), diastatic power (as is and dry basis, °IoB), diastatic power Windisch Kolbach (dry basis, °WK), wort β-glucan (mg/l), free amino nitrogen (mg/l), soluble nitrogen ratio (%), total soluble nitrogen (%) and total nitrogen (%) were measured using the IoB and EBC standard recommended methods of analysis.

5.2.3 Yeast activity analysis

Analysis of yeast activity was undertaken to determine whether wort produced from Chevallier or Tipple malt was more favourable for yeast metabolism and also to identify any potential QTL associated with fermentation. Grain samples were crushed to 0.7mm (coarse grind) and weighed to 50g per sample. In a THIEMT TMB mashing bath, 350ml ddH_2O (total volume) per sample was preheated to 65^oC. Milled grain samples were then added to 250ml of ddH_2O and mixed with a glass rod, before a further 100ml ddH_2O was added. Each sample was mashed for 1 hour at 65^oC with a stirrer speed of 50rpm and then cooled to 20^oC. The volume of each sample was adjusted to 450ml and aliquoted into 30ml tubes which were centrifuged for 10 min at 1000g. Samples were then aliquoted into 1ml tubes and centrifuged for 10 min at 3000g to remove microorganism contamination. Per sample, 180µl of wort was transferred into a 96-well microtitre plate. Yeast culture (Safale 04, Fermentis©) was adjusted to optical density OD 2.0 using ddH_2O and 20µl was added to each wort sample. Negative controls of wort without yeast were included. Three replicates per RIL and nine replicates per parental line were analysed. Plates were incubated at 25^oC for 23 hours using a Tecan plate reader and the OD_{595} of each sample was recorded every 30 minutes. Gen5 data analysis software was used to process the data and to calculate Vmax and lag phase values. This work was undertaken at the University of Sunderland and Brewlab Ltd.

5.2.4 Quantitative trait loci analysis

The combined 384-SNP BeadXpress and Genotyping-by-Sequencing genetic map for the C×T F_5 population was used for QTL analysis. The raw values for each trait were analysed in a single trait linkage analysis in Genstat 16th edition, using the Kosambi mapping function with a LOD threshold of 3.0 for detecting significant QTL. The maximum step size along the genome was reduced to 10cM to improve the localization of possible QTL. Simple interval mapping (SIM) was used for the initial QTL search, followed by composite interval mapping (CIM) to finalise the QTL location using the detected candidate QTL as co-factors. A final QTL model was then fitted to produce the estimated QTL effects. QTL images were produced using MapChart.

5.2.5 Statistical analysis

Two-sample t-tests within Genstat 16th edition (Lawes Agricultural Trust, Rothamsted Experimental Station, UK) were used to determine if the mean trait values of Chevallier and Tipple were significantly different from one-another. A general linear model was used to determine whether there were significant differences between batches (16 samples per batch) during the micromalting process.

5.3 Results

5.3.1 Malting quality analysis

Multiple measurements associated with quality traits were recorded during micromalting of the parental lines and the RILs. Tipple displayed a greater mean α-amylase (as is) content than Chevallier with means of 63.5 and 51.0du, respectively. These values were on the boundary of being statistically different (P = 0.054 level). The mean for the RILs was 65.2du (Table 5.1). Similar values were obtained for the mean α-amylase (dry basis) values, with a mean of 53.5du and 67.0du for Chevallier and Tipple, respectively, which was significantly different (P = 0.033). The mean of the RILs was 69.4du. Mean values for diastatic power (as is) were not significantly different in the parental lines (P = 0.120), with values of 100.5 and 139.5 °IoB for Chevallier and Tipple, respectively. The mean diastatic power value of the RILs was

177.5 °IoB (Table 5.1). No significant difference in diastatic power (dry basis) values was observed (P = 0.148), with both parental lines providing similar measurements. Diastatic power (Windisch Kolbach, dry basis) was also measured with Chevallier displaying a marginally lower value than Tipple, with 394.5 and 403.0 °WK being recorded for each parent, respectively (P = 0.346). The mean of the RILs was 595.3 °WK (Table 5.1). A significant difference in wort β-glucan values between the two parental lines was observed (P = 0.036), with Tipple displaying a greater wort β-glucan content than Chevallier, with mean values of 383.0 and 278.5mg/l, respectively (Table 5.1). A mean value of 228.1 mg/l was obtained for the RILs. Both the 'as is' and 'dry basis' measurements of IoB 0.7mm extract were obtained from the micromalting analysis. Mean extract (as is) values of 285.5 (300.0 for dry basis) and 290.5 1°/kg (306.0 for dry basis) were determined for Chevallier and Tipple, respectively. Neither the 'as is' nor the 'dry basis' values for the parental lines were significantly different (P = 0.748 and 0.645, respectively). The means for the RILs were 279.1 and 296.8 1°/kg for the 'as is' and 'dry basis' extract values (Table 5.1). FAN mean values were 153.5 and 184.0 mg/l in Chevallier and Tipple respectively (P = 0.612), whilst the mean for the RILs was 147.7 mg/l. Multiple measurements associated with the nitrogen levels of the malted samples were recorded. The SNR values for Chevallier and Tipple were 36.7 and 40.2% respectively, with a mean of 35.7% in the RILs. The mean parental values were not significantly different (P = 0.671). TSN (dry basis) mean values were 0.7 and 0.8% in Chevallier and Tipple respectively, values which were not statistically different (P = 0.616), whilst the mean value of the RILs was 0.7%. The mean Chevallier value for TN (dry basis) was 1.8%, whereas for Tipple it was 1.9% (Table 5.1). Again, these values did not differ significantly (P = 0.836). The mean value for the RILs was 1.9%.

Table 5.1. The mean values associated with malting traits for Chevallier and Tipple, and both the range and mean values for 105 C×T F_5 recombinant inbred lines.

	Parents		RILs		
Trait[†]	**Chevallier**	**Tipple**	**Mean**	**Range**	**t- probability**[*]
AA (as is)	51.00	63.50	65.23	41.00 – 138.00	0.054
AA (dry)	53.50	67.00	69.37	44.00 – 146.00	0.033
DP (as is)	100.50	139.50	177.54	54.00 – 323.00	0.120
DP (dry)	106.00	147.00	188.83	58.00 – 342.00	0.148
DP-WK (dry)	394.50	403.00	595.31	183.00 – 077.00	0.346
BG	278.50	383.00	228.14	103.00 – 894.00	0.036
IoB Extract (as is)	285.50	290.50	279.11	264.00 – 298.00	0.748
IoB Extract (dry)	300.00	306.00	296.79	279.00 – 318.00	0.645
FAN	153.50	184.00	147.70	103.00 – 208.00	0.612
SNR	36.70	40.20	35.71	28.80 – 45.60	0.671
TSN (dry)	0.65	0.76	0.69	0.53 – 0.86	0.616
TN (dry)	1.81	1.88	1.94	1.65 – 2.37	0.836

[†] Abbreviations and measurements for each trait: AA (α-amylase: dextrin units or du); DP (diastatic power: °IoB); DP-WK (diastatic power: °WK); BG (wort β-glucan: mg/l); IoB extract (1°/kg); FAN (free amino nitrogen: mg/l); SNR (soluble nitrogen ratio: %); TSN (total soluble nitrogen: %) and TN (total nitrogen: %).

[*] The statistical significance of the difference between mean values for Chevallier and Tipple was calculated from a t-test.

For some malting parameters, such as α-amylase or TN, the range of values of the RILs appears to exceed the values of the parental genotypes (Table 5.1). It is possible that transgressive segregation may be occurring in the population as the two parental cultivars are genetically diverse, which may result in some of the RILs displaying either lower or higher values than the parental lines. Significant differences between micromalting batches were also observed for 11 of the 12 malting parameters measured (Table 5.2), a factor which again may contribute towards the variation seen within the population. It is worth noting that the mean values and the ranges of the RILs are generated from a single replicate of 105 RILs from the wider C×T F_5 population due to the high cost of the assay. Increased replication would therefore give more confidence in the accuracy of some of the more extreme trait values.

Table 5.2. T-probabilities of the significant differences between micromalting batches, calculated from a general linear model.

Trait	t- probability
α-amylase (as is)	<0.001
α-amylase (dry)	<0.001
Diastatic power (as is)	<0.001
Diastatic power (dry)	<0.001
Diastatic power Windisch Kolbach (dry)	<0.001
β-glucan (in wort)	0.034
IoB Extract (as is)	0.054
IoB Extract (dry)	0.027
Free amino nitrogen	0.015
Soluble nitrogen ratio	<0.001
Total soluble nitrogen (dry)	0.001
Total nitrogen (dry)	<0.001

5.3.2 Yeast activity analysis

Yeast activity assays were conducted to determine whether there were any significant differences in yeast fermentation between Chevallier and Tipple wort. The results of the yeast analysis assays were highly variable however, with considerable variance displayed both within replicates on each plate and between plates. Negative or zero readings were also observed for multiple samples, which may be indicative of settling of the yeast cells within the plate during incubation preventing accurate OD values being recorded. Fewer replicates were analysed for the RILs due to the large population size and this resulted in high variability of the mean trait values for these lines. Within the parental lines, no significant difference between the mean values for lag time, Vmax or the first and final OD values could be determined between Chevallier and Tipple (Table 5.3).

Table 5.3. The mean values associated with yeast activity for Chevallier and Tipple.

	Means		
Trait	**Chevallier**	**Tipple**	**t- probability***
Lag time†	258.00	240.50	0.288
Vmax†	1.93	1.90	0.808
OD 1	0.16	0.16	0.900
OD final	1.25	1.26	0.910

† Lag time is expressed in minutes (min) and Vmax is expressed as the increase in OD units per minute (OD/min)).

* The statistical significance of the difference between mean values for Chevallier and Tipple was calculated from a t-test.

5.3.3 QTL analysis of quality traits

QTL associated with malting parameters were identified on every chromosome except 1H and 6H. On several chromosomes the malting quality QTL appeared to co-locate with agronomic trait QTL, such as height and heading date, identified within chapter 4. To determine whether the agronomic QTL would be present using a reduced dataset, the analyses for these QTL were repeated using only the phenotype data for the 105 C×T RILs. All agronomic trait QTL were identified to the same location when using both the 105 RIL subset and the complete 188 RIL dataset, suggesting that there is little loss of power during the analysis process when using a reduced dataset.

Three QTL were associated with α- amylase activity, using both the 'dry basis' and 'as is' values. The α- amylase dry basis QTL was identified on 5H at position 89.0cM, accounting for 10.3% of the variance with the contributing parental allele from Chevallier (Table 5.4). Two further QTL, one each for 'dry basis' and one for 'as is' values, were identified on 7H at position 162.9cM (Figure 5.5) with the higher value allele being provided by the Tipple parent. A single QTL for diastatic power (Windisch-Kolbach units) was detected on 3H at 50.36cM, accounting for 11.4% of the phenotypic variance within the population. This QTL also partially overlapped the heading date QTL identified in the C×T F_5 *Fusarium* trials in 2013 (Figure 5.2). QTL peaks for both diastatic power 'as is' and 'dry basis' IoB measurements were also

observed on 3H, however these were not significant at the threshold of LOD 3.0 used. Two QTL were identified for wort β-glucan content, with one on 2H at 214.9cM explaining 14.4% of the variance, and a further QTL detected on 3H accounting for 23.3% of the phenotypic variance (Table 5.4). Higher wort β-glucan was associated with the Tipple parent. A QTL for IoB extract was detected on 2H at position 56.5cM, with a LOD score of 3.3. Three FAN QTL were detected from the dataset, with the major QTL being located on 2H at 207.4cM overlapping the QTL identified for wort β-glucan content (Figure 5.1). Two partially overlapping FAN QTL were also identified on 4H at positions 58.9 and 90.5cM (Table 5.4). Higher FAN content was associated with the Chevallier parent for all three QTL. A QTL associated with SNR was present on 2H at 206.4cM, co-locating with both the FAN and wort β-glucan QTL and also partially overlapping with a minor QTL associated with heading date (Figure 5.1). The SNR QTL accounted for 8.2% of the phenotypic variance within the RIL population and a higher SNR was conferred by the Chevallier parent (Table 5.4). A further SNR QTL was detected on 4H at 91.9cM, coinciding with the FAN QTL present on 4H (Figure 5.3) and explaining 21.3% of the variance. A single QTL associated with TSN was detected within the dataset. This co-located with the FAN and SNR QTL on 4H at position 91.9cM. A TN QTL was also found to be present on 3H at 138.2cM, with the QTL interval overlapping with QTL identified for agronomic traits such as height, heading date, tillering and growth habit (Figure 5.2). Both of the QTL associated with total nitrogen explained a similar amount of phenotypic variance, for example 17.9 and 15.2% in the 4H and 3H QTL respectively, with the Chevallier parent contributing to a higher value for both QTL. No QTL associated with yeast activity (initial/final OD values, Vmax, lag time) could be detected from the datasets.

Table 5.4. Quantitative trait loci for malting quality traits identified from the C×T F_5 recombinant inbred line population.

Trait	Marker	Chr.†	Position (cM)	LB (cM)†	UB (cM)†	-LOG(P)≈	% Var†	Add.†	Allele†	s.e.†
α-amylase (as is)	52670	5	89.03	72.30	105.76	3.04	10.30	6.03	Chevallier	1.81
α-amylase (as is)	1561200	7	162.90	152.51	173.29	3.99	14.79	7.22	Tipple	1.77
α-amylase (dry basis)	1561200	7	162.90	153.48	172.32	3.91	16.01	7.91	Tipple	1.97
DP Windisch Kolbach (dry basis)	1567966	3	50.36	35.88	64.84	3.00	11.43	52.67	Chevallier	15.87
β-glucan in wort	1769678	2	214.90	204.20	225.60	3.60	14.44	64.66	Tipple	16.88
β-glucan in wort	2555870	3	185.13	179.07	191.19	5.33	23.34	82.21	Tipple	16.74
IOB Extract 0.7mm (dry basis)	368439	2	56.47	44.96	67.98	3.33	13.62	1.83	Tipple	0.50
Free amino nitrogen	106745	2	207.44	191.28	223.60	3.58	10.56	6.81	Chevallier	1.98
Free amino nitrogen	49161	4	58.94	19.91	97.98	3.25	6.36	5.29	Chevallier	2.06
Free amino nitroen	11_21490	4	90.49	67.77	113.21	3.34	8.42	6.09	Chevallier	2.28
Soluble nitrogen ratio	374975	2	206.44	182.79	230.00	3.40	8.22	0.94	Chevallier	0.32
Soluble nitrogen ratio	11_20012	4	91.90	85.19	98.61	4.21	21.34	1.51	Chevallier	0.36
Total soluble nitrogen (dry basis)	11_20012	4	91.90	83.63	100.17	3.29	17.85	0.06	Chevallier	0.01
Total nitrogen (dry basis)	11_10918	3	138.15	128.15	148.15	3.12	15.24	0.03	Chevallier	0.02

≈ -LOG(P) is equivalent to LOD score

† Abbreviations: Chromosome (Chr.); LB (lower bound of QTL position); UB (upper bound of QTL position); % Var (percentage of phenotypic variance accounted for); Add. (Additive effect); Allele (High value allele); s.e. (standard error).

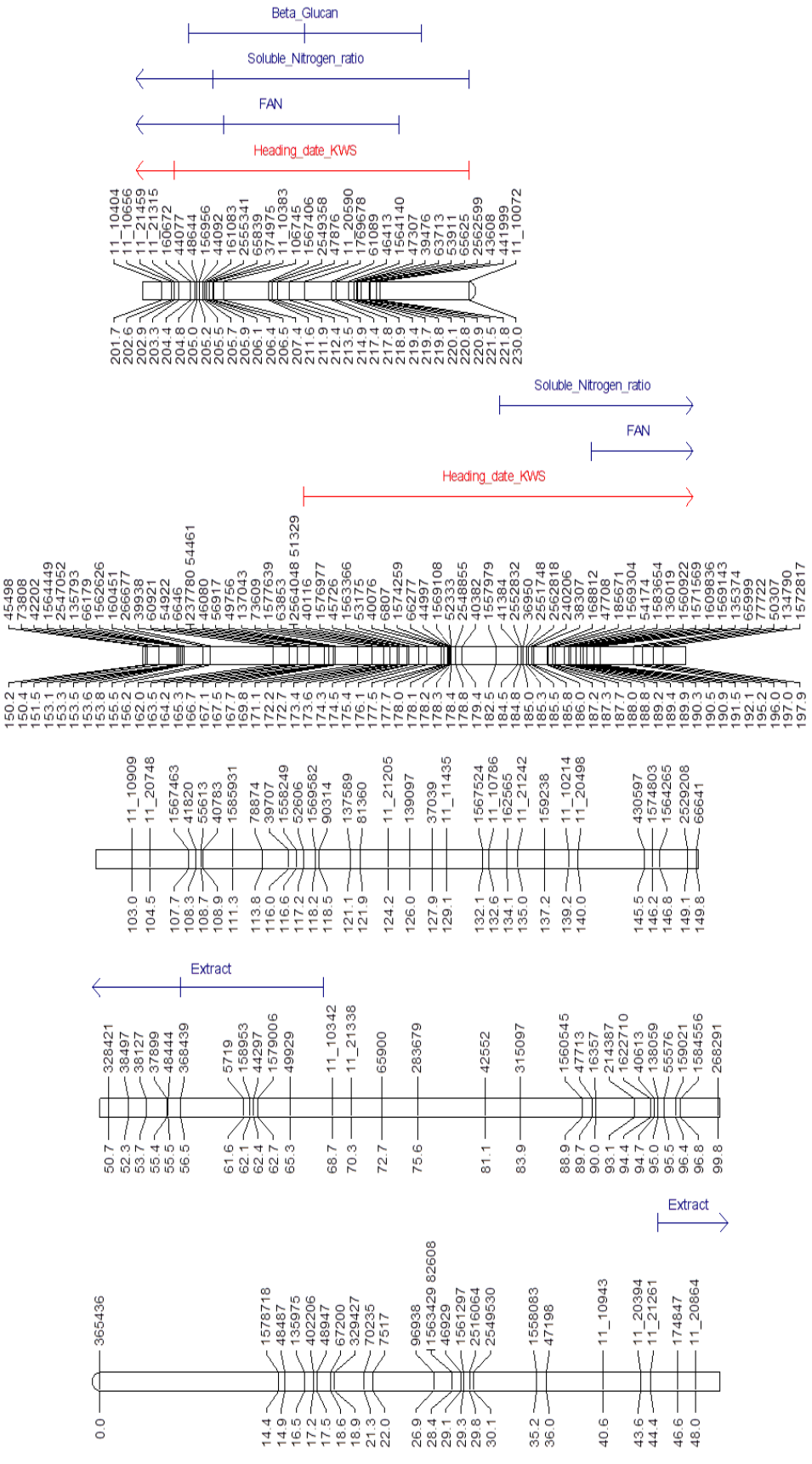

Figure 5.1. Quantitative trait loci identified on chromosome 2H of the Chevallier × Tipple F_5 mapping population by malt quality phenotyping.

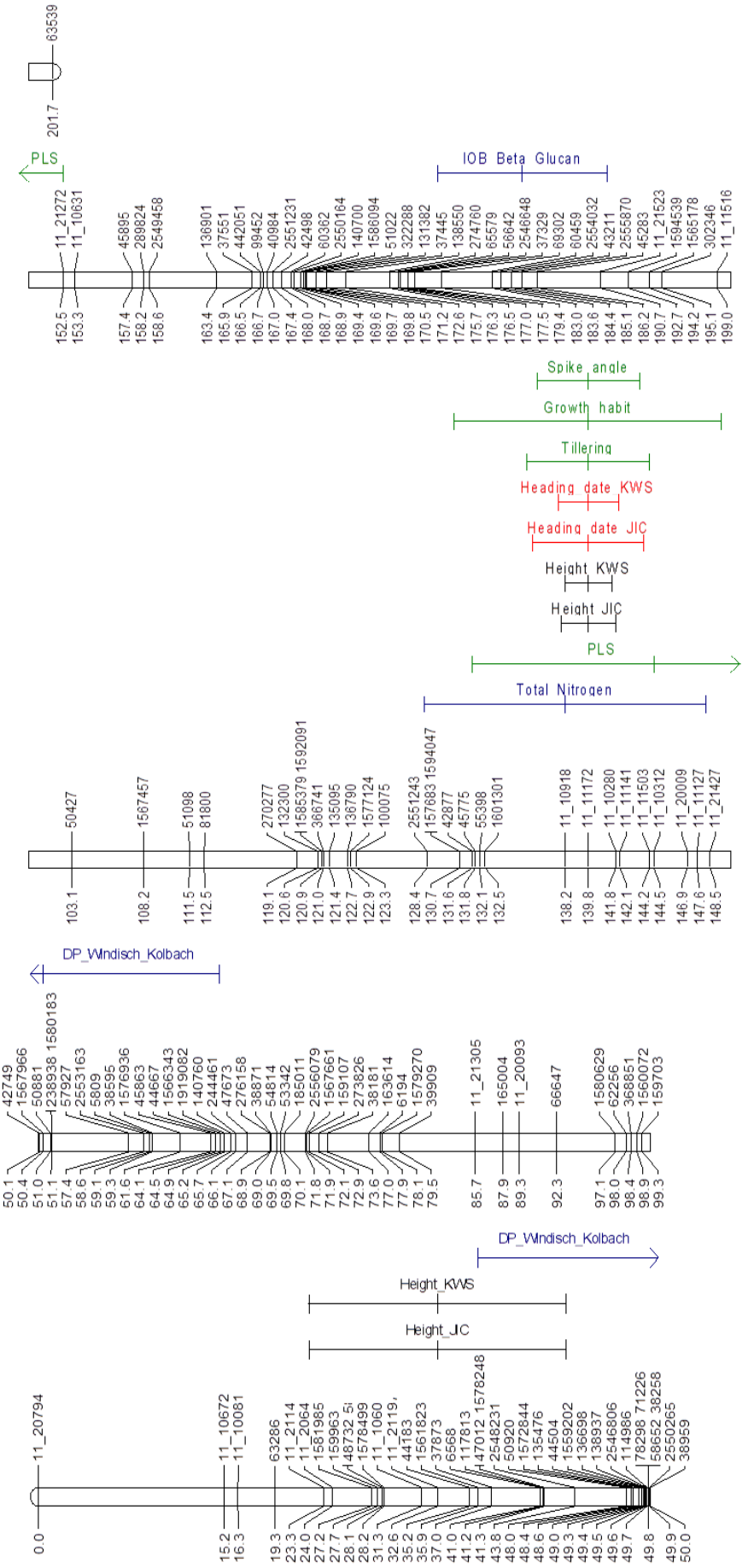

Figure 5.2. Quantitative trait loci identified on chromosome 3H of the Chevallier × Tipple F_5 mapping population by malt quality phenotyping.

Figure 5.3. Quantitative trait loci identified on chromosome 4H of the Chevallier × Tipple F_5 mapping population by malt quality phenotyping.

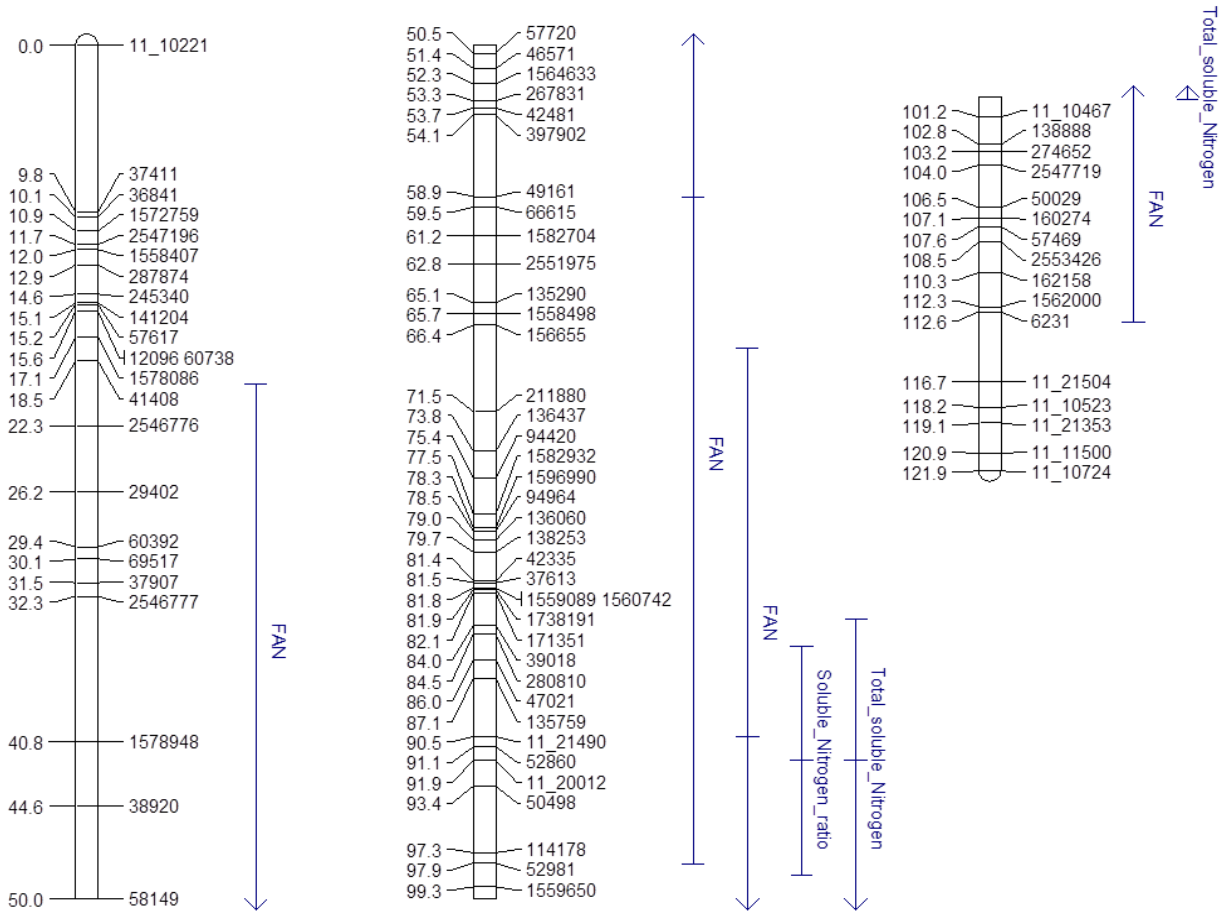

Figure 5.4. Quantitative trait loci identified on chromosome 5H of the Chevallier × Tipple F_5 mapping population by malt quality phenotyping.

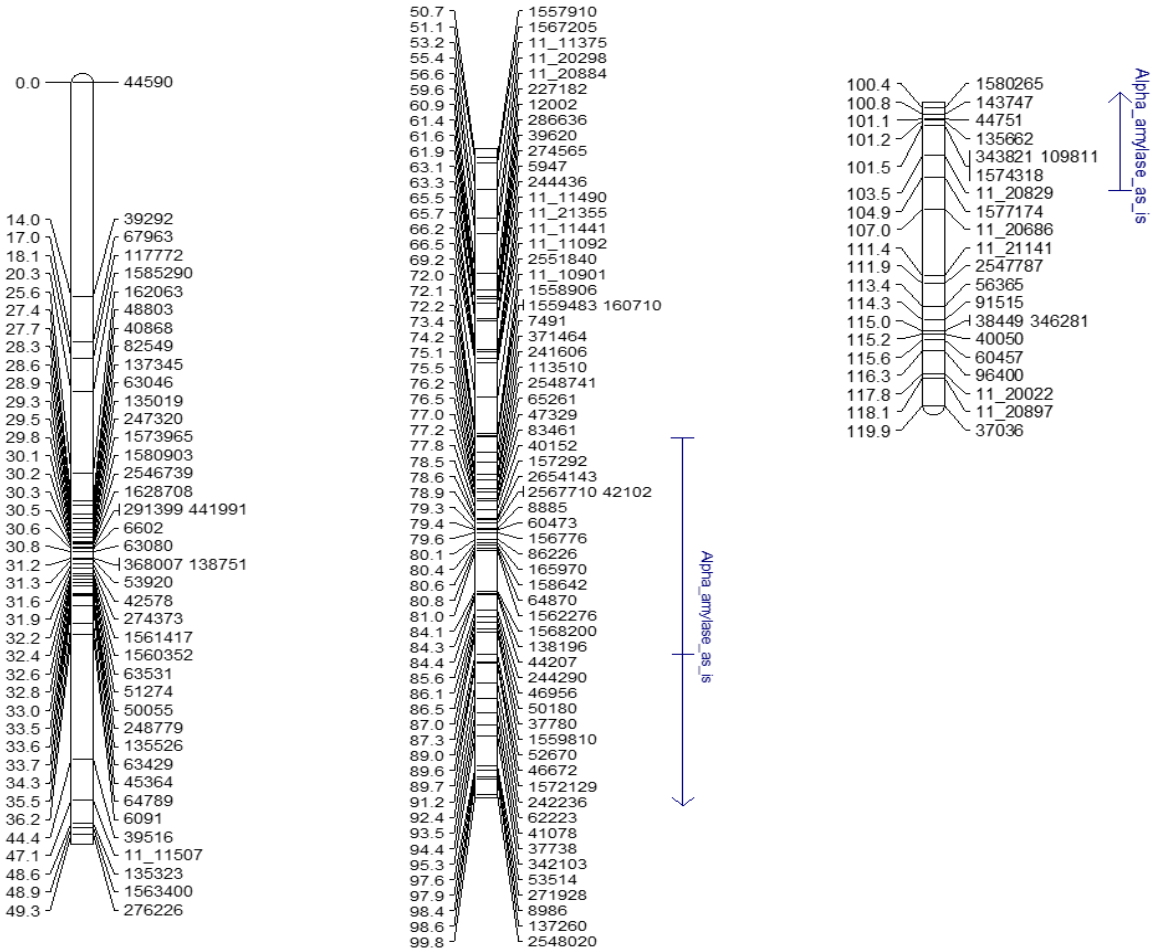

Figure 5.5. Quantitative trait loci identified on chromosome 7H of the Chevallier × Tipple F_5 mapping population by malt quality phenotyping.

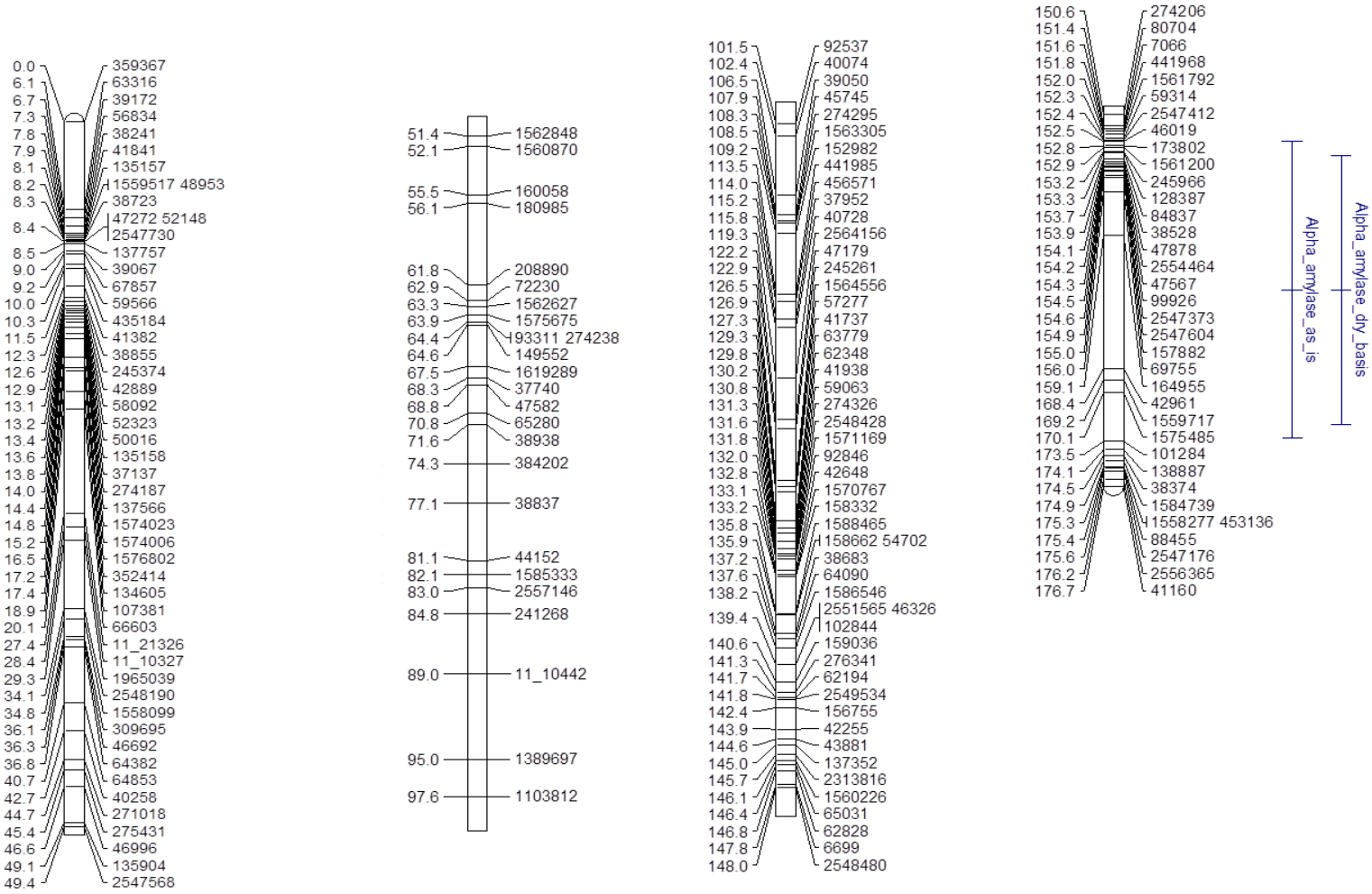

5.4 Discussion

QTL associated with malting quality have been identified on every barley chromosome (Wang et al. 2015), however within this study no QTL were detected for malting traits on chromosomes 1H and 6H. Four clusters of coincident QTL were detected on 2H, 4H, 5H and 7H; a feature not uncommon in malting quality studies (Han et al. 2004; Laido et al. 2009; Schmalenbach and Pillen, 2009).

QTL associated with wort β-glucan have been detected on each chromosome, with multiple studies identifying 1H, 2H and 7H as particular regions of interest (Emebiri et al. 2004; Gao et al. 2004; Han et al. 2004; Li et al. 2008; Gutiérrez et al. 2011). Within the current study, a minor QTL was detected on 2H and a major QTL was located on 3H. A minor QTL associated with wort β-glucan was previously identified on the long arm of 2H at 292cM in a VB9524 × ND11231*12 DH population (Emebiri et al. 2004) and significant marker-trait association with wort β-glucan was identified at position 150.7cM using cultivars from the Oregon State breeding program (Gutiérrez et al. 2011). The location of two previous wort β-glucan associated QTL on 2H suggests that the QTL detected in the current study may not be unique. Four genes associated with cellulose synthase-like (*CslF)* genes which are thought to mediate the synthesis of β-glucan have been previously mapped to 2H (Burton et al. 2008), but are located at the centromeric region suggesting these are unlikely to be associated with the 2H minor QTL. The major QTL for wort β-glucan segregating in the C×T population mapped to the long arm of chromosome 3H at 185.1cM, accounting for 23.3% of the variance within the population. β-glucan QTL have been detected on the short arm of 3H at position 32cM in a VB9524 × ND11231*12 DH population, which accounted for 22.6% of the variance, and at 99cM in a TR251 × CDC Bold population (Emebiri et al. 2004; Li et al. 2008). Several (1,3)-β-d-glucan synthase-like (*GSL*) genes have been detected in barley, with *HvGSL6* and *HvGSL7* both being located on chromosome 3H (Schober et al. 2009). Significant marker-trait associations between grain β-glucan content have been detected on 3H between 63.0 – 70.2cM in a GWAS of spring and winter elite barley germplasm pools (Houston et al. 2014). The most significant markers in the study by Houston et al. (2014) that were associated with β-glucan on 3H, SCRI_RS_237939 and 11_11314, are located in genomic regions which correspond to the presence of the candidate genes *HvGSL7* and a glycoside hydrolase,

respectively. The marker associated with wort β-glucan in the C×T F_5 map is located in the distal region of 3H at 185.1cM however, suggesting that the wort β-glucan QTL in the present study is unlikely to be due to an association with the candidate genes identified by Houston et al. (2014).

There are several parameters evaluated during malt analysis which relate to the nitrogen content, and therefore protein modification, of the malt. QTL associated with the TN, TSN, SNR or Kolbach-Index (K-I) and FAN content have been reported on chromosomes 1H, 2H, 3H, 4H, 5H and 7H and often co-locate (Emebiri et al 2004; Panozzo et al. 2007; Wang et al. 2015). Within the C×T population, four QTL for FAN, SNR and TSN were identified on 4H. Three of these QTL (FAN, SNR and TSN) co-located at 90.5 – 91.9cM, and the QTL interval of this cluster also partially overlapped the major FAN QTL located on 4H centred at 58.9cM. Chromosome 4H has been identified as region associated with nitrogen content, as QTL for FAN, SN and SNR/K-I have been identified on this chromosome in multiple studies (Panozzo et al. 2007; Szucs et al. 2009; Wang et al. 2015). Several QTL from previous studies map throughout the short arm of 4H, with a QTL mapping to 18.0cM in the study by Emebiri et al. (2004) and a QTL for FAN being located at 56.0cM, with a QTL interval of 51.6 – 95.0cM, within a TX9425 × Naso Nijo DH population (Wang et al. 2015). The positioning of these QTL suggests that the QTL associated with malt nitrogen content on 4H may not be unique to the C×T population. Two additional co-locating minor QTL for SNR and FAN were detected on chromosome 2H in the C×T population. QTL for TN and SNR/K-I have been associated with the short arm of 2H (Wang et al. 2015), but the detection of a QTL for FAN on 2H does not appear to have been previously reported. The 2H QTL in the C×T population partially overlap a minor QTL for wort β-glucan and as low β-glucan is associated with an increased Kolbach-Index or SNR (Jin et al. 2012), it is unsurprising that QTL for wort β-glucan and SNR appear to co-locate. A single QTL associated with TN was also detected on the long arm of chromosome 3H in my study. Two QTL associated with TN were also detected on 3H by Wang et al. (2015) which were found to be environmentally dependent. The same authors also identified two QTL for SN and FAN on 3H. This suggests that the identification of QTL on the long arm of 3H associated with malt nitrogen levels may be novel to the C×T population, but it is unclear how TN and SN/FAN traits may express themselves in different backgrounds.

QTL for α-amylase activity have been detected on each chromosome using several populations (Marquez-Cedillo et al. 2000; Han et al. 2004; Szucs et al. 2009; Mohammadi et al. 2015). Two of the major barley genes which encode α- amylases, *Amy1* and *Amy2*, are located on 6H and 7H, respectively (Matthies et al. 2009), and many QTL previously identified have been detected within the genomic regions containing these genes. Three QTL associated with the α-amylase content of the malt were identified in the C×T population, with two QTL on 7H and a single QTL on 5H. The α-amylase QTL on 7H (representing both the 'as is' and 'dry basis' values) was located at 162.9cM, which correlates with a previous study which identified α-amylase QTL at 161.5cM on 7H (Gutiérrez et al. 2011). The marker for the *Amy2* locus was recently mapped at 126cM on 7H in a GWAS of 254 European spring barleys (Shu and Rasmussen, 2014). α-amylase enzymes are separated into two major classes which are distinguished by the isoelectric point of each enzyme and the *Amy2* gene on 7H is thought to encode low isoelectric point α-amylases (Zwickert-Menteur et al. 1996). It is highly probable that the C×T 7H α-amylase QTL is due to the presence of the *Amy2* locus within this region. Whilst the 5H QTL identified within the C×T population is not associated with either of the major α-amylase genes, additional QTL for α-amylase have also been reported on 5H previously (Marquez-Cedillo et al. 2000; Ayoub et al. 2003; Gutiérrez et al. 2011; Mohammadi et al. 2015). A QTL for α-amylase was identified at position 280cM by Emebiri et al. (2004) and also at 183.0 – 188.0cM in five out of eight American breeding populations studied by Mohammadi et al. (2015). The 5H QTL in the present study was mapped to 89.0cM, suggesting that this QTL may be novel. The detection of three QTL associated with α-amylase, with the high value alleles being derived from either parent, may explain the range of values for α-amylase observed within the RILs which exceeded those of Chevallier and Tipple.

Diastatic power provides an estimate of all the amylolytic activity present during mashing. As with most malt quality traits, QTL for this characteristic have been identified on each of the seven barley chromosomes, with QTL associated with diastatic power and specific amylolytic enzymes often co-locating (Marquez-Cedillo et al. 2000; Gao et al. 2004; Han et al. 2004; Gutiérrez et al. 2011). A single QTL for diastatic power (Windisch-Kolbach), with a LOD score of 3.0, was identified on 3H in this study. A QTL associated with diastatic power was also detected on 3H at 200.9cM in a Morex × DH72 population by Larson et al. (1997), which was found to

co-locate with a serine carboxypeptidase I (*Cxp1*) gene which has been proposed to affect starch hydrolysis (Potokina et al. 2004). However, the QTL within this study and the study by Larson et al. (1997) map to different chromosomal arms of 3H, so are therefore unlikely to be associated. Diastatic power is an indicator of α-amylase, β-amylase and limit dextrinase activity, yet interestingly within this study the QTL for diastatic power (3H) did not co-locate with QTL associated with α-amylase (5H and 7H). It has been posited that β-amylase is a more reliable indicator of diastatic power than either α-amylase or limit dextrinase (Georg-Kraemer et al. 2001), however the activity of these enzymes were not specifically analysed in the present study. There are two known β-amylase genes in barley, with a gene specifying an endosperm specific β-amylase, known as *Bmy1*, on 4H and a second gene, *Bmy2*, encoding a ubiquitous β-amylase located on the short arm of 2H (Vinje et al. 2011). A gene encoding for limit dextrinase has been mapped to the short arm of 7H (Li et al. 1999). As the major genes encoding β-amylase and limit dextrinase are located on different chromosomes to the diastatic power QTL (3H) detected in the C×T population it is unlikely that they are associated with the differential diastatic power of these two varieties. However, analysis of the activity of these enzymes within the malt of the C×T RILs may provide more information regarding this QTL.

Malt extract is a measure of the sugar content derived from the malt. Many studies have identified 1H, 2H, 5H and 7H as being chromosomes frequently associated with this trait (Marquez-Cedillo et al. 2000; Gao et al. 2004; Han et al. 2004; Elia et al. 2010; Matthies et al. 2014). A single QTL for IoB extract (dry weight) was identified on 2H within this study which did not co-locate with any of the other malt quality traits. QTL associated with malt extract have been identified along chromosome 2H previously, with a major QTL on 2H at 29.0cM being identified in a study by Wang et al. (2015), a QTL locating near the *Vrs1* marker on 2H as detected by Elia et al. (2010) and two further QTL which were identified using the EBC analysis method mapping to 165.0 and 250cM on 2H in a study by Emebiri et al. (2004). The consistent detection of QTL for malt extract on 2H suggests that the QTL identified within the C×T population may not be novel.

Interestingly, it was not possible to detect any QTL associated with malt quality traits on chromosomes 1H and 6H in the C×T population. 1H is purported to be the site of multiple genomic regions that are associated with several co-locating malting traits.

QTL for α-amylase activity, β-glucan content, friability, wort viscosity, grain protein content, diastatic power and malt extract have all previously been detected on 1H (Emebiri et al. 2004; Molina-Cano et al. 2007; Laido et al. 2009; Schmalenbach and Pillen, 2009; Gutiérrez et al. 2011; Matthies et al. 2014; Wang et al. 2005). Malting QTL on 1H have also been demonstrated to cluster, with eight QTL overlapping in an 85cM interval in a study by Schmalenbach and Pillen (2009) and a marker-trait association for friability, malt extract and wort viscosity being detected at 58.7 – 59.4 cM detected by Matthies et al. (2014). It is therefore surprising that it was not possible to identify any QTL on 1H within the C×T population, which may indicate a lack of polymorphisms between Chevallier and Tipple on this chromosome. In contrast, malt quality QTL are less frequently reported on 6H (Marquez-Cedillo et al. 2000; Emebiri et al. 2004; Yang and Han, 2012; Wang et al. 2015). Fewer marker-trait associations were detected on 6H than on the other chromosomes in multiple GWAS of the Oregon Wolfe barley population (Gutiérrez et al. 2011) and only 12 significant associations were detected on 6H compared to the 40 that were identified on 5H in the study by Szucs et al. (2009).

Malting quality traits on 2H and 3H partially overlap with QTL associated with agronomic characteristics. The SNR and FAN QTL on 2H partially overlap the QTL interval of a minor QTL for heading date, whilst the diastatic power QTL on 3H overlaps a minor height QTL. The QTL identified for TN content also partially overlaps the agronomic QTL cluster on 3H, which is thought to be associated with the *sdw1* locus. Wang et al. (2015) also report the co-location of QTL for TN and heading date on both the short arm of 2H and 3H, whilst multiple studies have detected QTL associated with malt extract within the *sdw1* region on chromosome 3H (Collins et al. 2003; Elia et al. 2010). Further investigation within these regions of the genome is required to determine the possible associations between these traits.

Whilst different beer styles require specific quality parameters, there are preferential values for many traits within the brewing industry leading to an aim to breed cultivars which increasingly fit these criteria. Malts which do not conform to these standards may be more difficult to process and may result in the manufacture of products with variable quality. The malt specifications for diastatic power, FAN and wort β-glucan have been determined to be of particular importance for brewers due to their significant contribution towards the finished beer (Brewer's Association, 2014).

Diastatic power (Windisch-Kolbach) levels between 200 – 350°WK are generally preferable (Fox et al. 2003), yet the mean values for both Chevallier and Tipple exceed this range at 394.5 and 403.0°WK respectively. The diastatic power content of Chevallier is not significantly different from that of Tipple however, a cultivar which has full IBD approval for use as a malting cultivar (HGCA, 2014). This suggests that malt derived from Chevallier performs comparably with the modern variety Tipple for diastatic power activity. A FAN content of 140 – 180mg/l within malt is also desirable (Fox et al. 2003). Chevallier also compares well for FAN content at 153.5 mg/l, whilst Tipple only slightly exceeds the range of desired values at 184.0 mg/l. Whilst malt quality may differ between years, this suggests wort derived from Chevallier malt is likely to contain sufficient levels of FAN for adequate yeast fermentation but is less likely to contain excessive levels of FAN which contribute towards flavour instability. The preferred wort β-glucan content has been determined to be less than 200mg/l (O'Rourke, 2002), which should indicate sufficient grain modification without resulting in increased wort viscosity. Both the Chevallier and Tipple wort β-glucan content exceed this value, at 278.5 and 383.0 mg/l. Although the wort β-glucan content of Chevallier is larger than desired it is significantly lower than that of Tipple, suggesting that the heritage Chevallier malt better correlates with the favoured parameters for wort β-glucan than the modern Tipple variety.

The production of alcohol during brewing is dependent on the fermentation process. Immediately after the addition of yeast to unfermented wort, a process known as pitching, the yeast begins to metabolize amino acids within the wort. The initial stage of nitrogen uptake, synthesis of cell wall components such as sterols and fatty acids, and general acclimatisation is known as the lag phase and is critical for efficient fermentation (Stewart et al. 2013). Within 12 hours, the yeast begins a period of exponential growth where sugars such as glucose, maltose and fructose, are converted into ethanol and carbon dioxide. Whilst yeast has been considered a model organism for several decades, quantitative genetic studies using the budding yeast *Saccharomyces cerevisiae* have only become more prevalent within the last decade (Liti and Louis, 2012). Presently there are no reports of QTL associated with yeast performance during brewing, however two studies were recently published which identified QTL associated with the production of wine aroma compounds by *S. cerevisiae* (Marullo et al. 2007; Steyer et al. 2012). The current study attempted to

identify QTL associated with yeast growth parameters, including lag phase and maximum growth velocity, however no QTL were identified which may indicate that traits associated with yeast metabolism are not highly heritable. It may also suggest that whilst Chevallier and Tipple display significantly different malting traits, as evidenced by the detection of QTL, the wort derived from these cultivars is equally favourable for yeast growth. Different yeast strains, however, have also been demonstrated to utilise wort at different rates (Evans and Hamet, 2005). Safale 04 (Fermentis©), the yeast strain used within the present study, is known for its vigorous fermentation and it is possible that using a yeast strain which is more sensitive to the wort composition may reveal differences in growth activity influenced by parameters within the two barley varieties.

The present study provides the first investigation of malting quality associated with the heritage cultivar Chevallier. Analysis of malting traits requires large grain quantities and relies on the use of specialist equipment, meaning the process is both expensive and time-consuming. A single replicate of 105 RILs created from a cross with the modern cultivar Tipple were grown in one environment and were micromalted to provide preliminary knowledge of quality traits associated with Chevallier. Further studies with increased replication and a larger population may be undertaken to provide more robust data to detect more subtle differences between the varieties. Of the 15 QTL for malting traits identified within the RIL population the Chevallier parent was associated with nine of these QTL, whilst Tipple was associated with six. Chevallier contributed QTL for α-amylase, diastatic power (Windisch-Kolbach), FAN, SNR, TSN and TN, whereas Tipple contributed QTL for α-amylase and wort β-glucan content. As Chevallier was most widely grown over a century ago, it is surprising that this cultivar, and not the modern malting variety Tipple, contributes the more favourable high value alleles for diastatic power and malt nitrogen and also the low value allele associated with β-glucan. The malting quality of Chevallier is comparable to that of Tipple for a number of important characteristics, whilst for wort β-glucan Chevallier malt compares more favourably to the optimal quality parameters. As Tipple is a modern malting variety it was assumed that this cultivar would considerably outperform Chevallier in terms of quality, however the results presented here suggest that Chevallier displays remarkably good quality traits for a variety first grown in the early nineteenth century.

Chapter 6. General discussion

Fusarium head blight (FHB) is an economically important cereal disease caused by *Fusarium* species of hemibiotrophic fungi. Cultural practices aimed at reducing the impact of FHB, such as the application of triazole fungicides and crop rotation with soybean and sugar beet, are only moderately effective and therefore sources of genetic resistance must be identified to improve FHB resistance in commercial varieties (Paul et al. 2010; Marburger et al. 2015). QTL mapping studies have determined that much of the FHB resistance identified in both barley and wheat is associated with agronomic traits, particularly height (Zhu et al. 1999; Buerstmayr et al. 2009). There is a requirement to identify sources of genetic resistance that do not compromise the ability to combine favourable agronomic or quality characteristics and disease resistance within a single cultivar. A central theme of this thesis was to identify the potential for trade-off between FHB resistance and agronomic traits, particularly height, or quality characteristics.

Much of the resistance to FHB is associated with increased plant height. In wheat, cultivars that possess the semi-dominant gain-of-function *Reduced height* (*Rht*) *Rht-D1b* or *Rht-B1b* semi-dwarfing alleles display reduced Type 1 resistance (initial infection) to FHB infection, whilst *rht-tall* lines are significantly more resistant (Srinivasachary et al. 2008). Reduced plant height conferred by the *Rht-D1b* and *B1b* alleles in wheat is believed to be due to the alteration of signalling through the gibberellic acid (GA) pathway (Hedden, 2003). Similarly, a reduction in plant height is observed in barley lines which have a mutation in the Brassinosteroid-insensitive 1 (*BRI1*) gene, the receptor in the brassinosteroid (BR) phytohormone pathway (Chono et al. 2003). Such lines, known as '*uzu*' or *bri1*, exhibit reduced sensitivity to exogenously applied brassinosteroid and display a semi-dwarf phenotype (Chono et al. 2003). However unlike the GA-insensitive *Rht* alleles, little was known about the effect of this semi-dwarfing mutation on disease resistance in barley. In chapter 2 it was demonstrated that barley lines possessing the semi-dwarf *bri1* mutation display tissue specific resistance following *Fusarium culmorum* infection. The *bri1* semi-dwarf near-isogenic lines (NILs) were significantly more resistant to Fusarium crown rot (FCR) infection than the *BRI1* tall lines. This is in direct accordance with the studies of Chen et al. (2014) and Bai and Liu (2015), who observed that not only do

the *bri1* lines exhibit a reduction in visual FCR symptoms but they also display a decrease in the accumulation of fungal biomass within the leaf sheath tissues. Contrastingly, in response to FHB infection there was no significant difference observed in Type 1 resistance between the semi-dwarf *bri1* and tall *BRI1* barley NILs across two trial years. A similar response to floral infection with *F. culmorum* has also been observed in *Brachypodium distachyon* mutant lines which are disrupted in BR signalling. The *B. distachyon bri1* line, which displays a semi-dwarf phenotype, does not show an altered Type 1 resistance when compared to the tall *BRI1* line, but exhibits increased Type 2 resistance (Goddard et al. 2014). These results suggest it is possible that *BRI1* mutation offers increased resistance to the spread of the *Fusarium* fungus throughout the rachis and into adjacent spikelets (Type 2 resistance), but that the inherent Type 2 resistance of barley (Jansen et al. 2005) may have masked this effect within the results presented in my study. Importantly, the results in chapter 2 demonstrate that the *bri1* mutation is not associated with reduced Type 1 resistance as observed for the *Rht* dwarfing alleles (Srinivasachary et al. 2008; Saville et al. 2012). This suggests that this semi-dwarfing allele may be useful for introducing reduced height without negatively affecting resistance to initial infection.

Previous studies have reported that BR increases resistance to both FCR and FHB caused by *F. culmorum* (Ali et al. 2013). The study by Ali et al. (2013) observed the effects of exogenously applied BR to barley cultivars which were not altered in the BR signalling pathway, whilst the *bri1* NILs in the present study display constitutive disruption of BR signalling which is conferred by genetic mutation. The apparently contrasting results observed by Ali et al. (2013) may actually reflect the effect of increasing BR levels in plants with fully functional BR signalling pathways. Interestingly, *uzu* semi-dwarf *bri1* mutants also display a greater accumulation of castasterone, the biosynthetic precursor of the most bioactive BR brassinolide, than *BRI1* tall lines due to the disruption of signalling through the BR pathway (Chono et al. 2003). This response is similar to *Rht* wheat lines, where biologically active GA_1 accumulates in GA-non-responsive semi-dwarf lines (Appleford and Lenton, 1991). It is therefore possible that increased BR levels, resulting from either exogenous application of brassinolide as demonstrated by Ali et al. (2013) or as a consequence of *BRI1* mutation as seen in the *uzu* lines used in chapter 2, may increase resistance to *Fusarium* diseases.

Trade-offs associated with disease resistance have been widely reported in the literature. Barley cultivars displaying increased resistance to the obligate biotrophic pathogen *Blumeria graminis* f.sp. *hordei*, conferred by the recessive *mlo* alleles, display increased susceptibility to several fungal diseases. The caryopses of *mlo* cultivars are more easily colonised by the hemibiotroph *F. graminearum*, with the fungus being able to penetrate the endosperm and aleurone layer more quickly than in *Mlo* lines (Jansen et al. 2005). Barley *mlo* cultivars also exhibit increased susceptibility to the hemibiotrophs *Magnaporthe grisea* (Jarosch et al. 2003) and *Ramularia collo-cygni* (McGrann et al. 2014), and display increased susceptibility to lesion development caused by the necrotrophic fungus *Pyrenophora teres* (Makepeace, 2006). This suggests a trade-off between resistance to the biotroph *B. graminis* and pathogens with other trophic lifestyles, which therefore causes additional complexity when breeding for disease resistance. In chapter 2, the *bri1* semi-dwarf NILs were found to display altered resistance to fungal pathogens of differing trophic lifestyles when compared to the tall *BRI1* NILs. The *bri1* lines exhibited increased resistance to necrotrophic pathogens such as *Oculimacula acuformis* and *Gaeumannomyces graminis* var. *tritici*, and to hemibiotrophs with a short biotrophic phase such as *O. yallundae* and *M. oryzae*. However, no difference in resistance between semi-dwarf *bri1* and *BRI1* tall NILs was observed in response to infection by *R. collo-cygni*, a hemibiotroph with a prolonged endophytic phase. A similar resistance response to pathogens of differing trophic lifestyles has also been observed in the model species *B. distachyon*. The *B. distachyon* semi-dwarf *bri1* line displays increased resistance to *G. graminis* and *M. oryzae*, but not to *R. collo-cygni*, when compared to the respective *BRI1* tall line (Goddard et al. 2014). This suggests that the role of BR signalling in disease resistance is similar in both barley and *B. distachyon*. Importantly, within chapter 2 the barley *bri1* semi-dwarf lines do not show increased susceptibility to biotrophic pathogens such as *B. graminis* in comparison to the tall *BRI1* NILs. This is in contrast to the study of the GA-insensitive wheat *Rht* and *Slender 1* (*Sln1*), the barley *Rht* orthologue, semi-dwarfing alleles by Saville et al. (2012), who observed an increase in resistance to necrotrophic pathogens but also increased susceptibility to biotrophs. Chapter 2 demonstrates that alteration of the BR pathway through mutation of *BRI1* in barley, which confers a semi-dwarf phenotype, does not cause increased susceptibility to FHB and also does not confer a resistance trade-off between pathogens of differing trophic lifestyles like the GA-insensitive *Rht* or *Sln1* alleles

(Saville et al. 2012). This provides an alternate phytohormone pathway which may be investigated with regards to breeding cultivars with both a favourable height phenotype without compromising disease resistance.

Much of the study into FHB resistance in barley and wheat is conducted through the mapping of quantitative trait loci (QTL) and the development of new genotyping technologies throughout the last decade has enabled increasingly high density barley genetic maps to be produced for use in these studies (Yang et al. 2015). Chapter 3 detailed the use of two genotyping methods, the cultivar optimised 384-SNP assay developed by Moragues et al. (2010), designed from the original BOPA 1 and BOPA2 assays by Close et al. (2009), and the Genotyping-by-Sequencing technique (GBS) originally developed by Elshire et al. (2011) with the aim of producing the high density genetic maps for FHB QTL detection. The 384-SNP assay has been determined to be sufficient for SNP identification and genetic mapping studies in adapted germplasm (Moragues et al. 2010; McGrann et al. 2014; Bertholdsson et al. 2015), however the resultant Chevallier × Tipple (F_5 and F_7) and Armelle × Tipple (F_6) genetic maps were sparsely populated, particularly on chromosomes 1H and 7H. As the two barley populations within chapter 3 were derived from genetically distant parental lines it was expected that a larger number of SNPs would have been identified by the 384-SNP assay, yet the lack of SNPs within certain genomic regions suggests that the SNP assay may not always be suitable for the genotyping of diverse parents.

The GBS protocol identified a much larger initial pool of SNPs for mapping within both of the C×T populations; however 82% of these were removed through quality control processes before the initial mapping. Several barley GBS mapping studies have also reported large data losses throughout the GBS pipeline using mapping populations of a similar size developed from modern cultivars (Mascher et al. 2013; Liu et al. 2014; Honsdorf et al. 2014). This suggests that the data attrition observed in chapter 3 is a consequence of the genotyping method and not a result of the either the parental lines used or the population size. Whilst genetic maps in barley created using the GBS method produce a higher marker density, it has been noted that large gaps between markers still persist (Poland et al. 2012; Igartua et al. 2015), a detail which was also observed in the two C×T GBS maps created in chapter 3. QTL associated with FHB in barley have been identified from maps containing as few as 97 RFLP markers across the seven chromosomes (Zhu et al. 1999) or those displaying a mean

distance of over 10cM between genetic markers (Ma et al. 2001). However, the aim of this chapter was to create sufficiently dense maps to improve the resolution of QTL detection for both disease and agronomic traits. To this end, the SNPs from the GBS and the 384-SNP assays were combined to produce the two final C×T maps covering 1,224.4cM and 1,078.4cM in the F_5 and the F_7 populations, respectively. The map lengths created in chapter 3 are comparable to other GBS barley genetic maps formed from similar population sizes which have been used to successfully detect QTL for agronomic traits, such as the map created by Liu et al. (2014) who identified the row type locus *Vrs1* within a 1.5cM interval, suggesting that they were suitable for mapping of FHB QTL to sufficient resolution.

Many studies aiming to identify genetic resistance to FHB in barley and wheat have centred around the use of elite cultivars or breeding programs to develop mapping populations for either QTL or genome wide association studies. The results of such studies in both cereal species consistently identify FHB resistance which is associated with plant height (Ma et al. 2001; Gervais et al. 2003; Hori et al. 2005; Ban and Handa, 2008; Mao et al. 2011; Massman et al. 2011; Dahleen et al. 2012), heading date (HD) (Canci et al. 2004; Paillard et al. 2004; Horsley et al. 2006; Lamb et al. 2009; Liu et al. 2013) or other agronomic traits such as ear morphology (Choo et al. 2004; Hori et al. 2005; Gilsinger et al. 2005; Schmolke et al. 2005; Horsley et al. 2006). This suggests that the association between FHB and these traits may be due to pleiotropy or close linkage. At present, moderate resistance to FHB is achieved from a limited source of barley and wheat cultivars (Bai and Shaner, 2004) and studies using more diverse germplasm have been initiated to increase the potential of detecting potent FHB resistance. Chevallier is an English landrace barley which was originally discovered in 1823 (Beaven, 1936) that has significant Type 1 FHB resistance yet also displays a tall height phenotype. In chapter 4, the potential for linkage or pleiotropy between FHB resistance and plant height genes within the Chevallier background was investigated. Two height QTL were identified in both the F_5 and F_7 generations of the C×T population, with the major QTL being located on the long arm of 3H within the region of the *sdw1* gene (Malosetti et al. 2011). Whilst the candidate gene underlying this locus has been proposed to be a GA 20-oxidase (Jia et al. 2011) there was no differential in the response of Chevallier and Tipple to GA_3 application. This may indicate that at least in the C×T population, the QTL within this genomic region may

not be associated with a GA response. Interestingly the *uzu* semi-dwarf height gene investigated in chapter 2 is also present on the long arm of 3H; however the major height QTL within the C×T population is located at the distal end of 3HL whilst the *uzu* gene is located at the centromeric region (Li et al. 2015).

A potent QTL associated with Type 1 FHB resistance was identified in both the F_5 and F_7 C×T populations on chromosome 6H, with resistance derived from Chevallier. Surprisingly, this QTL was not associated with plant height, heading date or any of the morphological traits that are frequently identified with FHB resistance. This indicates that the resistance of Chevallier on 6H is not due to pleiotropy or linkage with genes for these traits, but may be a form of physiological resistance. As a potentially useful source of FHB resistance it is now important to begin to fine map the 6H QTL interval. The process of back-crossing recombinant inbred lines (RILs) displaying 6H resistance to the Tipple parent should eliminate genetic background noise that may affect phenotypic scoring and allow the interval to be further refined. There are a further 220 C×T RILs at the F_6 generation that have been developed which may also be used should additional material be required. The stacking of multiple minor effect QTL associated with FHB in a single variety has been demonstrated to be effective at reducing both FHB incidence and DON accumulation in wheat, due to the cumulative effects of these loci (Miedaner et al. 2006). This suggests that the three additional QTL for Type 1 FHB resistance identified on chromosomes 2H and 7H in the F_7 population trialled in 2015 may also be useful.

The detection of multiple QTL associated with accumulation of the mycotoxin DON within a single population is often observed in barley (Ma et al. 2001; Dahleen et al. 2003) and the effects of these QTL are often highly influenced by the environment. Within the C×T F_7 population four QTL associated with DON were identified from the 2015 trial data. A QTL on 6H was associated with increased DON levels from the F_7 population and lower DON levels within the F_5 population studied in 2013, suggesting the effect of this QTL is environmentally dependent. Two QTL associated with DON were identified on 3H, both of which co-located with agronomic trait QTL detected on the same chromosome. The minor DON QTL on the long arm of 3H was coincident with the major QTL complex in the region of the *sdw1* gene, suggesting there may be a pleiotropic effect associated with height or HD at this location. The major DON QTL on the short arm of 3H was found to be coincident with the minor

height/HD QTL. Interestingly, this suggests that lower DON levels associated with the major 3HS QTL are therefore less likely to be a result of disease escape due to increased plant height. In both barley and wheat, DON QTL are often non-coincident with QTL associated with FHB (Somers et al. 2003; Yu et al. 2010; Dahleen et al. 2012). Within the C×T F_7 population, a QTL on 6H, associated with higher DON levels in the 2015 trial, partially co-located with an FHB resistance QTL. However as the marker interval for the DON QTL is not precisely defined, as a result of the limited range of DON values observed in the 2015 trial, it may be possible that the two traits may not be associated although this cannot be discounted. A further three QTL for both traits were identified in the F_7 population, with FHB QTL being identified on 2H and 7H, and DON QTL being detected on 1H and 3H. Such results suggest that, as with previous studies, FHB resistance and DON accumulation are likely to be under separate genetic control.

Whilst it was possible to identify an apparently novel source of resistance to FHB within the Chevallier population, the screening of genetically diverse germplasm does not guarantee the identification of both unique and useful sources of resistance. A study of 23,255 wild (*Hordeum vulgare* ssp. *spontaneum*) and cultivated (*H. vulgare* ssp. *vulgare*) barley accessions by Huang et al. (2013) recurrently identified chromosome 2H as being particularly associated with FHB, although this region only conferred minor resistance and was often associated with the *Vrs1* row type locus. Mamo and Steffenson (2015) also investigated the resistance of 298 Ethiopian and Eritrean barley landraces to FHB and specifically selected lines from geographically diverse regions to increase the genomic diversity within the study. The authors also identified a QTL on 2HL associated with resistance to FHB severity and DON accumulation, though again this was associated with row type. In chapter 4, the A×T mapping population was evaluated to determine whether the FHB resistance of Armelle, a tall French cultivar released in 1974, was associated with plant height. In this population, QTL for FHB, plant height and heading date were coincident on chromosome 3H which is consistent with previous studies where these three traits have been observed to co-locate (Ma et al. 2001; Lamb et al. 2009; Dahleen et al. 2012). This again suggests that the FHB resistance of Chevallier identified on 6H, which is not associated with agronomic traits, is novel. Further heritage cultivars, in addition to those studied in chapter 4, are presently being screened for their resistance to FHB and

DON accumulation with the aim of identifying potential sources of resistance in both two-row and six-row barley.

Malting barley has many required characteristics which facilitate the production of beers with specific flavours and colours (Newton et al. 2011), yet contamination of malt by *Fusarium* species has been demonstrated to have a negative effect on these qualities. Altered levels of free amino nitrogen (FAN), β-glucan, starch and protein content are observed in contaminated malt compared to non-*Fusarium* infected malt (Oliveira et al. 2012a; Oliveira et al. 2012b) and the presence of *Fusarium* associated hydrophobins induces gushing in bottled beer (Sarlin et al. 2012). Therefore it is important that malting cultivars not only display specific malt quality characteristics, but also have favourable agronomic traits such as disease resistance. In chapter 4 Chevallier was demonstrated to display FHB resistance on chromosome 6H which was not associated with agronomic traits, as is usually observed in barley. It was not known however, how the Victorian malting variety Chevallier performed with respect to present-day micromalting standards and whether the cultivar possessed any favourable malting characteristics which may be of interest within modern brewing. In chapter 5, the malting quality of Chevallier was assessed through the QTL mapping of 105 C×T F_5 RILs. A total of 15 QTL associated with malt parameters were identified within the population. Whilst many factors contribute to malt quality, low β-glucan and adequate diastatic power and FAN levels are presently favoured to reduce wort viscosity and give flavour and product stability (Brewer's Association, 2014). Interestingly, the Chevallier allele was found to be associated with QTL for reduced wort β-glucan content and also higher FAN and diastatic power content within the malt. Whilst Chevallier was associated with higher malt FAN content, the measurement of the Chevallier malt was within the desired parameters for this trait (Brewer's Association, 2014). Similarly, the diastatic power activity in Chevallier malt slightly exceeded the favoured range for this trait (Fox et al. 2003), but was still lower than the measured activity within the malt derived from Tipple.

As with FHB QTL mapping studies, many of the previously reported malting quality QTL have been identified within modern germplasm with less information available for older varieties. The six-row cultivar Morex has been the common parental line in several reports due to the popularity of six-row varieties for malting in the U.S. (Marquez-Cedillo et al. 2000; Edney and Mather, 2004; Gao et al. 2004; Han et al.

2004; Elia et al. 2009) and several U.S. breeding programs, such as the Oregon Wolfe barley population, have also been studied (Szucs et al. 2009; Gutiérrez et al. 2011; Mohammadi et al. 2015). This has provided a more restricted gene pool for identifying QTL with which to improve malting quality. More recently, studies using diverse or uncultivated germplasm have detected sources of genetic variation associated with quality traits. Novel alleles for increased β-amylase activity at the *Bmy1* locus on 4H have been identified in both Tibetan wild barley and Chinese landraces (Gong et al. 2013), whilst wild barley lines from both Finland and Israel have been determined to show greater activity of the diastatic enzymes α-amylase and β-amylase in comparison to modern cultivars (Ahokas and Poukkula, 1999; March et al. 2012). The results presented in chapter 5 also illustrate that Chevallier displays favourable malting characteristics which are equivalent to those of the modern variety Tipple or are actually more desirable, such as low wort β-glucan. QTL analysis of Chevallier has demonstrated that beneficial alleles associated with malting quality are present within English landraces, suggesting another potential source of variation that may be exploited in the future for breeding of malting barley.

It was not possible to identify any QTL associated with malt quality on 1H or 6H, whereas multiple QTL were identified on each of the remaining five chromosomes. There appears to be a paucity of malting-related QTL identified on 6H in the literature (Marquez-Cedillo et al. 2000; Emebiri et al. 2004; Gutiérrez et al. 2011) suggesting that there may simply be fewer genes associated with malting traits located on this chromosome. However, 1H is commonly identified as the genomic region associated with multiple important malt characteristics such as β-glucan, wort viscosity, extract and grain protein content (Emebiri et al. 2004; Laido et al. 2009; Schmalenbach and Pillen, 2009; Gutiérrez et al. 2011). The basis of QTL mapping relies on the identification of polymorphisms between the parental lines (Collard et al. 2005). The absence of QTL on 1H within the C×T F_5 population, as evidenced in chapter 5, therefore suggests that Chevallier and Tipple do not possess polymorphic loci on chromosome 1H associated with the malting traits assessed. It may indicate that favourable alleles on 1H affiliated with malting characters were present in the Victorian era when Chevallier was first cultivated and were selected for in the cultivars developed at the time. It is possible that these alleles may have been retained through subsequent breeding selections into modern varieties such as Tipple, due to their

associations with advantageous characteristics, which would explain the lack of QTL on chromosome 1H within the present population.

Trade-offs within plant breeding often compromise the ability to introgress several favourable agronomic or quality characteristics into a single variety. Therefore the knowledge of whether specific agronomic or disease traits are associated is informative for determining their potential use within a breeding program. Within this thesis, several aspects of trade-off have been investigated. Chapter 2 determined that mutation of the BRI1 gene in barley, resulting in a semi-dwarf phenotype, does not cause a resistance trade-off between necrotrophic/hemibiotrophic pathogens and biotrophic pathogens. The same chapter also demonstrated that the reduced plant height of the *bri1* lines did not increase susceptibility to the incidence of FHB. Whilst most resistance to FHB in barley is associated with increased plant height, chapter 4 demonstrated that within the Chevallier genetic background resistance is present which is not associated with either height or heading date. Within chapter 5, the malting quality potential of Chevallier was determined for the first time. This chapter determined that not only does Chevallier possess potentially novel sources of resistance to FHB, it also has several favourable malting quality traits which may be of interest to modern brewers.

Bibliography

Abernathy DG, Spedding G, Starcher B, 2009. Analysis of protein and total usable nitrogen in beer and wine using a microwell ninhydrin assay. *Journal of the Institute of Brewing* **115**, 122-127.

Abu Qamar M, Liu ZH, Faris JD, et al. 2008. A region of barley chromosome 6H harbors multiple major genes associated with net type net blotch resistance. *Theoretical and Applied Genetics* **117**, 1261-1270.

Acevedo-Garcia J, Collins NC, Ahmadinejad N, et al. 2013. Fine mapping and chromosome walking towards the *Ror1* locus in barley (*Hordeum vulgare L.*). *Theoretical and Applied Genetics* **126**, 2969-2982.

Acevedo-Garcia J, Kusch S, Panstruga R, 2014. Magical mystery tour: MLO proteins in plant immunity and beyond. *New Phytologist* **204**, 273-281.

Achard P, Cheng H, De Grauwe L, et al. 2006. Integration of plant responses to environmentally activated phytohormonal signals. *Science* **311**, 91-94.

Adefila OA, Bakare MK, Adewale IO, 2012. Characterization of an α-amylase from sorghum (*Sorghum bicolor*) obtained under optimized conditions. *Journal of the Institute of Brewing* **118**, 63-69.

Aghnoum R, Marcel TC, Johrde A, Pecchioni N, Schweizer P, Niks RE, 2010. Basal host resistance of barley to powdery mildew: connecting quantitative trait loci and candidate genes. *Molecular Plant-Microbe Interactions* **23**, 91-102.

Ahokas H, Poukkula M, 1999. Malting enzyme activities, grain protein variation and yield potentials in the displaced genetic resources of barley landraces of Finland. *Genetic Resources and Crop Evolution* **46**, 251-260.

Albrecht C, Boutrot F, Segonzac C, et al. 2012. Brassinosteroids inhibit pathogen-associated molecular pattern-triggered immune signaling independent of the receptor kinase BAK1. *Proceedings of the National Academy of Sciences of the United States of America* **109**, 303-308.

Alexander NJ, Mccormick SP, Waalwijk C, Van Der Lee T, Proctor RH, 2011. The genetic basis for 3-ADON and 15-ADON trichothecene chemotypes in *Fusarium*. *Fungal Genetics and Biology* **48**, 485-495.

Ali SS, Gunupuru LR, Kumar GBS, et al. 2014. Plant disease resistance is augmented in *uzu* barley lines modified in the brassinosteroid receptor BRI1. *BMC Plant Biology* **14**.

Ali SS, Kumar GBS, Khan M, Doohan FM, 2013. Brassinosteroid enhances resistance to *Fusarium* diseases of barley. *Phytopathology* **103**, 1260-1267.

Alvey L, Harberd NP, 2005. DELLA proteins: integrators of multiple plant growth regulatory inputs? *Physiologia Plantarum* **123**, 153-160.

Andersen KF, Morris L, Derksen RC, Madden LV, Paul PA, 2014. Rainfastness of prothioconazole plus tebuconazole for Fusarium head blight and deoxynivalenol management in soft red winter wheat. *Plant Disease* **98**, 1398-1406.

Angelino S, Vanlaarhoven HPM, Vanwesterop JJM, Broekhuijse BM, Mocking HCM, 1997. Total nitrogen content in single kernel malting barley samples. *Journal of the Institute of Brewing* **103**, 41-46.

Appleford NEJ, Lenton JR, 1991. Gibberellins and leaf expansion in near-isogenic wheat lines containing *Rht1* and *Rht3* dwarfing alleles. *Planta* **183**, 229-236.

Arunachalam C, Doohan FM, 2013. Trichothecene toxicity in eukaryotes: Cellular and molecular mechanisms in plants and animals. *Toxicology Letters* **217**, 149-158.

Audenaert K, Callewaert E, Hofte M, De Saeger S, Haesaert G, 2010. Hydrogen peroxide induced by the fungicide prothioconazole triggers deoxynivalenol (DON) production by *Fusarium graminearum*. *BMC Microbiology* **10**.

Ayoub M, Armstrong E, Bridger G, Fortin MG, Mather DE, 2003. Marker-based selection in barley for a QTL region affecting α-amylase activity of malt. *Crop Science* **43**, 556-561.

Bai GH, Desjardins AE, Plattner RD, 2002. Deoxynivalenol-nonproducing *Fusarium graminearum* causes initial infection, but does not cause disease spread in wheat spikes. *Mycopathologia* **153**, 91-98.

Bai GH, Shaner G, 2004. Management and resistance in wheat and barley to Fusarium head blight. *Annual Review of Phytopathology* **42**, 135-161.

Bai ZY, Liu CJ, 2015. Histological evidence for different spread of Fusarium crown rot in barley genotypes with different heights. *Journal of Phytopathology* **163**, 91-97.

Bakan B, Giraud-Delville C, Pinson L, Richard-Molard D, Fournier E, Brygoo Y, 2002. Identification by PCR of *Fusarium culmorum* strains producing large and small amounts of deoxynivalenol. *Applied and Environmental Microbiology* **68**, 5472-5479.

Ban T, Handa H, 2008. Multiple traits QTL for Fusarium head blight resistance on the wheat chromosome 2DS, QFhs.kibr-2ds, and its relationship with plant height. *Cereal Research Communications* **36**, 83-84.

Bari R, Jones J, 2009. Role of plant hormones in plant defence responses. *Plant Molecular Biology* **69**, 473-488.

Bayry J, Aimanianda V, Guijarro JI, Sunde M, Latge JP, 2012. Hydrophobins-unique fungal proteins. *PLoS Pathogens* **8**.

Beaven ES, 1936. Barley for brewing since 1886. *Journal of the Institute of Brewing*. **42**, 487-495.

Beccari G, Covarelli L, Nicholson P, 2011. Infection processes and soft wheat response to root rot and crown rot caused by *Fusarium culmorum*. *Plant Pathology* **60**, 671-684.

Becher R, Hettwer U, Karlovsky P, Deising HB, Wirsel SGR, 2010. Adaptation of *Fusarium graminearum* to tebuconazole yielded descendants diverging for levels of fitness, fungicide resistance, virulence, and mycotoxin production. *Phytopathology* **100**, 444-453.

Behn A, Hartl L, Schweizer G, Baumer M, 2005. Molecular mapping of QTLs for non-parasitic leaf spot resistance and comparison of half-sib DH populations in spring barley. *Euphytica* **141**, 291-299.

Behn A, Hartl L, Schweizer G, Wenzel G, Baumer M, 2004. QTL mapping for resistance against non-parasitic leaf spots in a spring barley doubled haploid population. *Theoretical and Applied Genetics* **108**, 1229-1235.

Belkhadir Y, Jaillais Y, 2015. The molecular circuitry of brassinosteroid signaling. *New Phytologist* **206**, 522-540.

Belkhadir Y, Jaillais Y, Epple P, Balsemao-Pires E, Dangl JL, Chory J, 2012. Brassinosteroids modulate the efficiency of plant immune responses to microbe-associated molecular patterns. *Proceedings of the National Academy of Sciences of the United States of America* **109**, 297-302.

Bennett JW, Klich M, 2003. Mycotoxins. *Clinical Microbiology Reviews* **16**, 497-516.

Bertholdsson NO, Holefors A, Macaulay M, Crespo-Herrera LA, 2015. QTL for chlorophyll fluorescence of barley plants grown at low oxygen concentration in hydroponics to simulate waterlogging. *Euphytica* **201**, 357-365.

Bezant J, Laurie D, Pratchett N, Chojecki J, Kearsey M, 1996. Marker regression mapping of QTL controlling flowering time and plant height in a spring barley (*Hordeum vulgare L*) cross. *Heredity* **77**, 64-73.

Blandino M, Minelli L, Reyneri A, 2006. Strategies for the chemical control of Fusarium head blight: Effect on yield, alveographic parameters and deoxynivalenol contamination in winter wheat grain. *European Journal of Agronomy* **25**, 193-201.

Blein M, Levrel A, Lemoine J, Gautier V, Chevalier M, Barloy D, 2009. *Oculimacula yallundae* lifestyle revisited: relationships between the timing of eyespot symptom appearance, the development of the pathogen and the responses of infected partially resistant wheat plants. *Plant Pathology* **58**, 1-11.

Boddu J, Cho SH, Muehlbauer GJ, 2007. Transcriptome analysis of trichothecene-induced gene expression in barley. *Molecular Plant-Microbe Interactions* **20**, 1364-1375.

Boenisch MJ, Schafer W, 2011. *Fusarium graminearum* forms mycotoxin producing infection structures on wheat. *BMC Plant Biology* **11**.

Borutova R, Faix S, Placha I, Gresakova L, Cobanova K, Leng L, 2008. Effects of deoxynivalenol and zearalenone on oxidative stress and blood phagocytic activity in broilers. *Archives of Animal Nutrition* **62**, 303-312.

Both M, Csukai M, Stumpf MPH, Spanu PD, 2005. Gene expression profiles of *Blumeria graminis* indicate dynamic changes to primary metabolism during development of an obligate biotrophic pathogen. *Plant Cell* **17**, 2107-2122.

Bottalico A, Perrone G, 2002. Toxigenic *Fusarium* species and mycotoxins associated with head blight in small-grain cereals in Europe. *European Journal of Plant Pathology* **108**, 611-624.

Boyd LA, Smith PH, Green RM, Brown JKM, 1994. The relationship between the expression of defense-related genes and mildew development in barley. *Molecular Plant-Microbe Interactions* **7**, 401-410.

Brennan JM, Fagan B, Van Maanen A, Cooke BM, Doohan FM, 2003. Studies on in vitro growth and pathogenicity of European *Fusarium* fungi. *European Journal of Plant Pathology* **109**, 577-587.

Brewers Association, 2014. Malting barley characteristics for craft brewers. http://www.brewersassociation.org

Brinch-Pedersen H, Madsen CK, Holme IB, Dionisio G, 2014. Increased understanding of the cereal phytase complement for better mineral bio-availability and resource management. *Journal of Cereal Science* **59**, 373-381.

Brinch-Pedersen H, Sorensen LD, Holm PB, 2002. Engineering crop plants: getting a handle on phosphate. *Trends in Plant Science* **7**, 118-125.

Brown JKM, Wolfe MS, 1990. Structure and evolution of a population of *Erysiphe-graminis* f. sp. *hordei*. *Plant Pathology* **39**, 376-390.

Brown NA, Urban M, Van De Meene AML, Hammond-Kosack KE, 2010. The infection biology of *Fusarium graminearum*: Defining the pathways of spikelet to spikelet colonisation in wheat ears. *Fungal Biology* **114**, 555-571.

Buerstmayr H, Ban T, Anderson JA, 2009. QTL mapping and marker-assisted selection for Fusarium head blight resistance in wheat: a review. *Plant Breeding* **128**, 1-26.

Buerstmayr H, Lemmens M, Hartl L, et al. 2002. Molecular mapping of QTLs for Fusarium head blight resistance in spring wheat. I. Resistance to fungal spread (type II resistance). *Theoretical and Applied Genetics* **104**, 84-91.

Buerstmayr M, Buerstmayr H, 2015. Comparative mapping of quantitative trait loci for Fusarium head blight resistance and anther retention in the winter wheat population Capo x Arina. *Theoretical and Applied Genetics* **128**, 1519-1530.

Buerstmayr M, Lemmens M, Steiner B, Buerstmayr H, 2011. Advanced backcross QTL mapping of resistance to Fusarium head blight and plant morphological traits in a *Triticum macha* × *T. aestivum* population. *Theoretical and Applied Genetics* **123**, 293-306.

Burt C, Hollins TW, Powell N, Nicholson P, 2010. Differential seedling resistance to the eyespot pathogens, *Oculimacula yallundae* and *Oculimacula acuformis*, conferred by *Pch2* in wheat and among accessions of *Triticum monococcum*. *Plant Pathology* **59**, 819-828.

Burton RA, Jobling SA, Harvey AJ, et al. 2008. The genetics and transcriptional profiles of the cellulose synthase-like *HvCslF* gene family in barley. *Plant Physiology* **146**, 1821-1833.

Bushnell WR, Perkins-Veazie P, Russo VM, Collins J, Seeland TM, 2010. Effects of deoxynivalenol on content of chloroplast pigments in barley leaf tissues. *Phytopathology* **100**, 33-41.

Canci PC, Nduulu LM, Muehlbauer GJ, Dill-Macky R, Rasmusson DC, Smith KP, 2004. Validation of quantitative trait loci for Fusarium head blight and kernel discoloration in barley. *Molecular Breeding* **14**, 91-104.

Cartwright DA, Troggio M, Velasco R, Gutin A, 2007. Genetic mapping in the presence of genotyping errors. *Genetics* **176**, 2521-2527.

Champeil A, Dore T, Fourbet JF, 2004. Fusarium head blight: epidemiological origin of the effects of cultural practices on head blight attacks and the production of mycotoxins by *Fusarium* in wheat grains. *Plant Science* **166**, 1389-1415.

Chapman NH, Burt C, Dong H, Nicholson P, 2008. The development of PCR-based markers for the selection of eyespot resistance genes *Pch1* and *Pch2*. *Theoretical and Applied Genetics* **117**, 425-433.

Chen GD, Liu YX, Wei YM, et al. 2013. Major QTL for Fusarium crown rot resistance in a barley landrace. *Theoretical and Applied Genetics* **126**, 2511-2520.

Chen GD, Yan W, Liu YX, et al. 2014. The non-gibberellic acid-responsive semi-dwarfing gene *uzu* affects Fusarium crown rot resistance in barley. *BMC Plant Biology* **14.**

Chen X, Steed A, Travella S, Keller B, Nicholson P, 2009. *Fusarium graminearum* exploits ethylene signalling to colonize dicotyledonous and monocotyledonous plants. *New Phytologist* **182**, 975-983.

Chinchilla D, Zipfel C, Robatzek S, et al. 2007. A flagellin-induced complex of the receptor FLS2 and BAK1 initiates plant defence. *Nature* **448**, 497-500.

Chono M, Honda I, Zeniya H, et al. 2003. A semidwarf phenotype of barley *uzu* results from a nucleotide substitution in the gene encoding a putative brassinosteroid receptor. *Plant Physiology* **133**, 1209-1219.

Choo TM, Vigier B, Shen QQ, Martin RA, Ho KM, Savard M, 2004. Barley traits associated with resistance to Fusarium head blight and deoxynivalenol accumulation. *Phytopathology* **94**, 1145-1150.

Chutimanitsakun Y, Nipper RW, Cuesta-Marcos A, et al. 2011. Construction and application for QTL analysis of a restriction site associated DNA (RAD) linkage map in barley. *BMC Genomics* **12**.

Close TJ, Bhat PR, Lonardi S, et al. 2009. Development and implementation of high-throughput SNP genotyping in barley. *BMC Genomics* **10.**

Clouse SD, Langford M, Mcmorris TC, 1996. A brassinosteroid-insensitive mutant in *Arabidopsis thaliana* exhibits multiple defects in growth and development. *Plant Physiology* **111**, 671-678.

Collard BCY, Jahufer MZZ, Brouwer JB, Pang ECK, 2005. An introduction to markers, quantitative trait loci (QTL) mapping and marker-assisted selection for crop improvement: The basic concepts. *Euphytica* **142**, 169-196.

Collins HM, Panozzo JF, Logue SJ, Jefferies SP, Barr AR, 2003. Mapping and validation of chromosome regions associated with high malt extract in barley (*Hordeum vulgare L.*). *Australian Journal of Agricultural Research* **54**, 1223-1240.

Comadran J, Kilian B, Russell J, et al. 2012. Natural variation in a homolog of *Antirrhinum* CENTRORADIALIS contributed to spring growth habit and environmental adaptation in cultivated barley. *Nature Genetics* **44**, 1388-1392.

Cronn R, Knaus BJ, Liston A, et al. 2012. Targeted enrichment strategies for next-generation plant biology. *American Journal of Botany* **99**, 291-311.

Cuthbert PA, Somers DJ, Thomas J, Cloutier S, Brule-Babel A, 2006. Fine mapping *Fhb1*, a major gene controlling Fusarium head blight resistance in bread wheat (*Triticum aestivum L.*). *Theoretical and Applied Genetics* **112**, 1465-1472.

D'Angelo DL, Bradley CA, Ames KA, Willyerd KT, Madden LV, Paul PA, 2014. Efficacy of fungicide applications during and after anthesis against Fusarium head blight and deoxynivalenol in soft red winter wheat. *Plant Disease* **98**, 1387-1397.

D'Mello JPF, Placinta CM, Macdonald AMC, 1999. *Fusarium* mycotoxins: a review of global implications for animal health, welfare and productivity. *Animal Feed Science and Technology* **80**, 183-205.

Dahleen LS, Agrama HA, Horsley RD, et al. 2003. Identification of QTLs associated with Fusarium head blight resistance in Zhedar 2 barley. *Theoretical and Applied Genetics* **108**, 95-104.

Dahleen LS, Morgan W, Mittal S, Bregitzer P, Brown RH, Hill NS, 2012. Quantitative trait loci (QTL) for *Fusarium* ELISA compared to QTL for Fusarium head blight resistance and deoxynivalenol content in barley. *Plant Breeding* **131**, 237-243.

Dai F, Qiu L, Ye LZ, Wu DZ, Zhou MX, Zhang GP, 2011. Identification of a phytase gene in barley (*Hordeum vulgare L.*). *Plos One* **6**.

Davey JW, Hohenlohe PA, Etter PD, Boone JQ, Catchen JM, Blaxter ML, 2011. Genome-wide genetic marker discovery and genotyping using next-generation sequencing. *Nature Reviews Genetics* **12**, 499-510.

De Bruyne L, Hofte M, De Vleesschauwer D, 2014. Connecting growth and defense: The emerging roles of brassinosteroids and gibberellins in plant innate immunity. *Molecular Plant* **7**, 943-959.

De La Pena RC, Smith KP, Capettini F, et al. 1999. Quantitative trait loci associated with resistance to Fusarium head blight and kernel discoloration in barley. *Theoretical and Applied Genetics* **99**, 561-569.

De Sa RM, Palmer GH, 2004. Assessment of enzymatic endosperm modification of malting barley using individual grain analyses. *Journal of the Institute of Brewing* **110**, 43-50.

De Vleesschauwer D, Van Buyten E, Satoh K, et al. 2012. Brassinosteroids antagonize gibberellin- and salicylate-mediated root immunity in rice. *Plant Physiology* **158**, 1833-1846.

Del Ponte EM, Fernandes JMC, Bergstrom GC, 2007. Influence of growth stage on Fusarium head blight and deoxynivalenol production in wheat. *Journal of Phytopathology* **155**, 577-581.

Denschlag C, Rieder J, Vogel RF, Niessen L, 2014. Real-time loop-mediated isothermal amplification (LAMP) assay for group specific detection of important trichothecene producing *Fusarium* species in wheat. *International Journal of Food Microbiology* **177**, 117-127.

Desjardins AE, Hohn TM, 1997. Mycotoxins in plant pathogenesis. *Molecular Plant-Microbe Interactions* **10**, 147-152.

Desjardins AE, Proctor RH, 2007. Molecular biology of *Fusarium* mycotoxins. *International Journal of Food Microbiology* **119**, 47-50.

Desmond OJ, Manners JM, Stephens AE, et al. 2008. The *Fusarium* mycotoxin deoxynivalenol elicits hydrogen peroxide production, programmed cell death and defence responses in wheat. *Molecular Plant Pathology* **9**, 435-445.

Dhaliwal AS, Mares DJ, Marshall DR, 1987. Effect of 1B/1R chromosome-translocation on milling and quality characteristics of bread wheats. *Cereal Chemistry* **64**, 72-76.

Diamond M, Reape TJ, Rocha O, et al. 2013. The *Fusarium* mycotoxin Deoxynivalenol can inhibit plant apoptosis-like programmed cell death. *Plos One* **8**.

Dill-Macky R, Jones RK, 2000. The effect of previous crop residues and tillage on Fusarium head blight of wheat. *Plant Disease* **84**, 71-76.

Dockter C, Gruszka D, Braumann I, et al. 2014. Induced variations in brassinosteroid genes define barley height and sturdiness, and expand the green revolution genetic toolkit. *Plant Physiology* **166**, 1912-1927.

Doohan FM, Brennan J, Cooke BM, 2003. Influence of climatic factors on *Fusarium* species pathogenic to cereals. *European Journal of Plant Pathology* **109**, 755-768.

Draeger R, Gosman N, Steed A, et al. 2007. Identification of QTLs for resistance to Fusarium head blight, DON accumulation and associated traits in the winter wheat variety Arina. *Theoretical and Applied Genetics* **115**, 617-625.

Druka A, Franckowiak JD, Lundqvist U, et al. 2011. Genetic dissection of barley morphology and development. *Plant Physiology* 155, 617-627.

Edney MJ, Mather DE, 2004. Quantitative trait loci affecting germination traits and malt friability in a two-rowed by six rowed barley cross. *Journal of Cereal Science* **39**, 283-290.

Eifler J, Martinelli E, Santonico M, Capuano R, Schild D, Di Natale C, 2011. Differential detection of potentially hazardous *Fusarium* species in wheat grains by an electronic nose. *Plos One* **6**.

Elia M, Swanston JS, Moralejo M, et al. 2010. A model of the genetic differences in malting quality between European and North American barley cultivars based on a QTL study of the cross Triumph × Morex. *Plant Breeding* **129**, 280-290.

Elshire RJ, Glaubitz JC, Sun Q, et al. 2011. A robust, simple genotyping-by-sequencing (GBS) approach for high diversity species. *Plos One* **6**.

Emebiri LC, Moody DB, Panozzo JF, Read BJ, 2004. Mapping of QTL for malting quality attributes in barley based on a cross of parents with low grain protein concentration. *Field Crops Research* **87**, 195-205.

Emerson KJ, Merz CR, Catchen JM, et al. 2010. Resolving postglacial phylogeography using high-throughput sequencing. *Proceedings of the National Academy of Sciences of the United States of America* **107**, 196-200.

The European Union, 2006. Commission Regulation (EC) No 1881/2006 setting maximum levels of certain contaminants in foodstuffs. *Official Journal of the European Union* **L365**, 5-24.

The European Union, 2013. Commission recommendation on the presence of T-2 and HT-2 toxin in cereals and cereal products. *Official Journal of the European Union* **L91**, 12-15.

Evans DE, Hamet MaG, 2005. The selection of a dried yeast strain for use in the apparent attenuation limit malt analysis (AAL) procedure. *Journal of the Institute of Brewing* **111**, 209-214.

Fan M, Bai MY, Kim JG, et al. 2014. The bHLH transcription factor HBI1 mediates the trade-off between growth and pathogen-associated molecular pattern-triggered immunity in *Arabidopsis*. *Plant Cell* **26**, 828-841.

Foroud NA, Eudes F, 2009. Trichothecenes in cereal grains. *International Journal of Molecular Sciences* **10**, 147-173.

Fox GP, Panozzo JF, Li CD, Lance RCM, Inkerman PA, Henry RJ, 2003. Molecular basis of barley quality. *Australian Journal of Agricultural Research* **54**, 1081-1101.

Freeman J, Ward E, 2004. *Gaeumannomyces graminis*, the take-all fungus and its relatives. *Molecular Plant Pathology* **5**, 235-252.

Gale MD, Gregory RS, 1977. Rapid method for early generation selection of dwarf genotypes in wheat. *Euphytica* **26**, 733-738.

Gang G, Miedaner T, Schuhmacher U, Schollenberger M, Geiger HH, 1998. Deoxynivalenol and nivalenol production by *Fusarium culmorum* isolates differing in aggressiveness toward winter rye. *Phytopathology* **88**, 879-884.

Gao W, Clancy JA, Han F, et al. 2004. Fine mapping of a malting-quality QTL complex near the chromosome 4HS telomere in barley. *Theoretical and Applied Genetics* **109**, 750-760.

Gardiner SA, Boddu J, Berthiller F, et al. 2010. Transcriptome analysis of the barley-deoxynivalenol interaction: evidence for a role of glutathione in deoxynivalenol detoxification. *Molecular Plant-Microbe Interactions* **23**, 962-976.

Georg-Kraemer JE, Mundstock EC, Cavalli-Molina S, 2001. Developmental expression of amylases during barley malting. *Journal of Cereal Science* **33**, 279-288.

Gervais L, Dedryver F, Morlais JY, et al. 2003. Mapping of quantitative trait loci for field resistance to Fusarium head blight in an European winter wheat. *Theoretical and Applied Genetics* **106**, 961-970.

Gianinetti A, 2009. A theoretical framework for β-glucan degradation during barley malting. *Theory in Biosciences*. **128**, 97-108.

Gibson TS, Solah V, Holmes MRG, Taylor HR, 1995. Diastatic power in malted barley - contributions of malt parameters to its development and the potential of barley-grain β-amylase to predict malt diastatic power. *Journal of the Institute of Brewing* **101**, 277-280.

Giese H, Holmjensen AG, Jensen HP, Jensen J, 1993. Localization of the *Laevigatum* powdery mildew resistance gene to barley chromosome 2 by the use of RFLP markers. *Theoretical and Applied Genetics* **85**, 897-900.

Gilsinger J, Kong L, Shen X, Ohm H, 2005. DNA markers associated with low Fusarium head blight incidence and narrow flower opening in wheat. *Theoretical and Applied Genetics* **110**, 1218-1225.

Glazebrook J, 2005. Contrasting mechanisms of defense against biotrophic and necrotrophic pathogens. *Annual Review of Phytopathology.* **43**, 205-27.

Goddard R, Peraldi A, Ridout C, Nicholson P, 2014. Enhanced disease resistance caused by *BRI1* mutation is conserved between *Brachypodium distachyon* and barley (*Hordeum vulgare*). *Molecular Plant-Microbe Interactions* **27**, 1095-1106.

Gong X, Westcott S, Zhang XQ, et al. 2013. Discovery of novel B*my1* alleles increasing β-amylase activity in Chinese landraces and Tibetan wild barley for improvement of malting quality via MAS. *Plos One* **8**.

Goswami RS, Kistler HC, 2004. Heading for disaster: *Fusarium graminearum* on cereal crops. *Molecular Plant Pathology* **5**, 515-525.

Gottwald S, Samans B, Luck S, Friedt W, 2012. Jasmonate and ethylene dependent defence gene expression and suppression of fungal virulence factors: two essential mechanisms of Fusarium head blight resistance in wheat? *BMC Genomics* **13.**

Grenier B, Bracarense A, Schwartz HE, et al. 2012. The low intestinal and hepatic toxicity of hydrolyzed fumonisin B_1 correlates with its inability to alter the metabolism of sphingolipids. *Biochemical Pharmacology* **83**, 1465-1473.

Guenther JC, Trail F, 2005. The development and differentiation of *Gibberella zeae* (anamorph : *Fusarium graminearum*) during colonization of wheat. *Mycologia* **97**, 229-237.

Gupta S, Li CD, Loughman R, Cakir M, Westcott S, Lance R, 2011. Identifying genetic complexity of 6H locus in barley conferring resistance to *Pyrenophora teres f. teres*. *Plant Breeding* **130**, 423-429.

Gutierrez L, Cuesta-Marcos A, Castro AJ, Von Zitzewitz J, Schmitt M, Hayes PM, 2011. Association mapping of malting quality quantitative trait loci in winter barley: positive signals from small germplasm arrays. *Plant Genome* **4**, 256-272.

Haberle J, Schmolke M, Schweizer G, et al. 2007. Effects of two major Fusarium head blight resistance QTL verified in a winter wheat backcross population. *Crop Science* **47**, 1823-1831.

Hamalainen JJ, Reinikainen P, 2007. A simulation model for malt enzyme activities in kilning. *Journal of the Institute of Brewing* **113**, 159-167.

Han F, Clancy JA, Jones BL, Wesenberg DM, Kleinhofs A, Ullrich SE, 2004. Dissection of a malting quality QTL region on chromosome 1 (7H) of barley. *Molecular Breeding* **14**, 339-347.

Hedden P, 2003. The genes of the Green Revolution. *Trends in Genetics* **19**, 5-9.

Heslot N, Rutkoski J, Poland J, Jannink JL, Sorrells ME, 2013. Impact of marker ascertainment bias on genomic selection accuracy and estimates of genetic diversity. *Plos One* **8**.

Hickey LT, Lawson W, Platz GJ, et al. 2012. Mapping quantitative trait loci for partial resistance to powdery mildew in an australian barley population. *Crop Science* **52**, 1021-1032.

Hill NS, Neate SM, Cooper B, et al. 2008. Comparison of ELISA for *Fusarium*, visual screening, and deoxynivalenol analysis of Fusarium head blight for barley field nurseries. *Crop Science* **48**, 1389-1398.

Honsdorf N, March TJ, Hecht A, Eglinton J, Pillen K, 2014. Evaluation of juvenile drought stress tolerance and genotyping by sequencing with wild barley introgression lines. *Molecular Breeding* **34**, 1475-1495.

Horevaj P, Milus EA, Bluhm BH, 2011. A real-time qPCR assay to quantify *Fusarium graminearum* biomass in wheat kernels. *Journal of Applied Microbiology* **111**, 396-406.

Hori K, Kobayashi T, Sato K, Takeda K, 2005. QTL analysis of Fusarium head blight resistance using a high-density linkage map in barley. *Theoretical and Applied Genetics* **111**, 1661-1672.

Horsley RD, Schmierer D, Maier C, et al. 2006. Identification of QTLs associated with Fusarium head blight resistance in barley accession CIho 4196. *Crop Science* **46**, 145-156.

Home Grown Cereals Authority, 2014. HGCA Recommended Lists 2014/15 for cereals and oilseeds. http://www.cereals.ahdb.org.uk/varieties

Houston K, Russell J, Schreiber M, et al. 2014. A genome wide association scan for (1,3;1,4)-β-glucan content in the grain of contemporary two-row Spring and Winter barleys. *BMC Genomics* **15**.

Hu SM, Dong JJ, Fan W, et al. 2014. The influence of proteolytic and cytolytic enzymes on starch degradation during mashing. *Journal of the Institute of Brewing* **120**, 379-384.

Huang YD, Millett BP, Beaubien KA, et al. 2013. Haplotype diversity and population structure in cultivated and wild barley evaluated for Fusarium head blight responses. *Theoretical and Applied Genetics* **126**, 619-636.

Hueza IM, Raspantini PCF, Raspantini LER, Latorre AO, Gorniak SL, 2014. Zearalenone, an estrogenic mycotoxin, is an immunotoxic compound. *Toxins* **6**, 1080-1095.

Hussain A, Peng JR, 2003. DELLA proteins and GA signalling in *Arabidopsis*. *Journal of Plant Growth Regulation* **22**, 134-140.

Igartua E, Mansour E, Cantalapiedra CP, et al. 2015. Selection footprints in barley breeding lines detected by combining genotyping-by-sequencing with reference genome information. *Molecular Breeding* **35**.

Ilgen P, Hadeler B, Maier FJ, Schaefer W, 2009. Developing kernel and rachis node induce the trichothecene pathway of *Fusarium graminearum* during wheat head infection. *Molecular Plant-Microbe Interactions* **22**, 899-908.

Ilgen P, Maier FJ, Schafer W, 2008. Trichothecenes and lipases are host-induced and secreted virulence factors of *Fusarium graminearum*. *Cereal Research Communications* **36**, 421-428.

Imathiu SM, Edwards SG, Ray RV, Back MA, 2013. *Fusarium langsethiae* - a HT-2 and T-2 toxins producer that needs more attention. *Journal of Phytopathology* **161**, 1-10.

Imathiu SM, Hare MC, Ray RV, Back M, Edwards SG, 2010. Evaluation of pathogenicity and aggressiveness of *F. langsethiae* on oat and wheat seedlings relative

to known seedling blight pathogens. *European Journal of Plant Pathology* **126**, 203-216.

International Barley Genome Sequencing Consortium, 2012. A physical, genetic and functional sequence assembly of the barley genome. *Nature* **491**, 711-716.

Ittu M, Saulescu NN, Hagima I, Ittu G, Mustatea P, 2000. Association of Fusarium head blight resistance with gliadin loci in a winter wheat cross. *Crop Science* **40**, 62-67.

Jansen C, Von Wettstein D, Schafer W, Kogel KH, Felk A, Maier FJ, 2005. Infection patterns in barley and wheat spikes inoculated with wild-type and trichodiene synthase gene disrupted *Fusarium graminearum*. *Proceedings of the National Academy of Sciences of the United States of America* **102**, 16892-16897.

Jarosch B, Jansen M, Schaffrath U, 2003. Acquired resistance functions in *mlo* barley, which is hypersusceptible to *Magnaporthe grisea*. *Molecular Plant-Microbe Interactions* **16**, 107-114.

Jarosch B, Kogel KH, Schaffrath U, 1999. The ambivalence of the barley *Mlo* locus: Mutations conferring resistance against powdery mildew (*Blumeria graminis* f. sp, *hordei*) enhance susceptibility to the rice blast fungus *Magnaporthe grisea*. *Molecular Plant-Microbe Interactions* **12**, 508-514.

Jestoi M, 2008. Emerging *Fusarium*-mycotoxins fusaproliferin, beauvericin, enniatins, and moniliformin - a review. *Critical Reviews in Food Science and Nutrition* **48**, 21-49.

Jia QJ, Zhang JJ, Westcott S, et al. 2009. GA-20 oxidase as a candidate for the semidwarf gene *sdw1*/*denso* in barley. *Functional & Integrative Genomics* **9**, 255-262.

Jia QJ, Zhang XQ, Westcott S, et al. 2011. Expression level of a gibberellin 20-oxidase gene is associated with multiple agronomic and quality traits in barley. *Theoretical and Applied Genetics* **122**, 1451-1460.

Jiang QT, Wei YM, Andre L, et al. 2010. Characterization of omega-secalin genes from rye, triticale, and a wheat 1BL/1RS translocation line. *Journal of Applied Genetics* **51**, 403-411.

Jin Y, Du J, Zhang K, Xie L, Li P, 2012. Relationship between Kolbach index and other quality parameters of wheat malt. *Journal of the Institute of Brewing* **118**, 57-62.

Jørgensen JH, 1994. Genetics of powdery mildew resistance in barley. *Critical Reviews in Plant Sciences* **13**, 97–119.

Kang Z, Buchenauer H, 2003. Immunocytochemical localization of cell wall-bound thionins and hydroxyproline-rich glycoproteins in *Fusarium culmorum*-infected wheat spikes. *Journal of Phytopathology-Phytopathologische Zeitschrift* **151**, 120-129.

Kazan K, Manners JM, 2013. MYC2: The Master in Action. *Molecular Plant* **6**, 686-703.

Kikot EG, Hours AR, Alconada MT, 2009. Contribution of cell wall degrading enzymes to pathogenesis of *Fusarium graminearum*: a review. *Journal of Basic Microbiology* **49**, 231-241.

Klahr A, Zimmermann G, Wenzel G, Mohler V, 2007. Effects of environment, disease progress, plant height and heading date on the detection of QTLs for resistance to Fusarium head blight in an European winter wheat cross. *Euphytica* **154**, 17-28.

Kliebenstein DJ, Rowe HC, 2008. Ecological costs of biotrophic versus necrotrophic pathogen resistance, the hypersensitive response and signal transduction. *Plant Science* **174**, 551-556.

Knight NL, Sutherland MW, 2013. Histopathological assessment of wheat seedling tissues infected by *Fusarium pseudograminearum*. *Plant Pathology* **62**, 679-687.

Krogerus K, Gibson BR, 2013. 125th Anniversary Review: Diacetyl and its control during brewery fermentation. *Journal of the Institute of Brewing* **119**, 86-97.

Kuczynska A, Mikolajczak K, Cwiek H, 2014. Pleiotropic effects of the *sdw1* locus in barley populations representing different rounds of recombination. *Electronic Journal of Biotechnology* **17**, 217-223.

Kuczynska A, Surma M, Adamski T, Mikoajczak K, Krystkowiak K, Ogrodowicz P, 2013. Effects of the semi-dwarfing *sdw1/denso* gene in barley. *Journal of Applied Genetics* **54**, 381-390.

Lacey J, Bateman GL, Mirocha CJ, 1999. Effects of infection time and moisture on development of ear blight and deoxynivalenol production by *Fusarium* spp. in wheat. *Annals of Applied Biology* **134**, 277-283.

Laido G, Barabaschi D, Tondelli A, et al. 2009. QTL alleles from a winter feed type can improve malting quality in barley. *Plant Breeding* **128**, 598-605.

Lamb KE, Gonzalez-Hernandez JL, Zhang BX, et al. 2009. Identification of QTL Conferring resistance to Fusarium head blight resistance in the breeding line C93-3230-24. *Crop Science* **49**, 1675-1680.

Langevin F, Eudes F, Comeau A, 2004. Effect of trichothecenes produced by *Fusarium graminearum* during Fusarium head blight development in six cereal species. *European Journal of Plant Pathology* **110**, 735-746.

Lanubile A, Logrieco A, Battilani P, Proctor RH, Marocco A, 2013. Transcriptional changes in developing maize kernels in response to fumonisin-producing and nonproducing strains of *Fusarium verticillioides*. *Plant Science* **210**, 183-192.

Larson SR, Habernicht DK, Blake TK, Adamson M, 1997. Backcross gains for six-rowed grain and malt qualities with introgression of a feed barley yield QTL. *Journal of the American Society of Brewing Chemists* **55**, 52-57.

Lee JH, Graybosch RA, Peterson CJ, 1995. Quality and biochemical effects of a 1BL/1RS wheat-rye translocation in wheat. *Theoretical and Applied Genetics* **90**, 105-112.

Lee T, Lee SH, Shin JY, et al. 2014. Comparison of trichothecene biosynthetic gene expression between *Fusarium graminearum* and *Fusarium asiaticum*. *Plant Pathology Journal* **30**, 33-42.

Li CD, Zhang XQ, Eckstein P, Rossnagel BG, Scoles GJ, 1999. A polymorphic microsatellite in the limit dextrinase gene of barley (*Hordeum vulgare L.*). *Molecular Breeding* **5**, 569-577.

Li G, Yen Y, 2008. Jasmonate and ethylene signaling pathway may mediate Fusarium head blight resistance in wheat. *Crop Science* **48**, 1888-1896.

Li HH, Vikram P, Singh RP, et al. 2015. A high density GBS map of bread wheat and its application for dissecting complex disease resistance traits. *BMC Genomics* **16**.

Li JZ, Baga M, Rossnagel BG, Legge WG, Chibbar RN, 2008. Identification of quantitative trait loci for β-glucan concentration in barley grain. *Journal of Cereal Science* **48**, 647-655.

Li X, Shin S, Heinen S, et al. 2015. Transgenic wheat expressing a barley UDP glucosyltransferase detoxifies deoxynivalenol and provides high levels of resistance to *Fusarium graminearum*. *Molecular Plant-Microbe Interactions* doi:10.1094/MPMI-03-15-0062-R.

Lionetti V, Giancaspro A, Fabri E, et al. 2015. Cell wall traits as potential resources to improve resistance of durum wheat against *Fusarium graminearum*. *BMC Plant Biology* **15.**

Linkmeyer A, Gotz M, Hu L, et al. 2013. Assessment and introduction of quantitative resistance to Fusarium head blight in elite spring barley. *Phytopathology* **103**, 1252-1259.

Liti G, Louis EJ, 2012. Advances in quantitative trait analysis in yeast. *PLoS Genetics* **8**.

Liu H, Bayer M, Druka A, et al. 2014. An evaluation of genotyping by sequencing (GBS) to map the *Breviaristatum-e* (*ari-e*) locus in cultivated barley. *BMC Genomics* **15**.

Liu SX, Pumphrey MO, Gill BS, et al. 2008. Toward positional cloning of *Fhb1*, a major QTL for Fusarium head blight resistance in wheat. *Cereal Research Communications* **36**, 195-201.

Liu SY, Griffey CA, Hall MD, et al. 2013. Molecular characterization of field resistance to Fusarium head blight in two US soft red winter wheat cultivars. *Theoretical and Applied Genetics* **126**, 2485-2498.

Liu ZH, Holmes DJ, Faris JD, et al. 2015. Necrotrophic effector-triggered susceptibility (NETS) underlies the barley-*Pyrenophora teres* f. *teres* interaction specific to chromosome 6H. *Molecular Plant Pathology* **16**, 188-200.

Logrieco A, Rizzo A, Ferracane R, Ritieni A, 2002. Occurrence of beauvericin and enniatins in wheat affected by *Fusarium avenaceum* head blight. *Applied and Environmental Microbiology* **68**, 82-85.

Lott JNA, Kolasa J, Batten GD, Campbell LC, 2011. The critical role of phosphorus in world production of cereal grains and legume seeds. *Food Security* **3**, 451-62.

Lozano-Duran R, Macho AP, Boutrot F, Segonzac C, Somssich IE, Zipfel C, 2013. The transcriptional regulator BZR1 mediates trade-off between plant innate immunity and growth. *E-Life* **2**.

Lozano-Duran R, Zipfel C, 2015. Trade-off between growth and immunity: role of brassinosteroids. *Trends in Plant Science* **20**, 12-19.

Lu QX, Lillemo M, Skinnes H, et al. 2013. Anther extrusion and plant height are associated with Type I resistance to Fusarium head blight in bread wheat line 'Shanghai-3/Catbird'. *Theoretical and Applied Genetics* **126**, 317-334.

Lundqvist U, Franckowiak JD, Konishi T, 1997. Barley genetic stocks, new and revised descriptions. *Barley Genetics Newsletter* **26**, 44-516.

Lysoe E, Bone KR, Klemsdal SS, 2008. Identification of up-regulated genes during zearalenone biosynthesis in *Fusarium. European Journal of Plant Pathology* **122**, 505-516.

Ma LJ, Geiser DM, Proctor RH, et al. 2013. *Fusarium* Pathogenomics. *Annual Review of Microbiology*. **67**, 399-416.

Ma Z, Steffenson BJ, Prom LK, Lapitan NLV, 2001. Mapping of quantitative trait loci for Fusarium head blight resistance in barley. *Phytopathology* **91**, 1079-1088.

Maier FJ, Miedaner T, Hadeler B, et al. 2006. Involvement of trichothecenes in fusarioses of wheat, barley and maize evaluated by gene disruption of the trichodiene synthase (*Tri5*) gene in three field isolates of different chemotype and virulence. *Molecular Plant Pathology* **7**, 449-461.

Makandar R, Nalam V, Chaturvedi R, Jeannotte R, Sparks AA, Shah J, 2010. Involvement of salicylate and jasmonate signaling pathways in arabidopsis interaction with *Fusarium graminearum*. *Molecular Plant-Microbe Interactions* **23**, 861-870.

Makandar R, Nalam VJ, Lee H, Trick HN, Dong Y, Shah J, 2012. Salicylic acid regulates basal resistance to Fusarium head blight in wheat. *Molecular Plant-Microbe Interactions* **25**, 431-439.

Makepeace JC, 2006. The effect of the *mlo* mildew resistance gene on spotting diseases of barley. PhD thesis, University of East Anglia.

Makepeace JC, Havis ND, Burke JI, Oxley SJP, Brown JKM, 2008. A method of inoculating barley seedlings with *Ramularia collo-cygni*. *Plant Pathology* **57**, 991-999.

Makepeace JC, Oxley SJP, Havis ND, Hackett R, Burke JI, Brown JKM, 2007. Associations between fungal and abiotic leaf spotting and the presence of *mlo* alleles in barley. *Plant Pathology* **56**, 934-942.

Malinovsky FG, Batoux M, Schwessinger B, et al. 2014. Antagonistic regulation of growth and Immunity by the *Arabidopsis* basic helix-loop-helix transcription factor Homolog of brassinosteroid enhanced expression2 interacting with increased leaf inclination1 binding bHLH1. *Plant Physiology* **164**, 1443-1455.

Maloney PV, Petersen S, Navarro RA, et al. 2014. Digital image analysis method for estimation of Fusarium damaged kernels in wheat. *Crop Science* **54**, 2077-2083.

Malosetti M, Van Eeuwijk FA, Boer MP, et al. 2011. Gene and QTL detection in a three-way barley cross under selection by a mixed model with kinship information using SNPs. *Theoretical and Applied Genetics* **122**, 1605-1616.

Mamo BE, Steffenson B, 2015. Genome-wide association mapping of Fusarium head blight resistance and agromorphological traits in barley landraces from Ethiopia and Eritrea. *Crop Science* **55**, 1494-1512.

Mao SL, Wei YM, Cao W, et al. 2010. Confirmation of the relationship between plant height and Fusarium head blight resistance in wheat (*Triticum aestivum L.*) by QTL meta-analysis. *Euphytica* **174**, 343-356.

Marburger DA, Conley SP, Esker PD, Lauer JG, Ane JM, 2015. Yield response to crop/genotype rotations and fungicide use to manage *Fusarium*-related diseases. *Crop Science* **55**, 889-898.

March TJ, Richter D, Colby T, Harzen A, Schmidt J, Pillen K, 2012. Identification of proteins associated with malting quality in a subset of wild barley introgression lines. *Proteomics* **12**, 2843-2851.

Marquez-Cedillo LA, Hayes PM, Jones BL, et al. 2000. QTL analysis of malting quality in barley based on the doubled-haploid progeny of two elite North American varieties representing different germplasm groups. *Theoretical and Applied Genetics* **101**, 173-184.

Martin P, Gomez M, Carrillo JM, 2001. Interaction between allelic variation at the *Glu-D1* locus and a 1BL.1RS translocation on flour quality in bread wheat. *Crop Science* **41**, 1080-1084.

Marullo P, Aigle M, Bely M, et al. 2007. Single QTL mapping and nucleotide-level resolution of a physiologic trait in wine *Saccharomyces cerevisiae* strains. *FEMS Yeast Research* **7**, 941-952.

Mascher M, Wu SY, St Amand P, Stein N, Poland J, 2013. Application of genotyping-by-sequencing on semiconductor sequencing platforms: a comparison of genetic and reference-based marker ordering in barley. *Plos One* **8**.

Massman J, Cooper B, Horsley R, et al. 2011. Genome-wide association mapping of Fusarium head blight resistance in contemporary barley breeding germplasm. *Molecular Breeding* **27**, 439-454.

Matthies IE, Malosetti M, Roder MS, Van Eeuwijk F, 2014. Genome-wide association mapping for kernel and malting quality traits using historical European barley records. *Plos One* **9**.

Matthies IE, Weise S, Roder MS, 2009. Association of haplotype diversity in the α-amylase gene a*my1* with malting quality parameters in barley. *Molecular Breeding* **23**, 139-152.

McCartney CA, Somers DJ, Fedak G, et al. 2007. The evaluation of FHB resistance QTLs introgressed into elite Canadian spring wheat germplasm. *Molecular Breeding* **20**, 209-221.

McCormick SP, Stanley AM, Stover NA, Alexander NJ, 2011. Trichothecenes: from simple to complex mycotoxins. *Toxins* **3**, 802-814.

McGrann GRD, Stavrinides A, Russell J, et al. 2014. A trade off between *mlo* resistance to powdery mildew and increased susceptibility of barley to a newly important disease, Ramularia leaf spot. *Journal of Experimental Botany* **65**, 1025-1037.

McMullen M, Bergstrom G, De Wolf E, et al. 2012. A unified effort to fight an enemy of wheat and barley: Fusarium head blight. *Plant Disease* **96**, 1712-1728.

Meca G, Zinedine A, Blesa J, Font G, Manes J, 2010. Further data on the presence of *Fusarium* emerging mycotoxins enniatins, fusaproliferin and beauvericin in cereals available on the Spanish markets. *Food and Chemical Toxicology* **48**, 1412-1416.

Menke J, Weber J, Broz K, Kistler HC, 2013. Cellular development associated with induced mycotoxin synthesis in the filamentous fungus *Fusarium graminearum*. *Plos One* **8**.

Mennitti AM, Pancaldi D, Maccaferri M, Casalini L, 2003. Effect of fungicides on Fusarium head blight and deoxynivalenol content in durum wheat grain. *European Journal of Plant Pathology* **109**, 109-115.

Merhej J, Richard-Forget F, Barreau C, 2011. Regulation of trichothecene biosynthesis in *Fusarium*: recent advances and new insights. *Applied Microbiology and Biotechnology* **91**, 519-28.

Mesfin A, Smith KP, Dill-Macky R, et al. 2003. Quantitative trait loci for Fusarium head blight resistance in barley detected in a two-rowed by six-rowed population. *Crop Science* **43**, 307-318.

Mesterhazy A, 1995. Types and components of resistance to Fusarium head blight of wheat. *Plant Breeding* **114**, 377-386.

Miedaner T, 1997. Breeding wheat and rye for resistance to *Fusarium* diseases. *Plant Breeding* **116**, 201-220.

Miedaner T, Wilde F, Steiner B, Buerstmayr H, Korzun V, Ebmeyer E, 2006. Stacking quantitative trait loci (QTL) for Fusarium head blight resistance from non-adapted

sources in an European elite spring wheat background and assessing their effects on deoxynivalenol (DON) content and disease severity. *Theoretical and Applied Genetics* **112**, 562-569.

Mohammadi M, Blake TK, Budde AD, et al. 2015. A genome-wide association study of malting quality across eight US barley breeding programs. *Theoretical and Applied Genetics* **128**, 705-721.

Molina-Cano JL, Moralejo M, Elia M, et al. 2007. QTL analysis of a cross between European and North American malting barleys reveals a putative candidate gene for β-glucan content on chromosome 1H. *Molecular Breeding* **19**, 275-284.

Moller EM, Chelkowski J, Geiger HH, 1999. Species-specific PCR assays for the fungal pathogens *Fusarium moniliforme* and *Fusarium subglutinans* and their application to diagnose maize ear rot disease. *Journal of Phytopathology* **147**, 497-508.

Moragues M, Comadran J, Waugh R, Milne I, Flavell AJ, Russell JR, 2010. Effects of ascertainment bias and marker number on estimations of barley diversity from high-throughput SNP genotype data. *Theoretical and Applied Genetics* **120**, 1525-1534.

Morrison E, Kosiak B, Ritieni A, Aastveit AH, Uhlig S, Bernhoft A, 2002. Mycotoxin production by *Fusarium avenaceum* strains isolated from Norwegian grain and the cytotoxicity of rice culture extracts to porcine kidney epithelial cells. *Journal of Agricultural and Food Chemistry* **50**, 3070-3075.

Moscou MJ, Lauter N, Caldo RA, Nettleton D, Wise RP, 2011. Quantitative and temporal definition of the *Mla* transcriptional regulon during barley-powdery mildew interactions. *Molecular Plant-Microbe Interactions* **24**, 694-705.

Moseman JG, Macer RCF, Greeley LW, 1965. Genetic studies with cultures of *Erysiphe graminis* f. sp. *hordei* virulent on *Hordeum spontaneum*. *British Mycological Society Transactions* **48**, 479-489.

Mugode L, Portillo OR, Hays DB, Rooney LW, Taylor JRN, 2011. Influence of high protein digestibility sorghums on free amino nitrogen (FAN) production during malting and mashing. *Journal of the Institute of Brewing* **117**, 422-426.

Muhammed AA, 2012. Investigations into the characteristics of historic barley varieties with reference to fungal diseases and physiology. PhD thesis, University of Sunderland.

Muñoz-Amatriaín M, Moscou MJ, Bhat PR, et al. 2011. An improved consensus linkage map of barley based on flow-sorted chromosomes and single nucleotide polymorphism markers. ***The Plant Genome***. 4, 238-249.Nahar K, Kyndt T, Hause B, Hofte M, Gheysen G, 2013. Brassinosteroids suppress rice defense against root-knot nematodes through antagonism with the jasmonate pathway. *Molecular Plant-Microbe Interactions* **26**, 106-115.

Nakashita H, Yasuda M, Nitta T, et al. 2003. Brassinosteroid functions in a broad range of disease resistance in tobacco and rice. *Plant Journal* **33**, 887-898.

Nam KH, Li JM, 2002. BRI1/BAK1, a receptor kinase pair mediating brassinosteroid signaling. *Cell* **110**, 203-212.

Navarro L, Bari R, Achard P, et al. 2008. DELLAs control plant immune responses by modulating the balance and salicylic acid signaling. *Current Biology* **18**, 650-655.

Nduulu LM, Mesfin A, Muehlbauer GJ, Smith KP, 2007. Analysis of the chromosome 2(2H) region of barley associated with the correlated traits Fusarium head blight resistance and heading date. *Theoretical and Applied Genetics* **115**, 561-670.

Newton AC, Flavell AJ, George TS, et al. 2011. Crops that feed the world 4. Barley: a resilient crop? Strengths and weaknesses in the context of food security. *Food Security* **3**, 141-178.

Nicholson P, 2009. *Fusarium* and *Fusarium*–cereal interactions. John Wiley & Sons, Ltd.

Nicholson P, Lees AK, Maurin N, Parry DW, Rezanoor HN, 1996. Development of a PCR assay to identify and quantify *Microdochium nivale* var. *nivale* and *Microdochium nivale* var. *majus* in wheat. *Physiological and Molecular Plant Pathology* **48**, 257-271.

Nicholson P, Simpson DR, Weston G, et al. 1998. Detection and quantification of *Fusarium culmorum* and *Fusarium graminearum* in cereals using PCR assays. *Physiological and Molecular Plant Pathology* **53**, 17-37.

Nicholson P, Simpson DR, Wilson AH, Chandler E, Thomsett M, 2004. Detection and differentiation of trichothecene and enniatin-producing *Fusarium* species on small-grain cereals. *European Journal of Plant Pathology* **110**, 503-514.

Nielsen LK, Cook DJ, Edwards SG, Ray RV, 2014. The prevalence and impact of Fusarium head blight pathogens and mycotoxins on malting barley quality in UK. *International Journal of Food Microbiology* **179**, 38-49.

Nielsen LK, Justesen AF, Jensen JD, Jorgensen LN, 2013. *Microdochium nivale* and *Microdochium majus* in seed samples of Danish small grain cereals. *Crop Protection* **43**, 192-200.

Niks RE, Habekuss A, Bekele B, Ordon F, 2004. A novel major gene on chromosome 6H for resistance of barley against the barley yellow dwarf virus. *Theoretical and Applied Genetics* **109**, 1536-1543.

O' Rourke T, 2002. Malt specifications and brewing performance. *The Brewer International* **2**, 27-30.

Olcer Z, Esen E, Muhammad T, Ersoy A, Budak S, Uludag Y, 2014. Fast and sensitive detection of mycotoxins in wheat using microfluidics based real-time electrochemical profiling. *Biosensors & Bioelectronics* **62**, 163-169.

Oliveira P, Mauch A, Jacob F, Arendt EK, 2012a. Impact of *Fusarium culmorum*-infected barley malt grains on brewing and beer quality. *Journal of the American Society of Brewing Chemists* **70**, 186-194.

Oliveira PM, Mauch A, Jacob F, Waters DM, Arendt EK, 2012b. Fundamental study on the influence of *Fusarium* infection on quality and ultrastructure of barley malt. *International Journal of Food Microbiology* **156**, 32-43.

Oliveira PM, Waters DM, Arendt EK, 2013. The impact of *Fusarium culmorum* infection on the protein fractions of raw barley and malted grains. *Applied Microbiology and Biotechnology* **97**, 2053-2065.

Olsson J, Borjesson T, Lundstedt T, Schnurer J, 2002. Detection and quantification of ochratoxin A and deoxynivalenol in barley grains by GC-MS and electronic nose. *International Journal of Food Microbiology* **72**, 203-214.

Osborne LE, Stein JM, 2007. Epidemiology of Fusarium head blight on small-grain cereals. *International Journal of Food Microbiology* **119**, 103-108.

Pace JG, Watts MR, Canterbury WJ, 1988. T-2 Mycotoxin inhibits mitochondrial protein-synthesis. *Toxicon* **26**, 77-85.

Paillard S, Schnurbusch T, Tiwari R, et al. 2004. QTL analysis of resistance to Fusarium head blight in Swiss winter wheat (*Triticum aestivum L.*). *Theoretical and Applied Genetics* **109**, 323-332.

Panozzo JF, Eckermann PJ, Mather DE, et al. 2007. QTL analysis of malting quality traits in two barley populations. *Australian Journal of Agricultural Research* **58**, 858-866.

Paranidharan V, Abu-Nada Y, Hamzehzarghani H, et al. 2008. Resistance-related metabolites in wheat against *Fusarium graminearum* and the virulence factor deoxynivalenol (DON). *Botany-Botanique* **86**, 1168-1179.

Parchman TL, Gompert Z, Mudge J, Schilkey FD, Benkman CW, Buerkle CA, 2012. Genome-wide association genetics of an adaptive trait in lodgepole pine. *Molecular Ecology* **21**, 2991-3005.

Parker D, Beckmann M, Enot DP, et al. 2008. Rice blast infection of *Brachypodium distachyon* as a model system to study dynamic host/pathogen interactions. *Nature Protocols* **3**, 435-445.

Paul PA, Mcmullen MP, Hershman DE, Madden LV, 2010. Meta-analysis of the effects of triazole-based fungicides on wheat yield and test weight as influenced by Fusarium head blight intensity. *Phytopathology* **100**, 160-171.

Peng JR, Richards DE, Hartley NM, et al. 1999. 'Green revolution' genes encode mutant gibberellin response modulators. *Nature* **400**, 256-261.

Peraldi A, Beccari G, Steed A, Nicholson P, 2011. *Brachypodium distachyon*: a new pathosystem to study Fusarium head blight and other *Fusarium* diseases of wheat. *BMC Plant Biology* **11**.

Peraldi A, Griffe LL, Burt C, Mcgrann GRD, Nicholson P, 2014. *Brachypodium distachyon* exhibits compatible interactions with *Oculimacula* spp. and *Ramularia collo-cygni*, providing the first pathosystem model to study eyespot and ramularia leaf spot diseases. *Plant Pathology* **63**, 554-562.

Pereyra SA, Dill-Macky R, 2008. Colonization of the residues of diverse plant species by *Gibberella zeae* and their contribution to Fusarium head blight inoculum. *Plant Disease* **92**, 800-807.

Pereyra SA, Dill-Macky R, Sims AL, 2004. Survival and inoculum production of *Gibberella zeae* in wheat residue. *Plant Disease* **88**, 724-730.

Pestka JJ, 2010. Deoxynivalenol-induced proinflammatory gene expression: mechanisms and pathological sequelae. *Toxins* **2**, 1300-1317.

Pestka JJ, Zhou HR, Moon Y, Chung YJ, 2004. Cellular and molecular mechanisms for immune modulation by deoxynivalenol and other trichothecenes: unraveling a paradox. *Toxicology Letters* **153**, 61-73.

Plattner RD, 1999. HPLC/MS analysis of *Fusarium* mycotoxins, fumonisins and deoxynivalenol. *Natural Toxins* **7**, 365-370.

Poland J, Endelman J, Dawson J, et al. 2012. genomic selection in wheat breeding using genotyping-by-sequencing. *Plant Genome* **5**, 103-113.

Ponts N, Pinson-Gadais L, Boutigny AL, Barreau C, Richard-Forget F, 2011. Cinnamic-derived acids significantly affect *Fusarium graminearum* growth and in vitro synthesis of Type B trichothecenes. *Phytopathology* **101**, 929-934.

Poppenberger B, Berthiller F, Lucyshyn D, et al. 2003. Detoxification of the *Fusarium* mycotoxin deoxynivalenol by a UDP-glucosyltransferase from *Arabidopsis thaliana*. *Journal of Biological Chemistry* **278**, 47905-47914.

Potokina E, Caspers M, Prasad M, et al. 2004. Functional association between malting quality trait components and cDNA array based expression patterns in barley (*Hordeum vulgare L.*). *Molecular Breeding* **14**, 153-170.

Preiser V, Goetsch D, Sulyok M, et al. 2015. The development of a multiplex real-time PCR to quantify *Fusarium* DNA of trichothecene and fumonisin producing strains in maize. *Analytical Methods* **7**, 1358-1365.

Pritsch C, Muehlbauer GJ, Bushnell WR, Somers DA, Vance CP, 2000. Fungal development and induction of defense response genes during early infection of wheat spikes by *Fusarium graminearum*. *Molecular Plant-Microbe Interactions* **13**, 159-169.

Pumphrey MO, Bernardo R, Anderson JA, 2007. Validating the *Fhb1* QTL for Fusarium head blight resistance in near-isogenic wheat lines developed from breeding populations. *Crop Science* **47**, 200-206.

Ramsay L, Comadran J, Druka A, et al. 2011. *Intermedium-c*, a modifier of lateral spikelet fertility in barley, is an ortholog of the maize domestication gene *Teosinte branched 1*. *Nature Genetics* **43**, 169-172.

Rapp C, Lantzsch HJ, Drochner W, 2001. Hydrolysis of phytic acid by intrinsic plant or supplemented microbial phytase (*Aspergillus niger*) in the stomach and small intestine of minipigs fitted with re-entrant cannulas. 1. Passage of dry matter and total phosphorus. *Journal of Animal Physiology and Animal Nutrition* **85**, 406-413.

Rea PA, 2007. Plant ATP-binding cassette transporters. *Annual Review of Plant Biology* **58**, 347-375.

Rheeder JP, Marasas WFO, Vismer HF, 2002. Production of fumonisin analogs by *Fusarium* species. *Applied and Environmental Microbiology* **68**, 2101-2105.

Rife TW, Wu SY, Bowden RL, Poland JA, 2015. Spiked GBS: a unified, open platform for single marker genotyping and whole-genome profiling. *BMC Genomics* **16**.

Risk JM, Selter LL, Chauhan H, et al. 2013. The wheat *Lr34* gene provides resistance against multiple fungal pathogens in barley. *Plant Biotechnology Journal* **11**, 847-854.

Rittenour WR, Harris SD, 2010. An in vitro method for the analysis of infection-related morphogenesis in *Fusarium graminearum*. *Molecular Plant Pathology* **11**, 361-369.

Robert-Seilaniantz A, Grant M, Jones JDG, 2011. Hormone crosstalk in plant disease and defense: more than just jasmonate-salicylate antagonism. *Annual Review of Phytopathology* **49**, 317-343.

Rossi V, Languasco L, Pattori E, Giosue S, 2002. Dynamics of airborne *Fusarium* macroconidia in wheat fields naturally affected by head blight. *Journal of Plant Pathology* **84**, 53-64.

Rostoks N, Mudie S, Cardle L, et al. 2005. Genome-wide SNP discovery and linkage analysis in barley based on genes responsive to abiotic stress. *Molecular Genetics and Genomics* **274**, 515-527.

Rostoks N, Ramsay L, Mackenzie K, et al. 2006. Recent history of artificial outcrossing facilitates whole-genome association mapping in elite inbred crop varieties. *Proceedings of the National Academy of Sciences of the United States of America* **103**, 18656-18661.

Rostoks N, Schmierer D, Kudrna D, Kleinhofs A, 2003. Barley putative hypersensitive induced reaction genes: genetic mapping, sequence analyses and differential expression in disease lesion mimic mutants. *Theoretical and Applied Genetics* **107**, 1094-1001.

Ruan YF, Comeau A, Langevin F, et al. 2012. Identification of novel QTL for resistance to Fusarium head blight in a tetraploid wheat population. *Genome* **55**, 853-864.

Rudd JC, Horsley RD, Mckendry AL, Elias EM, 2001. Host plant resistance genes for Fusarium head blight: Sources, mechanisms, and utility in conventional breeding systems. *Crop Science* **41**, 620-627.

Salgado JD, Madden LV, Paul PA, 2014. Efficacy and economics of integrating in-field and harvesting strategies to manage Fusarium head blight of wheat. *Plant Disease* **98**, 1407-1421.

Sarlin T, Kivioja T, Kalkkinen N, Linder MB, Nakari-Setala T, 2012. Identification and characterization of gushing-active hydrophobins from *Fusarium graminearum* and related species. *Journal of Basic Microbiology* **52**, 184-194.

Sarlin T, Vilpola A, Kotaviita E, Olkku J, Haikara A, 2007. Fungal hydrophobins in the barley-to-beer chain. *Journal of the Institute of Brewing* **113**, 147-153.

Sarlin T, Yli-Mattila T, Jestoi M, Rizzo A, Paavanen-Huhtala S, Haikara A, 2006. Real-time PCR for quantification of toxigenic *Fusarium* species in barley and malt. *European Journal of Plant Pathology* **114**, 371-380.

Sato K, Hori K, Takeda K, 2008. Detection of Fusarium head blight resistance QTLs using five populations of top-cross progeny derived from two-row x two-row crosses in barley. *Molecular Breeding* **22**, 517-526.

Savatin DV, Gramegna G, Modesti V, Cervone F, 2014. Wounding in the plant tissue: the defense of a dangerous passage. *Frontiers in Plant Science* **5**.

Saville RJ, Gosman N, Burt CJ, et al. 2012. The 'Green Revolution' dwarfing genes play a role in disease resistance in *Triticum aestivum* and *Hordeum vulgare*. *Journal of Experimental Botany* **63**, 1271-1283.

Scherm B, Balmas V, Spanu F, et al. 2013. *Fusarium culmorum*: causal agent of foot and root rot and head blight on wheat. *Molecular Plant Pathology* **14**, 323-341.

Schmalenbach I, Koerber N, Pillen K, 2008. Selecting a set of wild barley introgression lines and verification of QTL effects for resistance to powdery mildew and leaf rust. *Theoretical and Applied Genetics* **117**, 1093-1106.

Schmalenbach I, Pillen K, 2009. Detection and verification of malting quality QTLs using wild barley introgression lines. *Theoretical and Applied Genetics* **118**, 1411-1427.

Schmolke M, Zimmermann G, Buerstmayr H, et al. 2005. Molecular mapping of Fusarium head blight resistance in the winter wheat population Dream/Lynx. *Theoretical and Applied Genetics* **111**, 747-756.

Schober MS, Burton RA, Shirley NJ, Jacobs AK, Fincher GB, 2009. Analysis of the (1,3)-β-D-glucan synthase gene family of barley. *Phytochemistry* **70**, 713-720.

Schmolke M, Zimmermann G, Schweizer G, et al. 2008. Molecular mapping of quantitative trait loci for field resistance to Fusarium head blight in a European winter wheat population. *Plant Breeding* **127**, 459-464.

Schroeder HW, Christensen JJ, 1963. Factors affecting resistance of wheat to scab caused by *Gibberella zeae*. *Phytopathology* **53**, 831-838.

Schwarz PB, Horsley RD, Steffenson BJ, Salas B, Barr JM, 2006. Quality risks associated with the utilization of Fusarium head blight infected malting barley. *Journal of the American Society of Brewing Chemists* **64**, 1-7.

Schweiger W, Boddu J, Shin S, et al. 2010. Validation of a candidate deoxynivalenol-inactivating UDP-glucosyltransferase from barley by heterologous expression in yeast. *Molecular Plant-Microbe Interactions* **23**, 977-986.

Scott PR, 1971. The effect of temperature on eyespot (*Cercosporella herpotrichoides*) in wheat seedlings. *Annals of Applied Biology* **68**,169-175.

Serfling A, Ordon F, 2014. Virulence and toxin synthesis of an azole insensitive *Fusarium culmorum* strain in wheat cultivars with different levels of resistance to Fusarium head blight. *Plant Pathology* **63**, 1230-1240.

Shen R, Fan JB, Campbell D, et al. 2005. High-throughput SNP genotyping on universal bead arrays. *Mutation Research-Fundamental and Molecular Mechanisms of Mutagenesis* **573**, 70-82.

Shen XR, Ittu M, Ohm HW, 2003. Quantitative trait loci conditioning resistance to Fusarium head blight in wheat line F201R. *Crop Science* **43**, 850-857.

Shin S, Torres-Acosta JA, Heinen SJ, et al. 2012. Transgenic *Arabidopsis thaliana* expressing a barley UDP-glucosyltransferase exhibit resistance to the mycotoxin deoxynivalenol. *Journal of Experimental Botany* **63**, 4731-4740.

Shtaya MJY, Marcel TC, Sillero JC, Niks RE, Rubiales D, 2006. Identification of QTLs for powdery mildew and scald resistance in barley. *Euphytica* **151**, 421-429.

Shu XL, Rasmussen SK, 2014. Quantification of amylose, amylopectin, and β-glucan in search for genes controlling the three major quality traits in barley by genome-wide association studies. *Frontiers in Plant Science* **5**.

Silvar C, Casas AM, Igartua E, et al. 2011. Resistance to powdery mildew in Spanish barley landraces is controlled by different sets of quantitative trait loci. *Theoretical and Applied Genetics* **123**, 1019-1028.

Simpson DR, Rezanoor HN, Parry DW, Nicholson P, 2000. Evidence for differential host preference in *Microdochium nivale* var. *majus* and *Microdochium nivale* var. *nivale*. *Plant Pathology* **49**, 261-268.

Simpson DR, Weston GE, Turner JA, Jennings P, Nicholson P, 2001. Differential control of head blight pathogens of wheat by fungicides and consequences for mycotoxin contamination of grain. *European Journal of Plant Pathology* **107**, 421-431.

Siou D, Gelisse S, Laval V, et al. 2014. Effect of wheat spike infection timing on Fusarium head blight development and mycotoxin accumulation. *Plant Pathology* **63**, 390-399.

Skinnes H, Semagn K, Tarkegne Y, Maroy AG, Bjornstad A, 2010. The inheritance of anther extrusion in hexaploid wheat and its relationship to Fusarium head blight resistance and deoxynivalenol content. *Plant Breeding* **129**, 149-155.

Somers DJ, Fedak G, Savard M, 2003. Molecular mapping of novel genes controlling Fusarium head blight resistance and deoxynivalenol accumulation in spring wheat. *Genome* **46**, 555-564.

Song SS, Qi TC, Wasternack C, Xie DX, 2014. Jasmonate signaling and crosstalk with gibberellin and ethylene. *Current Opinion in Plant Biology* **21**, 112-119.

Speers RA, Jin YL, Paulson AT, Stewart RJ, 2003. Effects of β-glucan, shearing and environmental factors on the turbidity of wort and beer. *Journal of the Institute of Brewing* **109**, 236-244.

Spindel J, Wright M, Chen C, et al. 2013. Bridging the genotyping gap: using genotyping by sequencing (GBS) to add high-density SNP markers and new value to

traditional bi-parental mapping and breeding populations. *Theoretical and Applied Genetics* **126**, 2699-2716.

Srinivasachary, Gosman N, Steed A, et al. 2009. Semi-dwarfing *Rht-B1* and *Rht-D1* loci of wheat differ significantly in their influence on resistance to Fusarium head blight. *Theoretical and Applied Genetics* **118**, 695-702.

Srinivasachary, Gosman N, Steed A, et al. 2008. Susceptibility to Fusarium head blight is associated with the *Rht-D1b* semi-dwarfing allele in wheat. *Theoretical and Applied Genetics* **116**, 1145-1153.

Stabentheiner E, Minihofer T, Huss H, 2009. Infection of barley by *Ramularia collo-cygni*: scanning electron microscopic investigations. *Mycopathologia* **168**, 135-143.

Steiner B, Kurz H, Lemmens M, Buerstmayr H, 2009. Differential gene expression of related wheat lines with contrasting levels of head blight resistance after *Fusarium graminearum* inoculation. *Theoretical and Applied Genetics* **118**, 753-764.

Steiner E, Auer A, Becker T, Gastl M, 2012. Comparison of beer quality attributes between beers brewed with 100% barley malt and 100% barley raw material. *Journal of the Science of Food and Agriculture* **92**, 803-813.

Steiner E, Becker T, Gastl M, 2010. Turbidity and haze formation in beer - insights and overview. *Journal of the Institute of Brewing* **116**, 360-368.

Stewart GG, Hill A, Lekkas C, 2013. Wort FAN - its characteristics and importance during fermentation. *Journal of the American Society of Brewing Chemists* **71**, 179-185.

Steyer D, Ambroset C, Brion C, et al. 2012. QTL mapping of the production of wine aroma compounds by yeast. *BMC Genomics* **13**.

Szabo-Hever A, Lehoczki-Krsjak S, Varga M, et al. 2014. Differential influence of QTL linked to Fusarium head blight, Fusarium-damaged kernel, deoxynivalenol contents and associated morphological traits in a Frontana-derived wheat population. *Euphytica* **200**, 9-26.

Szucs P, Blake VC, Bhat PR, et al. 2009. An integrated resource for barley linkage map and malting quality QTL alignment. *Plant Genome* **2**, 134-140.

Theis T, Stahl U, 2004. Antifungal proteins: targets, mechanisms and prospective applications. *Cellular and Molecular Life Sciences* **61**, 437-455.

Thole V, Peraldi A, Worland B, Nicholson P, Doonan JH, Vain P, 2012. T-DNA mutagenesis in *Brachypodium distachyon*. *Journal of Experimental Botany* **63**, 567-576.

Thomas WTB, Powell W, Swanston JS, 1991. The effects of major genes on quantitatively varying characters in barley .4. The *Gpert* and *denso* loci and quality characters. *Heredity* **66**, 381-389.

Thrane U, Adler A, Clasen PE, et al. 2004. Diversity in metabolite production by *Fusarium langsethiae*, *Fusarium poae*, and *Fusarium sporotrichioides*. *International Journal of Food Microbiology* **95**, 257-266.

Tonshin AA, Teplova VV, Andersson MA, Salkinoja-Salonen MS, 2010. The *Fusarium* mycotoxins enniatins and beauvericin cause mitochondrial dysfunction by affecting the mitochondrial volume regulation, oxidative phosphorylation and ion homeostasis. *Toxicology* **276**, 49-57.

Torp M, Nirenberg HI, 2004. *Fusarium langsethiae* sp. nov on cereals in Europe. *International Journal of Food Microbiology* **95**, 247-256.

Trail F, 2009. For Blighted Waves of Grain: *Fusarium graminearum* in the Postgenomics Era. *Plant Physiology* **149**, 103-110.

Trail F, Xu HX, Loranger R, Gadoury D, 2002. Physiological and environmental aspects of ascospore discharge in *Gibberella zeae* (anamorph *Fusarium graminearum*). *Mycologia* **94**, 181-189.

Tufan HA, Mcgrann GRD, Magusin A, Morel J-B, Miche L, Boyd LA, 2009. Wheat blast: histopathology and transcriptome reprogramming in response to adapted and nonadapted *Magnaporthe* isolates. *New Phytologist* **184**, 473-484.

Union for the Protection of New Varieties of Plants, 1994. Guidelines for the conduct of tests for distinctness, uniformity and stability. http://www.upov.int/en/publications/tg-rom/

Urashima AS, Lavorent NA, Goulart ACP, Mehta Y, 2004. Resistance spectra of wheat cultivars and virulence diversity of *Magnaporthe grisea* isolates in Brazil. *Fitopatologia Brasileira* **29**, 511-518.

US Food and Drug Administration, 2010. Guidance for industry and FDA: advisory levels for Deoxynivalenol (DON) in finished wheat products for human consumption and grains and grain by-products used for animal feed. Washington, DC.

van Loon LC, Rep M, Pieterse CMJ, 2006. Significance of inducible defense-related proteins in infected plants. *Annual Review of Phytopathology* **44,** 135-162.

van Ooijen JW, Voorips RE, 2001. JoinMap® 3.0: Software for the calculation of genetic linkage maps. Plant Research International, Wageningen, Netherlands.

van Poecke RMP, Maccaferri M, Tang JF, et al. 2013. Sequence-based SNP genotyping in durum wheat. *Plant Biotechnology Journal* **11**, 809-817.

Vinje MA, Willis DK, Duke SH, Henson CA, 2011. Differential expression of two β-amylase genes (*Bmy1* and *Bmy2*) in developing and mature barley grain. *Planta* **233**, 1001-1010.

Voorrips, RE, 2002. MapChart: Software for the graphical presentation of linkage maps and QTLs. *The Journal of Heredity* **93**, 77-78.

Wagner C, Schweizer G, Kramer M, Dehmer-Badani A, Ordon F, Friedt W, 2008. The complex quantitative barley-*Rhynchosporium secalis* interaction: newly identified QTL may represent already known resistance genes. *Theoretical and Applied Genetics* **118**, 113-122.

Walter S, Doohan FM, 2011. Transcript profiling of the phytotoxic response of wheat to the *Fusarium* mycotoxin deoxynivalenol. *Mycotoxin Research* **27**, 221-230.

Walter S, Kahla A, Arunachalam C, et al. 2015. A wheat ABC transporter contributes to both grain formation and mycotoxin tolerance. *Journal of Experimental Botany* **66**, 2583-2593.

Walter S, Nicholson P, Doohan FM, 2010. Action and reaction of host and pathogen during Fusarium head blight disease. *New Phytologist* **185**, 54-66.

Wang J, Yang J, Jia Q, et al. 2014. A new QTL for plant height in barley (*Hordeum vulgare L.*) showing no negative effects on grain yield. *Plos One* **9**.

Wang JM, Zhang GP, Chen JX, Wu FB, 2004. The changes of β-glucan content and β-glucanase activity in barley before and after malting and their relationships to malt qualities. *Food Chemistry* **86**, 223-228.

Wang N, Ning SZ, Pourkheirandish M, Honda I, Komatsuda T, 2013. An alternative mechanism for cleistogamy in barley. *Theoretical and Applied Genetics* **126**, 2753-2762.

Wang XL, Chory J, 2006. Brassinosteroids regulate dissociation of BKI1, a negative regulator of BRI1 signaling, from the plasma membrane. *Science* **313**, 1118-1122.

Wang XL, Zhang XL, Cai SG, et al. 2015. Genetic diversity and QTL mapping of thermostability of limit dextrinase in barley. *Journal of Agricultural and Food Chemistry* **63**, 3778-3783.

Wanjiru WM, Kang ZS, Buchenauer H, 2002. Importance of cell wall degrading enzymes produced by *Fusarium graminearum* during infection of wheat heads. *European Journal of Plant Pathology* **108**, 803-810.

Wild M, Daviere J-M, Cheminant S, et al. 2012. The *Arabidopsis* DELLA RGA-LIKE3 is a direct target of MYC2 and modulates jasmonate signaling responses. *Plant Cell* **24**, 3307-3319.

Willyerd KT, Li C, Madden LV, et al. 2012. Efficacy and stability of integrating fungicide and cultivar resistance to manage Fusarium head blight and deoxynivalenol in wheat. *Plant Disease* **96**, 957-967.

Wright SaI, Azarang M, Falk AB, 2013. Barley lesion mimics, supersusceptible or highly resistant to leaf rust and net blotch. *Plant Pathology* **62**, 982-992.

Wu YX, Von Tiedemann A, 2004. Light-dependent oxidative stress determines physiological leaf spot formation in barley. *Phytopathology* **94**, 584-592.

Wurschum T, 2012. Mapping QTL for agronomic traits in breeding populations. *Theoretical and Applied Genetics* **125**, 201-210.

Xiao J, Jin XH, Jia XP, et al. 2013. Transcriptome-based discovery of pathways and genes related to resistance against Fusarium head blight in wheat landrace Wangshuibai. *BMC Genomics* **14**.

Xie GQ, Zhang MC, Chakraborty S, Liu CJ, 2007. The effect of 3BS locus of Sumai 3 on Fusarium head blight resistance in Australian wheats. *Australian Journal of Experimental Agriculture* **47**, 603-607.

Xu, SZ, 2008. Quantitative trait locus mapping can benefit from segregation distortion. *Genetics* **180**, 2201-2208.f

Xu WH, Meng Y, Wise RP, 2014. *Mla*- and *Rom1*-mediated control of microRNA398 and chloroplast copper/zinc superoxide dismutase regulates cell death in response to the barley powdery mildew fungus. *New Phytologist* **201**, 1396-1412.

Xu X, Nicholson P, 2009. Community ecology of fungal pathogens causing wheat head blight. *Annual Review of Phytopathology* **47**, 83-103.

Yamamuro C, Ihara Y, Wu X, et al. 2000. Loss of function of a rice Brassinosteroid insensitive1 homolog prevents internode elongation and bending of the lamina joint. *Plant Cell* **12**, 1591-1605.

Yang F, Svensson B, Finnie C, 2011. Response of germinating barley seeds to *Fusarium graminearum*: The first molecular insight into Fusarium seedling blight. *Plant Physiology and Biochemistry* **49**, 1362-1368.

Yang HA, Li CD, Lam HM, Clements J, Yan GJ, Zhao SC, 2015. Sequencing consolidates molecular markers with plant breeding practice. *Theoretical and Applied Genetics* **128**, 779-795.

Yang RC, Ham BJ, 2012. Stability of genome-wide QTL effects on malt α-amylase activity in a barley doubled-haploid population. *Euphytica* **188**, 131-139.

Yang ZP, Gilbert J, Fedak G, Somers DJ, 2005. Genetic characterization of QTL associated with resistance to Fusarium head blight in a doubled-haploid spring wheat population. *Genome* **48**, 187-196.

Yin Y, Liu X, Li B, Ma Z, 2009. Characterization of sterol demethylation inhibitor-resistant isolates of *Fusarium asiaticum* and *F. graminearum* collected from wheat in China. *Phytopathology* **99**, 487-497.

Yoshida M, Kawada N, Nakajima T, 2007. Effect of infection timing on Fusarium head blight and mycotoxin accumulation in open- and closed-flowering barley. *Phytopathology* **97**, 1054-1062.

Yoshida M, Kawada N, Tohnooka T, 2005. Effect of row type, flowering type and several other spike characters on resistance to Fusarium head blight in barley. *Euphytica* **141**, 217-227.

Yoshida M, Nakajima T, Arai M, Suzuki F, Tomimura K, 2008. Effect of the timing of fungicide application on Fusarium head blight and mycotoxin accumulation in closed-flowering barley. *Plant Disease* **92**, 1164-1170.

Yoshida M, Nakajima T, Tomimura K, Suzuki F, Arai M, Miyasaka A, 2012. Effect of the timing of fungicide application on Fusarium head blight and mycotoxin contamination in wheat. *Plant Disease* **96**, 845-851.

Yu GT, Franckowiak JD, Neate SM, Zhang B, Horsley RD, 2010. A native QTL for Fusarium head blight resistance in North American barley (*Hordeum vulgare L.*) independent of height, maturity, and spike type loci. *Genome* **53**, 111-118.

Zadoks JC, Chang TT, Konzak CF, 1974. Decimal code for growth stages of cereals. *Weed Research* **14**, 415-421.

Zhan J, Fitt BDL, Pinnschmidt HO, Oxley SJP, Newton AC, 2008. Resistance, epidemiology and sustainable management of *Rhynchosporium secalis* populations on barley. *Plant Pathology* **57**, 1-14.

Zhang L, Lavery L, Gill U, et al. 2009. A cation/proton-exchanging protein is a candidate for the barley *NecS1* gene controlling necrosis and enhanced defense response to stem rust. *Theoretical and Applied Genetics* **118**, 385-397.

Zhao CH, Cui F, Wang XQ, et al. 2012. Effects of 1BL/1RS translocation in wheat on agronomic performance and quality characteristics. *Field Crops Research* **127**, 79-84.

Zhao J, Zheng SH, Fujita K, Sakai K, 2004. Jasmonate and ethylene signalling and their interaction are integral parts of the elicitor signalling pathway leading to β-thujaplicin biosynthesis in *Cupressus lusitanica* cell cultures. *Journal of Experimental Botany* **55**, 1003-1012.

Zhu H, Gilchrist L, Hayes P, et al. 1999. Does function follow form? Principal QTLs for Fusarium head blight (FHB) resistance are coincident with QTLs for inflorescence traits and plant height in a doubled-haploid population of barley. *Theoretical and Applied Genetics* **99**, 1221-1232.

Zhu JY, Sae-Seaw J, Wang ZY, 2013. Brassinosteroid signalling. *Development* **140**, 1615-1620.

Zhuang YB, Gala A, Yen Y, 2013. Identification of functional genic components of major Fusarium head blight resistance quantitative trait loci in wheat cultivar Sumai 3. *Molecular Plant-Microbe Interactions* **26**, 442-450.

Zwickert-Menteur S, Jestin L, Branlard G, 1996. *Amy2* polymorphism as a possible marker of β-glucanase activity in barley (*Hordeum vulgare L*). *Journal of Cereal Science* **24**, 55-63.

Appendix

Table A.1. ANOVA from GLM calculated from *M. oryzae* inoculations.

Term	d.f	m.s	v.r	F pr.
Experiment_Replicate	2	899.20	7.52	<0.001
Line	1	301.10	2.52	0.116
Line/Mutation	2	1008.70	8.43	<0.001
Residual	104	119.60		
Total	109	151.90		

Table A.2. ANOVA from GLM calculated from *G. graminis* inoculations.

Term	d.f	m.s	v.r	F pr.
Experiment	2	14.20	13.26	<0.001
Experiment/Replicate	12	1.78	1.66	0.077
Line	1	4.92	4.59	0.033
Line/Mutation	2	29.55	27.59	<0.001
Residual	253	1.07		
Total	270	1.43		

Table A.3. ANOVA from GLM calculated from combined *O. acuformis* and *O. yallundae* inoculations.

Term	d.f	m.s	v.r	F pr.
Experiment	1	63.37	36.88	<0.001
Line	1	0.94	0.54	0.461
Line/Mutation	2	48.08	27.98	<0.001
Residual	181	1.72		
Total	185	2.55		

Table A.4. ANOVA from the GLM calculated from *F. culmorum* FHB inoculations.

Term	d.f	m.s	v.r	F pr.
Experiment	1	1074.28	51.71	<0.001
Experiment/Score	2	197.31	9.50	<0.001
Line	1	23.09	1.11	0.294
Line/Mutation	2	20.47	0.99	0.377
Residual	97	20.77		
Total	103	34.45		

Table A.5. ANOVA from the GLM calculated from *F. culmorum* non-wounded FCR inoculations.

Term	d.f	m.s	v.r	F pr.
Experiment	2	207.57	182.16	<0.001
Experiment/Rep	16	2.30	2.02	0.012
Line	1	1.97	1.73	0.189
Line/Mutation	2	44.86	39.37	<0.001
Residual	327	1.14		
Total	349	3.22		

Table A.6. ANOVA from the GLM calculated from *F. culmorum* wounded FCR inoculations.

Term	d.f	m.s	v.r	F pr.
Experiment	1	16.82	17.97	<0.001
Experiment/Rep	2	1.64	1.75	0.181
Line	1	0.67	0.71	0.402
Line/Mutation	2	2.94	3.14	0.049
Residual	74	0.94		
Total	80	1.19		

Table A.7. ANOVA from the GLM calculated from *R. collo-cygni* inoculations.

Term	**d.f**	**m.s**	**v.r**	**F pr.**
Experiment	2	1281.8	80.88	<0.001
Line	1	1073.45	67.73	<0.001
Line/Mutation	2	24.21	1.53	0.222
Residual	108	15.85		
Total	113	47.76		

Table A.8. ANOVA from the GLM calculated from *B. graminis* inoculations.

Term	**d.f**	**m.s**	**v.r**	**F pr.**
Experiment	2	20.71	66.10	<0.001
Experiment/Replicate	9	0.42	1.34	0.227
Dpi score	1	11.28	36.00	<0.001
Line	1	40.50	129.25	<0.001
Line/Mutation	2	0.41	1.30	0.278
Residual	112	0.31		
Total	127	1.05		

Table A.9. ANOVA from GLM of C×T F_5 JIC 2013 trial, variate: FHB

Term	**d.f**	**m.s**	**v.r**	**F.pr**
Score	3	187.14	32.19	<.001
Score.Line	808	18.32	3.15	<.001
Row	10	88.47	15.22	<.001
Residual	38	5.81		
Total	859	19.17		

Table A.10. ANOVA from GLM of C×T F_5 KWS1 2013 trial, variate: FHB

Term	d.f	m.s	v.r	F.pr
Line	206	9.69	1.42	0.255
Row	17	5.69	0.83	0.628
Residual	16	6.84		
Total	239	9.32		

Table A.11. ANOVA from GLM of C×T F_5 KWS2 2013 trial, variate: FHB

Term	d.f	m.s	v.r	F.pr
Line	206	13.78	1.65	0.124
Row	17	23.37	2.79	0.023
Residual	16	8.37		
Total	239	14.10		

Table A.12. ANOVA from GLM of C×T F_5 JIC 2013 trial, variate: height

Term	d.f	m.s	v.r	F.pr
Line	203	467.22	57.33	0.017
Row	10	4.41	0.54	0.793
Residual	2	8.15		
Total	215	441.42		

Table A.13. ANOVA from GLM of C×T F_5 KWS1 2013 trial, variate: height

Term	d.f	m.s	v.r	F.pr
Line	206	349.26	17.87	<.001
Row	17	49.65	2.54	0.034
Residual	16	19.54		
Total	239	305.88		

Table A.14. ANOVA from GLM of C×T F_5 KWS2 2013 trial, variate: height

Term	d.f	m.s	v.r	F.pr
Line	206	379.05	14.09	<.001
Row	17	77.19	2.87	0.020
Residual	16	26.9		
Total	239	334		

Table A.15. ANOVA from GLM of C×T F_5 JIC 2013 trial, variate: heading date

Term	d.f	m.s	v.r	F.pr
Line	203	14.99	99.95	0.010
Row	10	13.65	91.02	0.011
Residual	2	0.15		
Total	215	14.79		

Table A.16. ANOVA from GLM of C×T F_5 KWS1 2013 trial, variate: heading date

Term	d.f	m.s	v.r	F.pr
Line	206	23.80	28.35	<.001
Row	17	1.44	1.71	0.144
Residual	16	0.84		
Total	239	20.67		

Table A.17. ANOVA from GLM of C×T F_5 KWS2 2013 trial, variate: heading date

Term	d.f	m.s	v.r	F.pr
Line	206	29.53	38.63	<.001
Row	17	1.02	1.33	0.286
Residual	16	0.76		
Total	239	25.58		

Table A.18. ANOVA from GLM of C×T F_7 JIC 2014 trial, variate: FHB

Term	d.f	m.s	v.r	F.pr
Score	3	3015.20	1247.67	<.001
Score/Line	752	22.59	9.35	<.001
Row	6	16.75	6.93	<.001
Residual	18	2.42		
Total	779	33.60		

Table A.19. ANOVA from GLM of C×T F_7 JIC 2015 trial, variate: FHB

Term	d.f	m.s	v.r	F.pr
Score	3	1322.47	432.94	<.001
Score/Line	756	15.06	4.93	<.001
Row	9	33.66	11.02	<.001
Rep	6	4.48	1.47	0.187
Residual	793	3.06		
Total	1567	11.55		

Table A.20. ANOVA from GLM of C×T F_7 JIC 2014 trial, variate: height

Term	d.f	m.s	v.r	F.pr
Line	188	338.88	17.38	<.001
Row	9	19.5	1.13	0.343
Residual	1	2		
Total	198	329		

Table A.21. ANOVA from GLM of C×T F_7 JIC 2015 trial, variate: height

Term	d.f	m.s	v.r	F.pr
Line	189	685.17	10.66	<.001
Row	9	112.93	1.76	0.079
Rep	6	57.36	0.89	0.501
Residual	187	64.26		
Total	391	365.41		

Table A.22. ANOVA from GLM of C×T F_7 JIC 2014 trial, variate: heading date

Term	d.f	m.s	v.r	F.pr
Line	188	19.92	31.87	<.001
Row	9	44.97	2.41	0.409
Residual	1	0.63		
Total	198	19.32		

Table A. 23. ANOVA from GLM of C×T F_7 JIC 2015 trial, variate: heading date

Term	d.f	m.s	v.r	F.pr
Line	189	17.18	5.81	<.001
Row	9	1.20	0.41	0.930
Rep	6	1.83	0.62	0.716
Residual	187	2.96		
Total	391	9.78		

Table A.24. ANOVA from GLM of A×T F_6 NIAB 2013 trial, variate: FHB

Term	d.f	m.s	v.r	F.pr
Score	1	1176.69	53.44	<.001
Score/Line	398	83.04	3.77	0.008
Row	9	70.44	3.2	0.037
Residual	11	22.02		
Total	419	83.78		

Table A. 25. ANOVA from GLM of A×T F_6 JIC 2014 trial, variate: FHB

Term	d.f	m.s	v.r	F.pr
Score	1	185.71	20.63	0.020
Score/Line	388	22.09	2.45	0.252
Row	9	32.00	3.56	0.156
Residual	3	9.00		
Total	401	22.431		

Table A.26. ANOVA from GLM of A×T F_6 NIAB 2013 trial, variate: height

Term	d.f	m.s	v.r	F.pr
Line	199	152.65	152.65	0.055
Row	9	24.70	24.7	0.155
Residual	1	1		
Total	209	146.41		

Table A.27. ANOVA from GLM of A×T F_6 JIC 2014 trial, variate: height

Term	d.f	m.s	v.r	F.pr
Line	196	240.5	1.22	0.249
Row	9	230.8	1.17	0.319
Residual	1	97.7		
Total	206	203.3		

Table A. 28. ANOVA from GLM of A×T F_6 JIC 2014 trial, variate: heading date

Term	d.f	m.s	v.r	F.pr
Line	196	144.31	9.22	<.001
Row	9	28.18	1.8	0.056
Residual	1	9.65		
Total	206	22.77		